



HAL
open science

Rab35 GTPase and initiation of apico-basal polarity in 3D renal cysts

Kerstin Klinkert

► **To cite this version:**

Kerstin Klinkert. Rab35 GTPase and initiation of apico-basal polarity in 3D renal cysts. Cellular Biology. Université Pierre et Marie Curie - Paris VI, 2016. English. NNT : 2016PA066320 . tel-01474942

HAL Id: tel-01474942

<https://theses.hal.science/tel-01474942>

Submitted on 23 Feb 2017

HAL is a multi-disciplinary open access archive for the deposit and dissemination of scientific research documents, whether they are published or not. The documents may come from teaching and research institutions in France or abroad, or from public or private research centers.

L'archive ouverte pluridisciplinaire **HAL**, est destinée au dépôt et à la diffusion de documents scientifiques de niveau recherche, publiés ou non, émanant des établissements d'enseignement et de recherche français ou étrangers, des laboratoires publics ou privés.

Université Pierre et Marie Curie

Ecole Doctorale Complexité du vivant

**Rab35 GTPase and initiation of apico-basal
polarity in 3D renal cysts**

Présentée par

Kerstin KLINKERT

Thèse de doctorat de Biologie cellulaire

Présentée et soutenue publiquement le 22/09/2016

Devant un jury composé de :

Prof. Joëlle SOBCZAK-THEPOT	Président
Prof. Fernando MARTIN-BELMONTE	Rapporteur
Dr. Grégoire MICHAUX	Rapporteur
Dr. Yohanns BELLAÏCHE	Examineur
Dr. Arnaud ECHARD	Directeur de thèse

Membrane Traffic and Cell Division Lab
Institut Pasteur - CNRS



Dedication

*This thesis is dedicated to my parents,
grandparents and my better half Simon
for their love, endless support
and encouragement.*

ACKNOWLEDGEMENT

Firstly, I would like to thank my advisor Arnaud Echard for giving me the opportunity to complete my PhD in his lab and for encouraging me throughout my PhD. I am thankful for his support, his advice and our long and lively discussions.

I would also like to thank my thesis advisory committee Fanny Jaulin, Xavier Morin and Didier Montarras. I would like to thank them all for their support and their great ideas, suggestions and discussions.

Furthermore, I would like to thank Fernando Martin-Belmonte, Grégoire Michaux, Yohanns Bellaïche and Joëlle Sobczak-Thépot for examining my thesis.

Thanks to the Pasteur-Paris University doctoral program for the funding, general support and the yearly retreats. I am glad to be part of this program and I would like to highlight the great atmosphere within this program, among the students, the steering committee and all organizers.

My fourth year of my PhD was funded by the “Fondation pour la Recherche Médicale” (FRM), and I would like to thank for their financial support.

I would like to thank the team of Anne Houdousse for the help with the interaction experiments.

Thanks to Sophie Saunier and Flora Legenre for discussions, protocols and the introduction into MDCK cyst cultures.

Thanks also to the whole team of Franck Perez for the discussions during our joint labmeetings.

Furthermore, I would also like to thank everyone who helped me out with reagents and protocols. Many experiments would have not been possible without the people who kindly share reagents on our campus and at the Institut Curie. I would like to apologize for not thanking everyone individually.

Thanks also the Flow Cytometry Platform at the Institut Pasteur and especially Pierre-Henri Commere who helped me with my experiments. Furthermore I thank the Imagopol for the use of microscopes and Jean-Yves Tinevez and Audrey Salles for their assistance.

Last but not least I want to thank all present and past members of the Membrane Traffic and Cell Division Lab. We always had a great atmosphere in the lab, I am thankful for all the help and support and I am happy to be part of this team. I would also like to thank Murielle for teaching me all the French expressions they don't teach you in school.

For the non-scientific side of my thesis I would like to thank all my friends and especially my family for their support and faith. Many thanks to my partner Simon, who believes in me, supports me and pushes me forward.

Thanks.

TABLE OF CONTENTS

1	Introduction	1
1.1	Epithelial lumen morphogenesis	1
1.1.1	Polarized epithelial tissues	1
1.1.2	Polarity complexes in epithelial polarity	2
1.1.3	Polarized traffic - Apical and basolateral sorting signals	8
1.1.4	Polarized Mechanisms of epithelial lumen formation <i>in vitro</i> and <i>in vivo</i>	10
1.1.5	MDCK cells as a model for epithelial lumen formation	16
1.1.5.1	<i>Polarity in MDCK cells cultures in 2D or 3D</i>	16
1.1.5.2	<i>The role of membrane traffic in MDCK cystogenesis</i>	18
1.1.5.3	<i>The role of the extracellular environment</i>	23
1.1.5.4	<i>Inversion of apico-basal polarity and other abnormal phenotypes in cysts</i>	24
1.1.5.5	<i>The role of cytokinesis in polarity establishment</i>	36
1.2	Podocalyxin	40
1.2.1	Structure	40
1.2.2	Tissue Expression	41
1.2.3	Discovery and Function	42
1.2.4	PODXL in polarity	47
1.2.5	PODXL in cancer and disease	51
1.3	Functions of the Rab35 GTPase	53
1.3.1	Rab GTPases	53
1.3.2	Rab35 - a regulator of endocytic recycling and cytokinesis	55
1.3.3	A role for Rab35 in polarity	59
1.3.4	Functions of Rab35 in cancer	60
1.3.5	Other functions of Rab35	63
1.4	Thesis rationale	65
2	Results	67
2.1	Summary	67
2.2	Published Manuscript	68
2.3	Reviewers comments and author's rebuttal letter	94
3	Discussion	105
3.1	Definition of the AMIS	106
3.2	How is Rab35 recruited to the AMIS?	108

3.3 Rab35 and other tethering mechanisms at the AMIS	109
3.4 Why does Rab35 depletion lead to inversion of AB polarity?	115
3.5 Significance of other Rab-cargo interactions	120
3.6 The role of Rab35 interacting proteins in apico-basal polarity establishment	122
3.7 Other potential functions for Rab35 in epithelial polarity	127
3.7.1 The role of Rab35 in subsequent cell divisions in MDCK cysts	127
3.7.2 The Role of Rab35 in adherence junction integrity	131
3.8 Is the Rab35/ PODXL interaction a general mechanism?	133
4 Conclusion and Future perspectives	135
List of References	138
Annex	I
Figure A: Rab35 depletion levels correlate with cyst phenotypes	II
Figure B: Inversion of apico-basal polarity inversion requires Rab35 depletion during the first cell division of cyst development	III
Review article: Klinkert K and Echard A. Rab35 GTPase: a central regulator of phosphoinositides and F-actin in endocytic recycling and beyond. <i>Traffic</i> (2016)	IV

1 INTRODUCTION

1.1 EPITHELIAL LUMEN MORPHOGENESIS

1.1.1 Polarized epithelial tissues

All epithelial tissues share common features, despite their morphological diversity. Epithelial cells can be organized into simple monolayers or stratified multiple layers and their morphology can be classified into squamous (thin and flat), cuboidal (square) or columnar (barrel-shaped). Regardless their different organizations, all epithelial cells are tightly packed, closely connected through adherence and tight junctions and highly polarized.

Epithelial cells are polarized in respects to their neighbouring cells in X and Y (planar cell polarity) as well as in respect to the luminal surface in Z (apico-basal polarity). In this thesis I will focus on the apico-basal cell polarization, which is characterized by clearly segregated plasma membrane domains as well as polarized distribution of cell organelles and the cytoskeleton. The apical and basolateral plasma membrane domains are segregated by tight junctions and characterized by distinct lipid and protein compositions. The apical domain faces the lumen, whereas the basal domain is in contact with the basal lamina, which in turn is linked to the extracellular matrix of connective tissue. During development or upon injury, epithelial cells undergo cell division, which is a critical process since the cells have to maintain the integrity of the tissue while experiencing drastic cell shape remodelling.

How exactly epithelial cells establish and maintain their apico-basal polarization in the context of cell division are long standing questions that I will discuss in detail during this thesis.

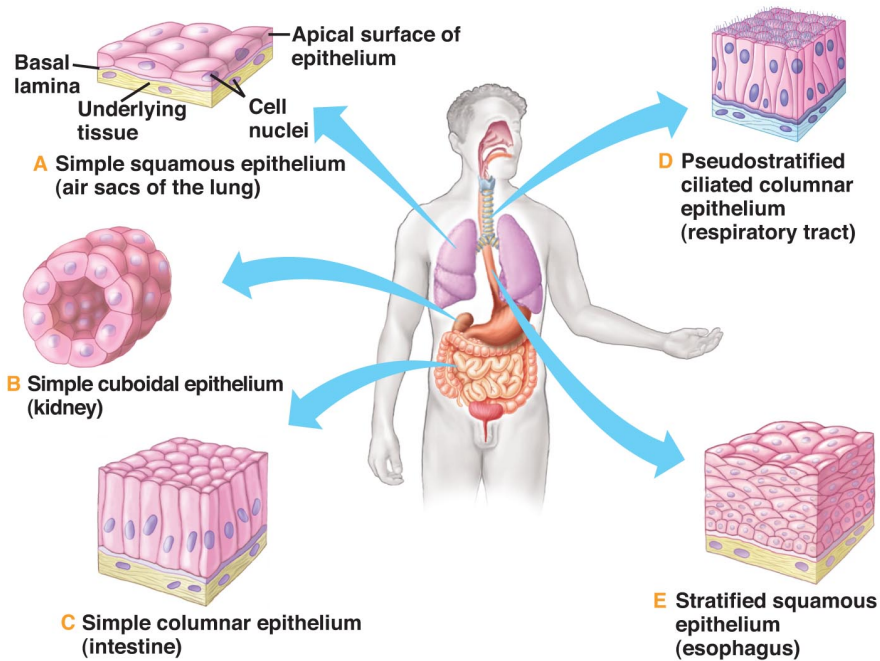


Figure 1: Classification of vertebrate epithelia.

This scheme illustrates the different types of epithelial tissues in respect to their localization in the human body.

From: <http://pharmaworld.pk.cws3.my-hosting-panel.com/BodySystemDetail.asp?tId=43>

1.1.2 Polarity complexes in epithelial polarity

Three evolutionary conserved polarity complexes play a major role in the establishment and maintenance of epithelial polarity: the Crumbs (Crumbs/PALS1/PATJ) complex, the PAR (Par6/Par3 /aPKC) complex and the Scribble (Scribble/Dlg/Lgl) complex. These polarity complexes, their functions and interactions are conserved from invertebrates to humans. Therefore many studies have been carried out in *C. elegans* and *Drosophila melanogaster*, due to the well-known cell fates and the ease of genetic manipulation.

The discovery of the Par complex

The Par (partitioning-defective) proteins 1-4 were initially identified in a genetic screen for maternal lethal mutants in *C. elegans* in 1988¹. Loss of Par proteins induces symmetric cell division through partition defects of cytoplasmic polarity regulators during early cell division. Interestingly, the idea that cell division is tightly coupled with polarity and cell fate in terms of asymmetric segregation of cytoplasmic regulatory proteins was already established in the early 1980s. Investigation of the distribution of P-granules during cell division in the early *C. elegans* embryos demonstrated that P-granules localized asymmetrically in the cytoplasm during cell division and determined which daughter cell would develop into a somatic cell and which one into a germ-line daughter cell².

Only one decade later the Par-5 (also called 14-3-3) and Par-6 were discovered in a screen for maternal effect lethal mutations in *C. elegans*³. The last component of the Par (Par6/Par3/aPKC) complex, aPKC, was also discovered in *C. elegans*, displaying the same phenotype as the Par mutants⁴. Furthermore it was demonstrated that Par3 interacts with aPKC and that their localization in the *C. elegans* embryo is mutually dependent⁴, whereas Par6 is required to maintain Par3 at the cell periphery^{3,5}. These studies discovered and described for the time the function of a polarity complex.

The function of polarity complexes in apico-basal polarity establishment

The apical plasma membrane domain of epithelial cells is defined by the Crumbs complex, which antagonizes with the subapical Par complex and with the basolateral localized Scribble complex in order to segregate two distinct membrane domains. Membrane segregation is achieved by different mechanisms that include mutual antagonism, positive or negative feed-back loops, inhibition, recruitment and formation of lateral diffusion barriers (tight junctions in vertebrate epithelial cells or the subapical complex/marginal zone in invertebrates).

The tight junctions (also called *zonulae occludentes*) are composed of Occludins, Claudins and Jam-A, which are anchored to the actin cytoskeleton via PDZ containing proteins such as ZO-1, -2, -3. The adherence junctions (*zonulae adhaerens*) are located underneath the tight junctions and are composed of Cadherins and Nectins, and are connected to the actin cytoskeleton via Catenins and Afadin. Adherence junctions are a prerequisite for tight junctions since Nectin, in cooperation with Cadherin, assist to recruit Jam-A, Occludin and Claudin to the apical side of adherence junctions^{6,7}. Nectin and Jam-A recruit Par3, a component of the Par complex, to the apical junctions, which is an important player in tight junction formation and apico-basal polarity establishment⁸⁻¹².

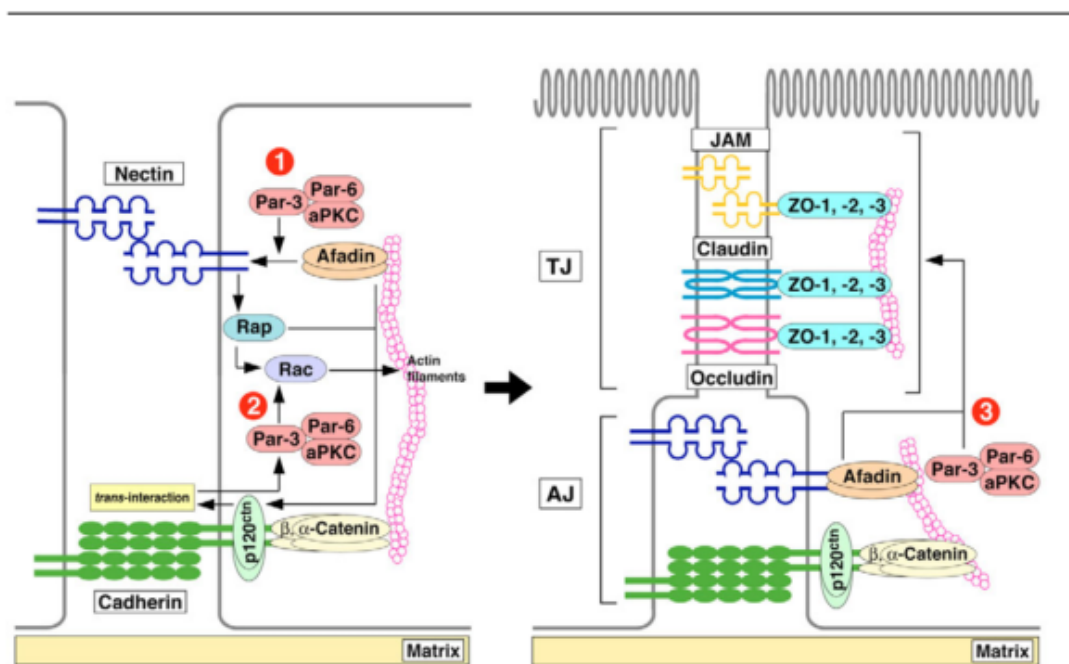


Figure 2: Polarity and junctional complexes in polarizing epithelial cells.

Localization of polarity complexes, adherence and tight junction proteins during the establishment of epithelial apico-basal polarity in vertebrate cells. Left: unpolarized epithelial cell, Right: polarized epithelial cell. From reference: ⁷

Depletion of Par3 in MDCK cysts leads to abnormal multiple lumen cysts and impaired tight junction formation through mistargeting of apical proteins¹². Interestingly, rescue experiments using a Par3 mutant unable to bind aPKC cannot rescue the MDCK single lumen formation, but can rescue tight junction formation. This indicates, that aPKC-mediated phosphorylation of Par3 is required for apical polarity establishment, but dispensable for tight junction formation¹².

This observation is in line with the fact that aPKC phosphorylation of Par3 occurs at the apical plasma membrane and leads to immediate dissociation of Par3 from the complex¹². Par3 phosphorylation is mediated through Par6, which is activated by Cdc42 and recruited to the apical domain through PALS1 and Crumbs¹². Moreover it was demonstrated in *Drosophila* that Par1 phosphorylates Par3, which induces Par3 binding to 14-3-3¹³. The binding to 14-3-3 competes with the binding of Par3 to aPKC and thus inhibits association of Par3 with aPKC/Par6. In addition Par1 binds to 14-3-3 and thus competes with Par3 for the binding site, thus leading to physical separation of the apical Par3 domain and the lateral Par1 domain.

Par3-mediated tight junction formation in contrast is independent of the Par complex but depends on binding to the Rac1 GEF Tiam1 and therefore local Rac1 activation¹¹. Active Rac1 assists PI3K activation, which activates Rac1 in a positive feed-back loop in *Drosophila*¹⁴ as well as during MDCK cysts development¹⁵. It was shown in *Drosophila* that apically-localized Crumbs represses this feed-back loop, while it is negatively regulated through Rac1 and PI3K¹⁴. This example of a tightly-regulated positive feed-back loop helps to restrict PI3K-induced conversion of $\text{PtdIns}(4,5)\text{P}_2$ into $\text{PtdIns}(3,4,5)\text{P}_3$ to the basolateral membrane, since it is inhibited by Crumbs at the apical membrane domain. Moreover PI3K is recruited to lateral junctions by E-cadherin where it recruits Disc Large and generates $\text{PtdIns}(3,4,5)\text{P}_3$, which in turn recruits Scribble to form the basolateral Scribble complex and antagonizes the apical Crumbs complex¹⁶⁻¹⁸.

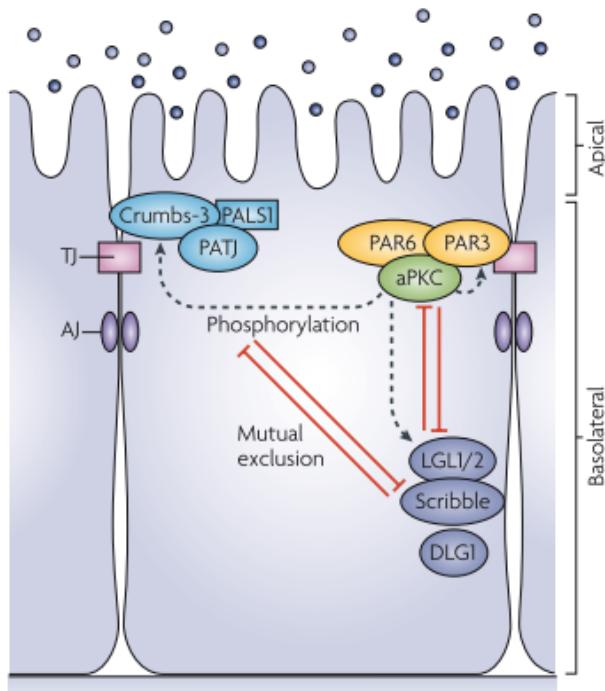


Figure 3: Polarity complexes in polarized vertebrate epithelial cells

This scheme illustrates the interaction between polarity complexes in polarized vertebrate epithelial cells. From reference: ¹⁹

The role of lipids in apico-basal polarity establishment

The apical plasma membrane domain is rich in $\text{PtdIns}(4,5)\text{P}_2$, whereas the basolateral domain is dominated by $\text{PtdIns}(3,4,5)\text{P}_3$ ²⁰. The segregation of these lipids is mainly achieved through polarized localization of the phosphatase PTEN and the kinase PI3K.

It was shown in *Drosophila* and MDCK cells that Par3 can bind PTEN through its PDZ3 domain and thus recruits PTEN to the apical membrane and apical junctions ²¹⁻²³. Par3 itself is recruited to the apical junctions via binding to cell adhesion molecules ⁸⁻¹², but also via its binding to phosphoinositides through its PDZ2 domain ^{21,22}. Furthermore Par3 can associate transiently with the apical aPKC/Par6 complex.

PTEN catalyses the conversion of $\text{PtdIns}(4,5,6)\text{P}_3$ into $\text{PtdIns}(4,5)\text{P}_2$ and therefore helps to recruit Cdc42 through Annexin2 (a $\text{PtdIns}(4,5)\text{P}_2$ -binding protein) ²⁴. Cdc42 in turn

participates in the activation of aPKC through Par6. Furthermore, aPKC phosphorylates Lgl, which induces its degradation and therefore suppresses basolateral identity at the apical pole.

However, Par3 also activates Rac1 and PI3K through binding to the Rac1 effector Tiam1 and thus promotes generation of $\text{PtdIns}(3,4,5)\text{P}_3$. Hence, Par3 with its localization at the apical adherence junctions triggers tight junction formation and the establishment of the apical domain through PTEN/ $\text{PtdIns}(4,5)\text{P}_2$ /Annexin/Cdc42 as well the establishment of the basolateral domain through Tiam1/Rac1/PI3K/ $\text{PtdIns}(3,4,5)\text{P}_3$.

Interestingly when $\text{PtdIns}(3,4,5)\text{P}_3$ is inserted ectopically into the apical membrane of MDCK cells, this is sufficient to locally change the membrane identity²⁰. $\text{PtdIns}(3,4,5)\text{P}_3$ insertion recruits PI3K to the apical membrane, thus inducing a positive feedback loop that induces transcytosis of basolateral proteins from the ECM facing membrane to the apical membrane domain. Indeed, a biotinylation assay demonstrated that basolateral proteins such as p58 and Syntaxin4 are endocytosed from the basolateral membrane and targeted towards the $\text{PtdIns}(3,4,5)\text{P}_3$ insertion site. In line with these results, addition of the PI3K inhibitor LY204002 reduces the cell height of MDCK 2D monolayers through inhibiting the expansion of the lateral domains²⁰. Thus, local PI3K activity is sufficient to initiate the formation of basolateral domains.

Similarly, addition of $\text{PtdIns}(4,5)\text{P}_2$ to the basolateral domain in MDCK 3D cysts is sufficient to target apical proteins such as actin and PODXL to the basolateral domain²⁴.

Hence, the distribution of different phosphoinositides, controlled by phosphatases and kinases, drives cell polarity through recruitment of polarity proteins that directly interact with lipids.

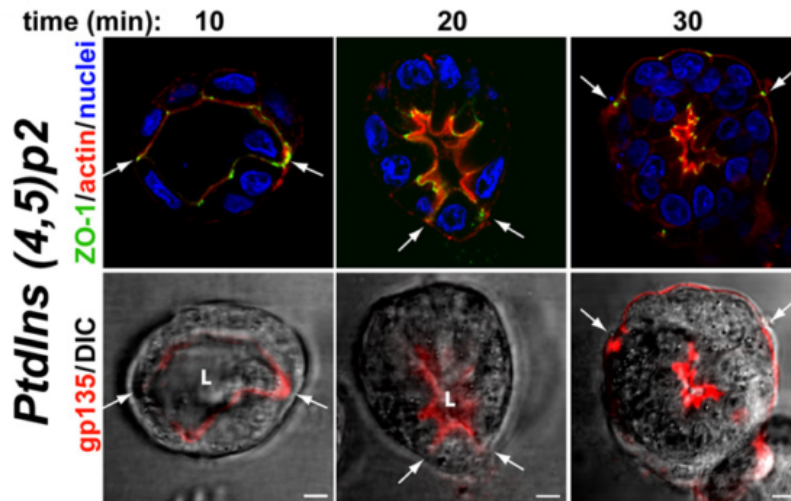


Figure 4: Exogenous PtdIns(4,5) P_2 reverses the orientation of the apical membrane

Exogenous addition of PtdIns(4,5) P_2 from the basolateral site of polarized MDCK cysts induces delocalization of PODXL(gp135), ZO-1 and actin from the apical membrane to the basolateral membrane. From reference: ²⁴

1.1.3 Polarized traffic - Apical and basolateral sorting signals

Newly synthesized membrane proteins are trafficked from the endoplasmic reticulum to the Golgi and through the trans-golgi network (TGN), where they are sorted and delivered to the correct plasma membrane domain. Some of these proteins will be sorted directly towards the apical or basolateral domain, others will be delivered to the basolateral domain from where they undergo transcytosis to the apical membrane. Upon endocytosis (clathrin-dependent or clathrin-independent), apical and basolateral cargo enter into Rab5-positive apical or basolateral early endosomes (AEE or BEE, respectively)²⁵⁻²⁷. From there, the cargo can be recycled back to the membrane of origin, transcytosed towards the opposite membrane domain or enter into late endosomes and lysosomes for degradation²⁸⁻³¹.

The sorting signals for basolateral proteins are usually located in the cytoplasmic tail. Most of these sorting signals are tyrosine-based or contain dileucine motifs such as "NPxY", "YxxO" or "D/ExxxLL"³²⁻³⁴. In some cases, these basolateral sorting motifs can also serve as endocytosis signals and can interact with subunits of clathrin adapter complexes. The clathrin adapter AP-1B is for example required for the basolateral sorting of vesicular stomatitis virus glycoprotein G (VSV-G), the low-density lipoprotein receptor (LDLR) and E-cadherin in mammalian epithelial cells^{35,36}. In *C. elegans* however, AP-1 is not only required for basolateral sorting but also for the apical sorting of essential polarity proteins such as Cdc42 and Par6³⁷. Interestingly, AP-1 regulates the sorting of E-cadherin both in vertebrates and in *C. elegans*, although E-cadherin localizes to the basolateral membrane in vertebrates and to the apical membrane in *C. elegans*³⁸, highlighting the plasticity of sorting mechanisms.

Apical sorting signals are often more complex than basolateral sorting signals and can include posttranslational modifications such as N- and O-linked glycosylation in combination with lipid raft association, dimerization of the protein or the presence of a GPI anchor or a PDZ domain^{32,33}. GPI-anchored proteins are often sorted from the TGN to the apical membrane in polarized epithelial cells. However, there are also GPI-anchored proteins that are sorted to the basolateral membrane. Fusion of GPI to the ectodomain of basolateral proteins was shown to redirect these proteins to the apical membrane^{39,40} and it was furthermore shown that GPI-mediated apical sorting requires oligomerization and raft-association of the proteins⁴¹⁻⁴³. Basolateral-sorted GPI-anchored proteins however, do not require oligomerization for their sorting⁴³. Interestingly, it was also shown that at least for some proteins that are naturally glycosylated and GPI-anchored such as the membrane dipeptidase (MDP), the glycosylation is required for apical sorting, but not the GPI anchor⁴⁴. Removal of the glycosylation therefore leads to basolateral targeting of MDP. It was shown for the p75 neurotrophin receptor (p75^{NTR}) that its O-glycosylation, but not the N-glycosylation important for its apical sorting and removal of the O-glycosylation is sufficient to target p75^{NTR} to the basolateral plasma membrane⁴⁵. The polymeric immunoglobulin receptor (pIgR) is biosynthetically targeted to the basolateral domain, where it can bind its ligand IgA and take the transcytosis

route to the apical membrane. For this protein it was shown that removal of the glycosylation reduces its transcytosis rate, but does not inhibit it completely⁴⁶. Instead a small sequence of 11 aminoacids in the cytoplasmic domain of plgR is sufficient for basolateral to apical transcytosis. Other proteins such as the P2Y₄ receptor rely on hydrophobic residues near the COOH-terminus for their apical targeting⁴⁷.

These examples show that there is no unique apical targeting signal and that several mechanisms are employed to ensure the correct apical sorting.

1.1.4 Polarized Mechanisms of epithelial lumen formation *in vitro* and *in vivo*

The formation of lumen is a highly conserved feature among vertebrates and invertebrates, though the mechanisms for lumen formation are very diverse even within the same species. Lumen can be established *de novo* from an already pre-existing epithelial monolayer or from unpolarized single cells or cell aggregates.

1.1.4.1 Lumen formation from polarized epithelia

A polarized monolayer can form lumen through processes called wrapping or budding (branching). In this case the monolayer undergoes either invagination to form tubes with an open lumen or folds and pinches of a tubular epithelium that are in both cases already polarized (Fig.5)⁴⁸. Wrapping can be found *in vivo* in the vertebrate neural tube, whereas budding is observed in the ureteric bud in the kidney and the lung epithelia⁴⁸.

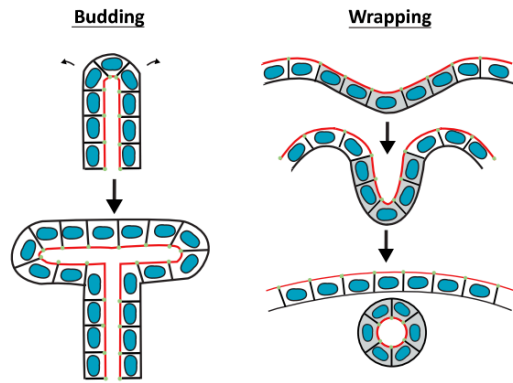


Figure 5: Two mechanisms of lumen formation in polarized epithelia.

This scheme illustrates epithelium lumen formation from polarized cells through two distinct processes called “budding” and “wrapping”. Apical membrane (red) and cell-cell junctions (green). From reference: ⁴⁸

1.1.4.2 Lumen formation from unpolarized epithelia

The major processes to establish a lumen from nonpolarized cells are described as cord hollowing, cell hollowing and cavitation.

Cavitation

Cavitation is the formation of a lumen within a cell aggregate through apoptosis of the inner lying cells. This process of lumen formation was initially studied *in vitro*, using MCF-10 cells (mammary gland cells) that were cultured in Matrigel. It has been shown that MCF-10 cell undergo a phase of proliferation and polarization that is followed by apoptosis of the inner lying cells that are not in contact with the extracellular matrix^{49,50}. These inner cells do not receive survival signals from the ECM and thus undergo apoptosis, leading to a hollow acini-like sphere. This model of cavitation can be found *in vivo* in the mammary and the salivary glands.

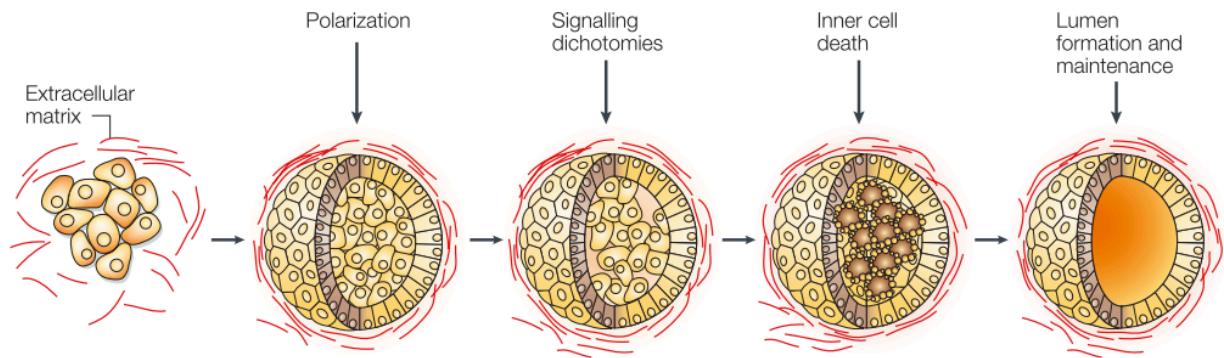


Figure 6: Cavitation - a mechanism of lumen formation in polarized epithelia.

This scheme illustrates *in vitro* lumen formation of mammary epithelia through apoptosis of the inner lying cells. From reference: ⁴⁹

Hollowing

Another mechanism of lumen formation is described as hollowing, where a lumen will form *de novo* between two or more cells from pre-existing cell-cell contacts through coordinated membrane traffic, cell division and polarization (cord hollowing). Hollowing can also occur within one cell through fusion of vesicles in the cytoplasm that form a lumen that traverse the whole cell (cell hollowing). Cord hollowing can be observed *in vitro* in intestinal epithelial Caco-2 cells as well as in canine Madin Derby kidney cells (MDCK). *In vivo*, it is observed for example in the *Drosophila melanogaster* tracheal system, in the Zebrafish gut and in the elongating nephron in the mouse kidney⁵¹. Cell hollowing in contrast has been described *in vivo* in the excretory cells of *C. elegans* as well as in the tracheal terminal cells in *Drosophila melanogaster*⁵².

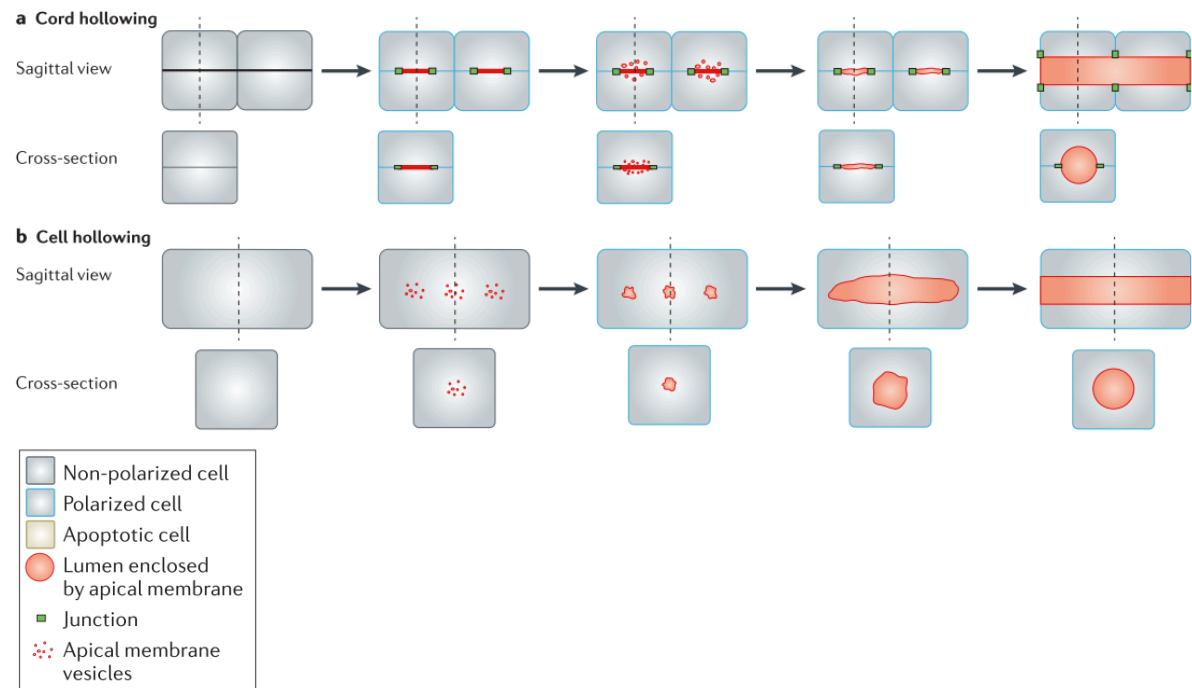


Figure 7: Hollowing - two mechanisms of lumen formation in polarized epithelia.

This scheme illustrates the differences between cord hollowing (a) and cell hollowing (b). Junctions are marked in green; apical vesicles and domains in red. From reference: ⁵²

Cell hollowing - Seamless tube formation in *Drosophila Melanogaster*

Seamless tubes consist of a single cell with an intracellular tube that can be found in the Zebrafish vasculature⁵³, the *Drosophila* trachea and the *C. elegans* excretory system⁵⁴. The tube forms through a process where intracellular vesicles coalesce and thereby form a tube, which requires endocytosis, endocytic recycling as well as pinocytosis⁵⁴⁻⁵⁸. In the *Drosophila* tracheal cells, it was shown that tube formation requires endocytosis since Rab5 and Syntaxin7 mutants show impaired seamless tube formation⁵⁶. Interestingly, perturbations of early endosome formation induce elevated levels of Crumbs and phosphorylated Moesin, which leads to cystic dilation of the seamless⁵⁶. It was further shown that Crumbs is required to recruit or to stabilize Moesin. Moesin in turn is required for luminal actin remodelling and targeting of Crumbs-positive vesicles in cooperation with the synaptotagmin like protein Bitesize⁵⁹.

Moreover it has been shown that tracheal seamless tube formation depends on minus-end directed microtubular trafficking of apical cargos. Importantly, the trafficking of apical cargos, such as Crumbs3, is mediated by the Rab35 GTPase and its GAP whacked, which will be discussed on page 59.

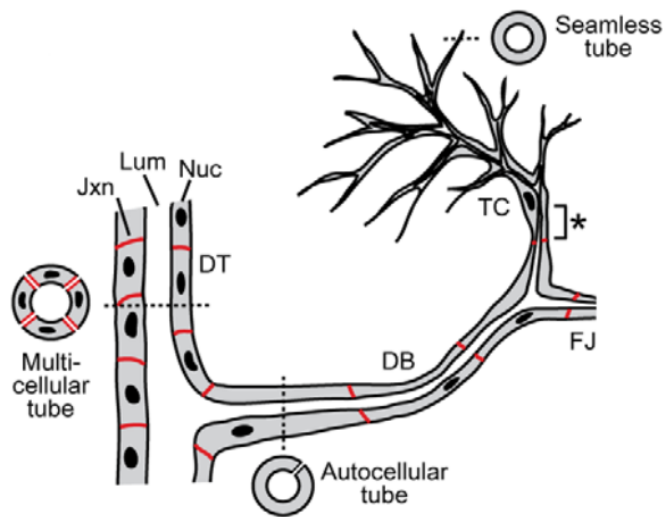


Figure 8: Dorsal trunk and dorsal branch of the *Drosophila* trachea

This scheme illustrates different types of tubules that can be found in the *Drosophila* trachea. The dorsal trunk (DT) consists of multicellular tubes that are separated by junctions (red). The dorsal branch (DB) consists two distinct types of tubes: The autocellular tube, a single cell wrapped around the luminal space and sealed by an autocellular junction. The seamless tube, a single cell with a lumen and without junctions. Terminal cells at each branch of the dorsal branch form seamless tubes. From reference: ⁶⁰

Cord Hollowing - Formation of the renal vesicle

During formation of the mammalian nephron for example, the cap mesenchyme becomes compacted to form a cell aggregate that undergoes MET and thus forms a sphere with an open lumen, which is called the renal vesicle⁵¹. The pre-tubular aggregate contains Par3-positive membrane domains that will coalesce to form the future apical membrane, which is mediated by the adherence junction protein Afadin. Consequently, depletion of Afadin leads to discontinuous, multiple lumen in the mouse

nephron. Then the renal vesicle elongates to form the s-shaped body that fuses to the ureteric bud tubule to form a continuous lumen. The process of the formation of the renal vesicles is very similar to the “hollowing” mechanism observed in renal MDCK cysts. However, to date, it is not known whether the formation of the renal vesicle is initiated by a single cell or by multiple cells. We do not know either whether this might be coupled to cell division, as it is the case in MDCK cystogenesis.

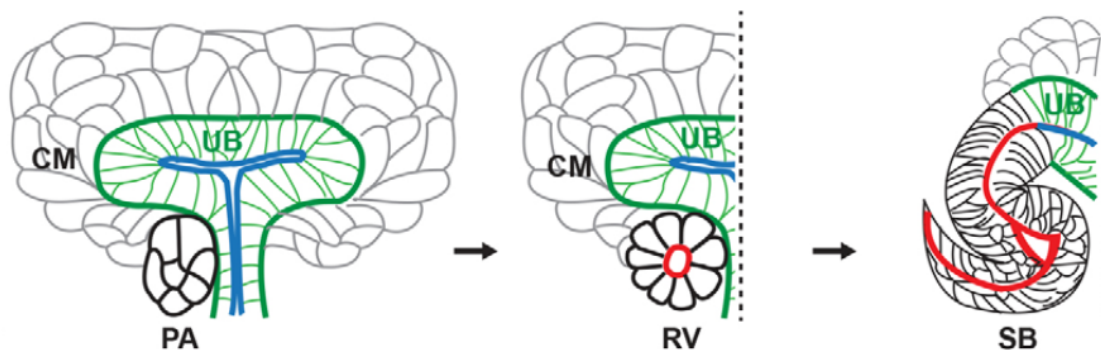


Figure 9: Lumen formation in the developing nephron.

This scheme illustrates the lumen formation of the developing nephron. The condensed mesenchyme (CM) forms the pre-tubular aggregate (PA) through compaction. The pre-tubular aggregate develops further to a polarized sphere that is called the renal vesicle (RV). The renal vesicle elongates and forms the S-shaped body (SB), which forms a continuous lumen with the ureteric bud (UB). Renal vesicle (black); apical membrane of the renal vesicle (red), ureteric bud (green); ureteric bud lumen (blue). From reference: ⁵¹

1.1.5 MDCK cells as a model for epithelial lumen formation

1.1.5.1 *Polarity in MDCK cells cultures in 2D or 3D*

MDCK cells are canine kidney tubule cells that are widely used as a model for epithelial polarity establishment and polarized membrane trafficking. When cultured on permeable filter supports, MDCK cells form a polarized monolayer with clearly segregates apical and basolateral plasma membrane domains. Already in 1976 Misfeldt et al demonstrated that MDCK monolayers formed functional epithelial tissues with physiological transport and permeability characteristics⁶¹. The epithelial morphology was described as asymmetrical with apical microvilli and occluding junctions in between the cells. Following studies described the segregation of certain membrane proteins to the apical or basolateral domain, such as the basolateral NaK-ATPase^{62,63} and the apical localized aminopeptidase⁶³ as well as the segregation of phospholipids⁶⁴. Bacallao et al further described an asymmetric organization of cell organelles in filter-grown MDCK monolayers⁶⁵. The authors describe continuous cellular remodelling, such as apical movement of the Golgi apparatus, the centrioles and tight junctions as well as apico-basal orientation of the microtubule network upon junction formation. These observations lead furthermore to the hypothesis that the microtubular arrangement in polarized epithelial cells as well as the apical localized Trans Golgi Network could promote polarized trafficking of apical proteins towards the apical plasma membrane⁶⁵.

Polarized MDCK 2-dimensional (2D) monolayers are widely used as a model to study epithelial cell -polarization, polarized membrane trafficking as well viral and pathogen infections. However, in comparison to in vivo epithelial tissues, 2D MDCK monolayers have acknowledgeable limits that can be only overcome using 3-dimensional (3D) MDCK cyst cultures.

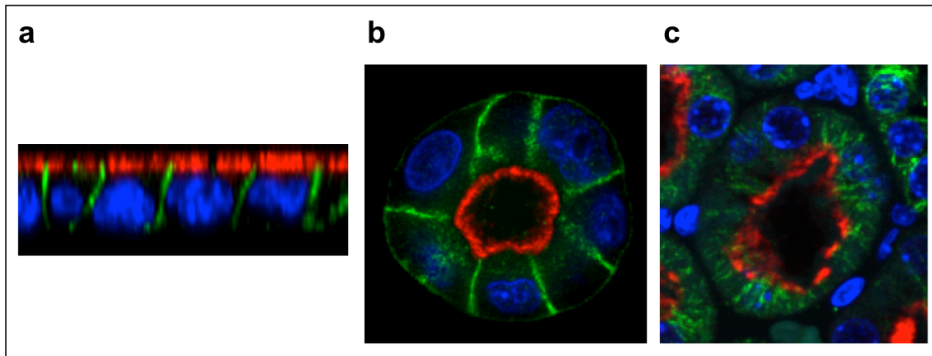


Figure 10: Polarized renal cells *in vitro* and *in vivo*.

These images show polarized renal MDCK cells in 2D (a) and 3D (b) *in vitro* and murine proximal tubular cells *in vivo*.

- (a) Polarized epithelial monolayer: MDCK cells grown for 7 days on a transwell filter. PODXL (red); β -catenin (green); DAPI (blue)
- (b) Polarized epithelial cyst: MDCK cells grown for 48 in Matrigel. PODXL (red); β -catenin (green); DAPI (blue)
- (c) Polarized proximal tubules: paraffin embedded mouse kidney section, showing a proximal tubule. The apical membrane is marked by the Megalin receptor (red), the cell volume is marked by β -tubulin (green) and the nuclei were stained with DAPI (blue).

When cultured in an extracellular matrix environment (Matrigel or collagen type I), MDCK cells establish an apical membrane and a lumen *de novo*. First, a single, unpolarized cell divides and establishes an apical membrane in between the two daughter cells, which will expand to form an open lumen. Subsequent cell divisions will occur perpendicular towards the apico-basal axis to establish a multi-cellular monolayered cyst with an open lumen.

These 3D MDCK cysts resemble *in vivo* epithelial tissues in many aspects. They represent a useful tool to study epithelial polarity establishment, cell-ECM interactions, epithelial to mesenchymal transition and tubulogenesis, which cannot be realized in 2D MDCK monolayers. Furthermore, it has been shown that MDCK cells cultured in an extracellular matrix such as Matrigel display different gene expression patterns than MDCK cells grown in 2D monolayers⁶⁶. Interestingly, genes that are upregulated in 3D versus 2D cultures are often found to be downregulated in glandular cancers⁶⁶.

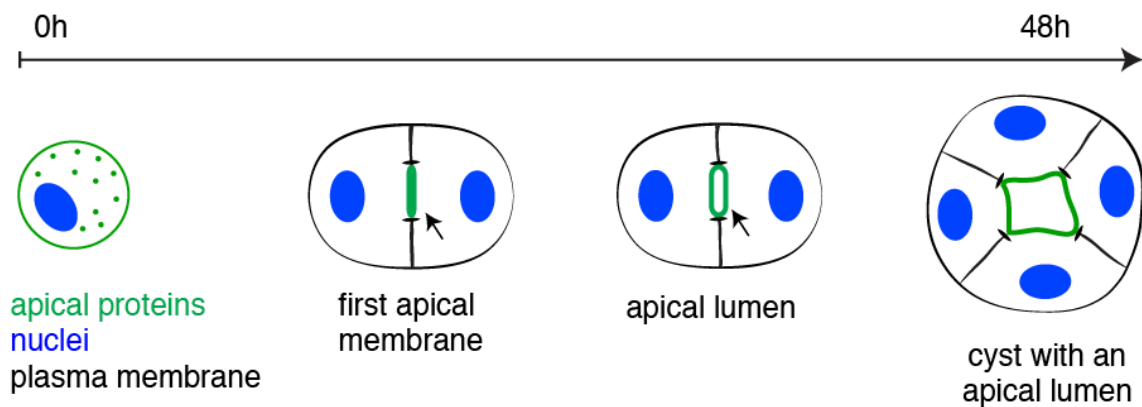


Figure 11: Model of cyst development.

This scheme illustrates the process of MDCK cyst development from a single unpolarized cell to a cyst with an open apical lumen.

1.1.5.2 *The role of membrane traffic in MDCK cystogenesis*

One of the first studies on MDCK 3D cystogenesis was performed by the group of James Nelson. They showed that MDCK cells grown in collagen formed cysts with an open apical lumen and a basolateral membrane that faces the extracellular matrix⁶⁷. MDCK cells in suspension, however, secreted and established a basal lamina in the centre of the cyst, while the apical membrane faced the ECM. Furthermore, this study demonstrated that cell-cell contacts between MDCK cells were sufficient to trigger the segregation of an apical and basolateral membrane and the formation of tight junctions. Later studies demonstrated that the establishment of the apical domain is mediated through the phosphatase PTEN that catalyses the conversion of $\text{PtdIns}(3,4,5)\text{P}_3$ to $\text{PtdIns}(4,5)\text{P}_2$ at the future apical membrane²⁴. As discussed previously, Annexin2 binds to $\text{PtdIns}(4,5)\text{P}_2$ and recruits Cdc42 to the future apical membrane, which in turn recruits aPKC to induce the formation of an apical membrane. Cdc42 has furthermore been shown to be crucial for the correct spindle orientation during cystogenesis.

Indeed, depletion of Cdc42 leads to a multiple lumen phenotype, as expected for defective spindle orientation (discussed in detail on page 127-130)⁶⁸.

Of note, the apical recruitment of Cdc42 and other cytosolic apical determinants such as aPKC was shown to be at least partially dependent on polarized membrane traffic^{69,70}. The recruitment of transmembrane proteins to the apical membrane in MDCK cysts relies, as expected, as well on directed membrane traffic. Ferrari et al demonstrated for the first time the stepwise formation of an apical membrane starting from the 2-cell aggregate to the formation of a pre-apical patch (PAP) at the contacting surface through insertion of Podocalyxin-positive vesicles from apical recycling endosomes (Figure 12). This is followed by maturation of the PAP through the formation of tight junctions and the enrichment of water and ion channels to expand the lumen⁷¹.

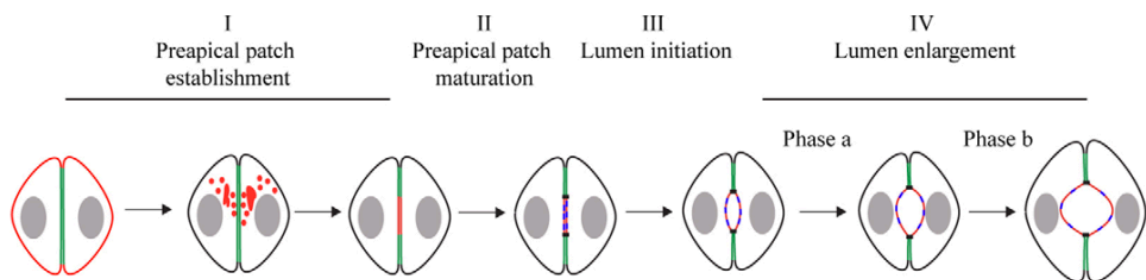


Figure 12: Lumen formation in MDCK cysts.

This scheme illustrates how MDCK cells (2-cell aggregate) establish a preapical patch through fusion of vesicles containing apical proteins at the cell-cell contact (I). The maturation of the preapical patch is characterized by insertion of water and ion channels into the preapical membrane (II) which allows lumen initiation (III) followed by lumen enlargement (IV). E-cadherin (green); PODXL (red; water and ion channels (blue). From reference: ⁷¹

A detailed description of the underlying mechanisms of apical membrane formation during MDCK cystogenesis was then provided by Bryant et al. in 2010⁷². Bryant and colleagues described how apical proteins undergo transcytosis from the ECM-facing membrane towards the future apical membrane to promote lumen formation. Apical proteins, including PODXL, are initially localized at the outer ECM-facing membrane of a so-called early aggregate (a 2-cell cyst), before internalization into Rab11-positive endosomes onto which Rab8 is recruited. Initially, PODXL is stabilized at the outer

membrane through RhoA/ROCKI-dependent phosphorylation of Ezrin (a binding partner of PODXL and NHERF1)⁷³. Integrins on the ECM facing membrane activate FAK-mediated phosphorylation of the RhoA GAP p190A and thereby inactivation of RhoA and its kinase ROCKI. The inactivation of RhoA/ROCKI causes a decrease of Ezrin phosphorylation, leading to destabilization of the PODXL/NHERF1/Ezrin complex. Complete destabilization of the complex and thus endocytosis of PODXL is achieved through PKC β II-mediated phosphorylation of PODXL and NHERF1. Complete destabilization of the complex and thus endocytosis of PODXL is achieved through PKC β II-mediated phosphorylation of PODXL and NHERF1.

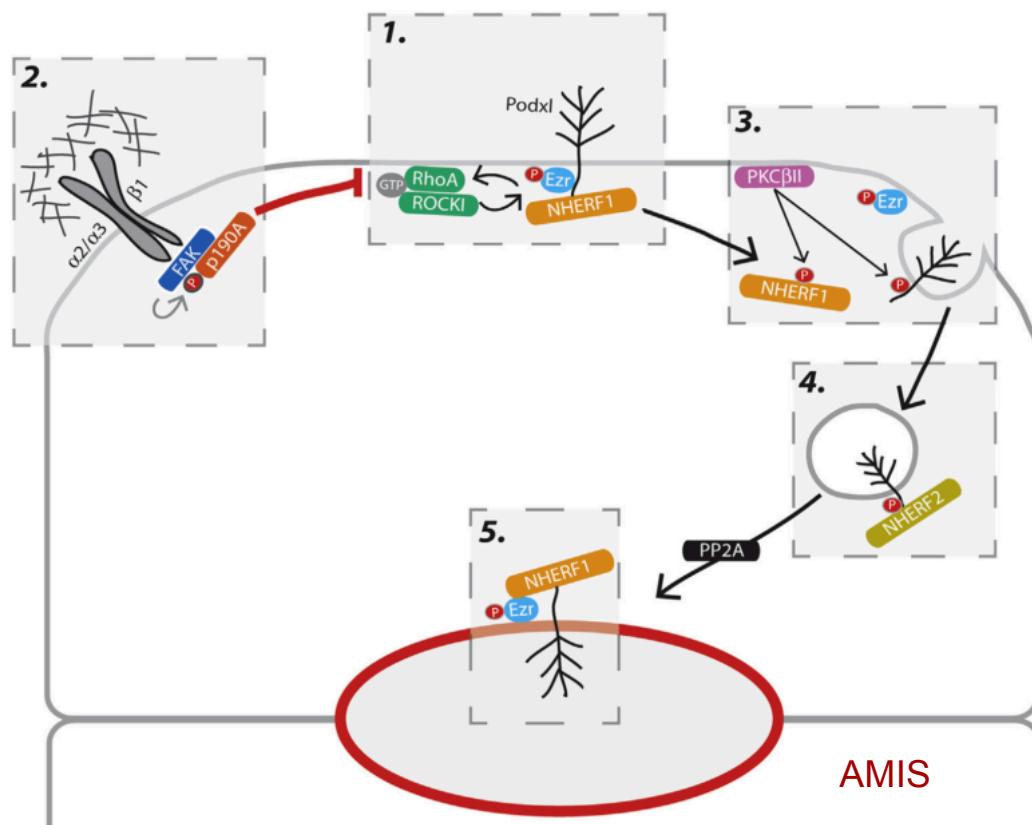


Figure 13: Model of PODXL transcytosis in early MDCK cysts.

This scheme illustrates the molecular cue of PODXL transcytosis during polarity establishment in early MDCK cysts.

1. PODXL is stabilized at the outer membrane through RhoA/ROCKI-dependent phosphorylation of Ezrin.
2. The PODXL/Ezrin/NHERF1 complex is destabilized through integrin mediated RhoA inactivation.
3. PKC β II-mediated phosphorylation of PODXL and NHERF1 induces PODXL endocytosis.
4. PODXL, in association with NHERF2, transcytoses to the AMIS.
5. PODXL exocytosis at the AMIS and re-formation of the PODXL/Ezrin/NHERF1 complex via PP2A. From reference: ⁷³

These PODXL positive vesicles are then trafficked towards the cell-cell contacts through association of Cdc42 and its GEF Tuba⁷². The apical vesicles are tethered through the exocyst, which in cooperation with aPKC and Par3 induces the formation of the Apical Membrane Initiation Site (AMIS). After fusion of the Rab8/Rab11/PODXL-positive vesicles to the AMIS, PODXL re-associates with NHERF and Ezrin after dephosphorylation through PP2A and give rise to the Pre-apical patch. The Pre-apical patch will then expand to an open lumen through pumps and channels. Here, PODXL was described as the earliest apical marker that could be detected at the AMIS.

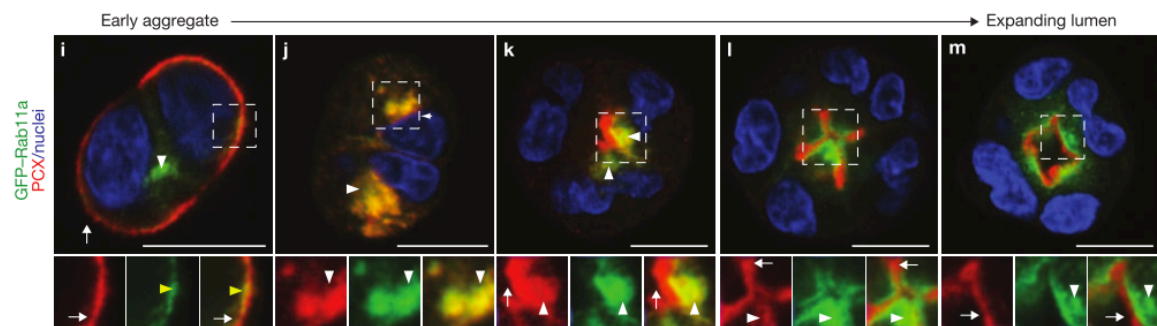


Figure 14: Localization of PODXL and Rab11 during cyst development.

In the early aggregate PODXL is localized at the ECM-facing membrane (i). Then PODXL is internalized into Rab11-positive recycling endosomes at the 2-cell stage (j). Following exocytosis of PODXL at the apical membrane (k), PODXL no longer co-localizes with (l,m), which is now localized subapical. From reference: ⁷².

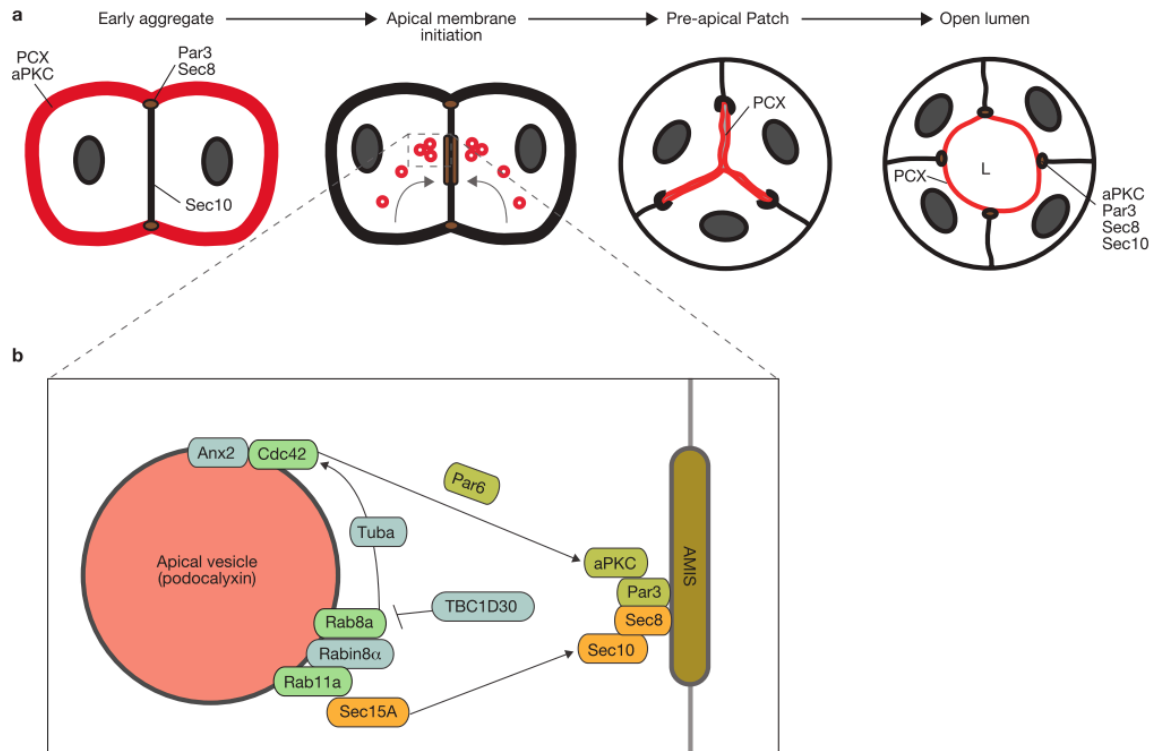


Figure 15: Stages of MDCK cyst development.

- (a) Localization of PODXL (red) in different stages of MDCK cyst development from an early aggregate to a multicellular cyst with an open apical lumen.
- (b) Illustration of proteins localized at the AMIS and on PODXL-positive vesicles. Par3, aPKC, Sec8 and Sec10 are the earliest proteins detected at the AMIS and assist in the recruitment of PODXL-positive vesicle. From reference: ⁷²

Furthermore, it was shown that Rab27A associates with PODXL vesicles prior to fusion at the apical membrane in 2D and 3D MDCK cultures^{66,74}. These Rab27A-positive vesicles are targeted to the apical membrane through Slp2-a and Slp4-a in cooperation with Rab27A, Rab3 and Stx3⁶⁶. Slp2-a targets Rab27A/PODXL vesicles to the apical membrane through binding to $\text{PtdIns}(4,5)\text{P}_2$, which is enriched at the apical membrane. Simultaneously, Slp4-a, which is bound to Rab3 and Rab27A on the vesicle, associates with membrane-bound Stx3 and thus tethers the vesicle to the apical membrane prior to fusion. Indeed, depletion of Stx3 or Slp4-a leads to an accumulation of PODXL vesicles due to impaired fusion. In contrast, Slp2-a depletion delays and mislocalizes the fusion of PODXL vesicles, thus showing a role for Slp2-a in apical targeting to $\text{PtdIns}(4,5)\text{P}_2$ enriched membranes⁶⁶.

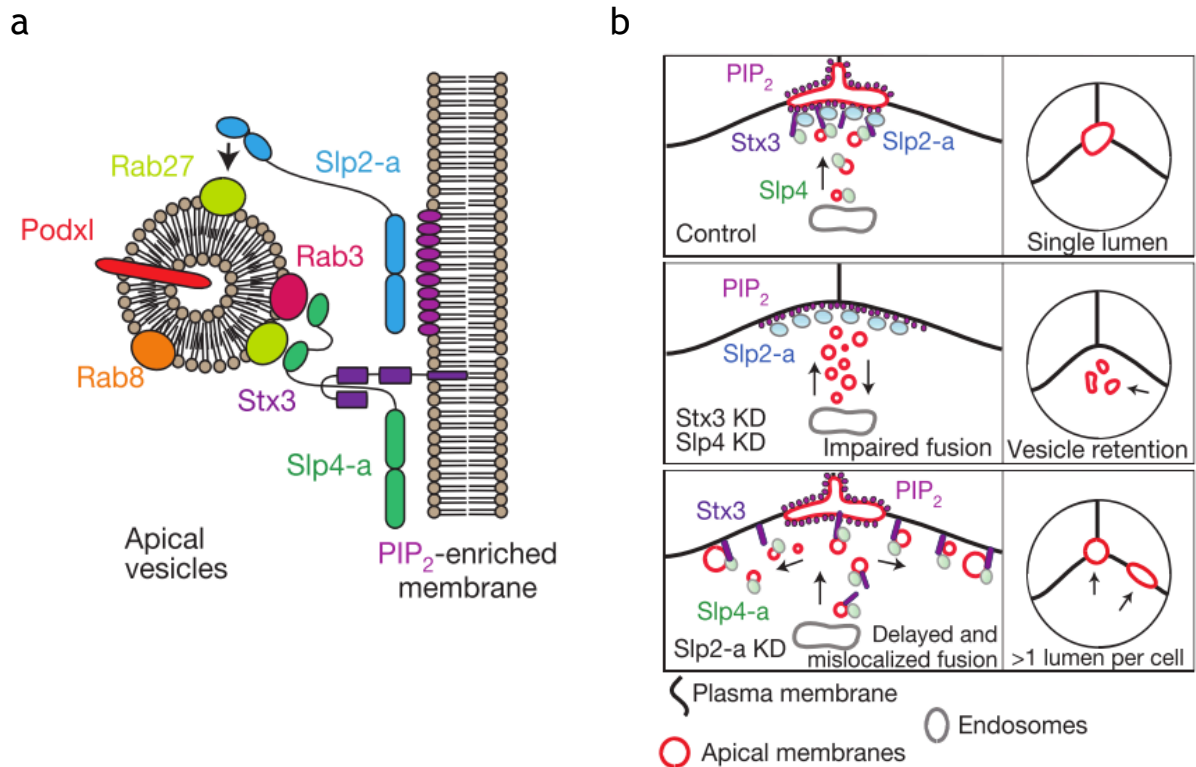


Figure 16: Fusion of PODXL-positive vesicles at the apical membrane.

(a) Slp2-a targets Rab27-positive vesicles to the PtdIns(4,5)P₂ enriched membrane. Tethering of the vesicle occurs via binding of Slp4-a to Stx3, Rab27 and Rab3.

(b) Depletion of Stx3 or Slp4-a impairs the tethering and fusion of Rab27-positive vesicle to the PtdIns(4,5)P₂ enriched future apical membrane. As a result these vesicles accumulate underneath the plasma membrane. Depletion of Slp2-a impairs the correct targeting of Rab27-positive vesicles and leads thus to mislocalized fusion. This results in the establishment of multiple lumen. From reference:⁶⁶

1.1.5.3 The role of the extracellular environment

The composition and stiffness of the extracellular matrix, as well as the cell confinement, play important roles in the establishment of epithelial polarity in MDCK cysts as well as *in vivo*⁷⁵. Loss-of function phenotypes of single ECM components in different *in vivo* models such as *M. musculus*, *D. rerio*, *X. laevis*, *G. galus* and *C. elegans* demonstrate prenatal or post-natal death for many of the tested components⁷⁵.

Furthermore ECM stiffness and composition is associated with tissue invasion and proliferation in epithelial cancers, and impaired lumen formation in 3D cell cultures⁷⁶⁻⁷⁸. Interestingly, high cell confinement combined with a stiff laminin matrix leads to junctional stability, aPKC activation at the cell contacts and polarized centrosome positioning and therefore correct lumen formation⁷⁹. This demonstrates that other parameters, such as cell confinement and ECM composition, can compensate for high ECM stiffness. Furthermore, the matrix stiffness is constantly regulated by the cell's secreted matrix metalloproteinases and lysyl oxidases that induce laminin proteolysis and collagen crosslinking⁷⁶. Dysregulation of ECM modifications was found in different types of carcinomas and cancer cell invasion, thus cancer cells can modulate the ECM to promote their own invasion^{76,80}. Moreover, it was shown in vitro in MCF-10 mammary acini that cancer derived mammary acini fail to assemble laminin and collagen type IV⁸¹. Interestingly, the assembly of laminin and collagen was shown to depend on a rotational movement of the acini within the matrix. MCF-10 mammary acini rotate 360° every 4 hours during cyst development to assemble secreted laminin and collagen type IV, whereas cancer derived acini do not exhibit this rotational movement.

Importantly, the composition of the ECM can also influence the apico-basal polarity axis through integrin signalling, which will be discussed in detail in the next chapter.

1.1.5.4 Inversion of apico-basal polarity and other abnormal phenotypes in cysts

Different cyst phenotypes

MDCK cells cultured in Matrigel give rise to cysts with a single open lumen. However, disruption of certain genes or manipulation of the extracellular environment results in a variety of cyst phenotypes such as multiple lumen, no lumen, filled lumen, cytoplasmic vesicles/vacuoles, expansion of the apical domain, luminal apoptosis inverted cysts and small cysts. Analysis, quantification and distinction between these

phenotypes rely on specific markers of the apical and basolateral domain as well as the tight- and adhesion junctions. As shown in Figure 17, different cysts phenotypes are categorized using PODXL as apical marker and β -catenin as basolateral marker.

In this chapter I will briefly introduce the most common cyst phenotypes and then focus on the rarely observed inverted cyst phenotype.

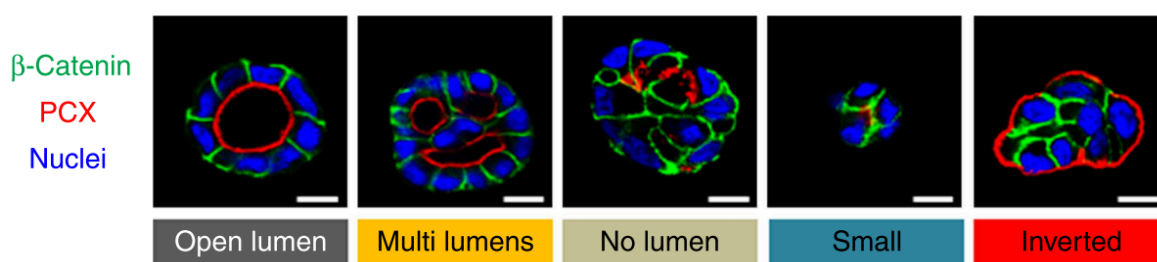


Figure 17: Overview of MDCK cyst phenotypes.

Representative images of various MDCK cyst phenotypes after 72h culture in Matrigel. The abnormal phenotypes were obtained by addition of different p110 inhibitors, giving rise to a variety of phenotypes. Cysts were stained with PODXL (red), β -catenin (green), DAPI (blue). From reference: ⁸²

The multiple lumen phenotype

One of the most frequently observed phenotypes is probably the multiple lumen phenotype, which will be discussed in detail on page 127-131. Disruption of genes that are involved in spindle orientation (eg. $Cdc42^{68,83,84}$, $aPKC^{85}$, $Par6^{85}$, $Par3^{86}$, LGN^{87}) often give rise to multi-luminal cysts. The axis of cell division and the localization of the cleavage furrow determine the site for apical vesicle fusion and lumen formation^{88,89}. In normal conditions, cells divide tangentially towards the lumen. In contrast, spindle orientation defects can lead to perpendicular cell divisions and thus formation of a second lumen between the two daughter cells. The disruption of tight junctions can also result in multiple lumen, as it was shown for $Par3^{86}$, $Pals1^{90}$, $PatJ^{91}$. The multiple lumen

phenotype has been associated with several cancers, such as non-invasive breast carcinomas and non-invasive ductal carcinomas, that are characterized by the presence of multiple lumen *in vivo*⁵⁰.

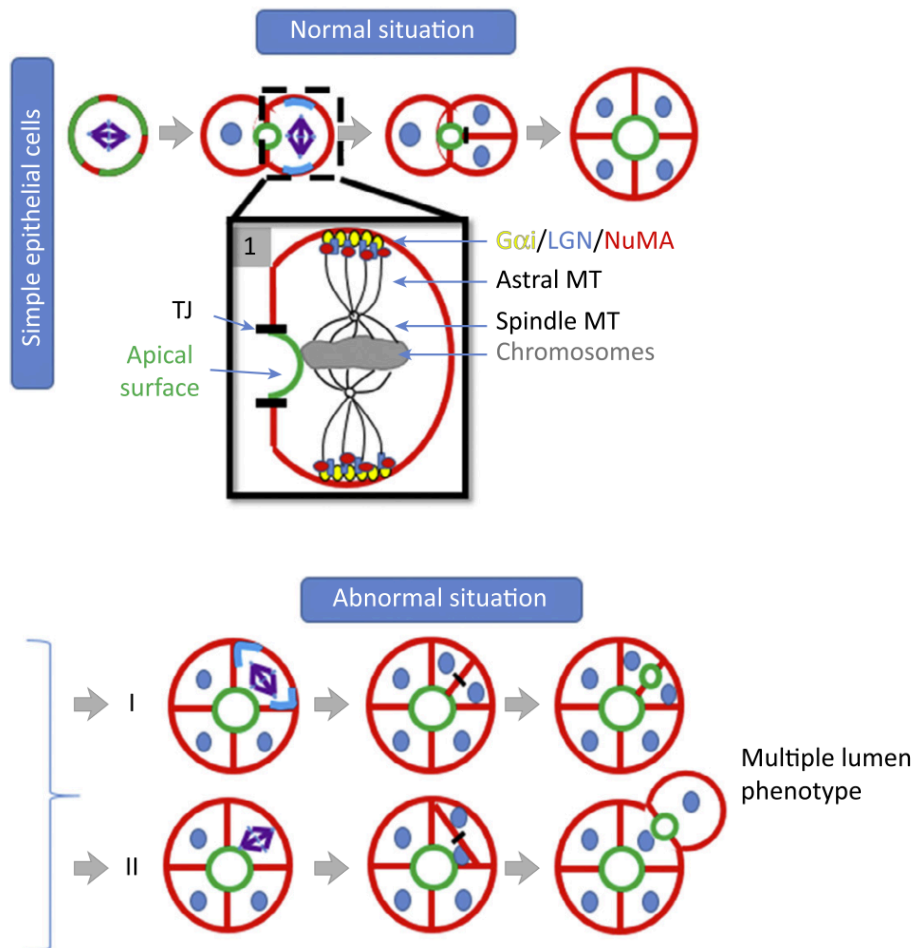


Figure 18: Spindle orientation in MDCK cysts.

In normal conditions, MDCK cells orientate their mitotic spindle perpendicular to the apico-basal axis, leading to symmetric cell division. Both daughter cells form an apical membrane at the central lumen. The midbody is closely localized to the apical lumen. In abnormal conditions however, perturbation of either the midbody localization (I) or the spindle positioning (II) can lead to the formation of an additional lumen. From reference: ⁹²

No lumen phenotypes: Filled lumen and apical vesicle accumulation

Transformation of MDCK cells with the Maloney sarcoma virus induces EMT and filling of the cyst lumen, a hallmark for most epithelial glandular cancers⁹³. The same phenotype was also observed upon over-activation of the well-known oncogene Ras⁹⁴. Another frequently observed cyst phenotype is the accumulation of internal vesicles that contain apical cargo proteins. This phenotype often entirely disrupts apico-basal polarity or leads to multiple small lumens. Depletion of genes involved in apical targeting/tethering such as Rab3⁶⁶, Rab8⁷², Rab11⁷², Rab27^{66,66}, Slp3⁶⁶, Slp4⁶⁶, Syntaxin3⁶⁶ and exocyst components^{66,72}, result in these defects.

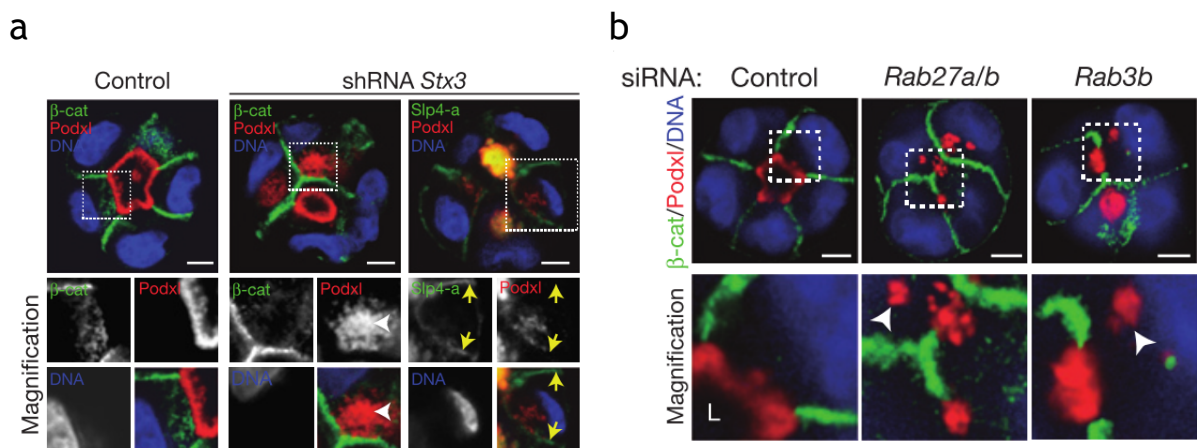


Figure 19: Apical vesicle accumulation in MDCK cysts after specific protein depletion.

- Localization of GFP-Slp4-a and PODXL in MDCK cysts depleted for Stx3. PODXL-positive vesicles accumulate in close proximity to the plasma membrane (also GFP-Slp4-a-positive). Additionally a pool of GFP-Slp4-a is mistargeted to the basolateral membrane (yellow arrows).
- Depletion of Rab27a/b or Rab3b leads to accumulation of PODXL-positive vesicles (arrowheads). From reference: ⁶⁶

Inverted cyst phenotype

The inverted cyst phenotype is characterized by the absence of a lumen and the presence of mis-localized apical proteins to the ECM facing membrane. Inversion of apico-basal polarity upon experimental perturbation is a rather rare, but very interesting phenotype, since this phenotype has been observed in different cancers as well as in cases of intestinal disorders such as multiple intestinal atresia (MIA)⁹⁵ and microvillus inclusion disease (MVID)⁹⁶.

Indeed, inversion of apico-basal polarity is characteristic for micropapillary breast carcinomas and micropapillary and is correlated to a high risk of metastasis and poor prognosis⁹⁷⁻¹⁰². Interestingly, polarity inversion has also been observed in micropapillary carcinomas of the intestine, the urether¹⁰³, the thyroid¹⁰⁴ and in colorectal micropapillary carcinomas^{99,105}. It is assumed that inversion of polarity could facilitate the secretion of metalloproteinases responsible for stromal and vascular invasion. Furthermore, polarity inversion could facilitate the detachment of tumour cells from the stroma and thus promote invasion¹⁰⁶. However the molecular mechanisms that causes polarity inversion in micropapillary carcinomas remains elusive.

MIA patients suffer from malformation of the intestine that can prevent the normal transit of the digestion products, which is often caused by mutation in the *TTC7A* gene, which encodes the tetratricopeptide repeat domain 7A⁹⁵. It was shown that patients display impaired apico-basal polarity with loss of the apical pole function. Interestingly, the apical brush boarder protein Villin was weakly detected at the luminal surface, thus indicating first signs of apico-basal polarity inversion. Furthermore intestinal organoids from MIA patients developed a complete apico-basal inversion and lacked an open lumen when cultured in Matrigel. This inverted polarity phenotype could be rescued by pharmacological inhibition of Rho kinase (ROCK) with Y-27632, suggesting that *TTC7A* directly or indirectly inhibits ROCK activity⁹⁵. The role of ROCK in apico-basal polarity will be discussed in detail later in this section.

Recently, also the intestinal disorder MVID has been linked to apico-basal polarity inversion⁹⁶. MVID is characterized by cytoplasmic microvillus inclusions and a loss of

apical microvilli, which is often caused by mutations of *MYO5B* or in some cases mutation of *STX3*^{96,107}. The establishment of apically localized microvilli and depends on functional myosin Vb and its interaction with Rab8 and Rab11¹⁰⁷. Furthermore, apical exocytosis of apical cargos such as GLUT5, CFTR and NHE3 depends on a functional of myosin Vb /Rab8/Rab11-dependent trafficking followed by Slp4-a /Stx3-dependent tethering and fusion at the apical membrane¹⁰⁸. Genome edited Caco-2 cells, carrying a human mutation of *Myo5B* display multiple disorganized lumen when cultured in Matrigel accompanied by loss of apical microvilli¹⁰⁸. However, recently it has been demonstrated that depletion of *Myo5B* in Caco-2 cells leads to an inversion of apico-basal polarity as marked by basolateral mislocalized Par6B, Ezrin and PKC⁹⁶. Importantly, a partial polarity inversion could also be found in some human intestinal samples from MVID patients⁹⁶.

Inversion of apico-basal polarity has also been observed in MDCK 3D cysts cultures. This phenotype was first observed by the group of James Nelson. This lab showed that MDCK cells cultured in suspension without addition of ECM components establish inverted cysts with the apical membrane facing towards the culture medium⁶⁷. Furthermore no real lumen establishes. However, cells secrete laminin, a component of the basal lamina, into the intercellular space. The importance of the extracellular environment was further demonstrated by Ojakian and Schwimmer, who showed that MDCK cysts in suspension could re-orientate their polarity upon addition of an extracellular matrix, such as collagen¹⁰⁹. Indeed, MDCK cells in suspension develop to inverted cysts, where the apical membrane faces the medium. Replacement of the culture medium with collagen I induces a reversion of apico-basal polarity, and microvilli can be observed in the centre of the cysts within 6 hours.

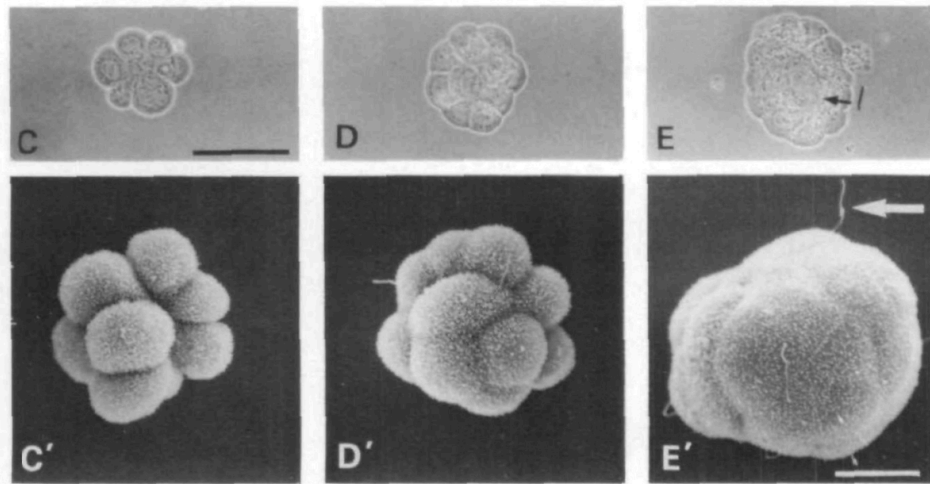


Figure 20: MDCK cells grown in suspension.

Phase-contrast images (C-E) and scanning electron microscopy (C'-E') of MDCK cells grown in suspension for 24h (C, C'), 2-3 days (D, D') and 4-5 days (E, E'). From reference: ⁶⁷

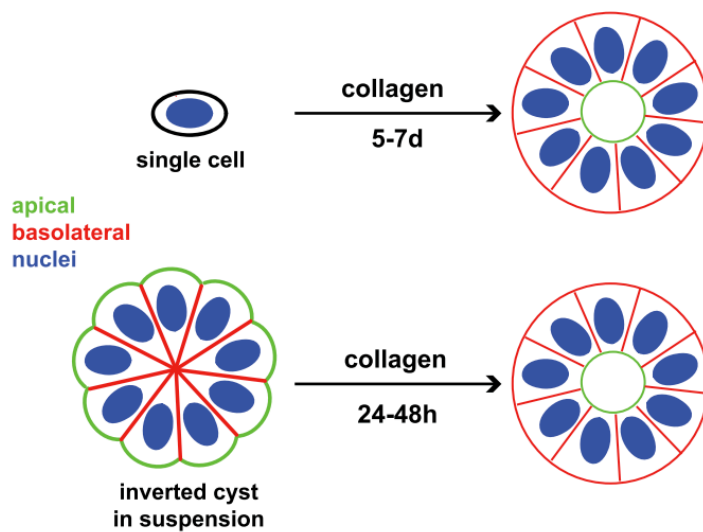


Figure 23: Re-orientation of apico-basal polarity.

MDCK cells cultured in either collagen to establish a cyst with an apical lumen or cultured in suspension to establish an inverted cyst without a lumen. The inversion of apico-basal polarity can be re-orientated by addition of collagen for 24-48h. From reference: ¹⁵

The interaction between the cell and the extracellular matrix is mediated through integrins and focal adhesions complexes. Integrins are non-covalently bound heterodimers consisting of an α - and a β -subunit. The composition of the α - and β -subunit determines the ligand specificity. For example $\alpha2\beta1$ binds primarily to collagen type I that is often used as ECM for MDCK 3D cysts cultures. The heterodimers $\alpha3\beta1$, $\alpha6\beta1$ and $\alpha7\beta1$ bind preferentially to laminin, the major component of Matrigel and only $\alpha1\beta1$ can bind to collagen I and laminin^{110,111}.

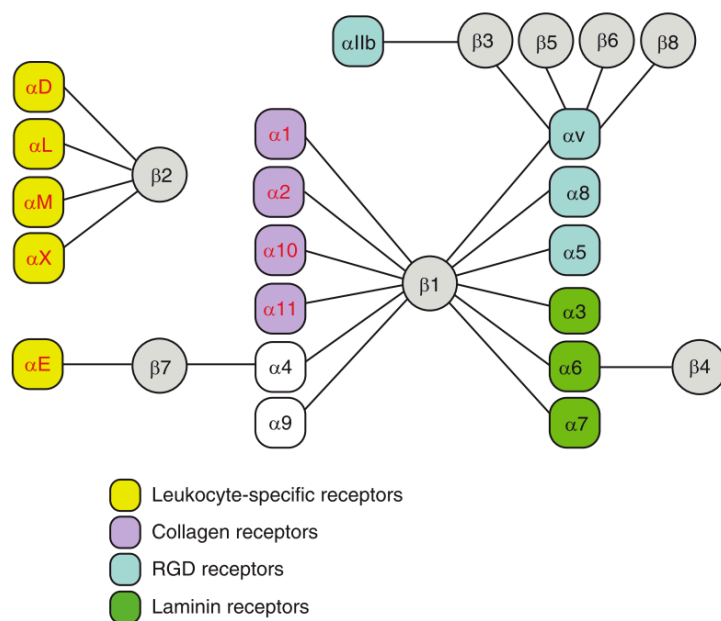


Figure 22: Classification of integrin heterodimers.

This scheme illustrates the ligand specificity of the different integrin heterodimers. From reference: ¹¹¹

In MDCK cysts $\beta1$ -integrins are localized exclusively to the basolateral membrane¹⁰⁹. Interestingly, blocking of $\beta1$ -integrin function using monoclonal blocking antibodies, inhibits re-orientation of apico-basal polarity upon collagen addition. This indicates that $\beta1$ -integrin is indeed the major integrin in MDCK cysts, required to sense and to interact with the extracellular environment.

Interestingly, a recent study showed that $\beta 1$ -integrin blockage or depletion of $\beta 1$ -integrin in MDCK cysts cultured in Matrigel (instead of collagen I) did not induce inversion of apico-basal polarity, but instead a front-rear polarity phenotype⁷³. This front-rear polarity is characterized by an inversion of apico-basal polarity of a few cells within the cyst, whereas the other cells exhibit normal polarity orientation, thus leading to a front-rear polarity of the entire cyst. Importantly, the leading cells with inverted polarity do not show an EMT-like behaviour: they do not migrate out of the cysts and they do not form tubular structures or thin protrusions as observed upon HGF induced tubulogenesis.

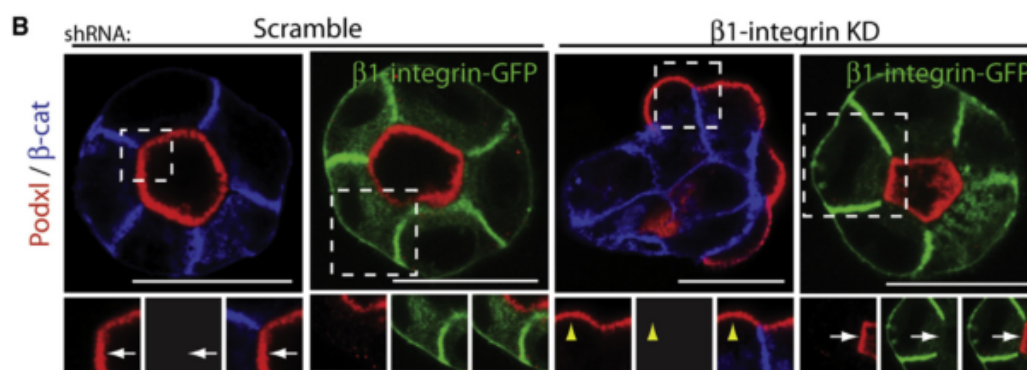


Figure 24: Depletion of $\beta 1$ -integrin leads to a front-rear polarity.

Parental or $\beta 1$ -integrin-GFP expressing MDCK cells were transfected with control shRNA or $\beta 1$ -integrin shRNA and cultured in Matrigel for 48h. Cysts were stained for PODXL (red) and β -catenin (blue). Cysts depleted of $\beta 1$ -integrin show a front-rear polarity phenotype. From reference:⁷³

The same front-rear phenotype was observed upon inhibition of PKC using either the PKC inhibitor GÖ-6976, depletion of PKC β or depletion of the focal adhesion kinase (FAK). These results describe a pathway where $\beta 1$ -integrin signalling through FAK and p190RhoGAP inhibits RhoA/ROCK activation and Ezrin phosphorylation at the ECM facing

membrane to destabilize the PODXL/NHERF1/Ezrin complex. PKC β II assists to the destabilization by phosphorylation of PODXL and NHERF1 and thus enables PODXL internalization and transcytosis towards the AMIS as described earlier on. Interestingly, cysts that exhibit the described front-rear polarity also show impaired rotational movement as observed in long-term time-lapse microscopy.

The front-rear polarity phenotype was described by the authors as a partial rescue of the inverted polarity phenotype due to the presence of other ECM components such as laminin, compared to pure collagen I. Previously, it was shown in pure collagen I-cultured MDCK cysts that β 1-integrin activates Rac1, which inhibits Rho-mediated ROCK1 activation¹¹². Consequently, expression of a constitutive active mutant of the Rac1 effector Pak1 induced polarity inversion, as observed upon β 1-integrin blockage. Interestingly, Pak1-mediated polarity inversion could be rescued by addition of exogenous laminin or Matrigel (contains laminin) into the collagen I matrix¹¹².

These results seem to be surprising, but could be simply explained by the presence of other integrin heterodimers that can bind to laminin. Indeed, blocking of β 1-integrins inhibits the binding to collagen receptors, but does not completely inhibit the binding to laminin since the heterodimer α 6 β 4-integrin would still be able to interact with laminin. α 6 β 4-integrin is indeed expressed in MDCK cells, however from previous studies it is not entirely clear whether α 6 β 4-integrin is required for laminin binding and could therefore compensate for the loss of β 1-integrins in the presence of laminin¹¹³.

Additionally, it has been shown that MDCK cells express another laminin receptor which is the heterodimeric glycoprotein Dystroglycan⁸². Dystroglycan is a high-affinity laminin receptor that consists of a β -subunit and a non-covalently bound α -subunit¹¹⁴. Moreover, depletion of Dystroglycan in MDCK cells induces complete inversion of apico-basal polarity in MDCK Matrigel cultures, thus indicating that Dystroglycan acts as a potent laminin receptor in MDCK cysts⁸².

Taken together, the presence of either Dystroglycan or α 6 β 4-integrin could potentially explain why exogenous laminin can rescue Pak1-mediated polarity inversion and why β 1-integrin blockage or depletion in Matrigel cultured MDCK cysts induces only a partial

polarity inversion. Moreover, these above mentioned studies demonstrate that the choice of the extracellular matrix in 3D cell cultures can have important impact on the obtained results.

The role of Rac1 in cystogenesis for example, was mainly studied in collagen I-based 3D cell cultures. It was demonstrated that Rac1 activation plays an important role in β 1-integrin mediated collagen/laminin signalling and polarity orientation in MDCK cysts and collagen overlay cultures¹¹⁵. Collagen I binding to β 1-integrin leads to Rac1 activation, which is required for the assembly of secreted laminin and thereby correct polarity orientation¹¹⁵. Moreover, blocking of β 1-integrin leads to RhoA activation, which by itself causes an inversion of apico-basal polarity¹¹⁶. In turn, inhibition of RhoA, ROCK I or myosin II restores normal polarity orientation after blockage of β 1-integrin or expression of DA Rac1¹¹⁶. Interestingly, it was furthermore shown that Arf6 activation is required for Rac1 activation, inducing laminin assembly and a positive feedback loop for Rac1 activation¹¹⁷. Depletion of Arf6 induces polarity inversion in collagen cultured or Matrigel cultured MDCK cysts due to Rac1 inactivation and impaired laminin assembly. However, the same study demonstrates that the inversion of polarity induced by Arf6 depletion can be rescued by ROCK inhibition in collagen cultures, but not in Matrigel cultures. Furthermore the sole presence of excess laminin in the Matrigel did not induce a partial rescue of polarity inversion induced by Arf6 depletion as reported for polarity inversion induced by blocking of β 1-integrin^{73,117}.

These results open the possibility that β 1-integrin-mediated Rac1 activation and Arf6-mediated Rac1 activation might function in two distinct pathways to orient apico-basal polarity.

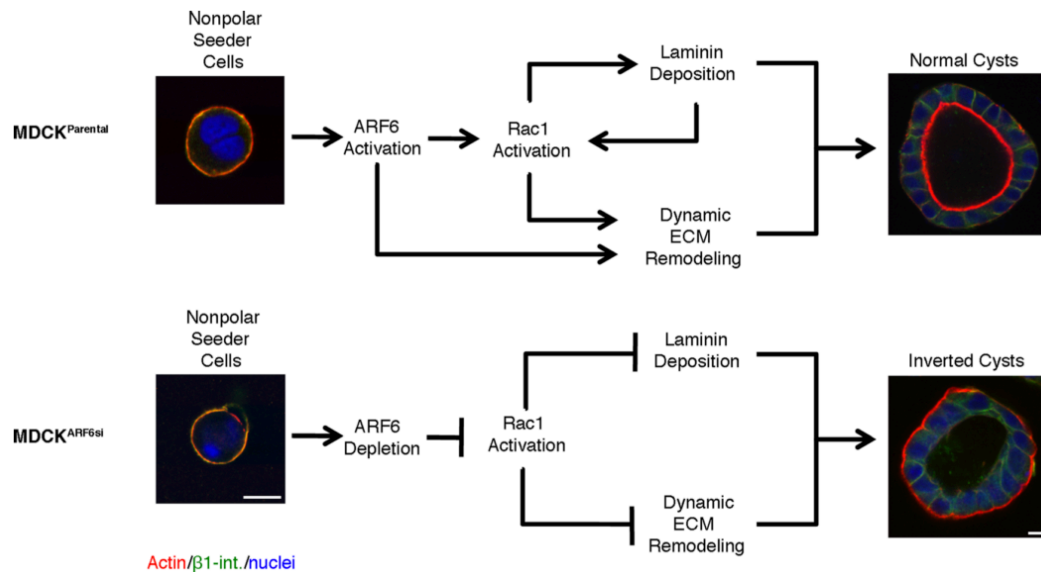


Figure 25: Model for Arf6-mediated activation of Rac1 and basement membrane remodelling.

This scheme illustrates how Arf6 activation in MDCK cysts activates Rac1, which positively regulates laminin deposition. Upon Arf6 depletion, Rac1 is not activated, leading to impaired laminin deposition and polarity inversion. From reference: ¹¹⁷

Rac1 activation was also shown to activate the PI3-kinase/protein kinase B pathway in collagen embedded MDCK cysts to correctly orientate apico-basal polarity¹⁵.

Of note, investigation of the role of PI3 kinase isoforms in 3D Matrigel cultures demonstrated that inhibition of the p110delta isoform induced complete apico-basal polarity inversion, which was not partially rescued through the laminin contained in the Matrigel as previously shown for Arf6-mediated polarity inversion^{82,117}. Depletion or inactivation of p110delta affected laminin and type IV collagen assembly around the cyst and decreased the expression of integrins. Furthermore p110delta expression is positively regulated by extracellular matrix components such as collagen type IV, Fibronectin, poly-D-lysine and laminin, indicating that PI3 kinase p110delta acts upstream of the β 1-integrin-laminin-Rac1 pathway⁸².

Referring to the possibility of having distinct Rac1 pathways that could be activated either by β 1-integrin or by Arf6, it is of interest that Arf6 activation has been recently linked to PI3K activity¹¹⁸. PI3K-mediated generation of PtdIns(3,4,5) P_3 recruits the Arf6 GEF ARNO (also known as CYTH2) to the plasma membrane, leading to Arf6 activation and thereby also Rac1 activation in COS-7 cells¹¹⁸.

Thus, inversion of epithelial apico-basal polarity seems to arise from distinct pathways, which are not inclusively coupled to ECM-induced signalling. However, ECM-independent polarity inversion has been reported in only two instances of Arf6 depletion and PI3K inactivation. Whether these two pathways could be indeed linked remains to be investigated.

1.1.5.5 *The role of cytokinesis in polarity establishment*

Cell division and epithelial cell polarity are two interdependent processes in multicellular organisms that must be well coordinated¹¹⁹⁻¹²¹. In an epithelial monolayer, the functional diffusion barrier of adherence and tight junctions must be maintained at all-time even when cells undergo morphological changes as during cell division. It has been suggested that epithelial cells maintain their apico-basal polarity as well their junctions during cell division¹²¹. It has been shown that E-cadherin and ZO-1 maintain their localization in dividing MDCK cells grown in a polarized monolayer as well as E-cadherin, Crumbs and Notch in the pupal *Drosophila* epithelium¹²²⁻¹²⁴. However, the localization of apically localized proteins during cell division is debated. In the *Drosophila* ectoderm for example the PAR complex was shown to remain apically, whereas its localization is disrupted during cell division in *Drosophila* ovary follicle cells^{125,126}.

During cytokinesis, which is the final step of cell division that physically separates the two daughter cells, a contractile actomyosin ring forms at the cell equator to drive

ingression of the furrow. Towards the end of cytokinesis, a dense structure called midbody will form at the central part of the intercellular bridge. It has been shown that the midbody could serve as a platform for the recruitment of the abscission machinery¹¹⁹. It was furthermore shown that the position of the midbody determines the site of apical membrane formation¹¹⁹. In the *Drosophila* follicular epithelium for example, ectopic positioning of the midbody initiates an apical domain at this location¹²⁷. The same concept of apical membrane initiation has been also suggested to occur in MDCK cysts. In early MDCK cysts the polarity protein Crumbs3 is trafficked in Rab11-positive recycling endosomes along the bridge microtubules towards the midbody⁸⁸. Here, Crumbs3 assists the recruitment of the Par-aPKC complex to initiate an apical membrane and thus links cytokinesis and midbody positioning to the establishment of apico-basal polarity⁸⁸.

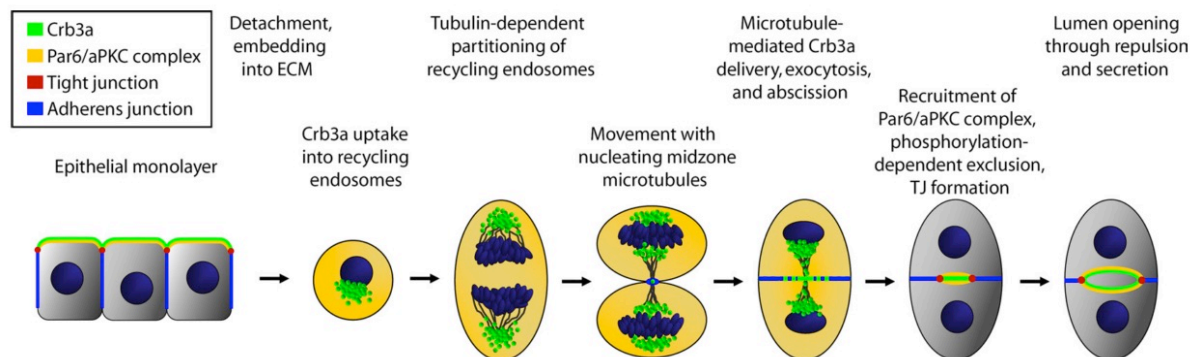


Figure 26: Coupling of MDCK lumen formation with cell division.

This scheme illustrates how a single unpolarized MDCK cell, embedded in Matrigel, divides, polarizes and gives rise to an apical lumen. Crb3a-positive vesicles are localized at the spindle poles before being transported along the bridge microtubules towards the site of cytokinesis, where they are exocytosed. This event marks the initiation of an apical membrane through recruitment of the Par6-aPKC complex, allowing the establishment of an apical membrane along with the establishment of tight junctions. From reference:⁸⁸

It was further shown that the Rab11 effector FIP5 was required to connect the Rab11-positive recycling endosomes to the microtubule motor Kinesin-2^{89,128}. During telophase FIP5 dephosphorylation leads to SNX18-dependent formation of FIP5 endosomes that contain apical cargo such as PODXL and Crumbs3. These endosomes move then with the help of Kinesin-2 along the bridge microtubules to fuse at the cleavage furrow plasma membrane where the apical membrane and later the lumen will be established^{89,128}.

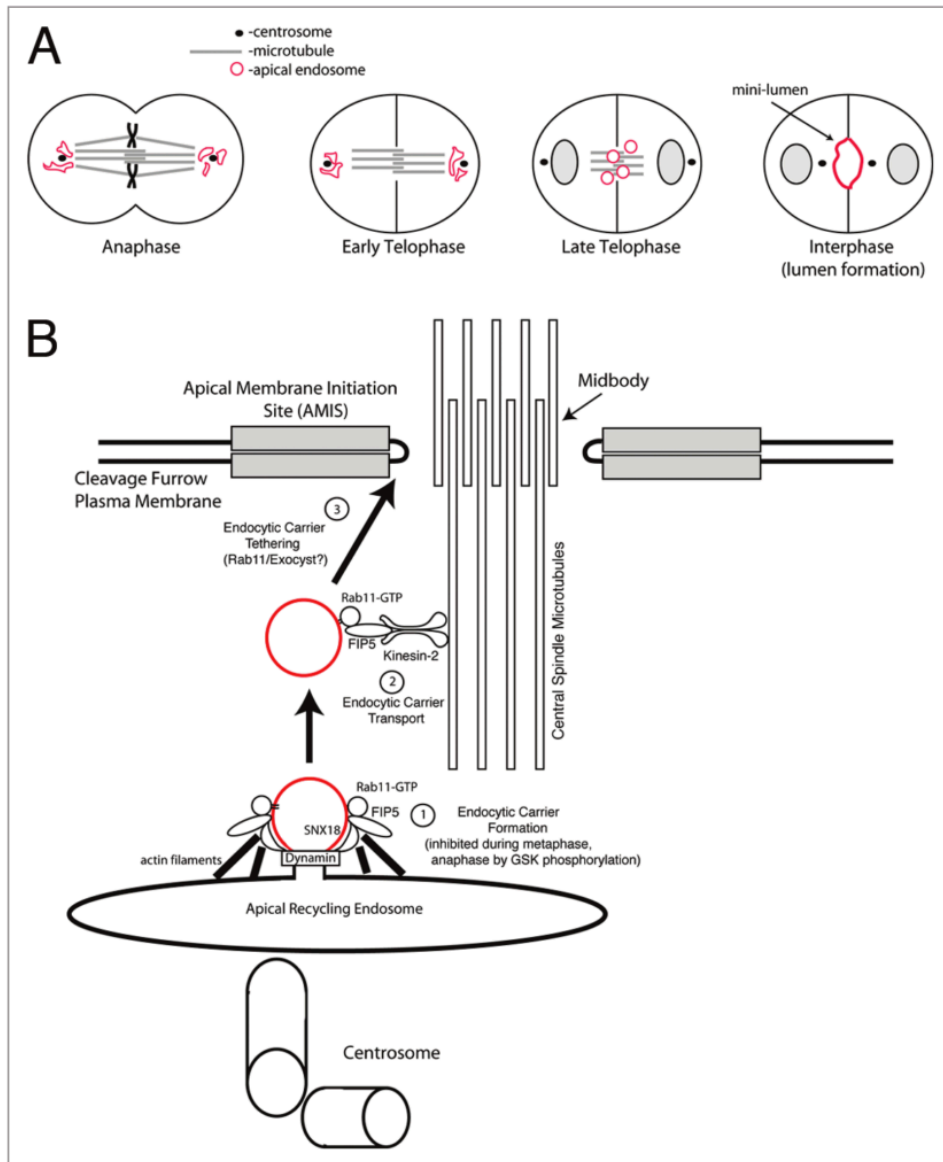


Figure 27: Model for apical lumen initiation.

- (A) This scheme illustrates how apical endosomes are transported along the bridge microtubules during cell division to initiate an apical lumen at the site of cytokinesis.
- (B) Illustration of Kinesin-2/FIP5-mediated trafficking of Rab11/FIP5-positive endosomes during cell division. From reference: ⁸⁹

These studies support the idea that regulators of cytokinetic abscission might be also involved in the establishment of polarity, as it is the case for Rab11. The Rab11 effectors FIP3 and FIP4 have furthermore been shown to interact with Arf6¹²⁹, a protein that is implicated in apico-basal polarity¹³⁰ as well as in cytokinesis^{131,132}. In addition, the regulation of the lipid composition of the plasma membrane seems to show analogies between cytokinesis and polarity¹³³. PTEN and PI3K are major regulators of the Phosphoinositides during polarity establishment and indeed it was shown that they are also required for the formation of the cleavage furrow for cytokinesis^{120,133,134}. Moreover it has been suggested that the $\text{PtdIns}(4,5)\text{P}_2$ enriched membrane of the cleavage furrow could be analogue to the $\text{PtdIns}(4,5)\text{P}_2$ enriched apical membrane in polarized epithelial cells^{120,133}. Nevertheless the exact localization and function of many polarity proteins during cell division needs yet to be determined.

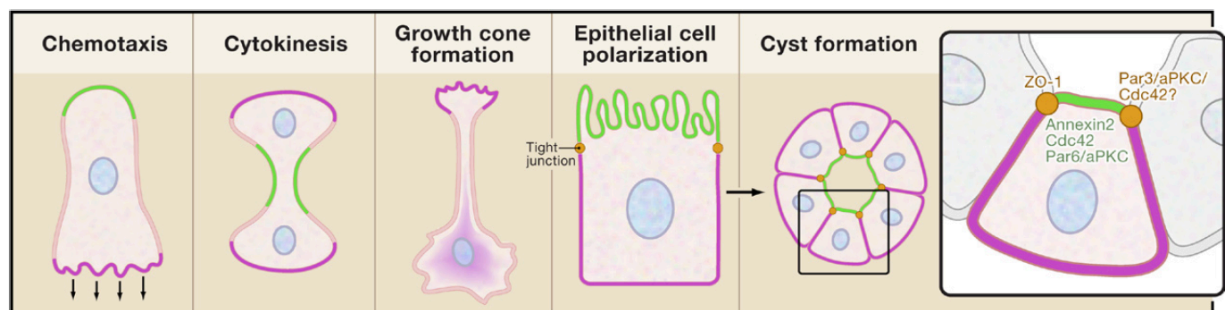


Figure 28: Membrane domains in polarized and dividing cells.

This scheme illustrates the cellular distribution of distinct membrane domains marked by $\text{PtdIns}(3,4,5)\text{P}_3$ (pink) and $\text{PtdIns}(4,5)\text{P}_2$ (green) during chemotaxis, cytokinesis, growth cone formation and epithelial cell polarization. Note that $\text{PtdIns}(4,5)\text{P}_2$ is enriched at the cleavage furrow in dividing cells as well as at the apical domain of polarized epithelial cells. From reference:¹³³

1.2 PODOCALYXIN

1.2.1 Structure

Podocalyxin (PODXL) is also known as podocalyxin-like protein, GP200, PC, PCLP, PCLP-1 or GP135 for the canin PODXL. PODXL belongs to the CD34 family of cell surface transmembrane proteins that comprises CD34, Endoglycan and PODXL. All of these three proteins have an extensively O- and N-glycosylated and sialylated extracellular domain and belong therefore also to the family of the sialomucins^{135,136}. Furthermore, they all have a single transmembrane helix and a highly conserved cytoplasmic tail. The cytoplasmic tail of PODXL is highly conserved between species (approx. 95% between rat, rabbit and human), while the extracellular domain has very little sequence homology, but a very similar structure. The cytoplasmic tail contains putative phosphorylation sites for PKC and CKII as well as a PDZ binding motif. Endoglycan and PODXL share the same PDZ binding motif DTHL, which is slightly different in CD34 (DTEL). Interestingly, the expression patterns in tissues are completely different between these three proteins, suggesting that they might exhibit similar functions in specific tissues¹³⁵.

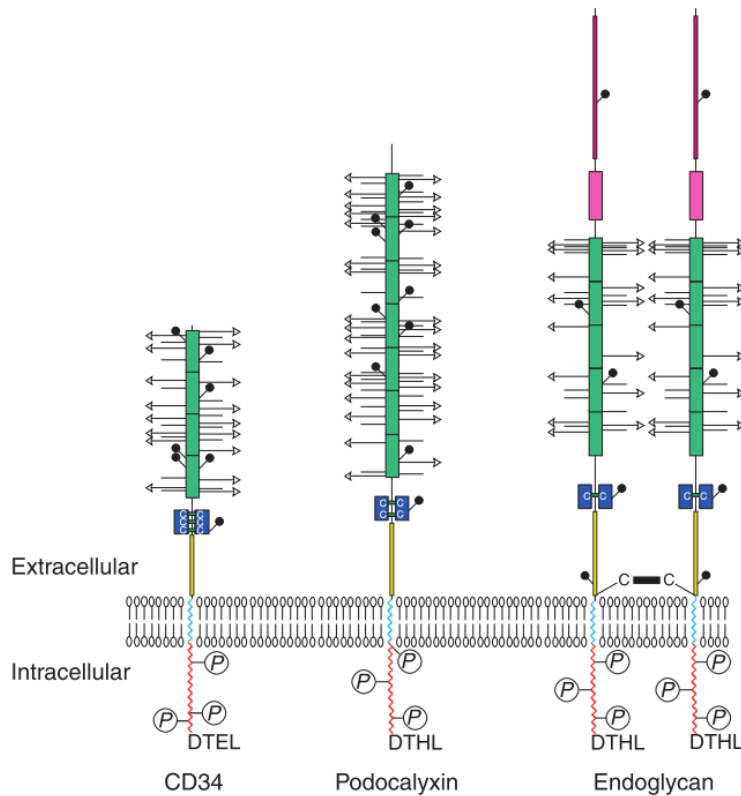


Figure 29: Protein structures of CD34 family members.

This scheme illustrates the similarities of the protein structures of the CD34 family members CD34, PODXL and Endoglycan. All members have an O-glycosylated (horizontal lines with arrowheads) and sialylated (horizontal lines) extracellular mucin domain with putative sites for N-glycosylation (lines with circles). Additionally all members have a cysteine-containing globular domain (dark blue), a juxtamembrane stalk region (yellow), a transmembrane domain (light blue) and a cytoplasmic tail (red) with putative phosphorylation sites and a PDZ-binding motif (DTEL or DTHL). Only Endoglycan contains a polyglutamic-acid-rich extracellular domain (pink) and unpaired cysteine residues that facilitate homodimerization. From reference: ¹³⁵

1.2.2 Tissue Expression

Although PODXL was first discovered as the most abundant glycoprotein in kidney podocytes¹³⁷, it is known today that its expression is very diverse. Just after the first discovery of PODXL, it was also detected lining the surface of vascular endothelia in the kidney¹³⁸ and other tissues¹³⁹. More recently it has been shown that PODXL is expressed

in all three germ layers during mouse embryogenesis¹⁴⁰. With maturation of the embryo its expression decreased, followed by a postnatal burst in hematopoietic progenitors when they colonize the spleen and the bone marrow. At 4 weeks after birth, the *PODXL* expression is restricted to Sca-1; c-kit+Lin- cells in the bone marrow with potential hematopoietic stem cell activities.¹⁴⁰ However, in more differentiated hematopoietic cells, *PODXL* expression is restricted to platelets, their precursors and megakaryocytes¹⁴⁰. Moreover *PODXL* expression was also found in the brain in a subset of neurons throughout development¹⁴¹.

The expression of *PODXL* is positively regulated through binding of WT1 to conserved elements within the *PODXL* gene promoter and negatively regulated through p53-mediated transcriptional repression¹⁴². WT1 is exclusively expressed in kidney cells and therefore cannot explain how *PODXL* expression is regulated in other tissues. Butta et al found that *PODXL* transcriptional regulation is supported by Spl sites and that DNA methylation of the CpG promoter islands contributes to control tissue specific expression.¹⁴³

1.2.3 Discovery and Function

Podocalyxin was initially identified in renal glomerular epithelial cells by the group of Farquhar in 1984¹³⁷. They identified a 140kDa protein as the major sialoprotein of the glomerulus and called it Podocalyxin since it is the major component of the glycocalyx of podocytes (**PODO**cyte glyco**CALYX** prote**IN**). The same group kept investigating *PODXL* in the new-born rat kidney, characterized its posttranslational modifications and suggested a role for *PODXL* in podocyte morphology¹³⁶. Further studies in *PODXL* null mice confirmed that *PODXL* was essential for kidney development, since new-born mice died within 24h after birth from anuric renal failure¹⁴⁴. During kidney development the glomerular epithelium undergoes remodelling from a typical polarized epithelium with

adherence and tight junctions to a specialized glomerular epithelium with remodelled junctions¹⁴⁵. The podocytes form footprocesses with intercellular spaces (filtration slits) to allow passage of glomerular filtrate, which is called the slit diaphragm. Podocytes from *PODXL* null mice did not form footprocesses and slit diaphragms but instead exhibited stable junctions, thus blocking glomerular ultrafiltration of the urine. Importantly, the opening of these intercellular spaces is mediated by sialylated proteins through their negative electrostatic repulsion¹⁴⁶, suggesting that *PODXL* is required for the opening of the filtration slits.

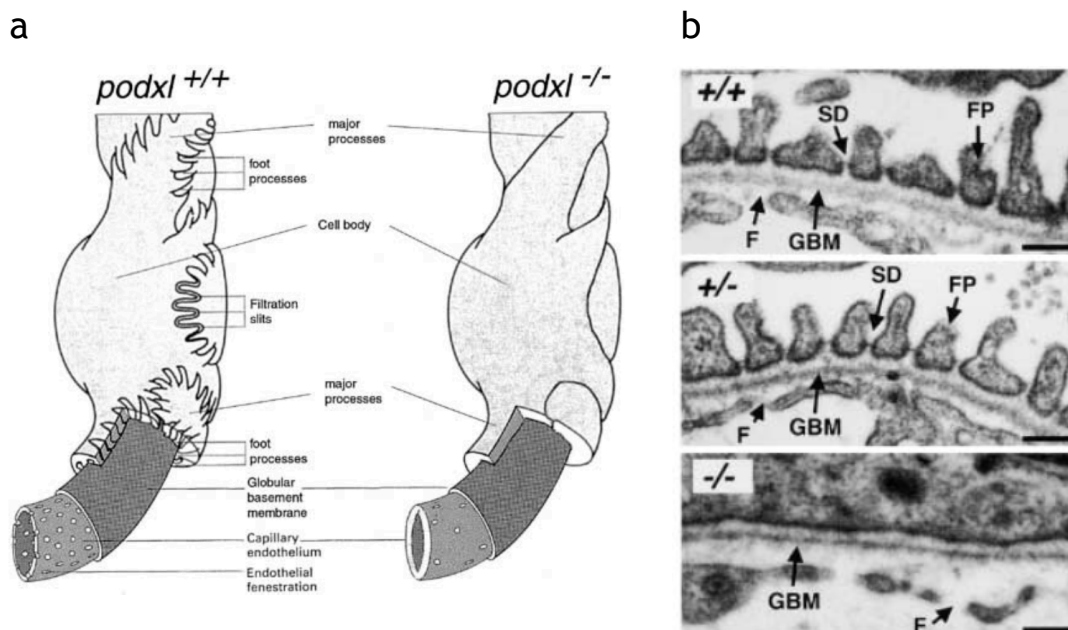


Figure 30: Glomerular filter in wild-type and *PODXL* null mice.

- (a) Schema of the glomerular filter: *PODXL* null mice lack the interdigitating foot processes, leading to a lack of of filtration slit area.
- (b) Transmission electron micrographs of E18 kidneys from *podxl*^{+/+} and *podxl*^{-/-} embryos. *podxl*^{-/-} mice show a complete loss of the slit diaphragm (SD) and foot processes (FP). GBM= glomerular basement membrane. From reference: ¹⁴⁷

Apart from the anuric renal failure, *PODXL* knock out (KO) mice were born with mild to severe edema and omphalocele, which means that the gut remained outside of the abdomen. The presence of edema suggests an additional role for *PODXL* during vascular development¹⁴⁴. Indeed *PODXL* was shown to play a role in vascular lumen formation in mice¹⁴⁸. Together with the sialomucin CD34, *PODXL* acts in separating the apical surfaces of contacting endothelial cells to induce vascular lumen formation through negative cell-surface repulsion. *PODXL* KO mouse embryos showed a delay in aortic lumen formation and failed to recruit Moesin and F-actin to the endothelial cell-cell contacts.

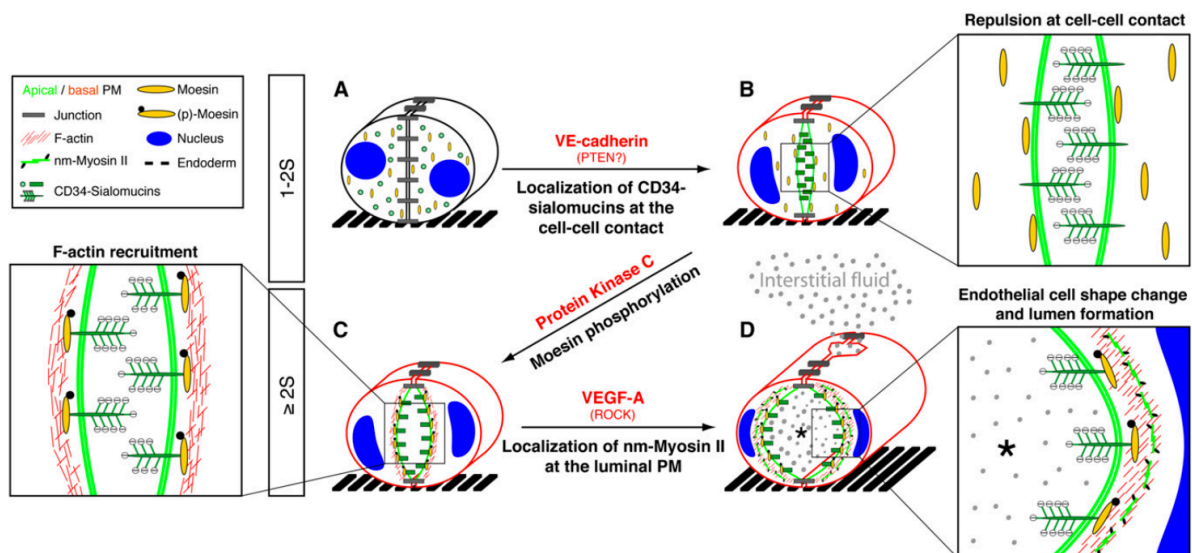


Figure 31: Vascular lumen formation in the developing aorta.

This scheme illustrates the establishment of polarity and progressive lumen formation in the vasculature.

- Endothelial cells form adherence junctions along their cell-cell contact.
- Recruitment of CD34-sialomucins (including *PODXL*) to the cell-cell contact site and repulsion of the two adjacent membranes.
- Recruitment of F-actin to the cell-cell contact by PKC mediated phosphorylation of Moesin.
- ROCK activation through VEGF-A induces recruitment of non-muscle Myosin II to the F-actin enriched cell-cell contact. Opening of the lumen occurs via ROCK mediated contractility and interstitial fluids infiltrate into the lumen. From reference: ¹⁴⁸

Due to its anti-adhesive properties, PODXL was described to act as a molecular “Teflon™”¹⁴⁴. *In vitro* studies in MDCK cells and CHO Chinese hamster ovary cells confirmed the anti-adhesive properties, since overexpression of PODXL decreased cell-cell aggregation and cell adhesion¹⁴⁹. Contrary to these results, two other studies showed that PODXL expression enhanced cell adhesion of CHO cells to vascular endothelial cells¹⁵⁰ and to platelets¹⁵¹. It has been suggested that these opposing observation of PODXL function in cell adhesion arose due to different expression levels. Nielsen and McNagny suggest that low levels of PODXL could drive integrins to the basolateral plasma membrane and thereby increase cell adhesion, whereas high levels of PODXL would induce apical membrane expansion, as reported in several studies¹⁵²⁻¹⁵⁴, which in turn reduces the basolateral surface and thus decreased cell adhesion.

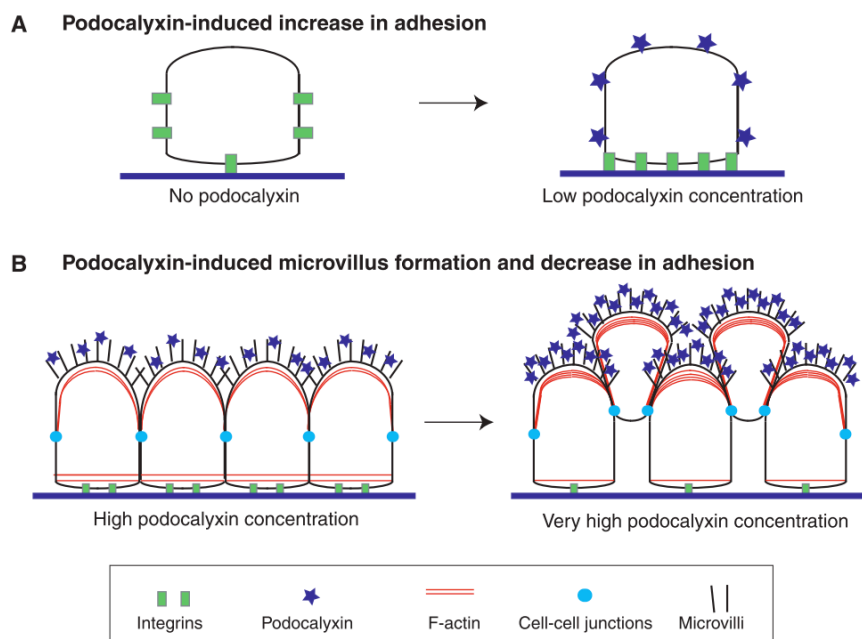


Figure 32: Role of PODXL in cell adhesion.

- (A) Membrane-protein-segregation model: Low levels of PODXL at the apical domain force integrins to the basal membrane, thereby increasing cell adhesion.
- (B) High levels of PODXL at the apical domain recruit F-actin and induce microvilli formation. Relocalization of F-actin to the apical domain leads to reduced F-actin at the basolateral domain, thereby decreasing integrin-mediated adhesion. From reference:¹³⁵

In addition to the anti- and pro-adhesive functions mediated by the negatively charged mucin domain, the cytoplasmic tail of PODXL was also shown to be essential for many functions. The group of Farquhar demonstrated that the cytoplasmic tail of PODXL plays an important role in podocyte architecture through association with Ezrin. They showed that PODXL forms a stable complex with active Ezrin and NHERF2, and is therefore linked to the actin cytoskeleton. NHERF2 functions here as a scaffolding protein linking PODXL to Ezrin and the actin cytoskeleton^{155,156}. Interestingly PODXL can interact with NHERF1 and NHERF2 *in vitro*, but only NHERF2 colocalizes with PODXL *in vivo* on podocytes. In contrast, NHERF1 is mainly localized in the proximal tubules where it interacts with NHE3¹⁵⁷. PODXL has also been shown to bind directly, and indirectly through NHERF2, to Ezrin in MDCK cells¹⁵⁸. Ezrin binds directly to the juxtamembrane region of the PODXL cytoplasmic tail and to the C-terminal FERM domain of NHERF. NHERF in turn binds directly to the C-terminus of PODXL via its PDZ domain, thus establishing an indirect link between Ezrin and PODXL¹⁵⁸. PODXL activates RhoA through NHERF and Ezrin, leading to redistribution of actin filaments to the apical membrane. A PODXL mutant lacking the NHERF2 binding site was not connected to actin did not induce redistribution of actin to the apical membrane and did not increase RhoA activity. The binding site for Ezrin was localized to the juxtamembrane region of PODXL “HQRISQRKDQQR”. In addition to the link to the actin cytoskeleton through Ezrin, PODXL also co-localizes with Cortactin at the apical membrane in rat glomerocytes and both proteins can be co-immunoprecipitated from glomerular rat cell lysate¹⁵⁹. Moreover PODXL was also found in a complex with CLIC5A together with Ezrin and NHERF2 in the mouse glomerulus. CLIC5A leads to PtdIns(4,5) P_2 accumulation at the PM through interaction with PIP5 kinases, enhances Ezrin activation by phosphorylation and therefore actin dependent cell-surface remodelling¹⁶⁰.

In conclusion these studies demonstrate that PODXL is involved in many different cellular processes through its negatively charged extracellular domain and through its cytoplasmic tail.

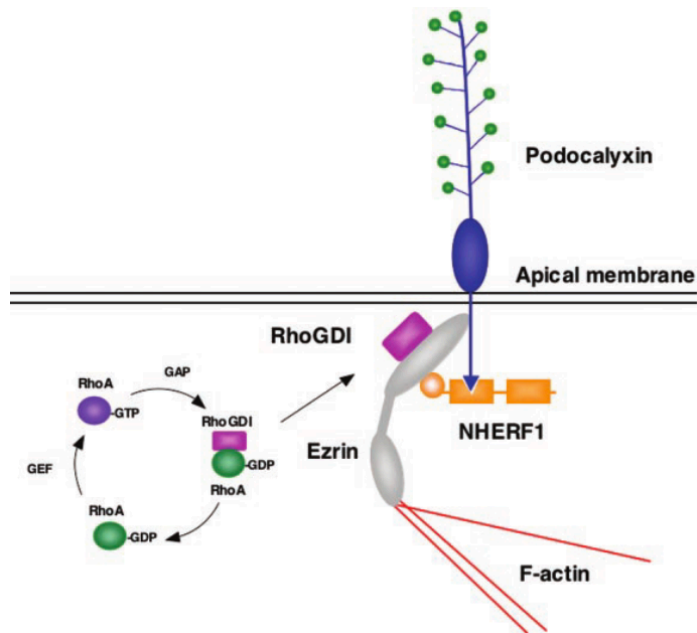


Figure 33: Interactions of the PODXL cytoplasmic tail.

PODXL interacts with Ezrin both directly and indirectly through NHERF1. PODXL interacts with NHERF1 via its PDZ-binding motif, which in turn interacts with Ezrin. Ezrin recruits Rho-GDI, leading to the release of Rho-GDP, which is converted to Rho-GTP in the presence of NHERF1 (likely because NHERF1 recruits a RHOA GEF). Active RhoA leads to Ezrin activation and allows its binding to F-actin. From reference: ¹⁵⁸

1.2.4 PODXL in polarity

Interestingly, at the same time when Podocalyxin was first identified in the kidney glomerulus, the group of Ojakian and Schwimmer worked on 135kDa glycoprotein gp135¹⁶¹. They found that GP135 localized exclusively to the apical membrane domain in polarized MDCK cells in an actin-dependent manner. Further studies on MDCK cells cultured in a collagen matrix used GP135 as a marker to define the apical membrane in MDCK cysts, without attributing any further function⁶⁷.

In 2005, the classical apical marker gp135 was identified as PODXL and its function in epithelial cell polarization was demonstrated 2D polarized monolayers and in 3D MDCK cysts¹⁵². Depletion of PODXL delayed apico-basal cell polarization when grown as 2D

monolayers on transwell filters and impaired single lumen formation in MDCK cysts. PODXL depletion also affected cell morphology: the cells appeared generally larger and flatter compared to control cells and apical markers such as GP114 and PLAP were less polarized. Interestingly, when cells were freshly plated onto coverslips, PODXL was the only apical protein that segregated into an apical domain without even junctions had formed. This apical localization of PODXL was independent of neosynthesized protein or endocytosis of basal localized PODXL. These results indicated that the restricted localization of PODXL on freshly plated cells was either due to membrane diffusion or more likely due to directed trafficking of a pre-existing internal pool of PODXL. Indeed, PODXL was found in Rab11-positive recycling endosomes that could quickly deliver PODXL to the dorsal plasma membrane. It was also previously shown that an internal pool of PODXL vesicles could replenish cell surface PODXL within 1h after removal of surface PODXL by trypsin¹⁶².

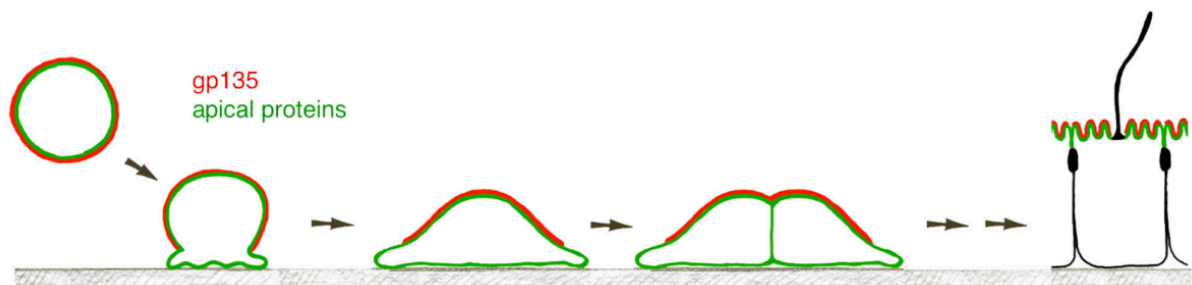


Figure 34: PODXL is restricted to a specialized the apical domain in MDCK cells.

In MDCK cells in suspension, PODXL is evenly distributed at the plasma membrane. Upon contact with a solid support, PODXL is excluded from the contact site, while other apical proteins are evenly distributed. Upon establishment of cell-cell contacts, PODXL becomes excluded from the junctions, but not other apical proteins. Only upon full polarization, also other apical proteins are excluded from the basolateral domain. From reference: ¹⁵²

In freshly plated cells, PODXL mutants lacking the cytoplasmic tail were found on the basal/ventral plasma membrane, indicating that the restriction and stability of PODXL at the dorsal membrane is likely due to its interaction with NHERF2, Ezrin and the actin cytoskeleton. In fully polarized MDCK monolayers, the apical sorting of PODXL depends on the extracellular O-glycosylation-rich region and the cytoplasmic PDZ-binding

motif^{152,154}. Deletion of either the O-glycosylation rich domain or the PDZ-binding motif leads to basolateral missorting of PODXL, which was even stronger when both domains were deleted. A fusion construct, substituting the PDZ binding motif with EBP50/NEHRF1 could rescue the PDZ-deleted mutant, but rescued only partially the mutant missing the O-glycosylation rich domain. Furthermore, it was shown that newly-synthesized PODXL binds to NHERF1 through its PDZ-binding motif at the TGN, which induced oligomerization during the sorting process (Figure 35). After delivery to the apical membrane, PODXL is stabilized by the actin cytoskeleton through binding to Ezrin and NHERF-1.¹⁵⁴ However, another study showed that it is PODXL that recruits NHERF-1 to the apical membrane, which depends on binding to the PDZ domain. This study demonstrates that deletion of the PDZ domain disrupts NHERF-1 recruitment but not the recruitment of Ezrin and actin to the apical membrane. Furthermore, the transmembrane and extracellular domains of PODXL were sufficient to induce microvilli formation in absence of NHERF-1¹⁵³.

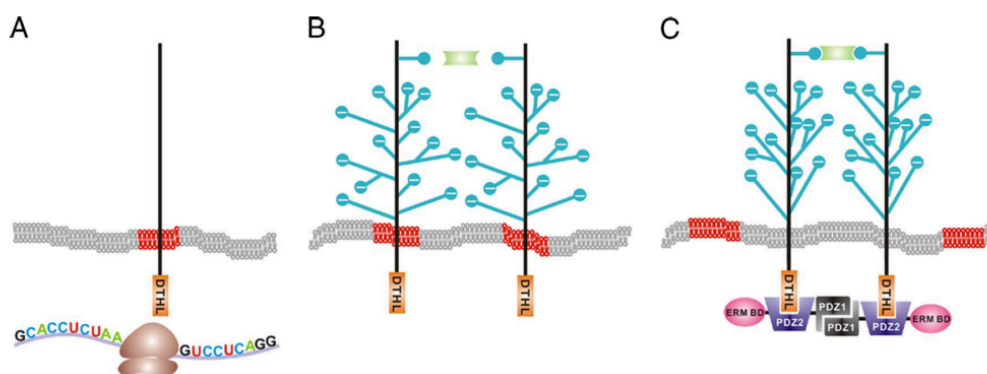


Figure 35: Biosynthetic route of PODXL from the ER to the apical plasma membrane.

- (A) PODXL is released from the membrane-associated ribosome and directed into the ER via its peptide signal.
- (B) The polypeptide becomes O- and N-glycosylated along the biosynthetic route.
- (C) Binding of NHERF1 to the cytoplasmic tail of PODXL induces clustering of PODXL through oligomerization of NHERF1. From reference:¹⁵⁴

Interestingly, it was suggested that also other proteins with PDZ binding domains such as NHE3, CFTR, Crb3 could bind to NHERF2 and therefore indirectly interact with PODXL. NHERF2 thereby could crosslink apical transmembrane proteins to stabilize the apical domain¹⁵².

The apical trafficking of PODXL is also mediated by Rab GTPases. It has been shown that PODXL is trafficked in Rab11- and Rab8-positive endosomes and that both Rab GTPases regulate its apical targeting in MDCK cyst 3D cyst cultures as described on page 19-21⁷². Furthermore, it was shown that Rab27A associated with PODXL vesicles prior to fusion at the apical membrane^{66,74}. These Rab27A/PODXL-positive vesicles are targeted to the apical membrane through Slp2-a and Slp4-a in cooperation with Rab27A, Rab3 and Stx3⁶⁶ as described on page 22-23.

PODXL-depleted MDCK cells grown in Matrigel fail to form single lumen cysts, but instead form either multiple lumen or filled cysts without a lumen^{73,152}. PODXL depletion impairs the apical localization of other apical proteins such as Crumbs3, Syntaxin-3 and CNT1, which accumulate in Rab11a-positive endosomes beneath the plasma membrane and therefore completely disrupt the establishment of an apico-basal polarity⁷³. We observed the same phenotype upon PODXL depletion in GFP-Crumbs3 expressing MDCK cysts (Figure 4g in the published manuscript).

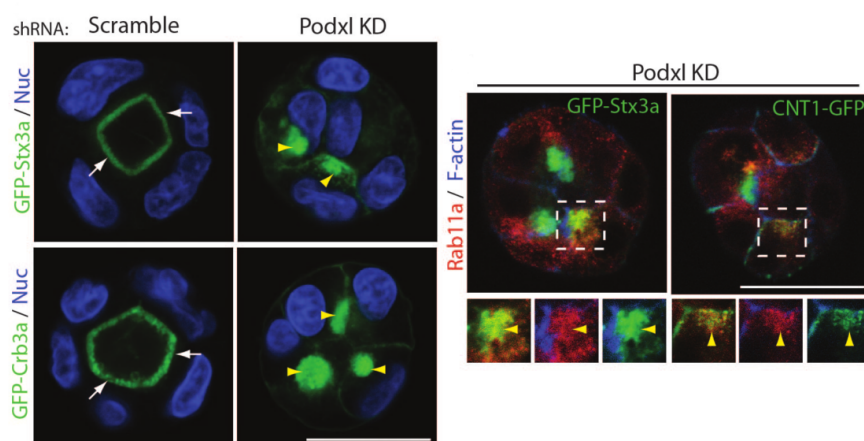


Figure 36: Depletion of PODXL leads to an accumulation of apical vesicles.

Depletion of PODXL in MDCK cysts leads to an accumulation of apical vesicles positive for Stx3, Crumbs3, Rab11 and CNT1. From reference: ⁷³

Another study in contrast did not observe any effects of PODXL depletion on cyst formation, but on tubulogenesis in MDCK cells cultured in collagen matrix. When MDCK cysts are exposed to HGF, cells will protrude out into the collagen matrix and form tubules. This study demonstrated that PODXL-depleted cells lost the ability of tube formation in a collagen matrix upon HGF stimulation¹⁶³. In a different model of cystogenesis, using human pluripotent stem cells (hPSCs), PODXL KO hPSCs retained their pluripotent characteristics, but failed to form lumen when cultured in a GelTrex matrix. PODXL KO hPSCs developed solid spheroids without lumen, showing that PODXL is required for epiblast spheroid lumenogenesis. The function of PODXL on lumen formation was dependent on the sialylated extracellular domain since treatment with protamine sulphate, a positively charged polycation, inhibited lumen formation in the presence of PODXL¹⁶⁴.

1.2.5 PODXL in cancer and disease

Most of the human cancers arise from epithelial cells due to misregulation of important regulatory or polarity proteins. Overexpression of PODXL has been found in many different kinds of tumors and has been especially associated with cancer progression of invasive and aggressive tumors with poor prognosis¹⁶⁵. For certain tumors, PODXL is even used as a diagnostic marker to assess the risk and prognosis as for renal cell carcinomas, kidney cancer (nephroblastoma), ovarian cancer, thyroid cancer, lung cancer, prostate cancer, brain cancer (astrocytoma), gastric cancer and colorectal cancer¹⁶⁵⁻¹⁶⁷. *In vitro* and *in vivo* studies showed that PODXL expression increases cell motility and invasion and that PODXL expression potentially downmodulates the immunosystem.

Expression of PODXL in glioblastoma cell lines increases soluble/intracellular β -catenin levels, MMP9 expression and therefore cell invasion and proliferation. PODXL expression furthermore induces p38 MAPK activity and inactivated GSK-3 β . Thus, PODXL promotes

invasion and proliferation through elevation of β -catenin signalling through p38 MAPK/GSK-3 β pathway, whereas depletion of PODXL has the reverse effects.¹⁶⁸ The role of PODXL in invasion was also confirmed in MCF-7 breast cancer and PC3 prostate cancer cells. The overexpression of PODXL in these cell types increased the migration and invasive potential through up-regulated expression of metalloproteinases such as MMP1 and MMP9 and elevated MAPK and PI3K activity¹⁶⁹. Injection of PODXL over-expressing MCF-7 breast cancer cells into the mouse mammary gland causes tumor invasion, which is not the case when control cells are injected¹⁷⁰.

Furthermore, expression of PODXL in MCF7 breast cancer cells impairs T-cell proliferation and induces resistance to NK -cell mediated cytotoxicity. PODXL decreases the expression of NK cell activating receptors on the cell surface in a contact-dependent manner. Interestingly, NK cells could acquire PODXL from MCF-7 cells by a process known as trogocytosis. This study suggests that PODXL expressed on tumor cells could have an immunomodulatory role that can help tumor cells to evade the immune response¹⁷¹. PODXL depletion in contrast attenuates the development of *in vitro* tumorspheres in different cell lines¹⁷². Correspondingly, depletion of PODXL decreases tumor growth and invasiveness *in vivo* when PODXL depleted-cells were injected into mice. Interestingly, injection of an anti-PODXL antibody effectively blocked tumor growth in mice and therefore suggest PODXL antibodies as a potential target for monoclonal antibody therapy¹⁷².

Recently, PODXL has also been suggested to play a role in neuronal development and *in vitro* studies in PC12 cells demonstrated that PODXL KO induces neurite outgrowth and enhances neurite branching. This was confirmed *ex vivo*, using primary neurons from PODXL KO mice¹⁷³. Interestingly, a frameshift mutation leading to the loss of PODXL protein was found to be the cause in some cases of Parkinson's disease, reinforcing the potential role for PODXL in neurodevelopment¹⁷⁴.

1.3 FUNCTIONS OF THE RAB35 GTPASE

1.3.1 Rab GTPases

Coordinated and polarized membrane traffic is essential for the establishment of apico-basal polarity. Newly synthesized proteins are either delivered directly to their destined basolateral or apical plasma membrane domain or are undergo transcytosis from the basolateral to the apical domain. Furthermore, maintenance of the apical and basolateral plasma membrane requires regulated endocytosis as well as recycling from both membrane domains. One of the major regulators of vesicular membrane traffic are Rab GTPases. More than 70 different Rab GTPases are expressed in mammals and together they regulate vesicle formation, motility, docking, and membrane remodelling and fusion (Figure 37). Rab GTPase activation and inactivation is tightly controlled by Guanine Exchange Factors (GEFs), which catalyze GTP loading and GTPase activating proteins (GAPs), which trigger GTP hydrolysis of bound GTP to GDP (Figure 38). Inactive GDP-bound Rabs are bound to GDI, which keeps them soluble in the cytoplasm. Upon dissociation of the GDI, Rab GTPases can bind to membranes via their prenyl anchor and are available for activation through specific GEFs. In their activated GTP-bound form, Rab GTPases can recruit specific effector proteins to their membrane, including coat proteins, motor proteins and SNAREs, thus promoting cargo sorting, trafficking and membrane fusion.

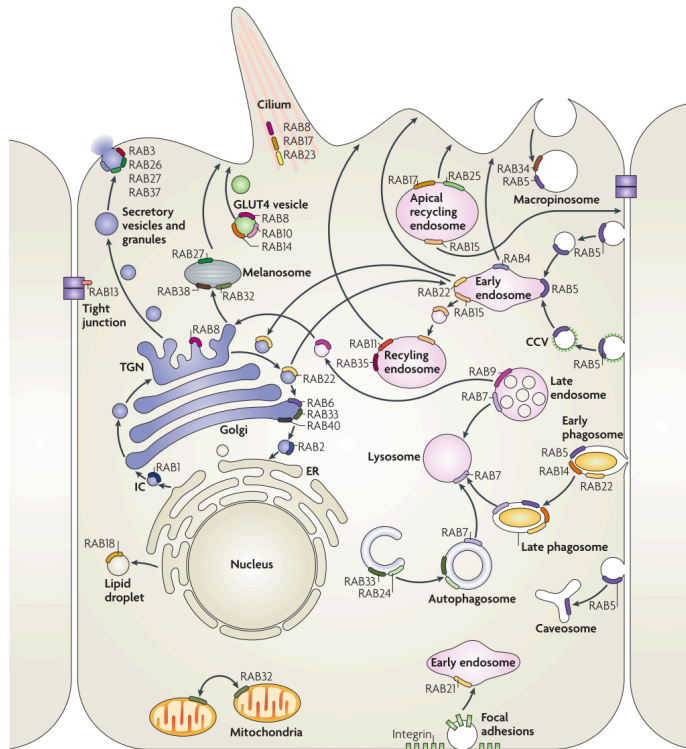


Figure 37: Localization of Rab GTPases.

This scheme illustrates the subcellular localization of Rab GTPases. Each membrane domain is marked by distinct Rab GTPases or a combination of multiple Rabs. From reference: ¹⁷⁵

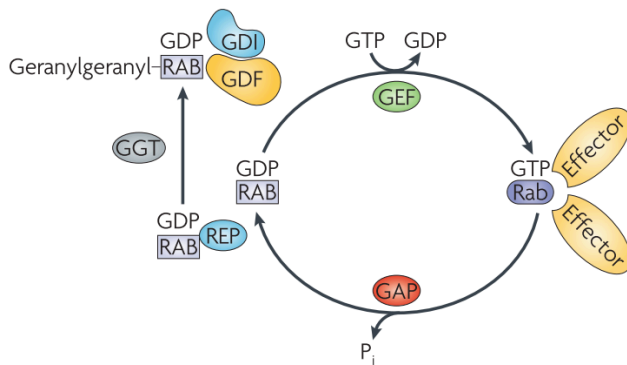


Figure 38: The Rab GTPase switch.

Newly synthesized Rab proteins, in the GDP-bound form, are recognized by Rab escort proteins (REPs), which present the Rab to a geranylgeranyl transferase leading to geranylgeranylation of the two C-terminal cysteine residues. Next, the Rab protein is recognized by a Rab GDP dissociation inhibitor (GDI), which associates Rabs to membrane via interaction with a membrane-bound GDI displacement factor (GDF). The inactive GDP-bound Rab is converted into its active GTP-bound state by exchange of GDP for GTP. This exchange is catalysed by a guanine nucleotide exchange factor (GEF), which causes conformational changes. In the GTP-bound state Rabs can bind to effector proteins. Active Rabs return to their inactive state through hydrolysis of GTP, which is catalysed by GTPase activating proteins (GAPs). From reference: ¹⁷⁵

Interestingly, it has been demonstrated that the plasma membrane localization of Rab35 is GTP-dependent and additionally requires its C-terminal polybasic region, which is not present in Rab1A and Rab1B^{176,177}. At the same time the lab identified Rab35 as a key regulator of endocytic recycling and cytokines in a RNAi screen in *Drosophila* S2 cells for cytokinesis defects¹⁷⁸. Depletion of Rab35 in *Drosophila* S2 cells leads to binucleated cells due to failure of cytokinetic abscission. Further investigations in HeLa cells revealed then that Rab35 controls a fast endocytic recycling pathway from early endosomes to the plasma membrane, required for the terminal steps of cytokinesis^{178,179}.

Since then, many studies confirmed the role of Rab35 in endocytic recycling of diverse cargo, including receptors and adhesion molecules, thus leading to a wide range of Rab35-mediated cellular functions. Apart from its role in endocytic recycling Rab35 has emerged as an important factor in cancer biology and cell polarity.

We wrote a comprehensive review on Rab35 functions, which have been appended in the annex.

1.3.2 Rab35 - a regulator of endocytic recycling and cytokinesis

The importance of Rab35 in membrane traffic and cytokinesis was first discovered in a RNAi screen in *Drosophila* S2 cell for cytokinesis defects in the lab¹⁷⁸. An increase of binucleated cells was observed upon depletion of Rab5, Rab11 and Rab35, with Rab35 leading to the strongest phenotype. Further investigations in HeLa cells revealed that Rab35 controls a fast endocytic recycling pathway from early endosomes to the plasma membrane, required for the terminal steps of cytokinesis^{178,179}. Consequently, depletion or inactivation of Rab35 led to an accumulation of endocytic carriers, such as transferrin and transferrin receptor. The key role of Rab35 in endocytic recycling was further strengthened when Rab35 was identified in a *C. elegans* genetic screen for yolk endocytosis.¹⁸⁰ The group of Grant found that loss of Rab35 in *C. elegans* results in an accumulation of yolk receptors in dispersed vesicles, confirming the role of Rab35 in

endocytic recycling. Rab35 dependent recycling has also been described for Megalin trafficking in L2 rat yolk sac cells¹⁸¹, KCa2.3 trafficking human embryonic kidney cells and human microvascular endothelial cells (HMEC-1)¹⁸², insulin stimulated GLUT4 trafficking in adipocytes¹⁸³ and MHC-1 trafficking in COS-7 cells.

Rab35 effectors in endocytic recycling and cytokinesis

Three effector proteins of Rab35 have been identified and characterized: OCRL, MICAL-L1 and ACAP2, which mediate Rab35 functions.

OCRL

OCRL is a phosphatidylinositol 5-phosphatase that preferentially hydrolyses PtdIns(4,5) P_2 to PtdIns4P. Loss-of function mutations in the *OCRL* gene lead to the Lowe Syndrome and Dent2 disease, both characterized by congenital cataract, mental retardation and reabsorption defects in proximal renal cells, thus leading to kidney failure. Interestingly, it has been shown that cells isolated from Lowe Syndrome patients exhibit an accumulation of clathrin-coated vesicles, positive for PtdIns(4,5) P_2 , actin and transferrin receptor, as previously observed in Rab35-depleted cells¹⁸⁴. Indeed, depletion of OCRL in Hela cells phenocopies the recycling and cytokinesis defects of Rab35 depletion¹⁷⁹. Rab35 activation is required to recruit OCRL onto early endosomes, in order to hydrolyse PtdIns(4,5) P_2 , thereby prevent F-actin polymerization to allow uncoating of the clathrin-coated vesicles¹⁸⁵. However, the activation of Rab35 on early endosomes is temporally tightly regulated by the GAP EPI64B and the GEF connecdenn1. During the formation of the clathrin-coated pit, the Arf6 GTPase recruits the Rab35 GAP EPI64B as well as the PI5-kinase to maintain PtdIns(4,5) P_2 levels high. Just after the scission of the clathrin-coated vesicle Rab35 becomes activated through connecdenn1, which binds to the clathrin adaptor AP-2. Active Rab35 recruits OCRL onto these newborn endosomes to hydrolyse PtdIns(4,5) P_2 ¹⁸⁵ (Figure 39).

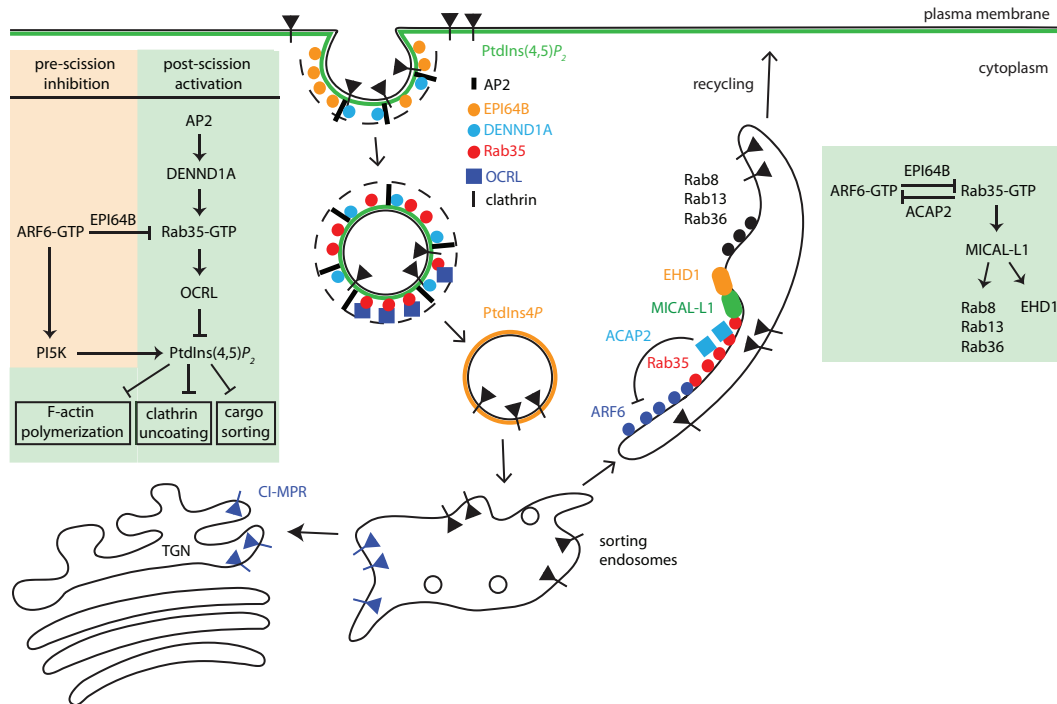


Figure 39: Rab35 in endocytic recycling.

This scheme illustrates the localization of Rab35 and its GAPs and GEFs during endocytosis and recycling. From reference: ¹⁸⁶

Interestingly the cytokinesis defects in OCRL- or Rab35-depleted cells can be explained by the same molecular mechanism. It was shown that Rab35 is enriched at the plasma membrane of the cleavage furrow during cell division. Here, Rab35 recruits OCRL to locally hydrolyse PtdIns(4,5) P_2 in order to prevent F-actin polymerization in the intercellular bridge and thereby allow successful cytokinesis¹⁷⁹ (Figure 40). Indeed, F-actin is highly enriched in Rab35- or OCRL-depleted cells, not only on endosomes, but also in the intercellular bridge, thus preventing cytokinesis. These cytokinesis defects can furthermore be rescued by low non-toxic doses of Latrunculin A¹⁷⁹.

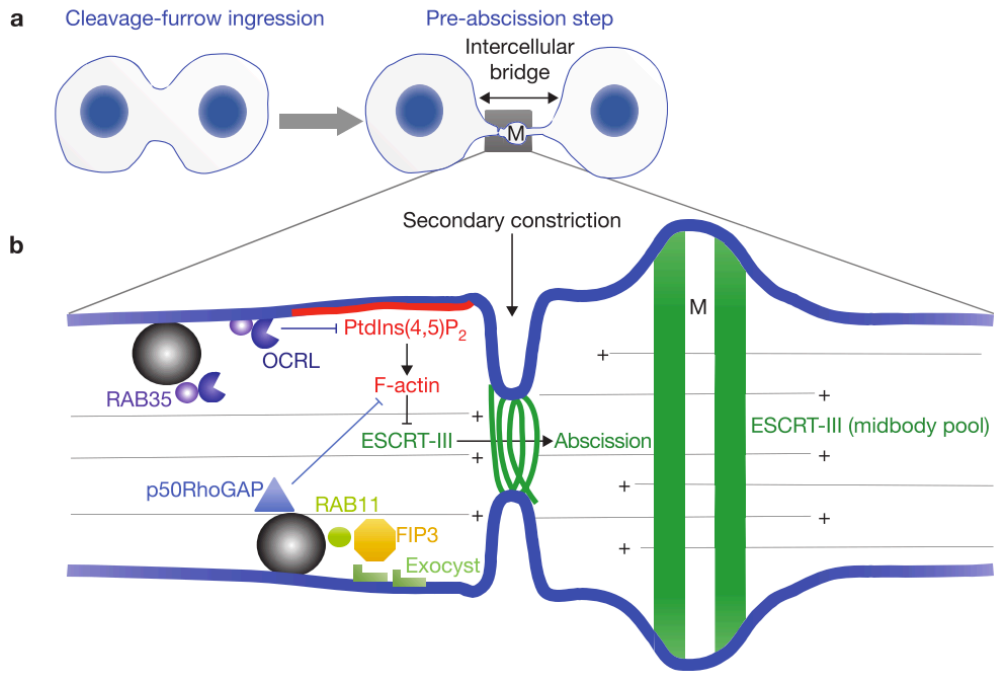


Figure 40: Function of Rab35 in cytokinesis.

- (a) Ingression of the cleavage furrow is mediated by F-actin and myosin II, leading to the formation of an intercellular bridge and the midbody (M).
- (b) A secondary constriction site occurs close to the midbody, driven by Rab11/FIP3 and ESCRT-III. The proper localization of ESCRT-III is inhibited by F-actin, which therefore needs to be cleared from the intercellular bridge. Rab35-GTP recruits the 5-phosphatase OCRL to the intercellular bridge in order to hydrolyse PtdIns(4,5)P₂, thereby preventing F-actin polymerization. Furthermore Rab11/FIP3 endosomes bring p50RhoGAP to the intercellular bridge, which assists to restrict F-actin. From reference: ¹⁸⁷

ACAP2 and MICAL-L1

Following clathrin-dependent or clathrin-independent endocytosis into early EEA1 positive endosomes, endocytic cargo can converge into Arf6 positive tubular recycling endosomes or take the lysosomal route to be degraded. Rab35 and Arf6 activation in these tubular endosomes is regulated through a mutual antagonism, which involves EPI64B and ACAP2. Active Arf6 recruits its effector EPI64B, which inactivates Rab35, whereas active Rab35 recruits its effector ACAP2, which is a GAP of Arf6.

Active Rab35 directly and indirectly through Arf6, recruits its effector MICAL-L1 onto Arf6 positive tubular endosomes¹⁸⁸⁻¹⁹⁰. MICAL-L1 together with ACAP2 promote the recruitment of EHD1, a protein which is known to induce membrane fission due to its similarities to Dynamin^{188,190}. MICAL-L1 associates directly with EHD1, whereas ACAP2 promotes EHD1 recruitment indirectly through inactivation of Arf6 and thereby maintenance of PtdIns4P, a scaffold factor for EHD1¹⁸⁸. Additionally MICAL-L1 also promotes recycling through recruitment of Rab8, Rab13 and Rab36 (Figure 39).

This pathway has been investigated in Hela cell and a human DCs in the case of MHC-II recycling from tubular endosomes to the plasma membrane¹⁹¹ as well as in a variety of neuronal cells during neurite outgrowth^{190,192-194}.

1.3.3 A role for Rab35 in polarity

To date, a role for Rab35 in polarity establishment has only been reported in the case of seamless tube formation in *Drosophila* tracheal terminal cells⁵⁷. Growth of seamless tubes is polarized along the proximodistal axis and regulated by Rab35 and its GAP Whacked (~30% identity to human EPI64A-C). Expression of a dominant active mutant of Rab35 or depletion of Whacked leads to tube overgrowth, whereas expression of a dominant negative mutant of Rab35 or overexpression of Whacked causes ectopic lumen formation due to distal overgrowth. As mentioned earlier on, seamless tubes form by cell hollowing, where vesicles are trafficked to the centre of the cell and fuse to form an internal tube (Figure 8). This study demonstrated that Whacked and Rab35 direct the transport of apical membrane vesicles to the distal tip of terminal cell branches to induce seamless tube growth.

1.3.4 Functions of Rab35 in cancer

Interestingly, the first functions of Rab35 that were discovered in 2004 and 2006 involved regulation of p53 transcriptional activity¹⁹⁵ and interaction with the oncogenic tyrosine kinase NPM-ALK¹⁹⁶. Overexpression of Rab35 suppresses the PRPK-induced p53 transcriptional activity through direct binding to PRPK, indicating a potential tumor suppressor function for Rab35, which need further investigation. The function of the direct interaction with the oncogenic tyrosine kinase NPM-ALK in contrast has not been studied so far. Furthermore it has been shown that Rab35 expression is up regulated in human ovarian cancers and it is suggested that Rab35 might be an androgen responsive gene and could function as a biomarker of androgen receptor function in ovarian cancer¹⁹⁷.

Cell adhesion and migration

More recently, Rab35 has been associated with cancer development through different mechanisms. Rab35 was shown to promote cell adhesion and inhibit cell migration through ACAP2-driven inactivation of Arf6 and subsequent down-regulation of Arf6-dependent β 1-integrin and EGF-receptor recycling¹⁹⁸. Of note the no effect of Rab35 depletion on integrin recycling could be detected in an earlier study by the same group in different cell culture conditions¹⁹⁹. Rab35 depletion in turn induces decreased cell adhesion and increased cell migration, which are characteristics of EMT as found in cancers. Interestingly, human cancer databases show that Rab35 expression is indeed down-regulated in some cancers with elevated Arf6 activity¹⁹⁸.

Furthermore Rab35 was shown to be negatively regulated by the microRNA-720 (miR-720), which is up regulated in cervical tumors²⁰⁰. In Hela cell miR-720 down regulates Rab35 expression and thereby promotes cell migration²⁰⁰.

However, another study demonstrated that Rab35 depletion does not promote, but instead inhibits cell migration in MCF-7 cells²⁰¹. It was found that Rab35 co-immunoprecipitates with Dvl2, a protein that plays a role in the signal transduction of the Wnt5a pathway²⁰¹. Wnt5a induces Rac1 and Dvl2 activation, which promotes cell migration in MCF-7 cells. Zhu et al showed that Wnt5a could activate Rab35 through Dvl2 and that Rab35 depletion was sufficient to inhibit Wnt5a induced Rac1 activation and cell migration. Rab35 acts here downstream of Wnt5a and Dvl2 and upstream of Rac1 to regulate cell migration²⁰¹.

PI3K/AKT signalling

Another mechanism by which Rab35 has been linked to cancer is the PI3K/AKT signaling pathway. Rab35 was identified in a screen for AKT phosphorylation in HeLa cells²⁰². Depletion of Rab35 suppressed AKT phosphorylation in HeLa cells and other cell types, whereas expression of a dominant active mutant of Rab35 induced constitutive AKT phosphorylation and therefore activation of the PI3K/AKT signalling pathway. Rab35 functions downstream of growth factor receptors and upstream of PDK1 and mTORC2, likely through regulation of PI3K, since Rab35-GTP co-immunoprecipitated with PI3K. In normal conditions, the growth factor receptor PDGFR- α is activated at the cell membrane by PDGF-AA ligand, then internalized and sorted into Lamp2-positive endosomes where liganded PDGFR- α drives PI3K/AKT signalling²⁰². Expression of a dominant active mutant of Rab35 is sufficient to drive PDGFR- α into Lamp2 positive endosomes even in absence of a ligand, leading to constitutive AKT phosphorylation. Rab35 expression did not affect other growth factor receptors such as EGFR²⁰², although Rab35 was previously reported to play a role in EGFR recycling¹⁹⁸. Moreover it has been demonstrated that AKT-dependent phosphorylation releases the autoinhibition of the Rab35 GEF connecdenn1, thus increasing GEF activity and the binding to Rab35 and therefore promoting Rab35 activation²⁰³. Hence, Rab35 activation and AKT phosphorylation likely act together in positive feedback loop.

Interestingly, two somatic Rab35 mutations were found in human cancers that constitutively activate PI3K/AKT signaling²⁰². The same mutations expressed in HeLa cells phenocopied the expression of a dominant active mutant of Rab35, suggesting that Rab35-dependent recycling of certain growth factor receptors could play an emerging role in cancer development.

Folliculin - a putative Rab35 GEF involved in tumorigenesis

Moreover, Rab35 has been shown to bind *in vitro* to the tumor suppressor Folliculin²⁰⁴. Mutations of Folliculin lead to the BHD syndrome, characterized by fibrofolliculomas, cystic lung disease and renal cell carcinoma²⁰⁵. Interestingly, it was shown that FLCN exhibit GEF activity towards Rab35, at least *in vitro*²⁰⁴. Depletion of FLCN *in vitro* leads to increased cell-cell adhesions and impaired cell polarization in 3D cysts in T84 cells in Matrigel and in IMCD3 cells in Geltrex matrix^{206,207}. Of note, also Rab35 is implicated in the formation and remodelling of adherence junctions²⁰⁸ and its activation might be thus regulated by FLCN. Rab35 has been shown to regulate the cadherin trafficking and stabilization at cell-cell contacts in C2C12 myoblasts and HeLa cells²⁰⁸.

Additionally, FLCN depletion causes cytokinesis defects resulting in binucleated cells²⁰⁶, another similarity to Rab35 regulated pathways, indicating that FLCN might act as a GEF for Rab35 in multiple cellular processes, potentially also in the establishment of epithelial apico-basal polarity. However, further studies will be necessary to investigate whether Rab35 plays a role in FLCN loss-of-function carcinomas and to confirm FLCN's GEF activity towards Rab35 *in vivo*.

1.3.5 Other functions of Rab35

Besides its function in endocytic recycling, cytokinesis and its emerging role in polarity and cancer, Rab35 is also involved in many other cellular processes including cell migration neurite outgrowth, phagocytosis and infection (Figure 41).

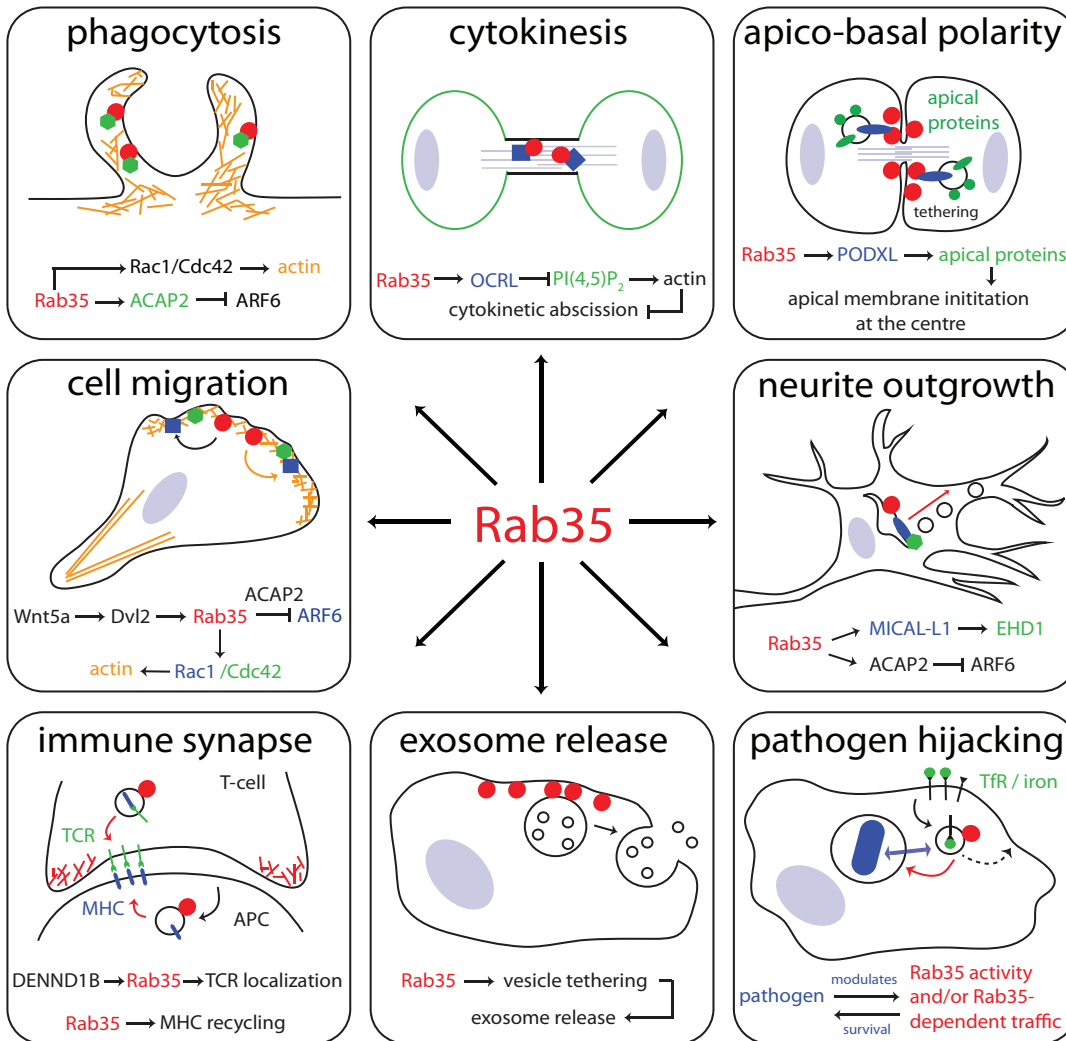


Figure 41: Functions of the Rab35 GTPase

This scheme illustrates the different cellular functions of Rab35 at the plasma membrane and its regulation by GAPs and GEFs. From reference: ¹⁸⁶

Notably, Rab35 is involved in many cellular processes that involve regulation of $\text{PtdIns}(4,5)\text{P}_2$ and F-actin through recruitment of different effectors. As mentioned above Rab35 regulates $\text{PtdIns}(4,5)\text{P}_2$ and F-actin levels on early endosomes and in the intercellular bridge through recruitment of OCRL.

Furthermore, Rab35 was shown to regulate actin dynamics in *Drosophila*. Depletion of Rab35 or expression of a dominant negative mutant of Rab35 during *Drosophila* development induces malformation of the bristles, such as sharp bends and forked ends²⁰⁹. These malformed bristles are caused by loose and disconnected actin organization, suggesting a role for Rab35 in actin remodelling. The protein that directly links Rab35 to actin dynamics is Fascin, an actin bundling protein that has been identified as a new effector for Rab35. It was further demonstrated that overexpression of Fascin can rescue the bristle phenotype induced by Rab35 depletion, putting Fascin downstream of Rab35. Using *Drosophila* S2 cells the authors demonstrated that active Rab35 ectopically expressed at the mitochondrial membrane was sufficient to induce actin bundling around the mitochondria²⁰⁹.

More recently the McPherson lab has investigated the differences between the 3 major Rab35 GEFs *connecdenn1-3*. Interestingly, *connecdenn3* but not *connecdenn1* and *2* can bind to actin and colocalizes with Rab35, Fascin and actin. Furthermore co-expression of Rab35 with *connecdenn3* induces the formation of actin protrusions but not co-expression with *connecdenn1* and *2*. This study suggests that *connecdenn3* recruits and activates Rab35 at actin filaments and Rab35 in turn recruits its effector Fascin to induce actin bundling²¹⁰.

A third Rab35-regulated pathway that acts on actin dynamics involves Rac1 and Cdc42. Although Rab35 does not interact directly with Rac1 or Cdc42, it has been shown that Rab35 promotes the recruitment of Cdc42 and Rac1 to the phagocytic cup in SL2 cells, where Rab35 promotes the formation of the phagocytic cup through Cdc42/Rac1-mediated actin remodelling²¹¹. Moreover Rab35 regulates neurite outgrowth in PC-12 cells and NHE-115 cells through via a Cdc42 dependent pathway¹⁹³. It was furthermore shown that Rab35 can activate Cdc42 *in vitro*, although the exact mechanism remains

elusive¹⁹³. A link between Rac1 and Rab35 was established in MCF-7 breast cancer cells, demonstrating that Rab35 form a complex with Dvl2, a protein involved in the Wnt5 signal transduction pathway²⁰¹. Wnt5a activates Rab35 through Dvl2, which induces Rac1 activation. However, the mechanism for this activation cascade remains to be established.

1.4 THESIS RATIONALE

De novo establishment of an apical membrane is a complex process that has been linked to symmetry breaking steps during cytokinesis in several instances^{88,89,128}. It has been furthermore suggested that proteins involved in epithelial cell polarization could also play a role during cytokinesis and vice-versa¹²⁰. Although cytokinesis failure as well as polarity defects are associated with tumorigenesis, investigation of underlying molecular mechanisms that couple cytokinesis with epithelia polarity have only been started recently.

The thesis project was initially based on the result of a Yeast-two hybrid screen using Rab35^{Q67L} (GTP-bound) as bait¹⁷⁹. This screen revealed a potential interaction between Rab35 and the cytoplasmic tail of the apical transmembrane protein Podocalyxin. Podocalyxin is implicated in many cellular processes that involve cell adhesion and membrane repulsion, cell morphology as well as epithelial cell polarity. Moreover PODXL overexpression is associated with tumor progression and poor prognosis in many different carcinomas. Rab35 is a known as a regulator for endocytic recycling and cytokinetic abscission, but raises increasing attention in cancer research in the last few years. The interaction between Rab35 and PODXL could therefore potentially link the known functions of Rab35 with PODXL mediated epithelial polarity and cancer progression and thus shed light on novel mechanisms and functions coupling cytokinesis with the initiation of apico-basal polarity through Rab35.

The major goals and questions of my thesis were initially the following:

- **Characterization of the PODXL/Rab35 interaction**
Is PODXL an effector protein of active GTP-bound Rab35?

- **Investigation of PODXL traffic/recycling in polarized (3D cysts) and unpolarized MDCK cells by time-lapse microscopy**
Do Rab35 and PODXL co-localize on endosomes?
Does Rab35 regulate the traffic/recycling of PODXL?
Is Rab35 required for the apical targeting of PODXL?

- **Investigation of the potential function for Rab35 in epithelial polarity using MDCK 3D cysts**
Does Rab35 inactivation/depletion affect apico-basal polarity?
Does Rab35 inactivation/depletion affect the apical localization of PODXL?

- **Deciphering the function/mechanism of the PODXL/Rab35 interaction**
Does blocking of the PODXL/Rab35 interaction phenocopy Rab35 inactivation/depletion?

2 RESULTS

2.1 Summary

Most of the human cancers arise from epithelial cells and the loss of epithelial apico-basal polarity is a hallmark in tumor progression. It has been shown that the initiation of epithelial polarity is tightly connected to cell division and polarized membrane traffic, but how this is coordinated at a molecular level remains unknown. During my thesis I addressed this question in renal MDCK cells, which develop 3D polarized cysts with an open apical lumen from a single cell when cultured in Matrigel. Unpolarized renal MDCK cells establish an apical membrane already at the first cell-cell interface during the two-cell stage, and this is coupled to cytokinesis by an unknown mechanism. Unexpectedly, I found that the Rab35 GTPase directly interacts with the cytoplasmic tail of the apical transmembrane protein Podocalyxin (PODXL, also known as GP135), a classical apical marker essential for epithelial polarity and lumen formation. Interestingly, Rab35 was enriched at the future apical membrane during the first cell division before PODXL or any other tested apical proteins could be detected. Depletion of Rab35 or replacement of endogenous PODXL by the mutant PODXL V496A/Y500A unable to interact with Rab35, prevented PODXL and other apical proteins to become enriched at the future apical membrane during the first cell division. Consequently, a complete inversion of apico-basal polarity was observed in these conditions. Furthermore, the experimental delocalization of Rab35 to mitochondrial membranes induced a striking accumulation of vesicles containing PODXL, Crb3, Cdc42 and aPKC around the mitochondria, leading to a loss of apico-basal polarity. From these results I conclude that Rab35 acts as a direct tether for transcytosed PODXL-containing vesicles at the future apical membrane, and thereby plays a crucial role in triggering the establishment of apical polarity. In addition, this work provides a molecular mechanism for coupling the site of cytokinesis to the initiation of polarity and lumen localization in 3D structures.

2.2 Published Manuscript

ARTICLE

Received 3 Sep 2015 | Accepted 25 Feb 2016 | Published 4 Apr 2016

DOI: 10.1038/ncomms11166

OPEN

Rab35 GTPase couples cell division with initiation of epithelial apico-basal polarity and lumen opening

Kerstin Klinkert^{1,2,3}, Murielle Rocancourt^{1,2}, Anne Houdusse⁴ & Arnaud Echard^{1,2}

Establishment and maintenance of apico-basal polarity in epithelial organs must be tightly coupled with cell division, but the underlying molecular mechanisms are largely unknown. Using 3D cultures of renal MDCK cells (cysts), we found that the Rab35 GTPase plays a crucial role in polarity initiation and apical lumen positioning during the first cell division of cyst development. At the molecular level, Rab35 physically couples cytokinesis with the initiation of apico-basal polarity by tethering intracellular vesicles containing key apical determinants at the cleavage site. These vesicles transport aPKC, Cdc42, Crumbs3 and the lumen-promoting factor Podocalyxin, and are tethered through a direct interaction between Rab35 and the cytoplasmic tail of Podocalyxin. Consequently, Rab35 inactivation leads to complete inversion of apico-basal polarity in 3D cysts. This novel and unconventional mode of Rab-dependent vesicle targeting provides a simple mechanism for triggering both initiation of apico-basal polarity and lumen opening at the centre of cysts.

¹Membrane Traffic and Cell Division Lab, Cell Biology and Infection Department, Institut Pasteur, 25–28 rue du Dr Roux, 75724 Paris, France.

²Centre National de la Recherche Scientifique UMR3691, 75015 Paris, France. ³Sorbonne Universités, Université Pierre et Marie Curie, Université Paris 06, Institut de formation doctorale, 75252 Paris, France. ⁴Institut Curie, Structural Motility Lab, 26 rue d'Ulm, 75005 Paris, France. Correspondence and requests for materials should be addressed to A.E. (email: arnaud.echard@pasteur.fr).

Many epithelial organs are composed of a polarized cell monolayer surrounding a central apical lumen. Renal Madin-Darby canine kidney (MDCK) cells cultured in Matrigel form polarized hollow spheres (cysts) that represent a powerful model for deciphering the establishment of epithelial polarity and lumen formation^{1–5}. The *de novo* apico-basal polarity in cysts arises from successive divisions of a single, non-polarized cyst-founding cell^{6,7}. During the first cell division, apical transmembrane proteins such as Podocalyxin (PODXL, a classical apical marker also known as GP135) and Crumbs3 are transcytosed from the plasma membrane facing the extracellular matrix (ECM) towards the first cell–cell contact site^{8–10}. Membrane traffic is therefore essential for this symmetry-breaking step, which specifies the location of the apical membrane initiation site (AMIS) and thus the central position of the future apical lumen^{10–12}. Recent data indicate that the location of the cytokinetic bridge between the first two daughter cells determines the location of the AMIS^{12–15}, yet the molecular mechanisms coupling the first cell division with apical lumen formation are largely unknown. We previously identified Rab35 as a unique Rab GTPase present at the cleavage site that promotes cytokinetic abscission in HeLa cells^{16–20}. Given the postulated analogy between the cytokinetic plasma membrane and the apical membrane of polarized epithelial cells²¹, we hypothesized that Rab35 might play a role in apico-basal polarity events. Here we show that the Rab35 GTPase is localized at the cell–cell interface and at the future AMIS during cytokinesis, where it captures vesicles transporting key apical determinants via a direct interaction with the cytoplasmic tail of PODXL. Through this original mechanism of vesicle tethering, Rab35 thus couples cell division with initiation of apico-basal polarity and lumen formation.

Results

Rab35 directly interacts with PODXL at the apical membrane.

We first identified a potential connection between Rab35 and PODXL through a yeast two-hybrid screen using the active, GTP-bound mutant of Rab35 (Rab35^{Q67L}) as a bait. We found that the cytoplasmic tail of PODXL (aa 476–551) interacted selectively with Rab35^{WT} and Rab35^{Q67L}, but not with Rab35^{S22N}, the GDP-bound, inactive form (Fig. 1a). In contrast, no interaction was detected between the PODXL tail and the GTP-locked mutants of Rab6A or Rab GTPases involved in cystogenesis like Rab8, Rab11A or Rab27A (Fig. 1a). Using recombinant proteins, we confirmed that the PODXL/Rab35 interaction was direct and specific for the GTP-bound conformation of Rab35 (Fig. 1b). In addition, endogenous PODXL could be co-immunoprecipitated from MDCK cells expressing Rab35^{WT} or Rab35^{Q67L}, but not from Rab35^{S22N}-, Rab6A^{Q72L}-, Rab8A^{Q67L}-, Rab11^{Q70L}- or Rab27A^{Q78L}-expressing cells (Fig. 1c). To examine where this direct interaction takes place during cystogenesis, we stained for endogenous PODXL in MDCK cells stably expressing mCherry-Rab35. During initial phases of three-dimensional (3D) cyst development, PODXL vesicles concentrated on endosomal recycling compartments at the two-cell stage (arrowheads) and then concentrated at the AMIS (arrow), as previously reported^{9,10,14} (Fig. 2a(iii)). Importantly, we noticed that Rab35 was present at the first cleavage furrow before any detectable co-localization with PODXL (Fig. 2a(ii)). Early signs of co-localization were observed when PODXL started to be trafficked towards the cytokinetic bridge (Fig. 2a(iii), and zoom (vii)). A remarkable close apposition between PODXL-containing vesicles and membrane-bound Rab35 was thus initially detected at the AMIS. Subsequently, PODXL strongly co-localized with Rab35 at the AMIS and at the apical membrane (Fig. 2a(iv–vi) and

Fig. 2b). We observed that Rab35 was not restricted to the AMIS (defined by ZO-1) and that part of Rab35 also localized on its sides (β -catenin positive) at the first cell–cell interface (Supplementary Fig. 1a,b and Discussion). Altogether, these results indicate that PODXL is a genuine Rab35-interacting protein and suggest that Rab35 could play a critical role in early steps of cyst development.

Rab35 depletion leads to a complete inversion of polarity.

To test the potential function of Rab35 in apico-basal polarity establishment and PODXL-dependent lumen formation, we depleted Rab35 using independent siRNAs (Fig. 3a and Supplementary Fig. 2a) or shRNAs (Supplementary Fig. 2b,c), and seeded single MDCK-depleted cells into Matrigel for 48 h. In control siRNA conditions, the majority of cysts (>75%) developed a single, PODXL-positive central lumen surrounded by an epithelial monolayer (Fig. 3b,c). In contrast, only 40% of Rab35-depleted cysts formed a single apical lumen. Remarkably, Rab35 depletion led to the appearance of cysts with inverted apico-basal polarity, characterized by mislocalization of PODXL to the outer, ECM-facing plasma membrane (Fig. 3b,c). The remaining Rab35-depleted cysts displayed either multiple lumens or intracellular vacuoles ('other abnormal cysts'; Fig. 3b,c and Supplementary Fig. 2a). All these phenotypes were fully rescued with siRNA-resistant Rab35^{WT} but not with the Rab35^{S22N} mutant (Fig. 3c). The same defects were confirmed using an shRNA targeting a different region of *Rab35* mRNA, and were similarly rescued with Rab35^{WT} but not with the GDP-bound Rab35 (Supplementary Fig. 2b,c). In addition, expression of the Rab35 GAP EPI64B/TBC1D10B (refs 22–24) phenocopied Rab35 depletion (Supplementary Fig. 2d,e). Thus, both depletion and inactivation of Rab35 lead to defects in cyst development.

Using a Rab35 shRNA-IRES-GFP MDCK cell line, we established that fluorescence-activated cell sorting (FACS)-sorted cells that expressed the highest levels of green fluorescent protein (GFP) corresponded to the most Rab35-depleted cells (Fig. 3d). Interestingly, the most-depleted cells were the most prone to develop into inverted cysts (up to 50% of cysts, Fig. 3d, and full rescue by Rab35^{WT} in Supplementary Fig. 2f), indicating that polarity inversion is observed when Rab35 is reduced below a critical threshold. We thus focused on understanding why Rab35 depletion led to this striking phenotype. We first investigated whether polarity markers other than PODXL were also inverted upon Rab35 depletion. Whereas the classical apical markers F-actin, aPKC and Crumbs3 were strongly enriched at the central apical membrane in control cysts, they were all delocalized to the peripheral membrane facing the ECM after Rab35 depletion (Fig. 3e). Consistent with genuine inversion of polarity, the basolateral marker β 1-integrin was absent from the membrane facing the ECM (Fig. 3e). Of note, lateral adherens junctions stained by E-cadherin formed correctly (Fig. 3e). In addition, ZO-1-labelled tight junctions were present, but with inverted location (Fig. 3e). Intracellular organization was also inverted, since sub-apical compartments such as the Golgi apparatus or the recycling compartment labelled by Rab11 were delocalized underneath the membrane facing the ECM (Fig. 3e). Finally, primary cilia, which always form at the apical luminal membrane in control cysts, sprouted from the ECM-facing membrane after Rab35 depletion (Fig. 3e). Altogether, we conclude that strong Rab35 depletion leads to a complete inversion of apico-basal polarity in cysts.

Ectopic fusion of PODXL vesicles upon Rab35 depletion.

We next addressed whether inversion of polarity upon Rab35 depletion occurred already in the initial steps of cyst development. As a first approach, we fixed control- and Rab35-depleted

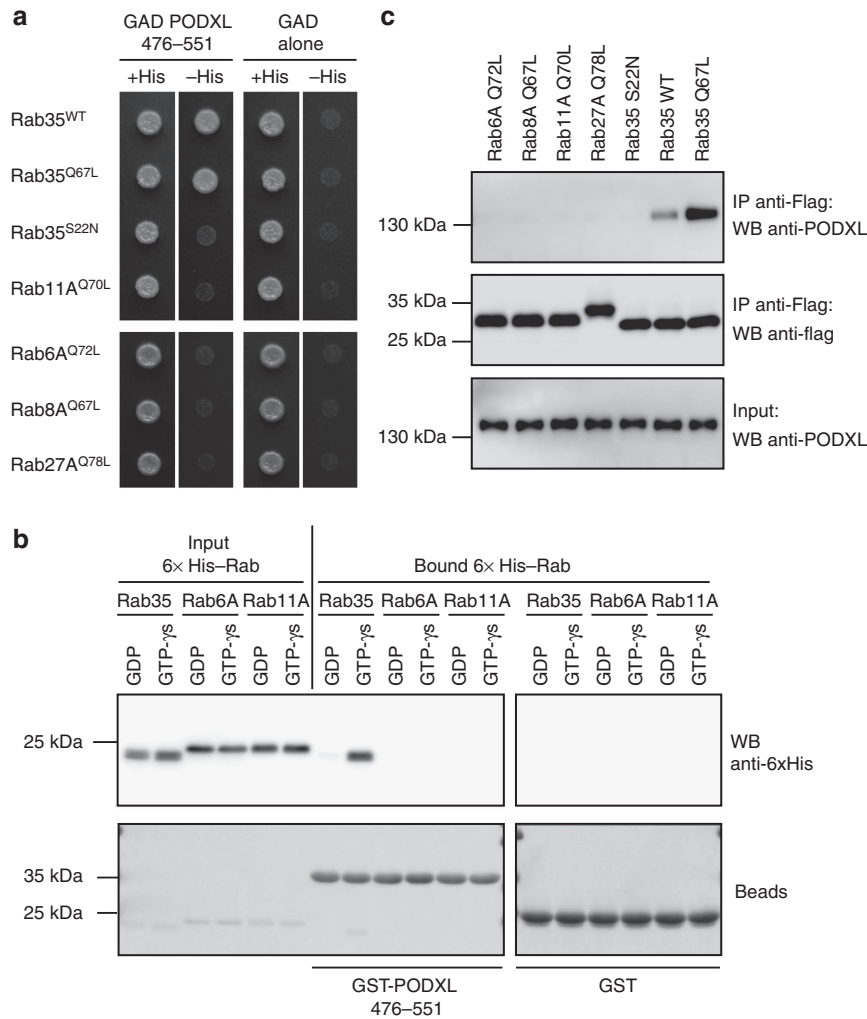


Figure 1 | GTP-bound Rab35 directly interacts with PODXL. (a) *Saccharomyces cerevisiae* L40 reporter strain was transformed with plasmids encoding GAD fused to PODXL cytoplasmic tail (aa 476–551) or GAD alone to examine interactions with LexA fused to Rab35^{WT}, Rab35^{Q67L} (GTP-bound mutant), Rab35^{S22N} (GDP-bound mutant), Rab11A^{Q70L} (GTP-bound mutant), Rab6A^{Q72L} (GTP-bound mutant), Rab8A^{Q67L} (GTP-bound mutant) and Rab27A^{Q78L} (GTP-bound mutant). Growth on a medium without histidine (– His) indicates an interaction with the corresponding proteins in this two-hybrid assay. (b) Recombinant GST or GST-PODXL (aa 476–551) immobilized on glutathione beads was incubated with recombinant 6xHis-tagged Rab35^{WT}, Rab11A^{WT} or Rab6A^{WT}, and loaded with either GDP or GTPγS. Top panel: Rab proteins directly bound to beads were detected by western blot with anti-6xHis antibodies. 5% of the Rab protein input are displayed in the first six lanes. Bottom panel: bead inputs in Ponceau staining. (c) Rab proteins were immunoprecipitated with anti-Flag antibodies (IP) from MDCK cells transfected with plasmids encoding 3xFlag-tagged Rab6A^{Q72L}, Rab8A^{Q67L}, Rab27A^{Q78L}, Rab11^{Q70L}, Rab35^{S22N}, Rab35^{WT} or Rab35^{Q67L}. Flag-proteins and co-immunoprecipitated endogenous PODXL were detected by western blot using anti-PODXL antibodies (top panel) and anti-Flag antibodies (middle panel). Corresponding inputs (5% of total lysates) are displayed in the bottom panel.

cysts 24 h after seeding single cells into Matrigel, and analysed PODXL localization at the two-cell stage (Fig. 4a). While 58% of control cysts displayed PODXL at the AMIS (Fig. 4a, arrow), this was the case in 38% of Rab35-depleted cysts (Fig. 4a,b). Interestingly, in line with the increase of inverted cysts observed at 48 h (Fig. 3c), Rab35 depletion led to an increase of cysts with PODXL abnormally located at the membrane facing the ECM already at 24 h (Fig. 4a, arrowheads). This abnormal localization was fully rescued by the expression of siRNA-resistant Rab35^{WT}, but not of GDP-locked Rab35^{S22N} (Fig. 4b). We next turned to time-lapse microscopy of cells expressing GFP-PODXL to precisely characterize how inversion of polarity arose in Rab35-depleted cysts (Fig. 4c). In control cysts, PODXL was present at the plasma membrane and on vesicles during the first metaphase, then it was internalized into internal recycling compartments during telophase, but not yet localized at the AMIS

(Supplementary Movie 1, Fig. 4c top panels, time 0:50; and also Fig. 2a(ii)). Finally, the recycling compartments from both cells moved towards the intercellular bridge and PODXL started to strongly accumulate at the AMIS (Fig. 4c, top panels, arrows). This first description in live cells of PODXL trafficking from the one-cell stage to the two-cell stage of cystogenesis is fully consistent with previous observations in fixed cysts, indicating that PODXL is transcytosed towards the AMIS at the two-cell stage¹⁰. Importantly, PODXL also reached the recycling compartments after Rab35 depletion (Fig. 4c, bottom panels, time 00:30–00:40; and Supplementary Movie 2). However, as these compartments moved towards the cell–cell interface, they became dimmer and a concomitant increase of PODXL back to the ECM-facing plasma membrane was observed. Two hours after mitosis onset, PODXL eventually localized abnormally to the ECM-facing membrane (Fig. 4c, bottom panels, arrowheads). Other examples of movie

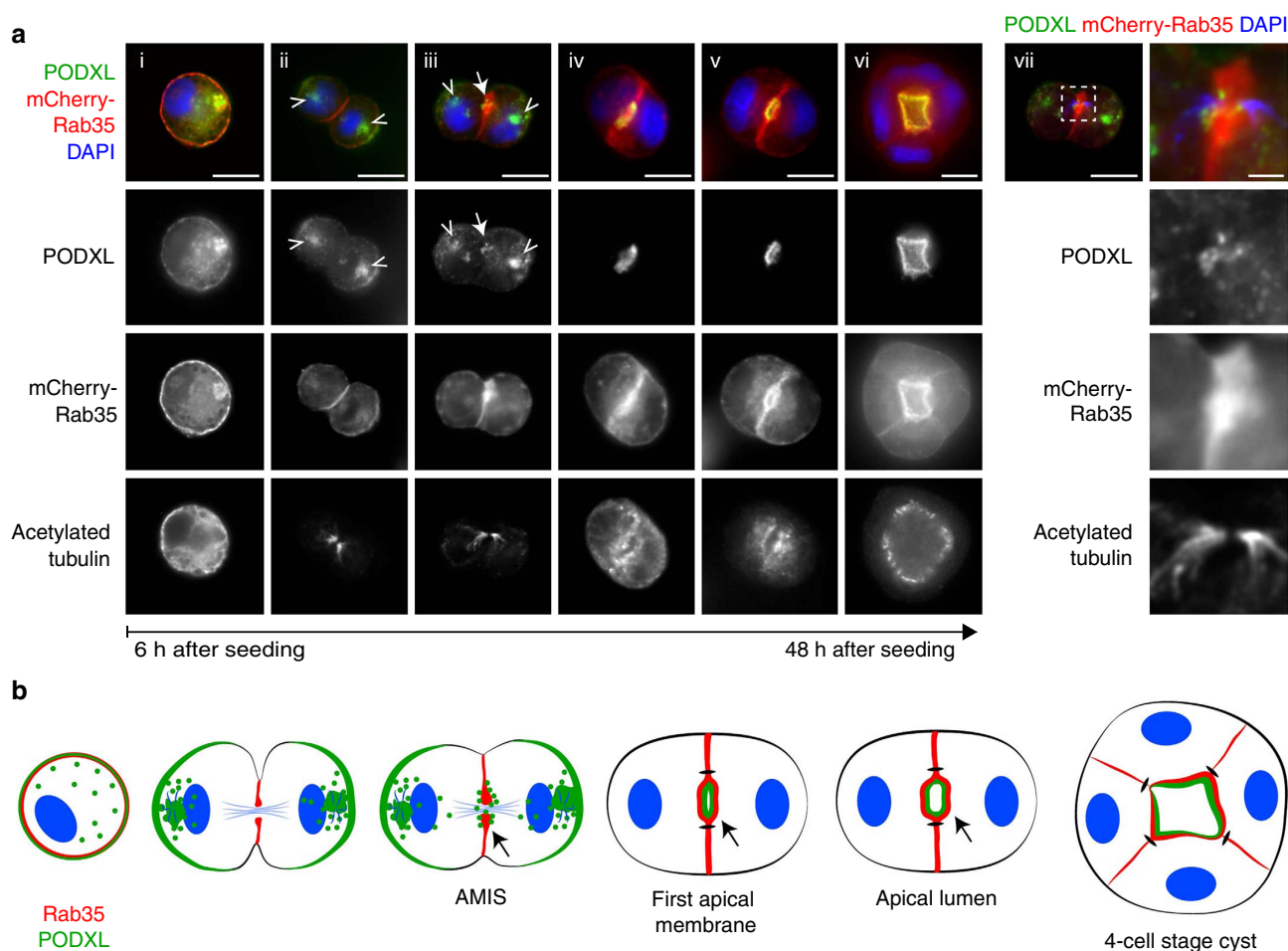


Figure 2 | Rab35 and PODXL co-localize at the apical membrane since the first cytokinesis of 3D cyst development. (a) MDCK cells stably expressing mCherry-Rab35 were cultured in Matrigel and fixed between 6 and 48 h after seeding. Merged pictures show endogenous PODXL (green), DAPI (blue) and mCherry-Rab35 (red) in immunofluorescence. Corresponding channels for PODXL, mCherry-Rab35 and acetylated tubulin are displayed in grey levels. Arrowheads and arrows point towards endocytic recycling compartments and AMIS, respectively. vii is the same cyst as in iii, and the right panels correspond to the intercellular bridge region at higher magnification (merged images and single channels, as indicated). Scale bars, 10 μ m (2 μ m for zoomed region). (b) Localization summary of PODXL (green) and Rab35 (red) through cell division of the cyst-founding cell, two-cell cyst and four-cell cyst. Blue lines: intercellular bridge microtubules. Nuclei are figured in blue. Arrows point towards the AMIS and the first apical membrane.

snapshots are presented in Supplementary Fig. 3. Taken together, these results indicate that inversion of polarity results from the inability of internalized PODXL-containing vesicles to fuse at the membrane surrounding the first cytokinetic bridge in Rab35-depleted cysts.

As Rab35 has been involved in the timing of cytokinetic abscission¹⁷, we investigated whether this could influence the establishment of polarity. We thus depleted Cep55, a protein critical for abscission in HeLa cells, and found indeed a strong delay in cytokinetic abscission in MDCK cells (Supplementary Fig. 4a). However, Cep55 depletion had no effect on apico-basal polarity in cysts (Supplementary Fig. 4b). Therefore, abscission delay cannot account for the inversion of polarity observed after Rab35 depletion.

To test whether the interaction between PODXL and Rab35 was essential for normal cyst polarity, we designed a C-terminal mutant of PODXL unable to bind Rab35 (Supplementary Fig. 4c). We reasoned that Rab GTPases usually interact with partners through hydrophobic amino acids, and screened for mutations that would disrupt the interaction. Using recombinant proteins, we found that the combination of the two point mutations V496A/Y500A in the PODXL cytoplasmic tail completely

abolished the binding to Rab35 (Fig. 4d). We then replaced endogenous PODXL with either GFP alone, siRNA-resistant version of GFP-PODXL WT or GFP-PODXL V496A/Y500A (Fig. 4e). In PODXL-depleted cysts expressing GFP alone, we observed a striking increase of cysts without lumen but no polarity inversion (Fig. 4f). This was accompanied by the accumulation of apical recycling endosomes (positive for Crumbs3) close to the plasma membrane (Fig. 4g), as reported previously in ref. 25. This is consistent with a role of PODXL upstream or at the fusion step of these vesicles with the future apical membrane, as well as for lumen opening^{25–27}. Ruling out off-target effects, the defects observed in PODXL-depleted cysts were fully rescued by expression of GFP-PODXL WT (Fig. 4f). Importantly, replacing endogenous PODXL with GFP-PODXL V496A/Y500A was sufficient to invert cyst polarity, without the need to deplete Rab35 (Fig. 4f, arrow). Time-lapse microscopy of the first cell division revealed that PODXL V496A/Y500A was internalized but failed to be correctly delivered to the presumptive AMIS, and instead accumulated back to the ECM-facing plasma membrane (Fig. 4h and Supplementary Movie 3). Thus, a PODXL mutant unable to interact with Rab35 triggers inversion of cyst polarity from the two-cell stage by preventing fusion of PODXL

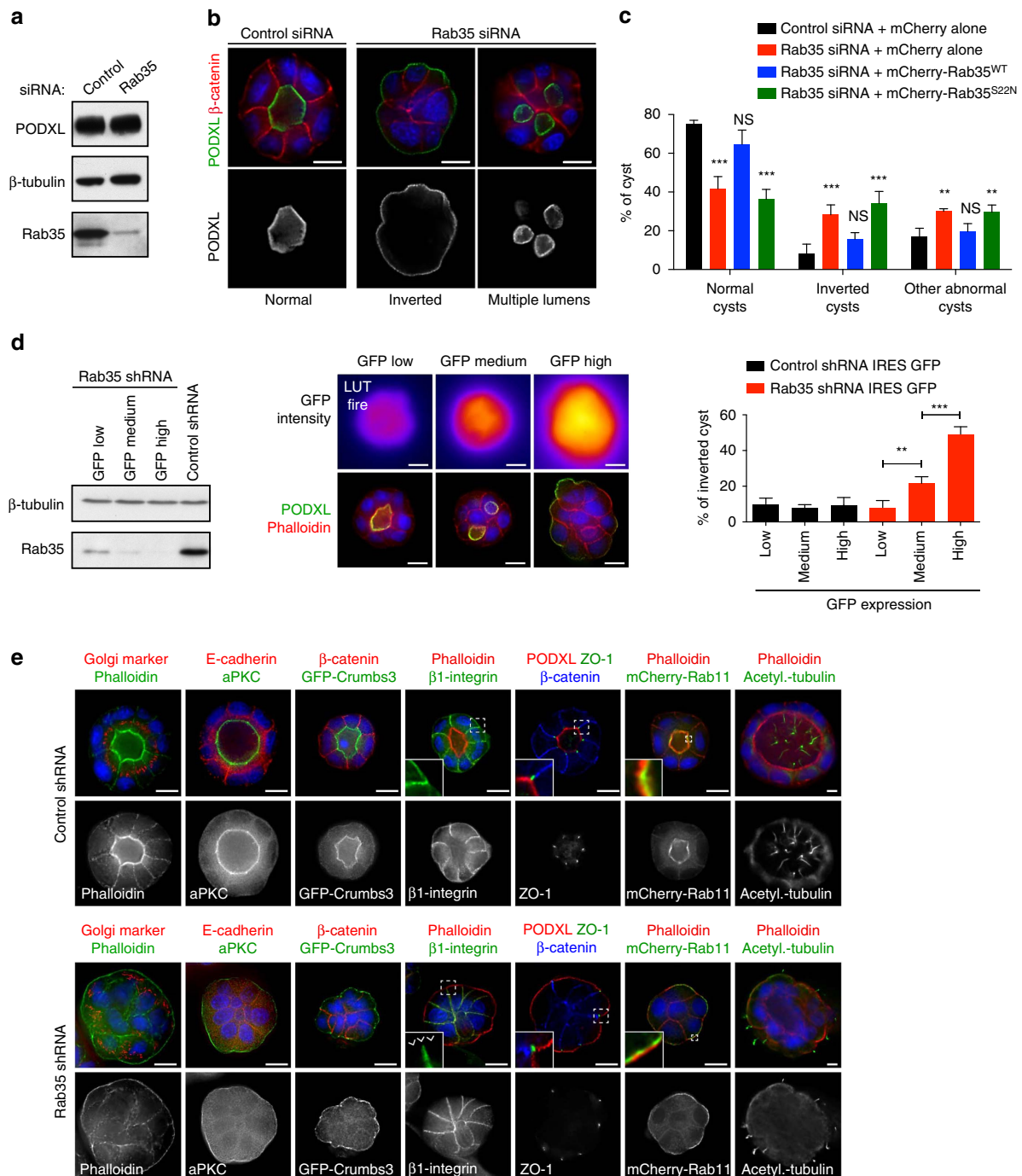


Figure 3 | Rab35 depletion leads to a complete inversion of cyst apico-basal polarity. (a) Western blot of MDCK cell lysates after control or Rab35 depletion, using antibodies detecting PODXL, β -tubulin and Rab35, as indicated. (b) MDCK cells were treated with control or Rab35 siRNAs and seeded into Matrigel for 48 h. Cysts were fixed and stained for DAPI (blue), PODXL (green) and β -catenin (red) or PODXL as single channel (grey), as indicated. Examples of an inverted cyst or a multiple lumen cyst observed after Rab35 depletion are displayed. Scale bar, 10 μ m. (c) MDCK cells were treated with control or Rab35 siRNAs, then transfected with plasmids encoding mCherry alone, siRNA-resistant mCherry-Rab35^{WT} or siRNA-resistant mCherry-Rab35^{S22N}. Cysts were fixed after 48 h in Matrigel and categorized as normal cysts, inverted cysts or other abnormal cysts based on PODXL staining. Mean \pm s.d., $N=3$ independent experiments, 300–900 cysts analysed per condition. Two-way analysis of variance (ANOVA): $^{**}P<0.01$; $^{***}P<0.001$; NS, not significant. (d) Left panels: lysates from Rab35 shRNA IRES GFP MDCK cells sorted according to low, medium and high levels of fluorescence were analysed by western blot, as indicated. Note that Rab35 levels are the most reduced in the highest GFP cells. Middle panels: cells with indicated intensity of GFP fluorescence (top row, LUT fire) were seeded into Matrigel for 48 h, fixed and stained for PODXL (green), F-actin by phalloidin (red) and DAPI (blue). Right panels: quantification of the proportion of inverted cysts based on PODXL localization in MDCK cells expressing either control shRNA (black) or Rab35 shRNA (red), and indicated categories of GFP intensity. Mean \pm s.d., $N=3$ independent experiments, 300–1,500 cysts analysed per condition. Two-way ANOVA: $^{**}P<0.01$; $^{***}P<0.001$; NS, not significant. (e) Control- or Rab35-depleted MDCK cells were cultured in Matrigel for 48 h (except for acetylated (acetyl.) tubulin: 7 days), fixed and stained for apical components (PODXL, F-actin (phalloidin), primary cilia (acetylated tubulin), aPKC, GFP-Crumbs3 and mCherry-Rab11 (sub-apical)), baso-lateral markers (β -catenin, E-cadherin and β 1-integrin) or Golgi apparatus (CTR433 marker), as indicated. Selected channels are also displayed in grey levels. Scale bar, 10 μ m.

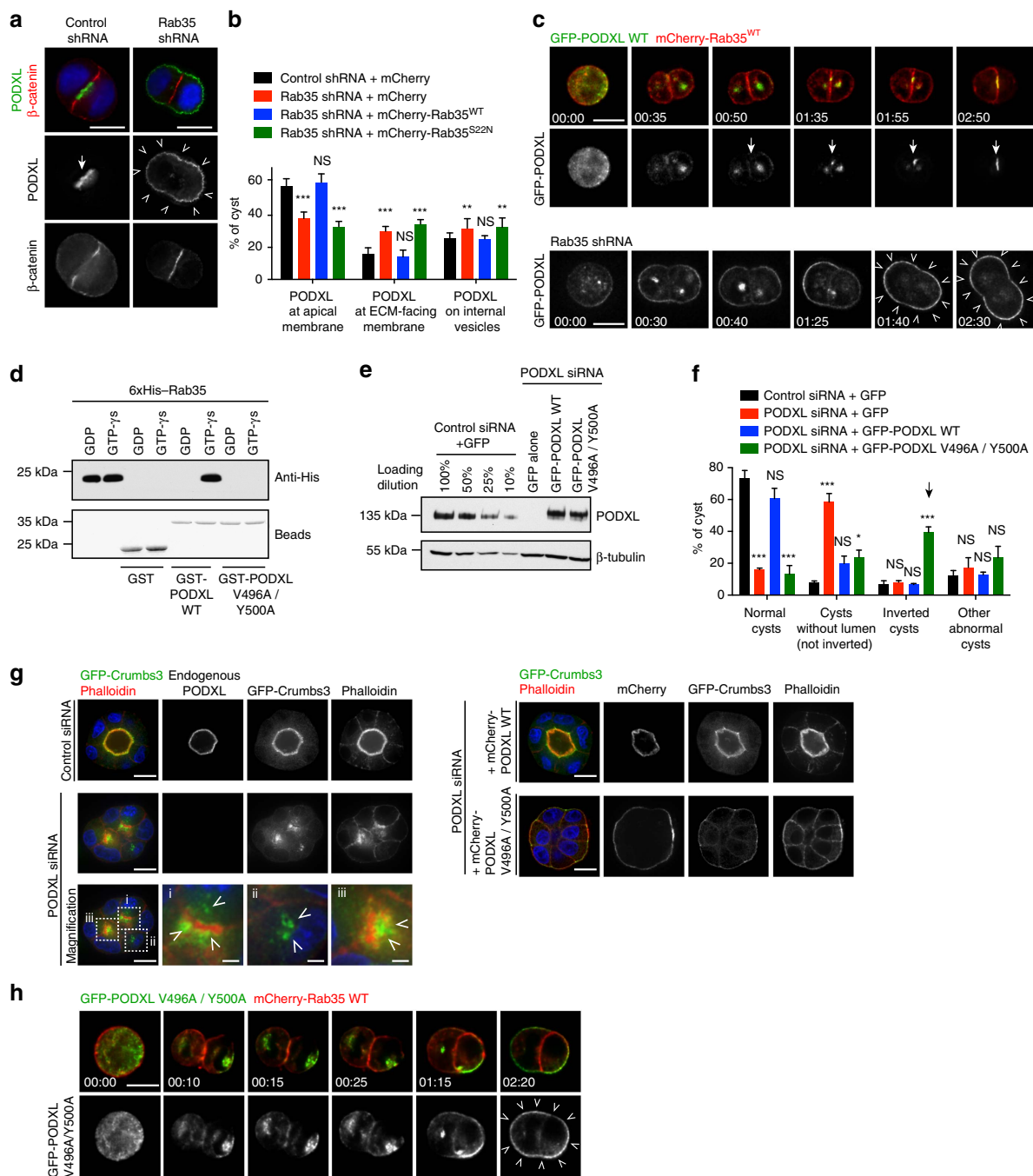


Figure 4 | Ectopic fusion of PODXL-positive vesicles to the ECM-facing membrane on Rab35 depletion or disruption of Rab35/PODXL interaction. (a) Staining for PODXL, β -catenin and DAPI in control- or Rab35-depleted two-cell cysts fixed 24 h after seeding in Matrigel (merge and single channels, as indicated). Scale bar, 10 μ m. (b) Localization of PODXL at the two-cell-stage cyst (24 h in Matrigel) after indicated depletion and plasmid transfection. Mean \pm s.d., $N = 3$ independent experiments, 150–200 two-cell cysts analysed per condition. Two-way analysis of variance (ANOVA): $**P < 0.01$, $***P < 0.001$, NS, not significant. (c) Top two rows: snapshots of time-lapse microscopy from control MDCK cells seeded into Matrigel and expressing mCherry-Rab35^{WT} (red) together with GFP-PODXL (green). Bottom row: snapshots of time-lapse microscopy from Rab35 shRNA MDCK cells seeded into Matrigel and expressing GFP-PODXL. Arrowheads indicate ectopic localization of PODXL after the first division. Scale bar, 10 μ m. Time stamps: (hour:min) using mitotic entry as origin. (d) GST-pull-down experiment as described in Fig. 1b, using either GST alone, GST-PODXL tail (aa 476–551) as in WT or GST-PODXL tail (aa 476–551) with the two substitutions V496A and Y500A. (e) MDCK cells treated with PODXL siRNAs for 3 days and transfected with indicated plasmids. Western blot showing PODXL (loading control: β -tubulin). For comparison, dilutions of lysates from control siRNA-treated MDCK cells transfected with plasmids encoding GFP alone have been used. 100% correspond to the amount loaded in the PODXL siRNA conditions. (f) Proportion of normal cysts, cysts without lumen (but not inverted), inverted cysts and other abnormal cysts following seeding of the cells described in e. in Matrigel for 48 h. Mean \pm s.d., $N = 3$ independent experiments, 150–500 cysts analysed per condition. Two-way ANOVA: $*P < 0.05$; $***P < 0.001$; NS, not significant. (g) MDCK cells as described in e were co-transfected with GFP-Crumbs3, fixed after 48 h in Matrigel and stained as indicated. Magnification: GFP-Crumbs3-positive vesicles close to the plasma membrane in displayed PODXL-depleted cyst. Scale bar, 10 μ m (2 μ m for zoomed region). (h) Snapshots of time-lapse microscopy from PODXL-depleted MDCK cells seeded into Matrigel and expressing mCherry-Rab35^{WT} (red) together with siRNA-resistant GFP-PODXL full-length V496A Y500A mutant (green). Single PODXL channel also displayed in grey levels. Arrowheads indicate ectopic localization of PODXL mutant after the first division. Scale bar, 10 μ m.

vesicles at the first cell–cell interface, exactly as observed after Rab35 depletion. Remarkably, fusion of the PODXL-positive vesicles to the ECM-facing membrane is sufficient to invert apical polarity, likely because they can transport key apical determinants such as aPKC, Cdc42 and Crumbs3 (refs 10,14 and see below).

GTP-bound Rab35 directly tethers PODXL-positive vesicles.

Given the physical interaction between Rab35 and the PODXL cytoplasmic tail, as well as the unique localization of Rab35 at the cleavage furrow before PODXL vesicle fusion, these results raised the exciting possibility that Rab35 might act as a direct tether that would capture internalized PODXL vesicles, and thus determine AMIS and lumen location at the cyst centre. To test this tethering model, we experimentally delocalized a GTP-locked mutant of Rab35 to the mitochondrial membrane, by fusing it to the mitochondria-targeting signal of *Listeria monocytogenes* ActA (ref. 28; Rab35^{Q67L}-Mito). As expected, this Rab35-chimera localized exclusively to the mitochondrial surface in MDCK cells (Fig. 5a–l). Strikingly, expression of this construct was sufficient to tether vesicles positive for PODXL at the surface of mitochondria, these vesicles appeared as dotted structures closely apposed to the smooth staining of Rab35^{Q67L}-Mito (Fig. 5a arrowheads). Importantly, no PODXL vesicles were tethered around mitochondria if the GDP-bound mutant of Rab35 was used (Rab35^{S22N}-Mito; Fig. 5b) or when GTP-locked Rab11A^{Q70L}-Mito was expressed (Supplementary Fig. 5a). Using live cell imaging, we confirmed that individual PODXL vesicles were tethered around mitochondria by Rab35^{Q67L}-Mito, but not by Rab35^{S22N}-Mito (Supplementary Movie 4). Using Rab35^{Q67L}-Mito to tether PODXL vesicles to mitochondria, we found that these vesicles also contained crucial apical determinants such as GFP-Crumbs3 (Fig. 5c), GFP-Cdc42 (Fig. 5e) and aPKC (Fig. 5g). This was not observed in Rab35^{S22N}-Mito-expressing cells (Fig. 5d,f,h). Furthermore, Rab11-positive vesicles were also tethered around mitochondria by Rab35^{Q67L}-Mito but not by Rab35^{S22N}-Mito (Supplementary Fig. 5b,c), consistent with PODXL and Rab11 being trafficked in the same vesicles^{9,10,14}. As expected for a direct tethering through Rab35 interaction with the PODXL cytoplasmic tail, the tethering of Rab11-positive vesicles crucially depended on the presence of PODXL, since it was lost upon PODXL depletion (Fig. 5i,j). To confirm the importance of the PODXL/Rab35 interaction in vesicle tethering, we analysed cells in which endogenous PODXL had been replaced by either siRNA-resistant GFP-PODXL V496A/Y500A or GFP-PODXL WT (Fig. 5l), vesicles containing GFP-PODXL V496A/Y500A failed to be tethered around mitochondria by Rab35^{Q67L}-Mito (Fig. 5k). Altogether, we conclude that GTP-bound Rab35 tethers intracellular vesicles containing key apical markers (PODXL, aPKC, Cdc42 and Crumbs3) through physical interaction with the cytoplasmic tail of PODXL.

Delocalizing Rab35 on mitochondria prevents AMIS formation.

If this Rab35-dependent tethering mechanism is important for apical membrane determination, one should expect profound polarity defects when Rab35 is delocalized from the plasma membrane. We thus analysed the consequences of delocalizing Rab35 at mitochondria during cystogenesis. Interestingly, we observed that the proportion of cysts with PODXL correctly localized at the AMIS was strongly reduced upon Rab35^{Q67L}-Mito expression, in line with ~50% of cysts displaying PODXL vesicles at mitochondria (Fig. 6a, 24-h cysts). This was accompanied by the absence of an apical membrane, as shown by a continuous β -catenin staining at the cell–cell interface

(Supplementary Fig. 5d,f,h,j, arrows). While Par3 localized to the tight junctions, other apical proteins such as Crumbs3, Cdc42 and aPKC were not correctly localized in the centre of the two-cell-stage cyst in Rab35^{Q67L}-Mito-expressing cells (Supplementary Fig. 5d,f,h,j). As expected, apical determinants localized normally at the two-cell stage in cysts expressing Rab35^{S22N}-Mito (Supplementary Fig. 5e,g,i,k). As a consequence, expression of Rab35^{Q67L}-Mito resulted in the appearance of disorganized cysts without lumen, since PODXL-positive vesicles were tethered around mitochondria throughout cyst development (Fig. 6b, 48-h cysts). In contrast, PODXL was normally enriched at the AMIS after Rab35^{S22N}-Mito expression (Fig. 6a), and cysts with a PODXL-positive apical lumen developed normally in this condition (Fig. 6b). Thus, delocalizing GTP-bound Rab35 on mitochondria displaced PODXL-positive vesicles from the plasma membrane, which prevented AMIS formation and apico-basal polarity establishment.

Discussion

Understanding how apical polarity is established *de novo* and how lumens form in epithelial organs represent crucial biological questions^{1–5}. In certain organs, such as the acini of exocrine glands, lumens result from the apoptosis of inner glandular cells, through a process called cavitation¹. In contrast, lumen formation can arise in other tissues through hollowing, for instance, during the development of vascular endothelia and kidneys¹. In the developing mouse aorta, apical membrane establishes *de novo* from pre-existing cell–cell contacts by targeted exocytosis of apical cargos towards the AMIS²⁷. In this system, lumen opening involves PODXL, whose anti-adhesive properties promote cell–cell repulsion. During kidney embryogenesis, the existence of an AMIS has also been described before lumen formation and its elongation into a tubular nephron²⁹. MDCK cells form cysts very similar to the embryonic renal vesicle, thus making them an attractive model to study apico-basal establishment and lumen morphogenesis *in vitro*. This led to the key concept that MDCK cysts establish an apical membrane at the two-cell stage through transcytosis of apical proteins, including PODXL, which will later delimit an open lumen^{9,10} (Fig. 2b). Interestingly, transcytosis events are temporally and spatially associated with the positioning of the cytokinetic bridge microtubules, which likely promote the delivery of apical recycling endosomes towards the AMIS at the centre of the two-cell cyst¹⁴. Accordingly, kinesin-2-dependent apical trafficking of the Rab11/FIP5-positive endosomes towards the AMIS during cytokinesis is important for the formation of a single, central apical lumen^{12,15}. Thus, the formation of the AMIS, which is defined by the tight junction marker ZO-1 (ref. 12), Par3/aPKC and the exocyst subunit Sec8 (ref. 10), must be coordinated with cytokinesis. However, the molecular mechanisms coupling cell division, delivery of apical initiation determinants and lumen formation remained elusive.

Here we propose that Rab35 acts as a molecular tether that captures PODXL-containing vesicles around the cytokinetic bridge of the cyst-founding cell (Fig. 7). This simple model explains how lumen formation is coupled with the position of the first division apparatus, at the centre of the cyst. Rab35 is indeed localized at the AMIS labelled by ZO-1 around the cytokinetic bridge (Supplementary Fig. 1a). There, we observed co-localization between Rab35 and β -catenin (Supplementary Fig. 1b, arrowheads). This suggests that at least at early stages when PODXL has not yet fused to the AMIS (Supplementary Fig. 1a,b), the AMIS overlaps with adherens junction markers. This observation has been confirmed with co-localization between ZO-1 and β -catenin on the side of the tubulin-positive bridge (Supplementary Fig. 1c). Later, after establishment of the apical membrane (positive for PODXL), there is a clear segregation

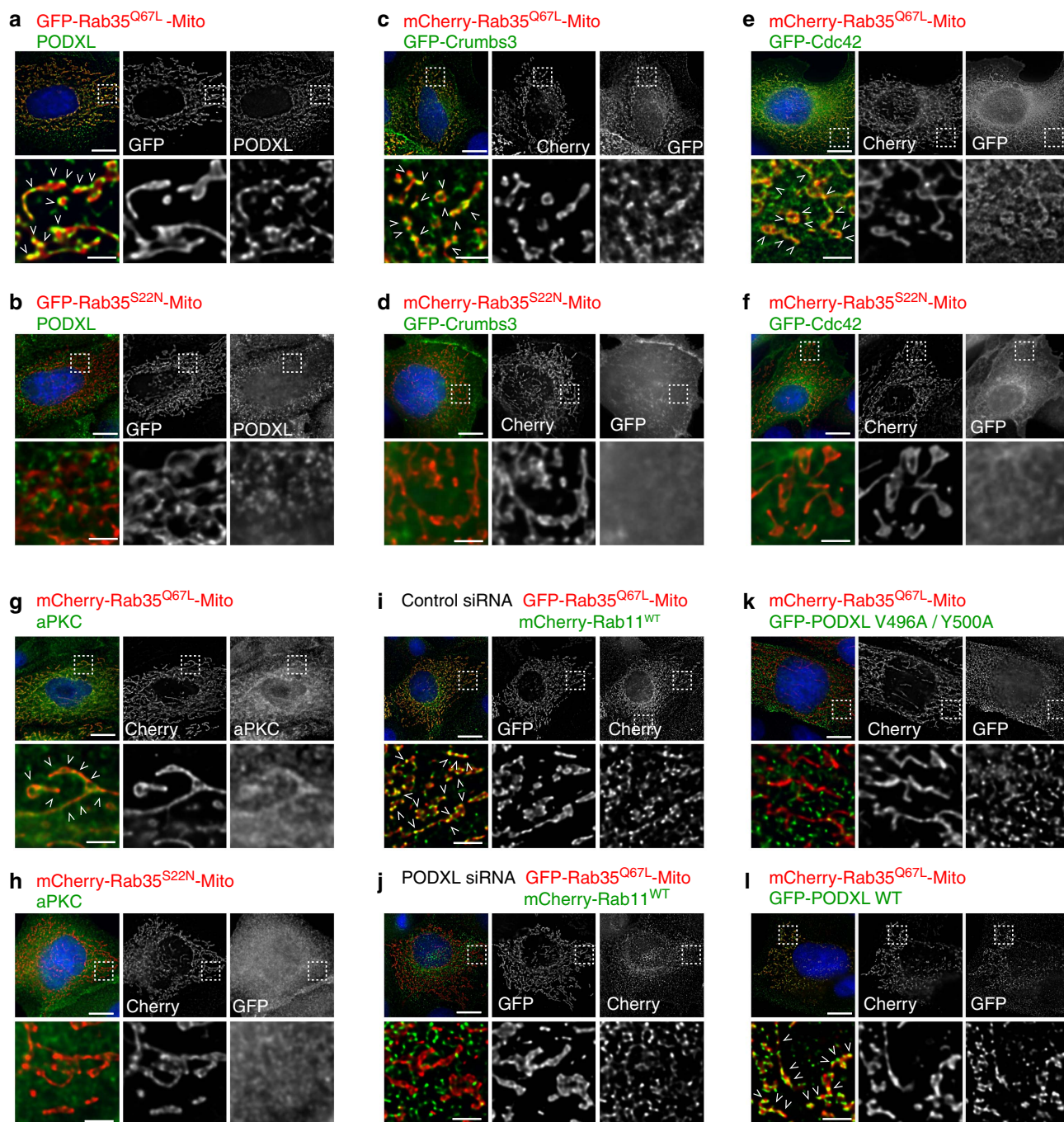


Figure 5 | GTP-bound Rab35 acts a direct molecular tether for PODXL-positive vesicles transporting key apical determinants. (a–h) MDCK cells were transfected for 72 h with plasmids encoding either fluorescently tagged Rab35^{Q67L} or Rab35^{S22N} fused to the mitochondrial targeting signal of ActA (-Mito), as indicated. In the merged images, Rab35-Mito proteins are displayed in red, and PODXL, GFP-Crumbs3, GFP-Cdc42 or aPKC in green. (i, j) MDCK cells were treated with either control or PODXL siRNAs for 72 h, and co-transfected for 72 h with plasmids encoding mCherry-Rab11^{WT} and either GFP-Rab35^{Q67L}-Mito or GFP-Rab35^{S22N}-Mito, as indicated. (k, l) MDCK cells were co-transfected for 72 h with plasmids encoding mCherry-Rab35^{Q67L}-Mito and either GFP-PODXL WT or GFP-PODXL V496A/Y500A. In the merged images, Rab35^{Q67L}-Mito is displayed in red, and PODXL^{WT} or mutant in green. For a–l individual channels in grey levels and higher magnification of the regions delimited by a dash line are displayed, as indicated. Scale bars, 10 μ m for unzoomed regions and 2 μ m for zoomed regions. Arrowheads indicate examples of close-apposition vesicles (green) with mitochondrial Rab35^{Q67L} (red).

between adherens junction markers and apical markers (Supplementary Fig. 1d), suggesting remodelling of the junctions. Thus, the AMIS is a dynamic compartment and its molecular definition changes with time. In addition, a pool of Rab35 also localizes at the cell–cell interface not labelled by ZO-1 (Supplementary Fig. 1b). Interestingly, we observed that PODXL

vesicles are tethered/fused mainly at the ZO-1-positive AMIS (as expected) but also on its sides (Supplementary Fig. 1e, arrowheads), where Rab35 is also present. This is consistent with the proposed tethering model, and suggests that a pool of POXL vesicles can also interact with β -catenin/Rab35-positive membranes close to the AMIS. This raises the possibility that vesicles

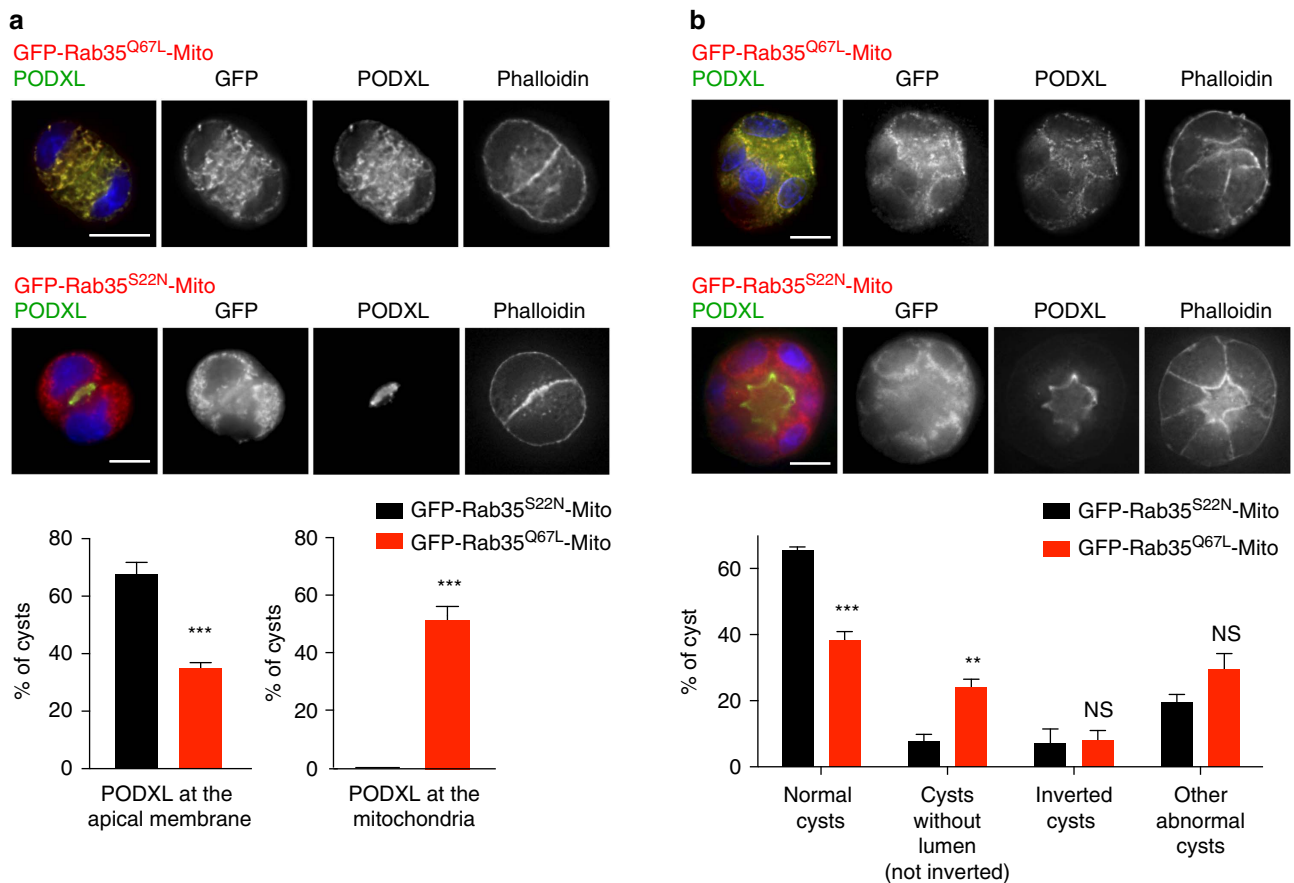


Figure 6 | Delocalizing GTP-bound Rab35 on mitochondria prevents AMIS formation and apico-basal polarity establishment. (a) MDCK cells transfected with either GFP-Rab35^{S22N}-Mito or GFP-Rab35^{Q67L}-Mito were seeded into Matrigel for 24 h, cysts were fixed and stained for PODXL and F-actin (phalloidin). Merged images and single channels in grey levels are displayed, as indicated. Scale bar, 10 mm. Graphs: proportion of cysts with PODXL normally localized at the apical membrane (left graph) or with PODXL localized at the mitochondria (right graph) in each condition. Mean \pm s.d., $N=3$ independent experiments, 100–200 two-cell cysts analysed per condition. Two-way analysis of variance (ANOVA): *** $P<0.001$. (b) MDCK cells were transfected for 24 h with plasmids encoding either GFP-Rab35^{Q67L}-Mito or GFP-Rab35^{S22N}-Mito and seeded into Matrigel for 48 h. Cysts were then fixed and stained for PODXL (green), F-actin (phalloidin, red) and DNA (DAPI). Merged images and individual channels in grey levels are displayed. Scale bar, 10 mm. Graphs: normal cysts, cysts without lumen, inverted cysts and other abnormal cysts were quantified based on PODXL and Phalloidin staining. Two-way ANOVA: ** $P<0.01$; *** $P<0.001$; NS, not significant. Mean \pm s.d., $N=3$ independent experiments, >100 cysts analysed per condition.

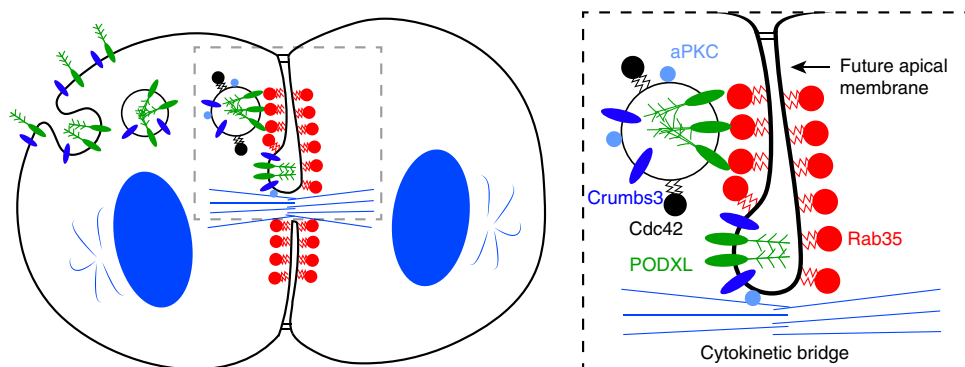


Figure 7 | Model for coupling the first cyst cytokinesis and the initiation of the apical lumen at the centre of cysts. Rab35 located at the cell-cell interface surrounding the first intercellular bridge (red) directly tethers internalized PODXL-positive vesicles (green) containing Crumbs3, aPKC and Cdc42 through direct binding to the PODXL cytoplasmic tail. This allows the targeting of vesicles transporting both lumen-promoting factors and key apical determinants to initiate apical polarity at the centre of the cyst-founding cell.

could deliver PODXL mainly at the membrane surrounding the bridge (AMIS) but also on its sides, and that apical proteins later coalesce into a single domain while junctions are being remodelled.

Contrary to known tethering machineries (for example, exocyst) that link membranes via assembly of protein sub-complexes found on either membrane, Rab35 tethers vesicles through a physical, direct interaction with the cytoplasmic tail of one of

their transmembrane cargo. This thus represents a new mode of tethering, through *trans* interaction between the acceptor compartment and intracellular vesicles. Indeed, Rab GTPases have been shown to be essential regulators of traffic by promoting vesicle formation, targeting and fusion of Rab-positive vesicles with the acceptor compartment^{18,19}. Here we provide the evidence that Rab GTPases can unexpectedly act as direct and specific receptors for vesicles. Several examples of Rab/transmembrane cargo interactions have been reported (for example, Rab4/CFTR cystic fibrosis chloride channel), but their mechanistic significance remains largely unclear³⁰. This novel tethering mode could thus resolve the function of Rab/cargo interactions beyond cyst development. Interestingly, nothing was known about Rab35 in epithelial polarity, except that it regulates branching of polarized seamless tracheal tubes in *Drosophila*³¹. We show here that Rab35 plays a critical role for selectively defining the destination of vesicles that initiate the establishment of polarity. Of note, Rab35 has been involved in the trafficking of a number of cargoes from the endosomes, such as TfR or CI-MPR (refs 16,17,32–34). However, there is no effect of Rab35 depletion on endogenous PODXL or GFP-PODXL internalization from the plasma membrane (Supplementary Fig. 6a–d). Thus, the inversion of polarity observed after Rab35 depletion does not result from the retention of PODXL at the ECM-facing membrane. In addition, depletion of the two known Rab35 effectors in trafficking (OCRL (ref. 32) and MICAL-L1 (refs 33,35)) did not lead to polarity inversion (Supplementary Fig. 6e–g), as previously shown for OCRL in pure Matrigel cultures³⁶. This suggests that Rab35 depletion does not impair PODXL trafficking through early endosomes, as reported for TfR and CI-MPR in HeLa cells³², and is in agreement with the presence of transcytosed PODXL in recycling endosome after Rab35 depletion (Fig. 4c and Supplementary Fig. 3a). Altogether, these observations are consistent with a function of Rab35 in targeting PODXL vesicles generated from the Rab11-positive recycling compartment to the future apical membrane (Fig. 7). Of note, the fusion of PODXL vesicles to the AMIS occurs between 1 and 10 h after the metaphase–anaphase transition in control situations, depending on the cysts (Supplementary Fig. 3b). The same cyst-to-cyst variability is observed in Rab35-depleted cysts, until internalized PODXL is fused back to the ECM-facing membrane (Supplementary Fig. 3b). Thus, the process of apical membrane establishment in wild-type cysts is robust but the timing varies.

Our study reveals that PODXL plays a pivotal and broader role in cyst development than previously expected. First, PODXL plays a role in lumen opening, likely by its negatively charged, anti-adhesive extracellular domain^{25–27}. Second, our data support the idea that PODXL, directly or more likely indirectly, is necessary for the fusion of the vesicles to the plasma membrane. Indeed, in the absence of PODXL, vesicles containing Crumbs3 do not fuse with the plasma membrane, but rather appear close to the cortex (Fig. 4g), confirming previous reports²⁵. Third, PODXL directly participates in the tethering of vesicles containing key determinants for the establishment of the apico-basal polarity to the future apical surface (this study). Accordingly, PODXL-positive vesicles transport other transmembrane apical proteins (for example, Crumbs3) and also a pool of the cytosolic apical determinants such as Cdc42 and aPKC (Fig. 5 and refs 10,37). While vesicular transport (in that case through the PODXL/Rab35 interaction) is the only way for targeting transmembrane apical proteins, this mechanism also possibly contributes to target a pool of Cdc42/aPKC at the future apical domain. However, other pathways (such as the PtdIns(4,5)P₂–Annexin2–Cdc42 pathway³) likely function in parallel to deliver cytosolic apical determinants. The importance

of PODXL-vesicle fusion at the first cell–cell interface likely explains why Rab35, together with multiple but non-redundant mechanisms of tethering (Rab11/exocyst, Rab11/FIP5/cingulin and Rab27/Slp4-a (refs 7,10–12,38)), is essential for correct initiation of apico-basal polarity in cysts. While Rab35 appears as a major factor promoting the establishment of the apical domain, it is likely the combination of different tethering and fusion factors, together with bridge microtubules and directed molecular motors^{12,15}, that collectively allow the definition of a robust and properly localized apical membrane.

Complete inversion of cyst polarity has been described in only a few instances^{39–45}. In particular, depletion of β 1-integrin interrupts laminin signalling from the extracellular matrix cues and leads to inverted cysts when cultured in pure collagen I matrices⁴¹. As Rab35 regulates β 1-integrin recycling in HeLa cells^{46,47}, one can wonder whether Rab35 depletion could additionally perturb polarity by preventing β 1-integrin trafficking to the cell surface. This is unlikely since Rab35 depletion, on the opposite, increases recycling of β 1-integrin to the plasma membrane⁴⁶. In addition, PODXL is not known to be involved in β 1-integrin trafficking and replacing endogenous PODXL by a PODXL mutant that cannot interact with Rab35 is sufficient to induce polarity inversion, even without depleting Rab35 (Fig. 4f,h). Finally, further work revealed that β 1-integrin depletion does not lead to complete inversion of polarity but rather to impaired polarity reorientation characterized by collective front–rear polarization and motility²⁵, when MDCK cells are cultured in Matrigel (our conditions).

Rab35 depletion and overexpression of the Rab35GAP EPI64B experiments revealed that both Rab35 and its level of activation are important for correct establishment of apico-basal polarity and lumen localization (Fig. 3c and Supplementary Fig. 2d,e). This is fully consistent with the observation that PODXL interacts specifically with active, GTP-bound Rab35 (Fig. 1a–c). Interestingly, the Rab35 GAP EPI64B can directly bind to NHERF1/EBP50 (ref. 48), which itself interacts with Ezrin and PODXL at the ECM-facing membrane²⁵. It is possible that the former interaction contributes to maintain low levels of GTP-bound Rab35 at the ECM-facing membrane. Conversely, since Rab35 is directly recruited by PtdIns(4,5)P₂ (ref. 49), it is likely that high levels of PtdIns(4,5)P₂ at the cleavage furrow, as well as the conversion of PtdIns(3,4,5)P₃ into PtdIns(4,5)P₂ via PTEN at the apical plasma membrane³ promote Rab35 localization at this site.

Finally, Rab35 and PODXL have been found to be differentially expressed in several cancers: Rab35 is downregulated in several tumours, including renal carcinomas^{46,50}, whereas PODXL overexpression has been identified as a potent marker for highly aggressive and metastatic cancers with poor prognosis^{51,52}. Since perturbed polarity is associated with tumour progression, the finding that Rab35 directly interacts with PODXL and that its inactivation perturbs both PODXL targeting and polarity may explain the emerging role of Rab35 and PODXL in tumorigenesis^{46,50–53}.

Note added in proof: The Fukuda laboratory identified through comprehensive RNAi screens the Rab GTPases mediating podocalyxin transcytosis and showed that different sets of Rabs, including Rab35, coordinate its transport during cell polarization in 2D and 3D MDCK cells. For more details, see: Mrozowska P. and Fukuda M. Regulation of podocalyxin trafficking by Rab small GTPases in 2D and 3D epithelial cell cultures. *The Journal in Cell Biology*, in press (2016).

Methods

Antibodies and plasmids. The following antibodies were used for immunocytochemistry experiments: mouse anti-PODXL (DSHB Hybridoma 3F2/D8

deposited by G.K. Ojakian); human anti-acetylated-tubulin C3B9-hFc (Institut Curie, Paris, France); goat anti- β -catenin (sc-31,000; Santa Cruz Biotechnology); rabbit anti-ZO-1 (61-7300, Invitrogen); rabbit anti-Par3 (07-330, Millipore); mouse anti-E-cadherin (610181; BD Transduction Laboratories); rabbit anti-aPKC ζ (C-20, Santa Cruz); mouse anti-integrin β 1 (4B4, Coulter Clone); mouse anti-CTR433 (a kind gift from M. Bornens, Institut Curie, Paris, France); and recombinant hVHH anti-GFP-hFc (Institut Curie, Paris, France). Fluorescently labelled secondary antibodies were purchased from Jackson Laboratories. Phalloidin 647 was purchased from Sigma-Aldrich. Mouse anti- β -tubulin (Clone Tub 2.1, Sigma-Aldrich), mouse anti-6xHis (Clone HIS-1, Sigma-Aldrich), mouse anti-GFP (11814460001; Roche), mouse anti-Flag (M2, Sigma-Aldrich), rabbit anti-Rab35 (described in ref. 16) and secondary horseradish-peroxidase-coupled antibodies (Jackson Laboratories) were used for western blot experiments.

The following plasmids were used for the yeast two-hybrid experiments presented in Fig. 1a: pGAD-rabbit PODXL cytoplasmic tail (aa 476–551); pGAD-rabbit PODXL V496A Y500A cytoplasmic tail (aa 476–551); pLex-human wild-type Rab35 K173 (aa 1–173); pLex-human Rab35^{Q67L} K173 (aa 1–173); pLex-human Rab35^{S22N} K173 (aa 1–173); pLex-human Rab11^{Q70L} Y173 (aa 1–173); pLex-human Rab6A^{Q72L} (aa 1–173); pLex-human Rab8A^{Q67L} (aa 1–183); and pLex-human Rab27A^{Q78L} (aa 1–201). Plasmids used for immunofluorescence were the following: pmCherry-human Rab35^{WT} (siRNA-resistant)¹⁷; pmCherry-human Rab35^{S22N} (siRNA-resistant)¹⁷; pEGFP-rabbit wild-type PODXL (a kind gift from K. Simons); GFP-human Crumbs3 (a kind gift from A. Le Bivic); pEGFP-human Cdc42 (a kind gift from S. Etienne-Manneville); pmCherry Rab11 (a kind gift from B. Goud); pEGFP canine Rab11 (a kind gift from Z. Lenkei); pEGFP-EPI64B^{WT}; pEGFP-EPI64B^{R409A}; and pmCherry-tubulin. The plasmids for the mitochondria-targeting experiments pGFP-Rab35^{Q67L}-Mito, pmCherry-Rab35^{Q67L}-Mito, pGFP-Rab35^{S22N}-Mito, pmCherry-Rab35^{S22N}-Mito, pGFP canine Rab11A^{Q70L}-Mito and pmCherry canine Rab11A^{Q70L}-Mito were constructed by PCR as followed: cDNA encoding Rab proteins lacking their last cysteines Rab35^{S22N} (aa 1–200), Rab35^{Q67L} (aa 1–200) and Rab11^{Q70L} (aa 1–212) were fused at their COOH terminus to DNA encoding the mitochondrial targeting sequence 'LILAMLAIGVFSLGAFIKIQLRKN' of *L. monocytogenes* ActA. All constructs were Rab35 shRNA-resistant. All mutations were obtained by Quickchange (Invitrogen).

RNA interference. The following siRNAs were used: canine Rab35, 5'-GCTCAC GAAGAACAGTAAA-3' (Sigma-Aldrich); canine PODXL, 5'-CACTGGAAGTGATGGAGACCT-3' (ref. 26; Sigma-Aldrich); canine Cep55, 5'-AGCAAGAAATCAAATAACA-3' (Smartpool Sigma-Aldrich); canine MICAL-L1, 5'-GAGAGAAGGTGCTGATGCA-3' (ref. 54; Sigma-Aldrich); canine OCRL, 5'-GGTTCCTGCCATT TTCA-3' (ref. 36; Sigma-Aldrich); and control luciferase, 5'-CGUACGCGGAAUACUUCGA-3' (Sigma-Aldrich). The following shRNAs were used: control shRNA, 3'-GTCTCCACGCGCAGTACATTT-5'; and Rab35 shRNA, 3'-CTGGTCCTCCGAGCAAAGAAA-5' (Amsbio). Lentiviral particles of pLenti-H1-shRNA-Rsv-IRES-Pyromycin and pLenti-H1-shRNA-Rsv-IRES-GFP-Pyromycin were provided by Amsbio. The shRNA expression is driven by a tetracycline inducible cytomegalovirus promoter. Rab35 siRNAs were transfected using Amaxa 2 days before seeding cells into Matrigel. Cep55 and PODXL siRNAs were transfected 24 and 48 h before seeding cells into Matrigel.

Yeast two-hybrid screen and experiments. A yeast two-hybrid screen with human Rab35^{Q67L} (aa 1–194) fused to LexA as a bait was carried out by Hybrigenics SA (Paris, France), using a human placenta complementary DNAGal4-activating domain (GAD)-fusion library¹⁷. Specificity experiments (Fig. 1a) were performed by co-transforming the *Saccharomyces cerevisiae* reporter strain L40 with either pGAD-rabbit PODXL (aa 476–551) or pGAD alone together with either pLex-human wild-type Rab35 (aa 1–173), pLex-human Rab35^{Q67L} (aa 1–173), pLex-human Rab35^{S22N} (aa 1–173), pLex-human Rab11^{Q70L} (aa 1–173), pLex-human Rab6A^{Q72L} (aa 1–173), pLex-human Rab8A^{Q67L} (aa 1–183) or pLex-human Rab27A^{Q78L} (aa 1–201). The later plasmids encode for Rab proteins without their COOH-terminal hypervariable regions. Transformed yeast colonies were selected on DOB agarose plates without tryptophan and leucine. Colonies were picked and grown on DOB agar plates with histidine (to select co-transformants) and without histidine (to detect interactions).

Cell cultures and transfections. MDCK II cells (ATCC) were grown in alpha-MEM medium supplemented with 10% fetal bovine serum, 100 U ml⁻¹ penicillin/streptomycin and 200 mM glutamine. Cells were transfected using Amaxa Kit L (Lonza) following the manufacturer's instructions.

Lentiviral transductions and stable cell lines. A stable cell line expressing mCherry-Rab35 was obtained by transfection using AMAXA, followed by selection with 100 ng ml⁻¹ Genetecin (G418) for 2 weeks and FACS sorting for mCherry-positive cells. Stable cell lines expressing control shRNA IRES GFP, Rab35 shRNA IRES GFP, control shRNA or Rab35 shRNA are obtained by lentiviral transduction (10 multiplicity of infection, 10⁷ particles per ml) in growth medium and 5 μ g ml⁻¹ Polybrene, following selection with 1 μ g ml⁻¹ Pyromycin 72 h after transduction. Cells expressing control shRNA IRES GFP or Rab35 shRNA IRES

GFP were sorted by FACS for low, medium and high levels of GFP fluorescence intensities.

Two-dimensional cell culture and immunofluorescence. MDCK cells grown on coverslips were fixed with 4% paraformaldehyde (PFA) for 10 min at room temperature, quenched with 50 mM NH₄Cl for 20 min, permeabilized in 0.1% Triton X-100 for 3 min and incubated in blocking buffer (0.2% BSA, 0.05% saponin and PBS) for 20 min. In Fig. 5a–l and Supplementary Fig. 5a–c, cells were stained with a primary antibody mouse anti-PODXL (1:1,000) and rabbit anti-aPKC ζ (1:1,000) in blocking buffer for 1 h, washed with PBS, incubated with a secondary antibody (1:1,000) in blocking buffer for 1 h, washed, stained with DAPI (4,6-diamidino-2-phenylindole) and mounted with Mowiol.

3D cultures in Matrigel and immunofluorescence. MDCK cells were resuspended in culture medium containing 0.3 mg ml⁻¹ phenol red-free Matrigel (Corning) and seeded into Matrigel-coated eight-well chamber slides (Millicell EZ slide eight-well glass; Millipore) at a concentration of 6,000 single cells per well. Chamber slides were coated with 10 μ l pure Matrigel per well and incubated at 37 °C for 2 min before cell seeding. The cells were incubated for the indicated period of time before fixation with 4% PFA for 30 min at room temperature. Cells were then treated with 50 mM NH₄Cl for 20 min, permeabilized with 0.5% Triton X-100 for 15 min and incubated with a primary antibody in PBS 0.3% saponin for 2 h at room temperature followed by 1 h incubation with a secondary antibody (1:1,000) or labelled Phalloidin (1:4,000) in PBS 0.3% saponin. Nuclei were stained with DAPI for 5 min, chambers were removed and the slides were mounted with Mowiol. The following concentration of primary antibodies were used: mouse anti-PODXL (1:1,000); human anti-acetylated-tubulin (1:200); goat anti- β -catenin (1:200); rabbit anti-ZO-1 (1:200); rabbit anti-Par3 (1:200); mouse anti-E-cadherin (1:200); rabbit anti-aPKC ζ (1:1,000); mouse anti-integrin β 1 (1:200); and mouse anti-CTR433 (1:50).

Immunofluorescence microscopy and deconvolution. Images were acquired with an inverted Ti E Nikon microscope, using a \times 100 1.4 NA (numerical aperture) PL-APO objective lens or a \times 60 1.4 NA PL-APO VC objective lens and MetaMorph software (MDS) driving a CCD (charge-coupled device) camera (Photometrics Coolsnap HQ)^{55,56}. Z-stacks were acquired with a distance of 130 μ m. The 16-bit images were deconvolved using Huygens Professional software (SVI) to reduce off-plane background fluorescence (2–20 iterations, signal/noise 40). Images were then converted into 8-bit images using ImageJ software (NIH). Images in Fig. 4g, Supplementary Figs 1, 2d, 5d–k, 6f were acquired using an inverted Eclipse Ti E Nikon microscope equipped with a CSU-X1 spinning disk confocal scanning unit (MDS), driving a EMCCD Camera (Evolve 512 Delta, Photometrics) Images were acquired with a \times 100 1.4 NA PL-APO objective lens and MetaMorph software (MDS).

Time-lapse microscopy. Two-dimensional cultures (Supplementary Movie 4 and Supplementary Fig. 4a): For time-lapse phase-contrast microscopy, transient or stably transfected MDCK cells were plated on 35-mm glass dishes (MatTek) and put in an open chamber (Life Imaging) equilibrated in 5% CO₂ and maintained at 37 °C. Time-lapse sequences were recorded every 5 min for 48 h (Supplementary Fig. 2a) or every second (Supplementary Movie 4) using a Nikon Eclipse Ti inverted microscope with a \times 20 0.45 NA Plan FluorELWD objective (Supplementary Fig. 4a) or a \times 100 1.4 NA PL-APO objective (Supplementary Movie 4) controlled by Metamorph 6.1 software (Universal Imaging). This microscope was equipped with a cooled CCD camera (HQ2; Roper Scientific). In Supplementary Fig. 4a, cytokinetic abscission time was quantified in mCherry-tubulin-transfected cells by time-lapse microscopy starting from furrow ingression until the cut of the intracellular bridge. In all, 100 cells per condition were analysed. Supplementary Movie 4 was deconvolved using Huygens Professional software SVI (2 iterations, signal/noise 10).

3D cultures for time-lapse microscopy. Transient or stably transfected MDCK cells were resuspended in culture medium containing 0.3 mg ml⁻¹ phenol red-free Matrigel (Corning) and seeded into coated glass bottom 24-well plates (MatTek) at a concentration of 10,000 single cells per well. The glass was coated with poly-L-lysine- γ -polyethyleneglycol (SuSoS) to create an anti-adhesive surface, followed by coating with 5 μ l pure Matrigel before cell seeding. Time-lapse sequences were recorded with a Nikon Eclipse Ti inverted microscope at 5 min for 24 h, \times 100 1.4 NA PL-APO objective. Image sequences were deconvolved using Huygens Professional software (SVI) as described above and assembled with ImageJ software (Supplementary Movie 1–3).

Antibody internalization assay. MDCK cells stably expressing control shRNA or Rab35 shRNA (Supplementary Fig. 6a,b) were plated into six-well plates (500,000 cells per well), washed with cold medium, incubated on ice for 10 min and then incubated with anti-PODXL antibodies 1:400 for 30 min on ice. MDCK cells were washed twice with cold medium; warm medium was added and cells were shifted at

37 °C for various time points. Cells were then shifted back on ice and remaining surface-bound antibodies were removed by treatment with 1 mg ml⁻¹ Pronase (Sigma-Aldrich) for 30 s on ice. The cells were fixed with 4% PFA for 10 min at room temperature, quenched with 50 mM NH₄Cl for 20 min, permeabilized in 0.1% Triton X-100 for 3 min, incubated in blocking buffer (0.2% BSA, 0.05% saponin and PBS) for 20 min and stained with secondary anti-mouse PE antibodies (1:200) before FACS analysis. FACS analysis was carried using MoFlo Astrios, FACS machine (Beckman Coulter) and FlowJo software. For Supplementary Fig. 6c,d MDCK cells stably expressing Rab35 shRNA were transfected with GFP-PODXL WT for 24 h; MDCK cells stably expressing control shRNA were depleted of endogenous PODXL using siRNAs for 3 days and transfected with either GFP-PODXL WT or GFP-PODXL^{V496A/Y500A} for 24 h. The antibody internalization and FACS analysis was performed as described above, but using anti-GFP primary antibodies (recombinant hVHH anti-GFP-hFc; 1:400) and anti-human PE secondary antibodies.

Co-immunoprecipitation assays. MDCK cells were transfected with either 3xFlag-tagged Rab35^{WT}, Rab35^{S22N}, Rab35^{Q67L}, Rab11A^{Q70L}, Rab6A^{Q72L}, Rab8A^{Q67L} or Rab27A^{Q78L} for 24 h using Amaxa. Cells were lysed in 25 mM Tris (pH 7.5), 150 mM NaCl, 10 mM MgCl₂ and 0.1% Triton X-100 (lysis buffer). Post-nuclear supernatants (20 min at 20,000g) were incubated with anti-Flag M2 affinity gel (Sigma-Aldrich) for 2 h, washed with lysis buffer, resuspended into 1 × Laemmli buffer and boiled at 95 °C for 5 min. The amount of co-immunoprecipitated PODXL in each condition was probed by western blot analysis using anti-Flag antibodies (1:2,000).

Bacterial expression and recombinant protein purification. 6xHis-Rab11A^{WT} full-length, 6xHis-Rab6A^{WT} full-length, 6xHis-Rab35^{WT} full-length, GST-PODXL WT (aa 476–551), GST-PODXL V4496A Y500A (aa 476–551) or glutathione S-transferase (GST) alone were expressed in the BL21 pLysS strain of *Escherichia coli* after induction with 1 mM isopropyl-β-D-thiogalactopyranoside at 37 °C for 3 h. Cells were lysed with PBS containing 1 mg ml⁻¹ lysozyme, 1 mM dithiothreitol and protease inhibitor (Roche) by sonication on ice. The GST fusion proteins were affinity-purified using glutathione Sepharose 4B (GE Healthcare) and eluted with 20 mM HEPES at pH 7.5, 150 mM NaCl and 20 mM reduced glutathione. 6xHis-fused proteins were affinity-purified using Ni-NTA Magnetic Agarose Beads (Qiagen) and were eluted in 50 mM Tris (pH 8), 150 mM NaCl, 2 mM MgCl₂ and 250 mM imidazole.

GST-pull down and western blot experiments. 6xHis-Rab35^{WT}, 6xHis-Rab11A^{WT} and 6xHis-Rab6A^{WT} were exchanged with either 1 mM GDP or 200 μM GTPγS in 25 mM Tris (pH 7.5), 100 mM NaCl, 10 mM EDTA, 5 mM MgCl₂ and 1 mM dithiothreitol for 1 h at 37 °C. Nucleotides were then stabilized with 20 mM MgCl₂. GST-PODXL WT (aa 476–551), GST-PODXL V496A Y500A (aa 476–551) or GST alone were loaded onto glutathione Sepharose 4B beads (Pharmacia) in 25 mM Tris (pH 7.5), 1 mM MgCl₂ and 0.2% BSA for 1 h at 4 °C. Beads were then incubated with exchanged 6xHis-Rab proteins in 25 mM Tris (pH 7.5), 50 mM NaCl, 10 mM MgCl₂, 0.1% Triton X-100 and 0.2% BSA. Beads were washed, resuspended into 1 × Laemmli buffer and boiled at 95 °C for 5 min. Pulled-down 6xHis-Rab proteins were detected by western blot using anti-6xHis antibodies (1:5,000) and GST-tagged proteins loaded on beads were detected by Ponceau red staining. Full scans of all western blots are displayed in Supplementary Figs 7 and 8.

Statistical analysis. MDCK cysts were scored into categories and displayed as mean proportions ± s.d. from three independent experiments. Significance was calculated using a two-way analysis of variance with a Tukey *post hoc* test. For abscission times, a non-parametric Kolmogorov–Smirnov test was used. In all statistical tests *P* > 0.05 was considered as not significant.

References

- Sigurbjornsdottir, S., Mathew, R. & Leptin, M. Molecular mechanisms of de novo lumen formation. *Nat. Rev. Mol. Cell Biol.* **15**, 665–676 (2014).
- Bryant, D. M. & Mostov, K. E. From cells to organs: building polarized tissue. *Nat. Rev. Mol. Cell Biol.* **9**, 887–901 (2008).
- Martin-Belmonte, F. *et al.* PTEN-mediated apical segregation of phosphoinositides controls epithelial morphogenesis through Cdc42. *Cell* **128**, 383–397 (2007).
- Jaffe, A. B., Kaji, N., Durgan, J. & Hall, A. Cdc42 controls spindle orientation to position the apical surface during epithelial morphogenesis. *J. Cell Biol.* **183**, 625–633 (2008).
- Datta, A., Bryant, D. M. & Mostov, K. E. Molecular regulation of lumen morphogenesis. *Curr. Biol.* **21**, R126–R136 (2011).
- Rodriguez-Boulán, E. & Macara, I. G. Organization and execution of the epithelial polarity programme. *Nat. Rev. Mol. Cell Biol.* **15**, 225–242 (2014).
- Eaton, S. & Martin-Belmonte, F. Cargo sorting in the endocytic pathway: a key regulator of cell polarity and tissue dynamics. *Cold Spring Harb. Perspect. Biol.* **6**, a016899 (2014).
- Ojakian, G. K. & Schwimmer, R. The polarized distribution of an apical cell surface glycoprotein is maintained by interactions with the cytoskeleton of Madin-Darby canine kidney cells. *J. Cell Biol.* **107**, 2377–2387 (1988).
- Ferrari, A., Veligodskiy, A., Berge, U., Lucas, M. S. & Kroschewski, R. ROCK-mediated contractility, tight junctions and channels contribute to the conversion of a preapical patch into apical surface during isochoric lumen initiation. *J. Cell Sci.* **121**, 3649–3663 (2008).
- Bryant, D. M. *et al.* A molecular network for de novo generation of the apical surface and lumen. *Nat. Cell Biol.* **12**, 1035–1045 (2010).
- Galvez-Santisteban, M. *et al.* Synaptotagmin-like proteins control the formation of a single apical membrane domain in epithelial cells. *Nat. Cell Biol.* **14**, 838–849 (2012).
- Li, D., Mangan, A., Cicchini, L., Margolis, B. & Prekeris, R. FIP5 phosphorylation during mitosis regulates apical trafficking and lumenogenesis. *EMBO Rep.* **15**, 428–437 (2014).
- Wang, T., Yanger, K., Stanger, B. Z., Cassio, D. & Bi, E. Cytokinesis defines a spatial landmark for hepatocyte polarization and apical lumen formation. *J. Cell Biol.* **127**, 2483–2492 (2014).
- Schluter, M. A. *et al.* Trafficking of Crumbs3 during cytokinesis is crucial for lumen formation. *Mol. Biol. Cell* **20**, 4652–4663 (2009).
- Li, D., Kuehn, E. W. & Prekeris, R. Kinesin-2 mediates apical endosome transport during epithelial lumen formation. *Cell. Logist.* **4**, e28928 (2014).
- Kouranti, I., Sachse, M., Arouche, N., Goud, B. & Echard, A. Rab35 regulates an endocytic recycling pathway essential for the terminal steps of cytokinesis. *Curr. Biol.* **16**, 1719–1725 (2006).
- Dambournet, D. *et al.* Rab35 GTPase and OCRL phosphatase remodel lipids and F-actin for successful cytokinesis. *Nat. Cell Biol.* **13**, 981–988 (2011).
- Stenmark, H. Rab GTPases as coordinators of vesicle traffic. *Nat. Rev. Mol. Cell Biol.* **10**, 513–525 (2009).
- Wandinger-Ness, A. & Zerial, M. Rab proteins and the compartmentalization of the endosomal system. *Cold Spring Harb. Perspect. Biol.* **6**, a022616 (2014).
- Chaineau, M., Ioannou, M. S. & McPherson, P. S. Rab35: GEFs, GAPs and effectors. *Traffic* **14**, 1109–1117 (2013).
- Hehny, H. & Doxsey, S. Polarity sets the stage for cytokinesis. *Mol. Biol. Cell* **23**, 7–11 (2012).
- Chesneau, L. *et al.* An ARF6/Rab35 GTPase cascade for endocytic recycling and successful cytokinesis. *Curr. Biol.* **22**, 147–153 (2012).
- Fuchs, E. *et al.* Specific Rab GTPase-activating proteins define the Shiga toxin and epidermal growth factor uptake pathways. *J. Cell Biol.* **177**, 1133–1143 (2007).
- Patino-Lopez, G. *et al.* Rab35 and its GAP EPI64C in T cells regulate receptor recycling and immunological synapse formation. *J. Biol. Chem.* **283**, 18323–18330 (2008).
- Bryant, D. M. *et al.* A molecular switch for the orientation of epithelial cell polarization. *Dev. Cell* **31**, 171–187 (2014).
- Meder, D., Shevchenko, A., Simons, K. & Fullekrug, J. Gp135/podocalyxin and NHERF-2 participate in the formation of a preapical domain during polarization of MDCK cells. *J. Cell Biol.* **168**, 303–313 (2005).
- Strilic, B. *et al.* The molecular basis of vascular lumen formation in the developing mouse aorta. *Dev. Cell* **17**, 505–515 (2009).
- Zhang, J., Fonovic, M., Suyama, K., Bogyo, M. & Scott, M. P. Rab35 controls actin bundling by recruiting fascin as an effector protein. *Science* **325**, 1250–1254 (2009).
- Yang, Z. *et al.* De novo lumen formation and elongation in the developing nephron: a central role for afadin in apical polarity. *Development* **140**, 1774–1784 (2013).
- Aloisi, A. L. & Bucci, C. Rab GTPases-cargo direct interactions: fine modulators of intracellular trafficking. *Histol. Histopathol.* **28**, 839–849 (2013).
- Schottenfeld-Roames, J. & Ghabrial, A. S. Whacked and Rab35 polarize dynein-motor-complex-dependent seamless tube growth. *Nat. Cell Biol.* **14**, 386–393 (2012).
- Cauvin, C. *et al.* Rab35 GTPase triggers switch-like recruitment of the low syndrome lipid phosphatase OCRL on newborn endosomes. *Curr. Biol.* **26**, 120–128 (2015).
- Kobayashi, H., Etoh, K., Ohbayashi, N. & Fukuda, M. Rab35 promotes the recruitment of Rab8, Rab13 and Rab36 to recycling endosomes through MICAL-L1 during neurite outgrowth. *Biol. Open* **3**, 803–814 (2014).
- Allaire, P. D. *et al.* The Connecden DENN domain: a GEF for Rab35 mediating cargo-specific exit from early endosomes. *Mol. Cell* **37**, 370–382 (2010).
- Rahajeng, J., Giridharan, S. S., Cai, B., Naslavsky, N. & Caplan, S. MICAL-L1 is a tubular endosomal membrane hub that connects Rab35 and Arf6 with Rab8a. *Traffic* **13**, 82–93 (2012).
- Rbaibi, Y. *et al.* OCRL1 modulates cilia length in renal epithelial cells. *Traffic* **13**, 1295–1305 (2012).

37. Elias, S., McGuire, J. R., Yu, H. & Humbert, S. Huntingtin is required for epithelial polarity through RAB11A-mediated apical trafficking of PAR3-aPKC. *PLoS Biol.* **13**, e1002142 (2015).
38. Yasuda, T., Saegusa, C., Kamakura, S., Sumimoto, H. & Fukuda, M. Rab27 effector Slp2-a transports the apical signaling molecule podocalyxin to the apical surface of MDCK II cells and regulates claudin-2 expression. *Mol. Biol. Cell* **23**, 3229–3239 (2012).
39. Wang, A. Z., Ojakian, G. K. & Nelson, W. J. Steps in the morphogenesis of a polarized epithelium. I. Uncoupling the roles of cell-cell and cell-substratum contact in establishing plasma membrane polarity in multicellular epithelial (MDCK) cysts. *J. Cell Sci.* **95**, 137–151 (1990).
40. O'Brien, L. E. *et al.* Rac1 orientates epithelial apical polarity through effects on basolateral laminin assembly. *Nat. Cell Biol.* **3**, 831–838 (2001).
41. Yu, W. *et al.* Beta1-integrin orients epithelial polarity via Rac1 and laminin. *Mol. Biol. Cell* **16**, 433–445 (2005).
42. Torkko, J. M., Manninen, A., Schuck, S. & Simons, K. Depletion of apical transport proteins perturbs epithelial cyst formation and ciliogenesis. *J. Cell Sci.* **121**, 1193–1203 (2008).
43. Montealeon, C. L. *et al.* Establishing epithelial glandular polarity: interlinked roles for ARF6, Rac1, and the matrix microenvironment. *Mol. Biol. Cell* **23**, 4495–4505 (2012).
44. Akhtar, N. & Streuli, C. H. An integrin-ILK-microtubule network orients cell polarity and lumen formation in glandular epithelium. *Nat. Cell Biol.* **15**, 17–27 (2013).
45. Peng, J. *et al.* Phosphoinositide 3-kinase p110delta promotes lumen formation through the enhancement of apico-basal polarity and basal membrane organization. *Nat. Commun.* **6**, 5937 (2015).
46. Allaire, P. D. *et al.* Interplay between Rab35 and Arf6 controls cargo recycling to coordinate cell adhesion and migration. *J. Cell Sci.* **126**, 722–731 (2013).
47. Argenzio, E. *et al.* CLIC4 regulates cell adhesion and beta1 integrin trafficking. *J. Cell Sci.* **127**, 5189–5203 (2014).
48. Reczek, D. & Bretscher, A. Identification of EPI64, a TBC/rabGAP domain-containing microvillar protein that binds to the first PDZ domain of EBP50 and E3KARP. *J. Cell Biol.* **153**, 191–206 (2001).
49. Heo, W. D. *et al.* PI(3,4,5)P3 and PI(4,5)P2 lipids target proteins with polybasic clusters to the plasma membrane. *Science* **314**, 1458–1461 (2006).
50. Jones, J. *et al.* Gene signatures of progression and metastasis in renal cell cancer. *Clin. Cancer Res.* **11**, 5730–5739 (2005).
51. Casey, G. *et al.* Podocalyxin variants and risk of prostate cancer and tumor aggressiveness. *Hum. Mol. Genet.* **15**, 735–741 (2006).
52. Somasiri, A. *et al.* Overexpression of the anti-adhesin podocalyxin is an independent predictor of breast cancer progression. *Cancer Res.* **64**, 5068–5073 (2004).
53. Wheeler, D. B., Zoncu, R., Root, D. E., Sabatini, D. M. & Sawyers, C. L. Identification of an oncogenic RAB protein. *Science* **350**, 211–217 (2015).
54. Abou-Zeid, N. *et al.* MICAL-like1 mediates epidermal growth factor receptor endocytosis. *Mol. Biol. Cell* **22**, 3431–3441 (2011).

55. Miserey-Lenkei, S. *et al.* Rab and actomyosin-dependent fission of transport vesicles at the Golgi complex. *Nat. Cell Biol.* **12**, 645–654 (2010).
56. Crowell, E. F., Gaffuri, A. L., Gayraud-Morel, B., Tajbakhsh, S. & Echard, A. Midbody remnant engulfment after cytokinesis abscission in mammalian cells. *J. Cell Sci.* **127**, 3840–3851 (2014).

Acknowledgements

We thank F. Jaulin, G. Michaux, N. Gupta-Rossi, X. Morin and F. Schweisguth for critical reading of the manuscript; G. Michaux, X. Morin and the Echard Lab members for helpful discussions; K. Simons (MPI, Dresden), P. Cossart and S. Etienne-Manneville (Institut Pasteur, Paris), B. Goud (the Plateforme Anticorps Recombinant, Institut Curie, Paris), A. Le Bivic (IBDM, Marseille) and the DHSB (University of Iowa) for reagents and plasmids. We thank the imaging facility Imagopole Institut Pasteur. We thank P.H. Commere from the Cytometry platform Institut Pasteur for FACS analysis. We thank Dr F. Legendre, S. Saunier and R. Salomon (Hôpital Necker, Paris, France) and F. Jaulin (IGR, Villejuif, France) for protocols and discussion. This work has been supported by Institut Pasteur, CNRS, FRM (Equipe FRM DEQ20120323707) and INCA (2014-1-PL BIO-04-IP1) to A.E. K.K. has been awarded a doctoral fellowship from the Pasteur Paris Universités International PhD programme and Carnot-Pasteur MI, and a fellowship from FRM (FDT20150532389).

Author contributions

K.K. carried out all experiments and M.R. provided technical help; A.H. helped for the design of PODXL mutant; K.K. and A.E. designed and interpreted the experiments; K.K. and A.E. wrote the manuscript; A.E. secured funding.

Additional information

Supplementary Information accompanies this paper at <http://www.nature.com/naturecommunications>

Competing financial interests: The authors declare no competing financial interests.

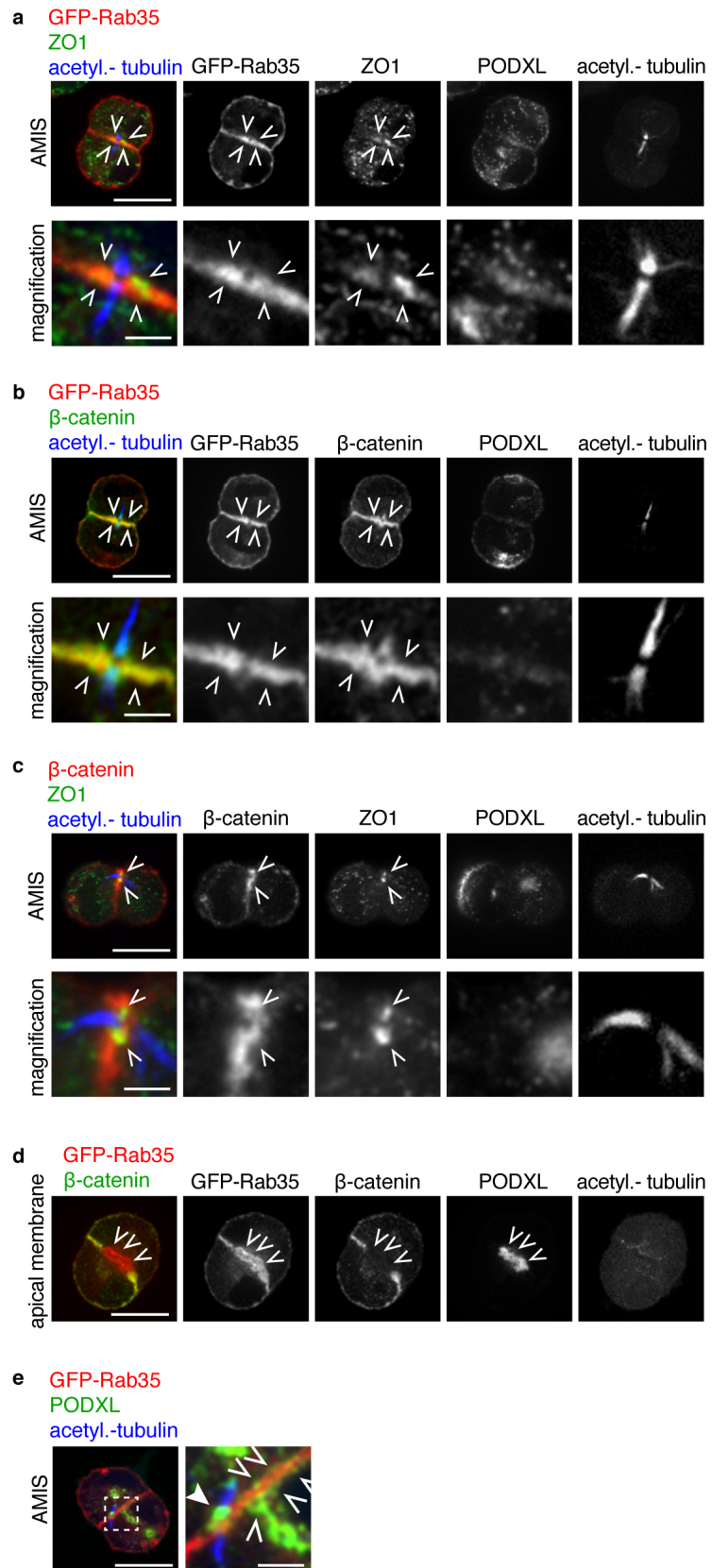
Reprints and permission information is available online at <http://npg.nature.com/reprintsandpermissions/>

How to cite this article: Klinkert, K. *et al.* Rab35 GTPase couples cell division with initiation of epithelial apico-basal polarity and lumen opening. *Nat. Commun.* **7**:11166 doi: 10.1038/ncomms11166 (2016).



This work is licensed under a Creative Commons Attribution 4.0 International License. The images or other third party material in this article are included in the article's Creative Commons license, unless indicated otherwise in the credit line; if the material is not included under the Creative Commons license, users will need to obtain permission from the license holder to reproduce the material. To view a copy of this license, visit <http://creativecommons.org/licenses/by/4.0/>

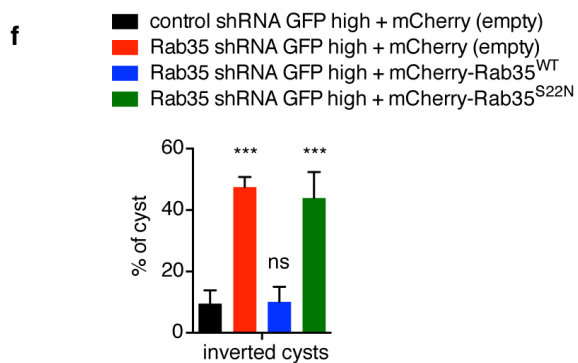
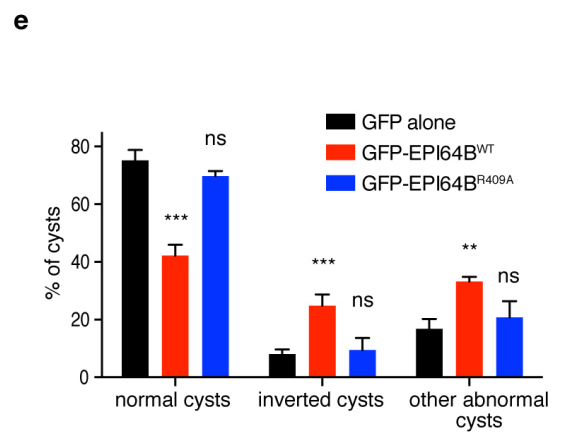
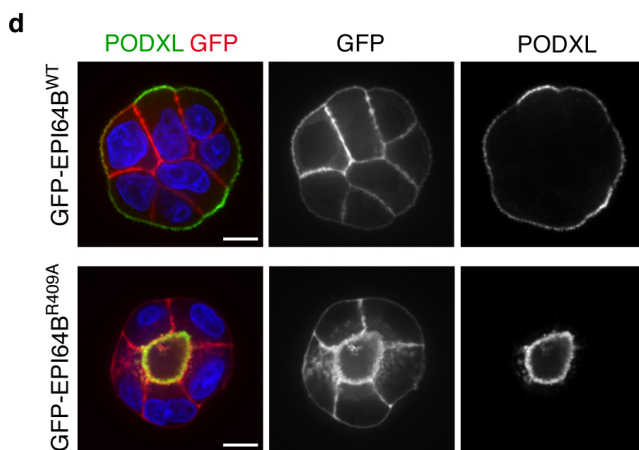
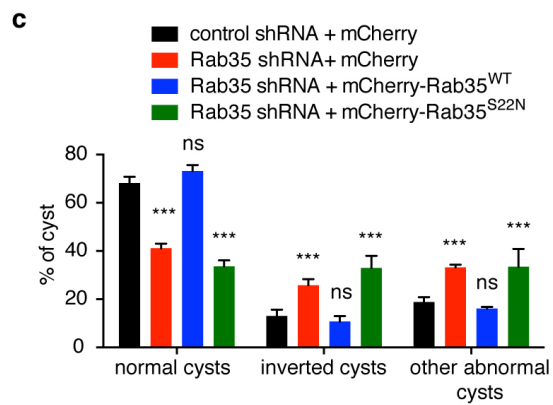
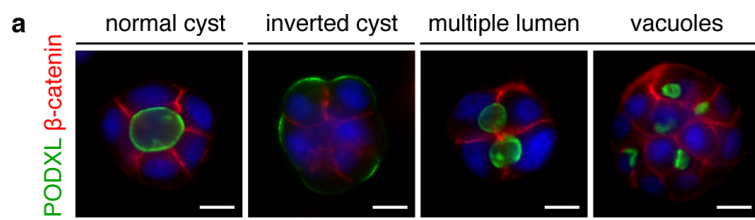
SUPPLEMENTARY INFORMATION



Supplementary Figure 1

Supplementary Figure 1: Rab35 is present at the AMIS

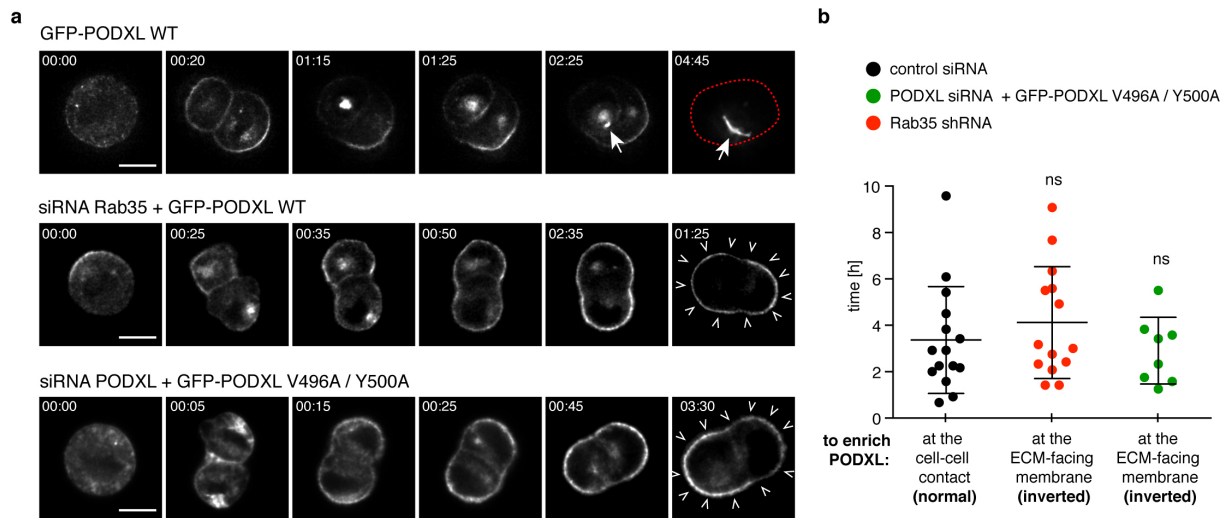
MDCK cells stably expressing GFP-Rab35^{WT} were cultured in Matrigel for 16h and stained for PODXL, acetylated tubulin and ZO1 **(a)** or b-catenin **(b,d)**. Arrowheads indicate the localization of the AMIS (a-b) or the apical membrane (d). Bar: 10 μ m (zoom: 2 μ m) **(c)** MDCK cells were cultured in Matrigel for 16h and stained for PODXL, acetylated tubulin, ZO1 and b-catenin. **(e)** MDCK cells stably expressing GFP-Rab35^{WT} (displayed in red) were cultured in Matrigel for 16h and stained for PODXL (green) and acetylated tubulin (blue). Magnification shows the accumulation of PODXL-vesicles around the Rab35 positive membrane. Bar: 10 μ m (zoom: 2 μ m)



Supplementary Figure 2

Supplementary Figure 2: Rab35 depletion by either siRNAs or shRNAs leads to abnormal cyst development.

(a) MDCK cells were treated with Rab35 siRNAs for 48 h and seeded into Matrigel for 48 h. Cysts were fixed and stained for PODXL (green), β -catenin (red) and DNA (DAPI, blue). Examples of normal cysts, inverted cysts and other abnormal cysts (multiple lumen shared by neighbouring cells or with intracellular vacuoles) upon Rab35 depletion. Bar: 10 μ m. **(b)** Western blot of MDCK cell lysates that stably express shRNAs targeting *Rab35* mRNA, using antibodies detecting PODXL, β -tubulin and Rab35, as indicated. 100% or dilutions of the lysate from control shRNA were loaded for comparison (lysate from Rab35 depletion corresponds to 100%). Rab35 depletion reduced by >90% of endogenous Rab35 levels. **(c)** MDCK cells that stably expressed either shRNAs targeting luciferase (control) or *Rab35* mRNAs were transfected with plasmids encoding mCherry alone, siRNA-resistant mCherry-Rab35^{WT} or siRNA-resistant mCherry-Rab35^{S22N}, as indicated. 48 h after seeding in Matrigel, the proportion of normal cysts, inverted cysts or other abnormal cysts based on PODXL staining was quantified. Mean \pm SD, N= 3 independent experiments, 300-600 cysts analysed per condition. Two-way ANOVA: p<0.001(***), ns: not significant. **(d)** MDCK cells were transfected with either GFP-EPI64B^{WT}, GFP-EPI64B^{R409A} or GFP alone and seeded into Matrigel for 48h. Cysts were fixed and stained for PODXL. Merged images and single channels in grey levels are displayed, as indicated. Bar: 10 μ m. **(e)** Proportion of normal cysts with a single lumen, inverted cysts and other abnormal cysts in each condition. Mean \pm SD, N= 3 independent experiments, >500 cysts analysed per condition. Two-way ANOVA: p<0.001(***), p<0.01(**). **(f)** MDCK cells that stably expressed either control shRNA IRES GFP or Rab35 shRNA IRES GFP were sorted for high levels of fluorescence (GFP high). Cells were then transfected with plasmids encoding mCherry alone, shRNA-resistant mCherry- Rab35^{WT} or shRNA-resistant mCherry-Rab35^{S22N}, as indicated, and seeded into Matrigel for 48 h. The proportion of inverted cysts based on PODXL staining was quantified in each condition. Mean \pm SD, N= 3 independent experiments, 100-600 cysts analysed per condition. Two-way ANOVA: p<0.001(***), ns: not significant.

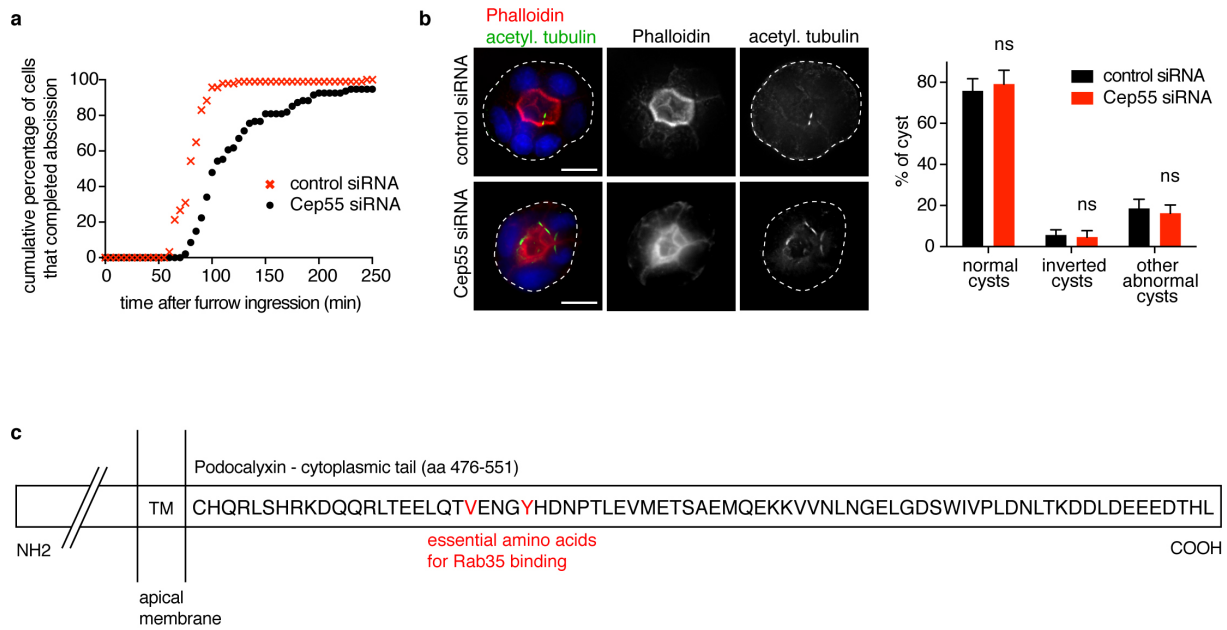


Supplementary Figure 3

Supplementary Figure 3: Additional time-lapse examples of control and Rab35-depleted cysts, and time to form the first apical membrane.

(a) Snapshots of time-lapse microscopy (as in Fig. 4) from control MDCK cells expressing GFP-PODXL^{WT} seeded into Matrigel (top row), Rab35-depleted cells expressing GFP-PODXL^{WT} (middle row) and PODXL-depleted cells expressing GFP-PODXL^{V496A Y500A} (bottom row). Arrows indicate the apical membrane in control cysts and arrowheads the inverted apical membrane in Rab35 depleted or PODXL mutant expressing cells. Bar: 10 μ m. Time stamps: [hour:min] using mitotic entry as origin.

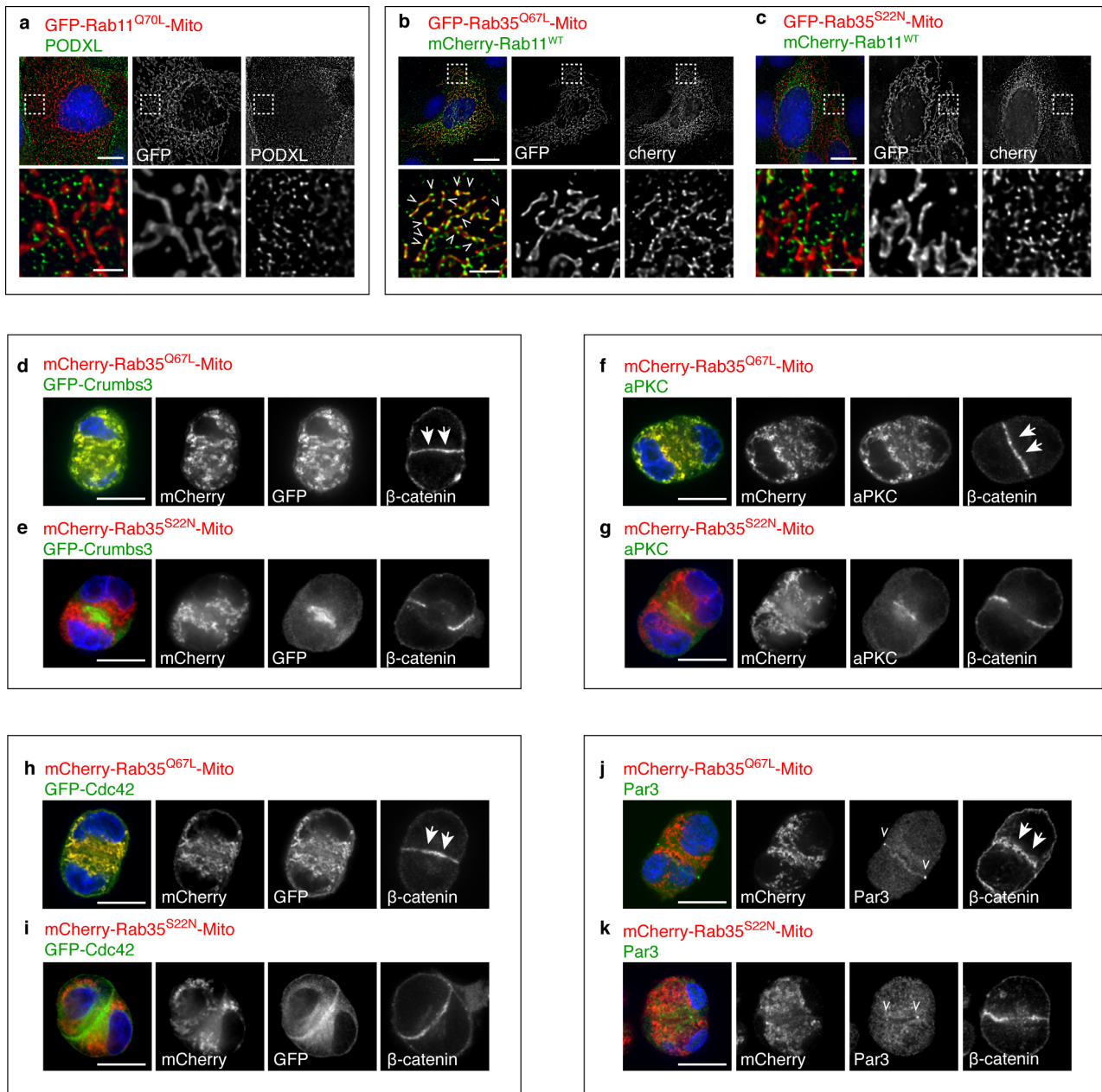
(b) Quantification of the time to establish an apical membrane from mitosis onset until PODXL enrichment at the cell-cell contact (control cysts) or PODXL enrichment at the ECM-facing membrane (Rab35 depleted cysts or GFP-PODXL mutant expressing cysts).



Supplementary Figure 4

Supplementary Figure 4: Defects in cytokinesis abscission does not perturb cyst development.

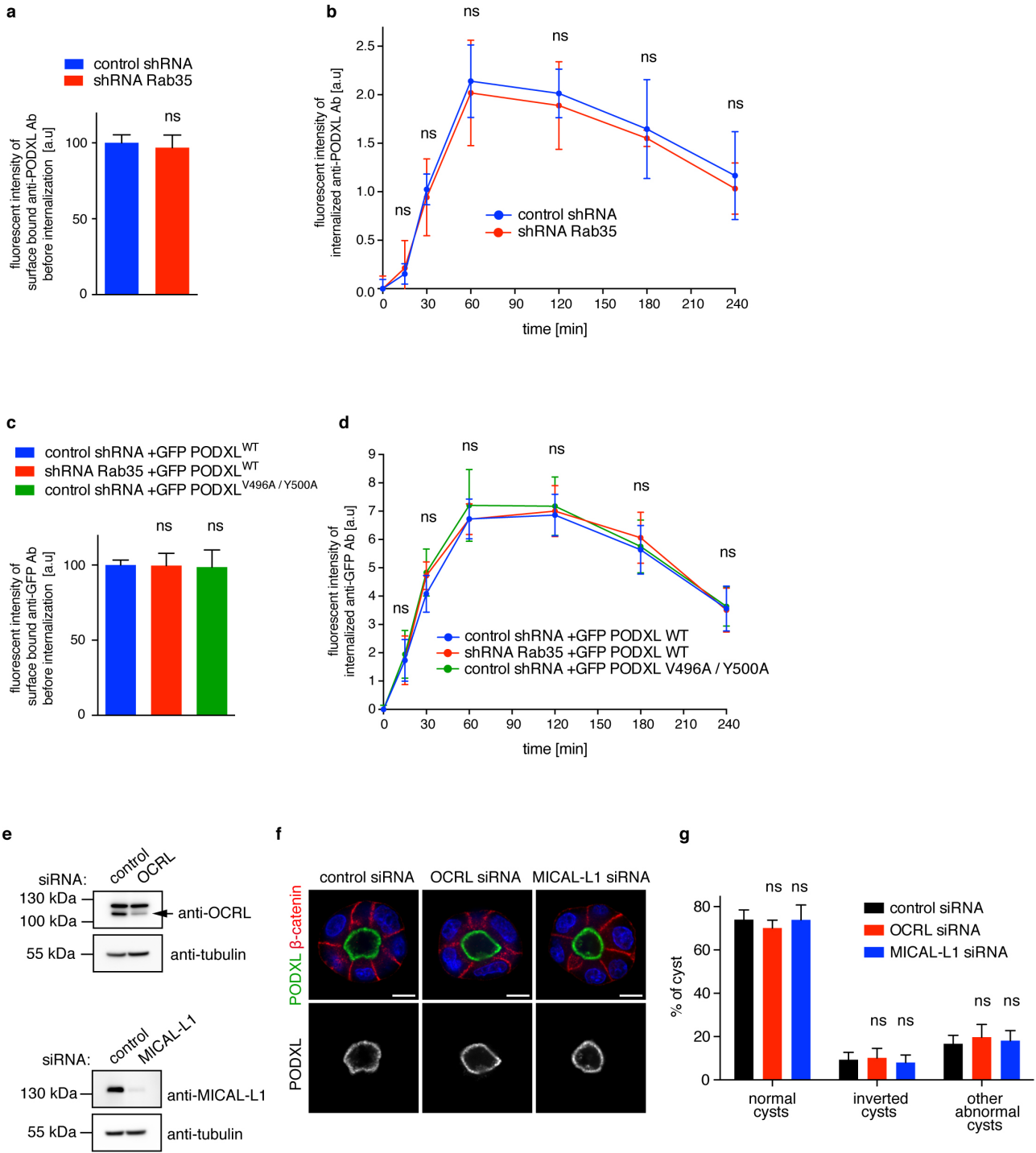
(a) MDCK cells were treated with either control (red) or Cep55 (black) siRNAs for 72 h and recorded by phase-contrast time-lapse microscopy for 48 h. Abscission time counted from furrow ingression to actual abscission (x-axis) are presented as cumulative percentage (y-axis). Note the strong delay in abscission observed after Cep55 depletion. **(b)** MDCK cells were treated with either control or Rab35 siRNAs for 48 h and seeded into Matrigel for 48 h. Left panels: Cysts were fixed and stained with phalloidin to detect apical F-actin (red), anti-acetylated-tubulin antibodies to visualize cytokinetic bridges (green) and DAPI (blue). Projections of z-stacks are presented. Single channel for acetylated-tubulin is also displayed in grey levels. Note the accumulation of cytokinetic bridges upon Cep55 depletion, indicating delayed cytokinesis in 3D cysts. Bar: 10 μ m. Right panel: Proportion of normal and abnormal cysts after control or Cep55 depletion, based on PODXL staining. Mean \pm SD, N= 3 independent experiments, 300-500 cysts analysed per condition. Two-way ANOVA: ns: not significant. **(c)** Carboxy-terminal sequence of PODXL cytoplasmic tail (aa 476-551). The position of Valine 496 and Tyrosine 500 essential for Rab35 binding are indicated in red.



Supplementary Figure 5

Supplementary Figure 5: Rab35^{Q67L}-Mito tethers vesicles containing PODXL and Rab11 around mitochondria.

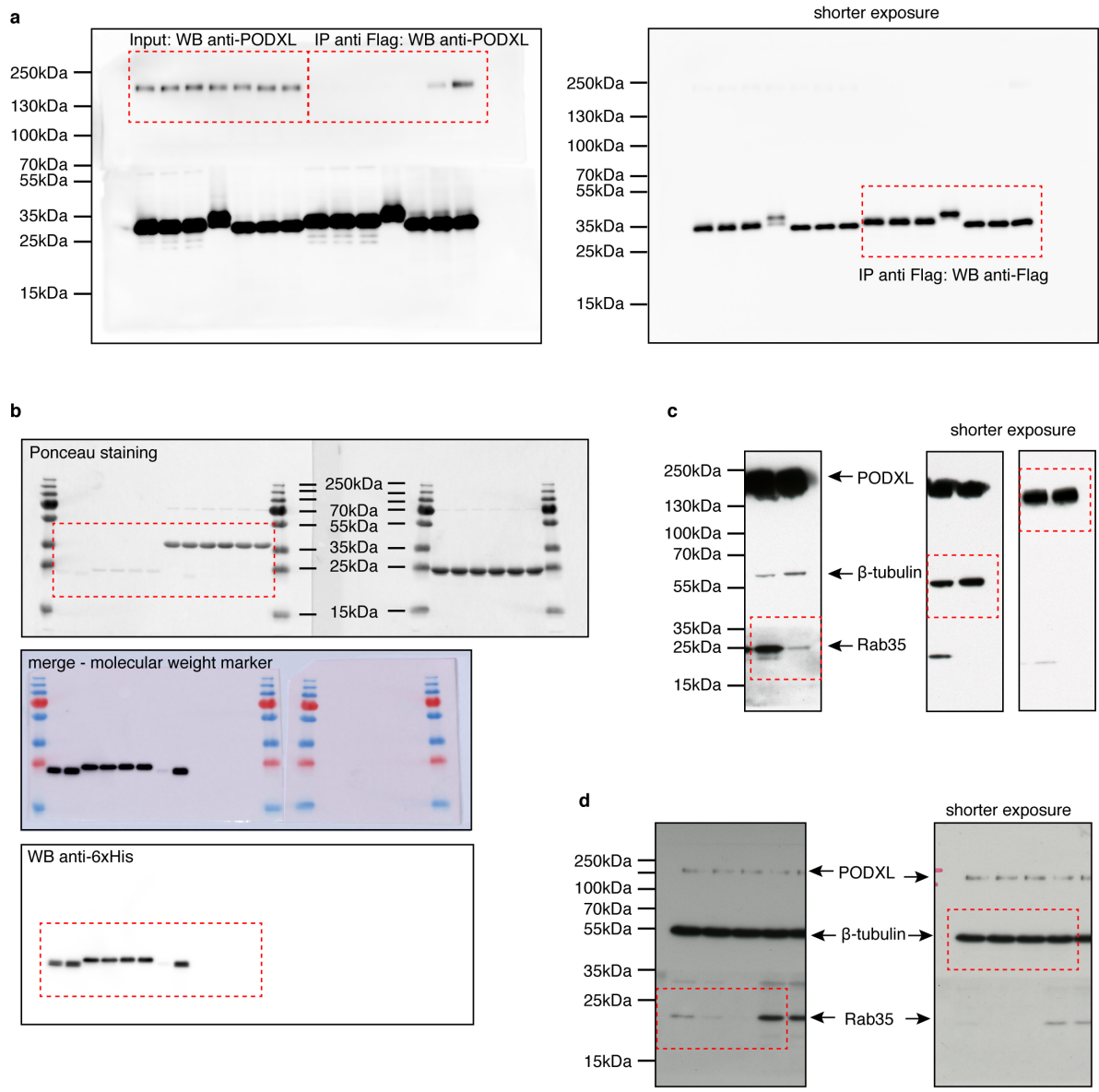
(a) MDCK cells were transfected for 72 h with plasmids encoding GFP-Rab11^{Q70L} fused to the mitochondrial targeting signal of ActA (-Mito), fixed and stained for PODXL. **(b-c)** MDCK cells were co-transfected for 72 h with plasmids encoding mCherry-Rab11^{WT} and either GFP-Rab35^{Q67L}-Mito **(b)** or GFP-Rab35^{S22N}-Mito **(c)**, fixed and stained with DAPI. **(a-c)**: merged images, individual channels in grey levels and higher magnification of the regions delimited by a dash line are displayed, as indicated. Bar: 10 μm for unzoomed regions and 2 μm for zoomed regions. Arrowheads indicate examples of close apposition vesicles (green) with mitochondrial Rab35^{Q67L} (red). **(d-k)** MDCK cells were co-transfected with plasmids encoding either GFP-Rab35^{Q67L}-Mito (d, f, h, j) or GFP-Rab35^{S22N}-Mito (e, g, i, k), together with GFP-Crumbs3 (d-e) or GFP-Cdc42 (h-i). Cells were seeded into Matrigel for 24h, fixed and stained with β -catenin (d-e, h-i), β -catenin and aPKC (f-g) or β -catenin and Par3 (j-k) as indicated. Arrows indicate the β -catenin marked basolateral membrane. Bar: 10 μm



Supplementary Figure 6

Supplementary Figure 6: Rab35 depletion does not affect PODXL endocytosis.

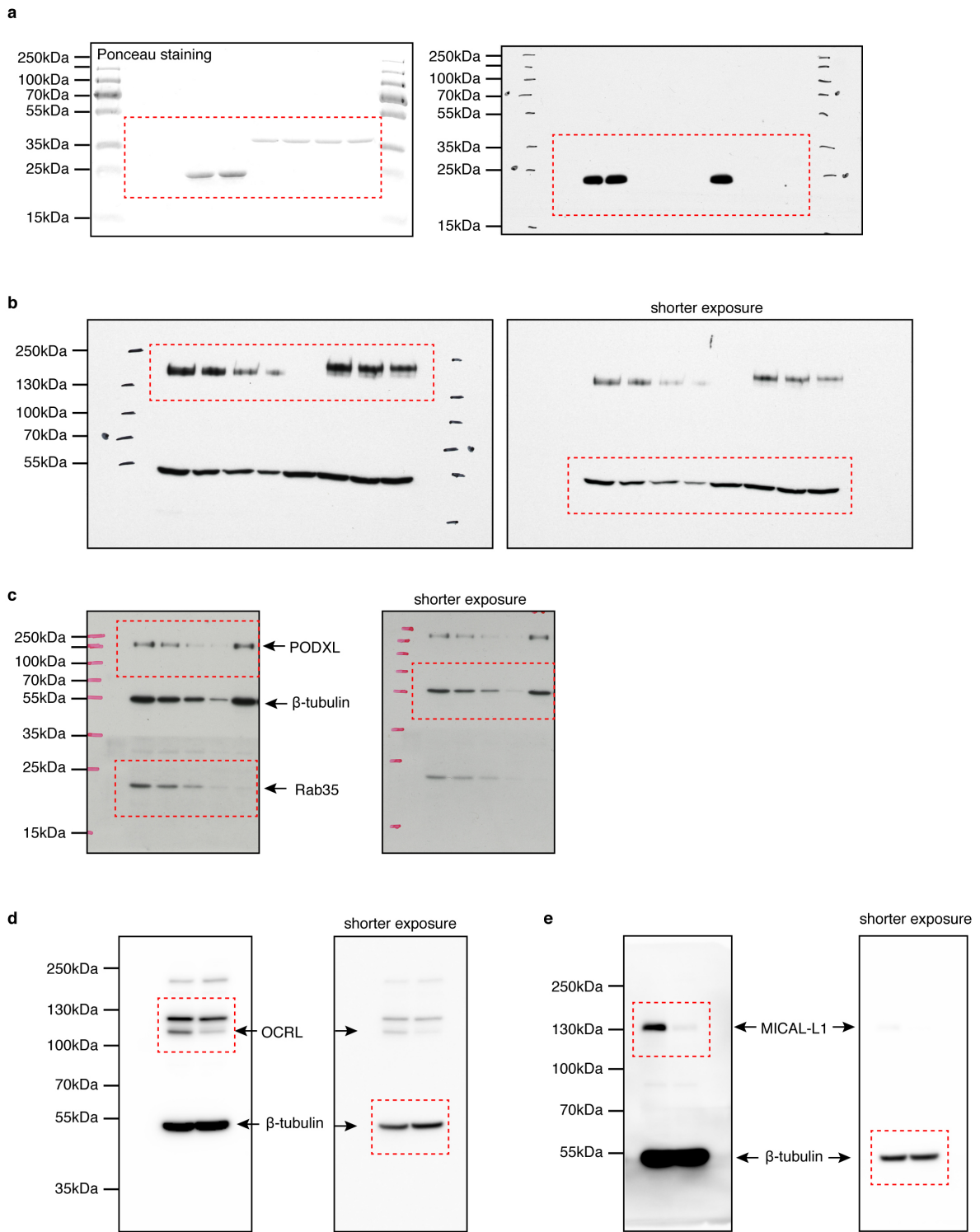
(a-b) MDCK cells stably expressing control shRNA or Rab35 shRNA were incubated with anti-PODXL antibodies at 4°C and then shifted to 37°C to allow antibody internalization for various time points as indicated. Remaining surface bound antibodies were removed by pronase treatment (except for baseline control cells were fixed, permeabilized and stained with secondary fluorescent antibodies before being analysed by FACS. The graph in (a) presents the fluorescent intensity of surface bound anti-PODXL antibody before internalization. **(c-d)** Endogenous PODXL was depleted with siRNAs and replaced by either GFP-PODXL^{WT} (blue line) or GFP-PODXL^{V496A Y500A} (green line) in MDCK cells stably expressing control shRNA. The red line shows MDCK cells stably expressing Rab35 shRNA that were transfected with GFP-PODXL^{WT} (red line). Internalization of exogenous PODXL was analyzed as in (a-b), by using anti-GFP antibodies. All graphs present triplicates of representative experiments. Mean ± SD. In b and d, values are normalized to baseline (surface bound antibodies before internalization) and subtracted from background fluorescent at t0. **(e)** Western Blot of MDCK cells transfected with either OCRL siRNA, MICAL-L1 siRNA or control siRNA for 3 days. **(f)** MDCK cysts transfected with either OCRL siRNAs, MICAL-L1 siRNAs or control siRNAs were seeded into Matrigel for 48h and stained for PODXL (green), β-catenin (red), DAPI (blue). Bar: 10 μm **(g)** Proportion of normal cysts, inverted cysts and other abnormal cysts of control cysts, OCRL-depleted cysts and MICAL-L1-depleted cysts after 48h in Matrigel. Mean ± SD, N= 3 independent experiments, >300 cysts analysed per condition. Two-way ANOVA: ns: p>0.05.



Supplementary Figure 7

Supplementary Figure 7: uncropped images for presented Western Blots (I)

(a) corresponds to Fig. 1c; (b) corresponds to Fig. 1b; (c) corresponds to Fig. 3a; (d) corresponds to Fig. 3d. Red squares indicate cropped regions as displayed in the Figures.



Supplementary Figure 8

Supplementary Figure 8: uncropped images for presented Western Blots (II)

(a) corresponds to Fig. 4d; (b) corresponds to Fig. 4e; (c) corresponds to Supplementary Fig. 2b; (d-e) corresponds to Supplementary Fig. 6e. Red squares indicate cropped regions as displayed in the Figures.

2.3 Reviewers comments and author's rebuttal letter

Response to Reviewers

" Rab35 GTPase couples cell division with initiation of epithelial apico-basal polarity and lumen opening"

We thank the three Reviewers for their positive comments and suggested experiments. We have provided additional experiments and Figures as well as explanations in the revised manuscript to address all their comments.

New experimental data have been added as Fig.1, Fig.4 and Supplementary Fig. S1, S2, S3, S4, S5, S6.

We provide below a full response to each comment raised by the Reviewers. We believe that the added experimental data and Reviewer's suggestions helped us to reinforce the conclusions of the manuscript.

Reviewer #1 (Remarks to the Author): Expert in apical-basal polarity and morphogenesis

This is an elegant study showing that Rab35 is essential for directing apical targeting to the cytokinetic cleavage site to establish apical-basal polarity in MDCK cells. Klinkert and colleagues provide extensive and very convincing data that Rab35 binds directly to podocalyxin to recruit apical polarity proteins to the Apical Membrane Initiation Site, and that lumen formation is dependent on this interaction.

I have no major concerns with the work presented and only one minor recommendation that further discussion be included as to whether apical trafficking coupled to cytokineses is a general mechanism of lumen formation.

We thank the Reviewer for this very positive evaluation of our work. We now provide a full discussion of the presented data and, in particular, of this point (p. 12/13)

Reviewer #2 (Remarks to the Author): Expert in Rabs and epithelial polarity

This is a well-written and very interesting manuscript that focuses on understanding the machinery governing the targeting of apical cargo-containing endosomes during apical lumen formation. Apical lumen formation is a new and emerging field, yet the mechanisms targeting apical organelles to the apical lumen initiation site (AMIS) remains unclear. As the result, this is a very timely and potentially very interesting study. However, study has multiple inconsistencies and technical issues that makes some of the data difficult to interpret. As consequence of that, I do not believe that data, as presented, supports author's conclusions. First, in order to serve as a specific apical endosome targeting factor, Rab35 needs to be specifically enriched at AMIS. Shown data does to demonstrate that. Actually, it appears that Rab35 is as enriched at AMIS as at adherens junctions. Second, Rab35 has been shown to have several functions (many actually shown by this group). It is crucial to show that Rab35 is actually AMIS tether, rather than regulator of PODXL

endocytosis. Actually, in my opinion, data better fits with the model that Rab35 affects the internalization of PODXL at the plasma membrane, thus affecting its transport to the AMIS. Thirdly, it is unclear why PODXL knock-down does not give the same phenotype as rab35 knock-down. Finally, while mitochondria recruitment studies are very elegant, the fact that Rab35 affects aPKC and Cdc42 recruitment is very puzzling. I strongly believe that all these issues need to be addressed before manuscript can be published. Detailed list of concerns/questions is shown below.

We thank the Reviewer for his/her comments and questions that helped us clarify several points in the revised manuscript. We have now addressed all points in new Figures 1 and 4 and Supplementary Figures S1, S2, S3, S4, S5, S6.

All the questions raised above are answered in the response to the specific points below.

The new experimental data now

- demonstrate that Rab35 has no effect on PODXL internalization,
- clarify the localization of Rab35 with respect to AMIS components and AJ markers
- explain why PODXL and Rab35 depletions lead to distinct phenotypes
- and provide an explanation for the observed Cdc42/aPKC recruitment on vesicles.

We believe that these new experiments strengthen the conclusions of the manuscript and support the proposed model.

1) Figure 1. Rab11 is probably not the best negative control for Rab35 and PODXL binding. Some of the known Rab35 effectors, such as OCRL, are also known to bind Rab6. As the result, it is important to test the ability of Rab6 to bind PODXL. Additionally, binding data to Rab8 and Rab27 needs to be shown (at least in supplemental figures). I am also confused about panel c. Why FLAG-Rab11-Q70L is so much bigger than FLAG-Rab35? Even with FLAG tag, Rab11 should only about 22-23 kDa in size.

As requested, we now thoroughly investigated possible interactions between Rab6 and PODXL, and found no interaction between these two proteins. Indeed, GTP-Rab6 does not interact by 2-hybrid (new Fig. 1a). Moreover, recombinant Rab6 loaded with GTP- γ S does not bind to PODXL (Fig 1b). Finally, GTP-locked mutant of Rab6 does not coIP with PODXL (Fig. 1c).

The binding data for Rab8/Rab27 previously mentioned as “data not shown” are now displayed in the new Fig. 1a, as suggested. The absence of binding was also confirmed by co-IP experiments (new Fig. 1b).

We expressed Rab proteins tagged with 3 Flag tags and a linker, which shifts the calculated molecular weights of Rab11 and Rab35 to 30 kDa and 26 kDa, respectively. The relative apparent molecular weights in SDS-PAGE/Western blot are consistent with the predicted values (new Fig. 1c).

We now dedicated a full figure (new Figure 1) to describe these additional negative controls.

2) Figure 1d. While Rab35 is clearly enriched at the site of adhesion between two cells, it does not appear to be that enriched and the AMIS. From previous work by Keith Mostov lab, it is clear that most of the interface between two cells is actually zona adherens, that contains cadherin and catenin based cell-cell adhesion junctions. AMIS usually is only small portion located in the middle of cell-cell interface. It contains several tight junction proteins (such as ZO1) and lacks cadherin/catenin. If authors want to conclude that Rab35 is enriched at AMIS, they need to show co-staining of Rab35 enriched in AMIS using known AMIS markers, such as ZO1 or Par3/6. Lack of Rab35 in cadherin/catenin containing adherens junctions also needs to be shown.

As requested, we now provide evidence that Rab35 is indeed localized at the AMIS labeled by ZO1 around the cytokinetic bridge (Fig. S1a). There, unexpectedly, we observed colocalization between Rab35 and b-catenin (Fig. S1b, arrowheads). This suggests that, at least at early stages when PODXL has not yet fused to the AMIS (Fig. S1a-b), the AMIS overlaps with adherens junction markers. This observation has been confirmed with colocalization between ZO1 and b-catenin on the side of the tubulin-positive bridge in Supplementary Fig. S1c. As expected, after establishment of the apical membrane (PODXL+), there is a clear segregation between adherens junction markers and apical markers (Fig. 1d), suggesting remodeling of the junctions. Thus, the AMIS appears as a dynamic compartment and its molecular definition changes with time, a noteworthy point that is now discussed (page 13/14).

In addition, a pool of Rab35 also localizes at the cell-cell interface not labeled by ZO1 (Fig. S1c). Interestingly, we observed that PODXL vesicles are tethered/fused mainly at the ZO1-positive AMIS (as expected, Fig. S1e solid arrowhead) but also on its sides (Fig. S1e, arrowheads), where a fraction of Rab35 is also present. This is consistent with the proposed tethering model, and suggests that a pool of PODXL vesicles can also interact with beta-catenin/Rab35-positive membranes close to the AMIS (discussed on page 14). This raises the possibility that vesicles could deliver PODXL mainly at the membrane surrounding the bridge (AMIS) but also on its sides, and that apical proteins later coalesce into a single domain while junctions are being remodeled.

A detailed description of Rab35 localization with respect to ZO1/beta-catenin is now included in the result section (page 5) and in the discussion (page 13/14).

3) Data of Rab35 GAP EPI64B needs to be shown (including GAP-dead EPI64B mutant).

The data showing that overexpression of the Rab35 GAP EPI64B (but not the GAP-dead mutant R409A, as expected) leads to polarity inversion is now displayed in the new Supplementary Fig. S2d and S2e.

4) Figure 3C. It seems that in Rab35 knock-down cells PODXL is not efficiently endocytosed (compare plasma membrane staining to that of control cells). Why authors focus on Rab35

as a targeting factor rather than endocytosis factor? That is especially puzzling since authors previously published that Rab35 regulates endocytosis. Affecting endocytosis rather than targeting better explain "inverted cyst" phenotype. Authors need to add quantitative analysis of the effect of Rab35 on PODXL endocytosis.

We thank the Reviewer for pointing out this question of a possible role of Rab35 in endocytosis, that we have now extensively addressed in the experiments presented in new Figure S6.

Indeed Rab35 has been shown to regulate endocytic recycling of TfR from endosomes to the plasma membrane¹⁻³ and endosomes-to-TGN retrograde traffic of CI-M6PR⁴. However, it should be pointed out that no effect of Rab35 inactivation on internalization has been detected¹. This makes sense since Rab35 is loaded on endosomes only after the fission of Clathrin-coated vesicles from the plasma membrane, as described recently⁴.

We nevertheless carefully tested the Reviewer's hypothesis that Rab35 might affect PODXL internalization in MDCK cells.

First, we depleted Rab35 and observed no differences in steady state amounts of endogenous PODXL at the cell surface (Fig. S6a). In addition, we performed a quantitative internalization assay of endogenous PODXL (antibody uptake after binding at 4°C and chase at 37°C for up to 4h). We observed no differences in the internalization kinetics between control-depleted and Rab35-depleted cells (Fig. S6b).

Second, we followed the internalization of GFP-PODXL and, again, no difference in the trafficking of exogenous GFP-PODXL was observed upon Rab35 depletion (Fig. S6d, blue vs. red line). As a consequence, Rab35 depletion did not increase GFP-PODXL localization at the plasma membrane (Fig. S6c). Importantly, polarity inversion was also observed by introducing mutations in the PODXL tail making it unable to interact with Rab35, even if Rab35 was not depleted. Again, this is not because the GFP-PODXL V496A Y500A mutant was not properly internalized (Fig. S6d, green line).

Finally, we analyzed polarity after depletion of OCRL⁴ and MICAL-L1^{5,6}, which are the two known Rab35 effectors in trafficking. Depletion of these Rab35 effectors did not lead to polarity inversion (consistent with previous work testing the effect of OCRL knock-down in matrigel⁷).

Altogether, we conclude that the inversion of polarity observed upon Rab35 depletion does not result from a defect in PODXL internalization from the plasma membrane. The fact that internalization is not blocked after Rab35 depletion is also consistent with the observation that a major pool of PODXL is present on recycling endosomes before disappearing from this compartment during the inversion process (Fig. 4c and S3a).

Nevertheless, even in control cysts, a small pool a PODXL can be seen at the plasma membrane at the 2-cell stage while most PODXL is internalized before delivery to the AMIS, and this varies from cyst to cyst. We provide additional videos in new Fig. S3b (and kept the original ones) to document this variability. In addition, the time between mitotic exit and apical membrane formation lies between 1 and 10 hours, depending on cysts, both

in controls (PODXL in the center) and in Rab35-depleted cells (PODXL at ECM-facing membrane) (new Fig. S3b). We think that describing for the first time these two levels of variability is an important finding for researchers interested in MDCK cysts, and we now discussed this on page 15.

Additionally, some of PODXL does appear at the AMIS, but then disappear again, leading to very specific accumulation only at the plasma membrane facing matrix. How do authors explain that? Affecting targeting should not lead to active exclusion of PODXL from AMIS membranes.

We agree that a small fraction of PODXL can be initially detected at the cell-cell interface in Rab35-depleted cells, then progressively disappears from this location and eventually exclusively localizes to the ECM-facing membrane.

In both normal and depleted cysts, we expect that once the amount of PODXL (and other co-transported transmembrane proteins such as Crumbs3) has reached a threshold on a given membrane, this now defines the apical-like membrane. On the contrary, low levels of PODXL are characteristic of the basolateral-like membrane.

We assume that, in the absence of Rab35, fusion of internalized vesicles could initially happen anywhere at plasma membrane of the cell, but more frequently at the ECM facing membrane due to the surface difference between ECM-facing membrane vs. cell-cell contact membrane. We therefore expect that the small pool of PODXL at the cell-cell contact (basolateral-like) will be iteratively removed by endocytosis (as at the basolateral membrane in normal cells) and thus progressively targeted to the ECM-facing membrane (apical-like).

This explanation is coherent if Rab35 is not required for the fusion process, but rather helps tethering vesicles containing apical markers (PODXL, Crumbs3) at the right place. We now clearly discuss that Rab35 is a major factor (obviously not the only one) that promotes the establishment of the apical domain. Indeed, in wild-type situation, it is likely the combination of different tethering and fusion factors, together with bridge microtubules and directed molecular motors^{8,9}, that collectively allow the definition of a robust and properly localized apical membrane (page 16).

5) Figure 3F. Images of phenotypes need to be shown (also showing other polarity markers, such as Crumbs and ZO1). I do not understand why PODXL knock-downs lead to cysts without lumens. PODXL may affect lumen opening, but should not affect cell ability to form lumens. Additionally, if PODXL is key to forming normal lumens, I would expect that knock-down should also lead to inverted cysts.

The requested images are provided in new Fig. 4g, both for Rab35-depleted cysts and for cysts in which PODXL has been replaced by wild-type or mutant PODXL (unable to interact with Rab35).

Consistent with previous reports^{10,11} and with the data presented in the initial manuscript, depletion of PODXL leads to cysts without lumen and without polarity inversion (Fig. 4f). The reason for the absence of lumen and for the lack of polarity inversion is explained by the accumulation of apical recycling endosomes (Crumbs3+ and Rab11+), close to the plasma membrane¹¹ (see examples in new Fig. 4g). This accumulation can also be seen underneath the plasma membrane facing the ECM (see example below, Fig.A).

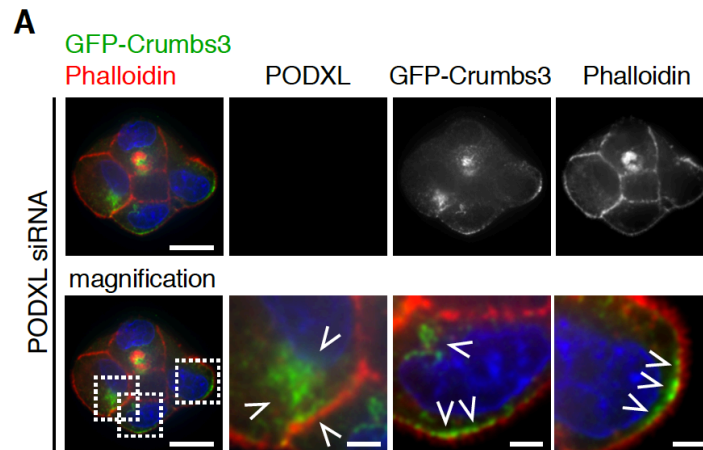


Figure A: MDCK cells treated with PODXL siRNAs for 3 days and co-transfected with GFP-Crumbs3. Cysts were fixed after 48h and stained for Phalloidin (red) and for endogenous PODXL (greyscale, single channel), as indicated. The magnification of the PODXL depleted cyst shows GFP-Crumbs3-positive vesicles close to the ECM-facing membrane marked by Phalloidin. Bar: 10 μ m (2 μ m for zoomed region).

Therefore, upon PODXL depletion, key apical polarity determinants are not delivered to the plasma membrane, consistent with ref.¹¹. This indicates that PODXL is (directly or indirectly) necessary for the fusion of the vesicle to the plasma membrane, besides its function in lumen opening.

In contrast, PODXL is expressed at normal levels in Rab35-depleted cells (western blot Fig. 3a). In the absence of the tethering factor Rab35, PODXL-positive vesicles can still fuse to the plasma membrane (since PODXL is present), but this does not occur at the correct location, leading to the observed inversion of polarity. Consistent with this explanation, the inversion of polarity after Rab35 depletion depends on the presence of PODXL, since double Rab35/PODXL depletion phenocopies the single PODXL depletion (see below, Fig. B and compare to Fig. 4f).

The additional data (Fig. A, B) could be included in a supplementary Figure if the Reviewer feels that it is important.

In summary, as now discussed on page 16, PODXL has multiple functions: it promotes 1) fusion of the vesicles to the plasma membrane, directly or more likely indirectly; 2) Rab35-dependent tethering of apical recycling endosomes to the future apical membrane; and 3) lumen opening.

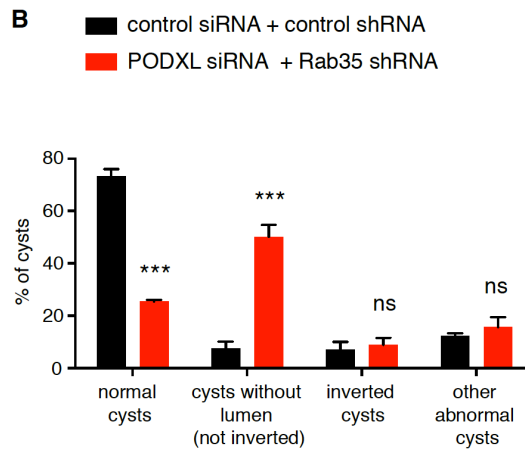


Figure B: MDCK cells stably expressing control shRNA or Rab35 shRNA were transfected with control siRNA or PODXL siRNA for 3 days and cultured in Matrigel for 48h. The graph displays the proportion of normal cysts, cysts without lumen (but not inverted), inverted cysts and other abnormal cysts. Mean \pm SD, N= 3 independent experiments, 150-500 cysts analysed per condition. Two-way ANOVA: $p < 0.001$ (***), ns: not significant.

6) Figure 4. I am a bit puzzled that Rab35-mito mediated recruitment of Cdc42 and aPKC to endosomes. None of these proteins relay of endosomes to be delivered to tight junctions and AMIS. Instead, it is well established that their recruitment is mediated by Par3/6 complex. How do authors explain that? Does Par3/6 are also recruited to mitochondria?

It has been previously shown that a pool of Cdc42 is trafficked on Rab11/PODXL-double positive endosomes during cystogenesis¹². aPKC can also be transported on these endosomes¹³. Of note, endosomes have also been implicated in the transport of a fraction of Cdc42 to the plasma membrane in other circumstances, such as during migration of astrocytes¹⁴. Altogether, this explains why a fraction of Cdc42/aPKC could be detected around mitochondria upon delocalization of Rab35 to mitochondria. Although aPKC, Par6 and Par3 are known to form a complex, we did not detect Par3 on tethered Rab11+/PODXL+ endosomes (data not shown, and see below). However, it is has been suggested that Par3 could dissociate from this complex upon phosphorylation by aPKC through active Cdc42¹⁵.

7) Figure 5. Where does Cdc42, aPKC and Par3/6 localize in 3D cultures when Rab35-mito is expressed (see comments above).

As requested, we have addressed this question experimentally (new Fig. S5f-k).

Consistent with the results of the mitochondrial targeting experiment (Fig. 5), we observed that PODXL (Fig. 6), Crumbs3a (new Fig. S5d), aPKC (new Fig. S5f) and Cdc42 (new Fig. S5h) are recruited to mitochondria upon expression of Rab35 Q67L-Mito in 3D cultures. As expected from the comments in point #6 above, Par3 localized to the tight junctions and was not detected around mitochondria (new Fig. S5j).

Reviewer #3 (Remarks to the Author): Expert in epithelial polarity and podocalyxin

The manuscript by Klinkert et al describes a novel interaction and function interplay between the Rab35 GTPase and the apical polarity protein Podocalyxin in spheroid lumen formation. The authors demonstrate that Rab35 directly binds the cytoplasmic domain in a GTP-dependent fashion. During lumen formation in the MDCK epithelial cell spheroid model, Rab35 is targeted to the so-called apical membrane initiation site ('AMIS') prior to Podxl vesicles to be delivered to form the lumen. In contrast to other pathways describing membrane traffic of Podxl to the lumen from the Mostov, Prekeris, and Martin-Belmonte labs, Rab35 does not appear to co-localize to transcytosing Podxl vesicles. Instead, Rab35 appears to tether Podxl to the AMIS, in order to form lumens during 3D culture of MDCK epithelial cells. The authors define key residues in Podxl required for the interaction of Podxl with Rab35. Interestingly, knockdown of Rab35 or a combination of Podxl knockdown and re-expression of non-Rab35-binding Podxl demonstrates that Podxl is internalized during polarity reorientation, but in the absence of functional interaction with Rab35 is not stabilized at the AMIS, and returns to the periphery of early aggregates. The net outcome of all of this is defective lumen formation - either total inversion of cysts, or formation of multiple, instead of single, lumens. Mistargeting Rab35 to mitochondria similarly disrupts lumen formation. Strikingly, this also results in the mistargeting of several other apical factors - Crumbs3, Cdc42, aPKC.

The work is elegantly performed and presented, and was a pleasure to review. The impact is likely broad for cell polarity, membrane traffic, and cell division fields. I have no experimental criticisms or suggestions.

We thank the Reviewer for this very positive evaluation of our work. We have modified the Figures 2b, added new data in Fig. S6, and rewritten extensively our discussion to take into account all the minor comments below.

Minor comments

In the model and images in figure 1, there is a stage missing from what was originally described by the Kroschewski lab (Ferrari et al, PMID: 18946028), between single cell and two cell stages. After division, Podxl is localized at the plasma membrane in an inverted fashion before transcytosis to the lumen. This is quantified in the authors' own data in Figure 3b. This should be included in the schema.

To clarify this point, we have modified the schematic drawing as requested (new Fig. 2 bB).

The discussion section is brief and not sufficient: this needs to be significantly expanded and rewritten to discuss their results in the context of what is known about apical polarity. How does their mechanism fit into the mechanism for polarity orientation described by Keith Mostov's lab where beta1-integrin controls polarity reorientation and gives polarity defect similar to this work ? Given that Rab35 has been shown to regulate b1-integrin

trafficking (PMID: 23264734; PMID: 25344254), how does their Rab35 mechanism relate? (The data in Fig. 3g likely show this is a separate, parallel mechanism).

We have now discussed why it is unlikely that Rab35 depletion leads to inversion of polarity by perturbing β 1-integrin (p. 17). Of note, β 1-integrin depletion does not lead to complete inversion of polarity (as described in the present study) but rather to impaired polarity reorientation characterized by collective front-rear polarization and motility {Bryant, 2014 #2194}, when MDCK cells are cultured in Matrigel (our conditions). We did not observe such collective front-rear polarization after Rab35 depletion.

How Rab35 is regulated should be discussed. Is the Rab35 GEF known? Similarly, the Rab35 GAP EPI64B (which the authors state the overexpression of which phenocopies Rab35 knockdown) binds to the Podxl-binding protein EBP50, which is critical for lumen formation in this system. These potential interplays should be discussed.

We have now discussed the interaction between EPI64B and EBP50/NHERF1, and possible significance in the discussion (page 17). Connecdenn1 is a major Rab35 GEF (work from McPherson Lab), but future work will be needed to determine if it activates Rab35 during cystogenesis. We also now mention that Rab35 localization depends on PtdIns(4,5)P2 interaction, a property that we discuss in the line of the PtdIns(4,5)P2-Annexin2-Cdc42 polarity pathway described in Martin-Belmonte et al. 2007.

What does binding of Rab35 to Podxl do? Are there endocytic motifs present in Podxl? Information about the mutant forms of Podocalyxin is missing. How were these mutations selected and defined? Does Rab35 binding mask a potential endocytic motif?

We experimentally addressed whether Rab35 could affect PODXL internalization (new Fig. S6). We found that Rab35 depletion had no effect on PODXL endocytosis. This is now detailed in the discussion (page 15).

We also added information about the characterization and the rationale behind the selection of the double PODXL mutant V496A Y500A that lost its ability to bind to Rab35 (page 8).

Overall, the data and manuscript are excellent. If the discussion were updated with the above comments, this will greatly enhance an already great work.

Thank you for this enthusiastic consideration of our work.

1. Kouranti, I., Sachse, M., Arouche, N., Goud, B. & Echard, A. Rab35 regulates an endocytic recycling pathway essential for the terminal steps of cytokinesis. *Curr. Biol.* **16**, 1719–25 (2006).
2. Dambournet, D. *et al.* Rab35 GTPase and OCRL phosphatase remodel lipids and F-actin for successful cytokinesis. *Nat. Cell Biol.* **13**, 981–8 (2011).
3. Allaire, P. D. *et al.* Interplay between Rab35 and Arf6 controls cargo recycling to coordinate cell adhesion and migration. *J. Cell Sci.* **126**, 722–31 (2013).
4. Cauvin, C. *et al.* Rab35 GTPase Triggers Switch-like Recruitment of the Lowe Syndrome Lipid Phosphatase OCRL on Newborn Endosomes. *Curr. Biol.* 120–128 (2015).
5. Giridharan, S. S. P., Cai, B., Naslavsky, N. & Caplan, S. Trafficking cascades mediated by Rab35 and its membrane hub effector, MICAL-L1. *Commun. Integr. Biol.* **5**, 384–7 (2012).
6. Kobayashi, H., Etoh, K., Ohbayashi, N. & Fukuda, M. Rab35 promotes the recruitment of Rab8, Rab13 and Rab36 to recycling endosomes through MICAL-L1 during neurite outgrowth. *Biol. Open* **3**, 803–14 (2014).
7. Rbaibi, Y. *et al.* OCRL1 modulates cilia length in renal epithelial cells. *Traffic* **13**, 1295–305 (2012).
8. Schlu, M. A. *et al.* Trafficking of Crumbs3 during Cytokinesis Is Crucial for Lumen Formation. **20**, 4652–4663 (2009).
9. Li, D., Mangan, A., Cicchini, L., Margolis, B. & Prekeris, R. FIP5 phosphorylation during mitosis regulates apical trafficking and lumenogenesis. *EMBO Rep.* **15**, 428–37 (2014).
10. Meder, D., Shevchenko, A., Simons, K. & Füllekrug, J. Gp135/podocalyxin and NHERF-2 participate in the formation of a preapical domain during polarization of MDCK cells. *J. Cell Biol.* **168**, 303–313 (2005).
11. Bryant, D. M. *et al.* A molecular switch for the orientation of epithelial cell polarization. *Dev. Cell* **31**, 171–87 (2014).
12. Bryant, D. M. *et al.* A molecular network for de novo generation of the apical surface and lumen. *Nat. Cell Biol.* **12**, 1035–45 (2010).
13. Elias, S., McGuire, J. R., Yu, H. & Humbert, S. Huntingtin Is Required for Epithelial Polarity through RAB11A-Mediated Apical Trafficking of PAR3-aPKC. *PLoS Biol.* **13**, e1002142 (2015).
14. Osmani, N., Peglion, F., Chavrier, P. & Etienne-Manneville, S. Cdc42 localization and cell polarity depend on membrane traffic. *J. Cell Biol.* **191**, 1261–1269 (2010).
15. Y, N.-T., K, M., T, H., A, S. & S, O. Regulated protein-protein interaction between aPKC and PAR-3 plays an essential role in the polarization of epithelial cells. *Genes to Cells* **7**, 1161–1171 (2002).

3 DISCUSSION

The Rab35 GTPase plays a crucial role in the initiation of apico-basal polarity establishment in MDCK 3D renal cysts. During the first cell division of cyst development apical transmembrane proteins such as PODXL are transcytosed from the outer ECM-facing membrane towards the AMIS where the apical membrane will be established. At this stage Rab35 localizes to the membrane surrounding the intercellular bridge (the AMIS) and the adjacent adherence junctions and acts as a tether for PODXL-vesicles through direct and GTP-dependent binding to its cytoplasmic tail. Ectopic expression of GTP-bound Rab35 on the mitochondrial membrane induces the accumulation of PODXL-vesicles around the mitochondria and reveals that these vesicles carry important apical determinants such as Crumbs3, apKC and Cdc42.

Hence, active Rab35 tethers apical determinants at the AMIS to initiate apical membrane formation through direct binding of PODXL (Figure 42).

Expression of the PODXL mutant V496A/Y500A that cannot bind to Rab35 or depletion of Rab35 equally leads to mistargeting of PODXL-vesicles to the ECM-facing plasma membrane and consequently to an inversion of apico-basal polarity.

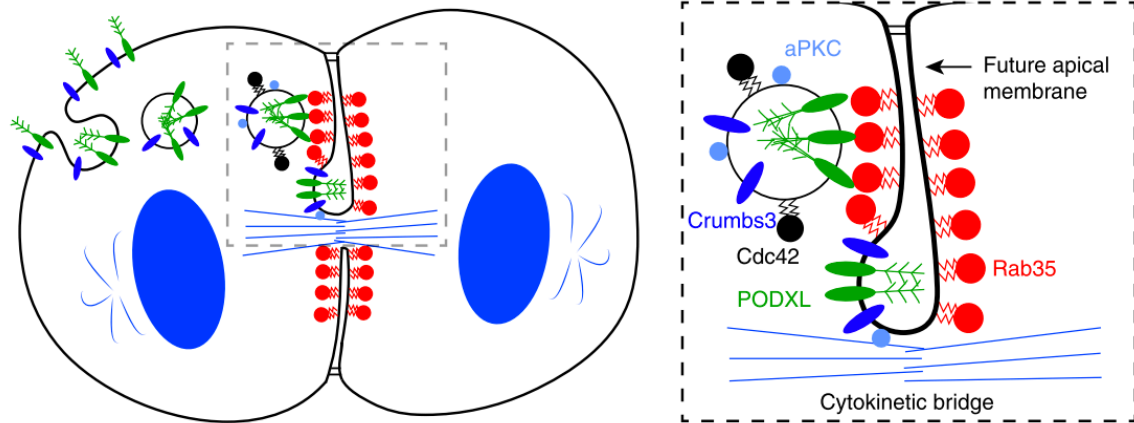


Figure 42: Model for coupling cell division and the initiation of apico-basal polarity.

This model shows how the first cyst cytokinesis is linked with the initiation of the apical lumen at the centre of the cyst. Rab35 (red) is localized at the cell-cell contacts, surrounding the intercellular bridge. There, Rab35 tethers PODXL-positive (green) vesicles through direct binding of the PODXL cytoplasmic tail. The PODXL-positive vesicles carry other important polarity determinants such as aPKC, Cdc42 and Crumbs3, which can initiate an apical membrane at the centre of the cyst. From reference:²¹²

3.1 Definition of the AMIS

The Apical Membrane Initiation Site (AMIS) was first described by Bryant et al in 2010, who defined the AMIS as a special zone of the cell-cell contacts of a 2-cell stage cyst, where the first fusion of PODXL vesicles can be observed⁷². PODXL co-localizes there with Par3 and Sec8 just before the expansion and segregation of the apical plasma membrane. Maturation of the AMIS requires activation of the Cdc42-Par6/aPKC complex, recruited by Rab11 and Rab8. At the same time another study demonstrated that the initiation of the apical membrane and the future lumen is coupled to cell division through delivery of Crumbs3 positive vesicles along the bridge microtubules⁸⁸. Although Schlüter and colleagues did not introduce the term “AMIS”, they nevertheless described a membrane domain around the bridge microtubules that becomes enriched in Crumbs3 and PODXL, and hence represents an apical membrane initiation site, which expands after completion of cytokinesis. The group of Prekeris further described the

formation of the midbody during cytokinesis as a symmetry breaking event that sets a landmark for AMIS formation^{89,128}. Vesicles positive for Crumbs3, PODXL and Rab11-FIP3/FIP5 are trafficked via Kinesin-2 along the bridge microtubules towards the midbody where they fuse the adjacent plasma membrane (AMIS). The AMIS is positive for tight junction markers such as ZO-1 and Cingulin, as well as the Exocyst complex (Figure 43).

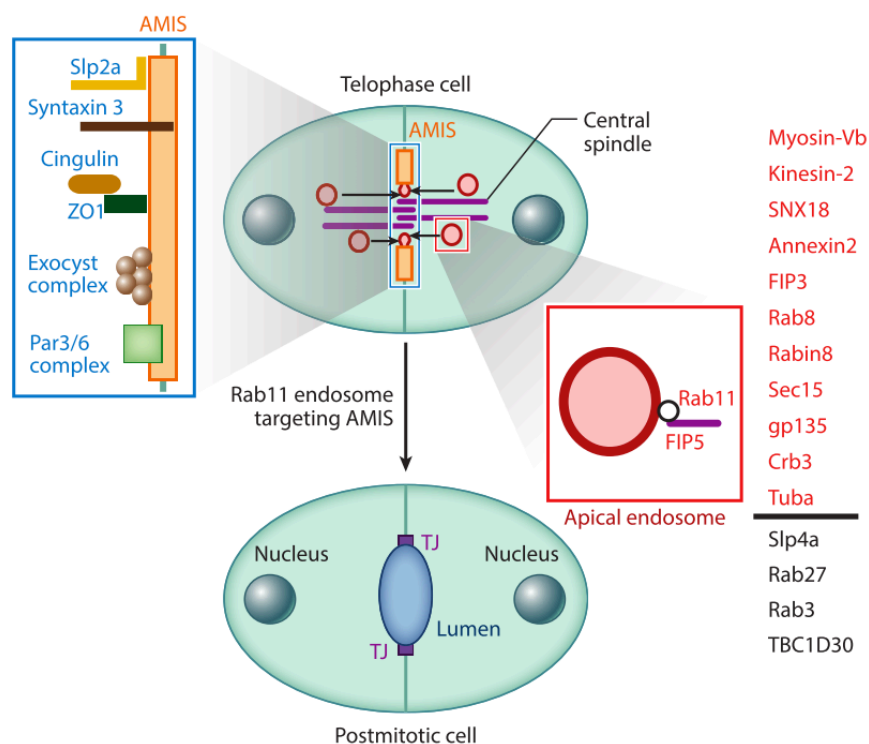


Figure 43: The Apical Membrane Initiation Site (AMIS).

This scheme illustrates the composition of the AMIS in early MDCK cysts. The blue box highlights proteins and protein complexes known to be localized at the AMIS. The red box highlights the apical endosomes and the associated proteins (red). From reference: ²¹³

Furthermore it was demonstrated that lipids play an important role in AMIS formation. AMIS formation at the previously basolateral cell-cell contacts requires the conversion of $\text{PtdIns}(3,4,5)\text{P}_3$ to $\text{PtdIns}(4,5)\text{P}_2$ via the phosphatase PTEN^{21,24,214}. The enrichment of

PtdIns(4,5) P_2 is essential for the recruitment of Annexin2 and Cdc42, the Exocyst subunits Exo70a and Sec3, as well as Slp2-a and Rab35.

However, the AMIS seems likely to be a transient membrane domain that can harbour apical proteins, tight junction proteins as well as basolateral proteins at the same time before segregation of clearly defined membrane domains occurs. Here, we demonstrate that basolateral markers such as β -catenin co-localize with the tight junction marker ZO-1 at the AMIS (Supplementary Figure 1 in the published manuscript). Furthermore, we show that PODXL vesicles fuse mainly in close proximity to the intracellular bridge, as described in previously^{88,89,128}, but also, unexpectedly, at its sides (Supplementary Figure 1 in the published manuscript). This indicates that either the AMIS is indeed demarcated by the tight junction-positive zone and thus fusion of apical vesicles is not limited to the AMIS, or the AMIS stretches over the cell-cell contacts and is thus not as restricted as believed. In any case it seems that remodelling of previous adherence junctions and newly formed tight junctions play an important role during AMIS formation.

3.2 How is Rab35 recruited to the AMIS?

Inactive GDP-bound geranylated Rab GTPases are delivered from the cytosol to specific membrane domains with help of a GDI and inserted into the membrane by a GDI dissociation factor (GDF)^{215,216}. Membrane bound Rab GTPases are then activated by Rab-specific GEFs that enable them to recruit Rab-specific effector proteins. How exactly Rab GTPases are recruited to specific membrane domains is incompletely understood, but it is suggested that a combination of features such as specific GEFs, specific effector proteins as well the hypervariable domain of each Rab GTPase determines its membrane localization^{176,217,218}.

It is known that Rab35 is targeted to the plasma membrane via its polybasic-prenyl plasma membrane targeting motif^{176,177}. This polybasic domain interacts with negatively charged phosphatidylinositide lipids, preferentially with PtdIns(4,5) P_2 . It has been shown that the AMIS is highly enriched in PtdIns(4,5) P_2 through conversion of PtdIns(3,4,5) P_3 to PtdIns(4,5) P_2 via the phosphatase PTEN²⁴, thus increasing the affinity for Rab35 binding. However, GEF mediated nucleotide exchange is also necessary for the insertion of prenylated Rab35 into the membrane¹⁷⁷, and it remains speculative which GEF mediates Rab35 activation at the AMIS. Therefore it would be of great interest to investigate the known Rab35 GEFs connecdenn1-3 and Folliculin during MDCK cystogenesis.

3.3 Rab35 and other tethering mechanisms at the AMIS

Fusion of vesicles to their target membrane is mediated through tethering steps and engagement with SNARE proteins that mediate membrane fusion²¹⁹⁻²²³. Typically a Rab GTPase is activated and recruited onto vesicular membranes by its specific GEF. The Rab GTPase can then bind molecular motors to mediate vesicle targeting along microtubules or actin cables. Once the vesicles reach their target membrane, Rab GTPases can interact with tethering factors located on the acceptor membrane, while v-SNAREs located on the vesicle interact with t-SNAREs at the acceptor membrane to mediate vesicle docking and fusion (Figure 44).

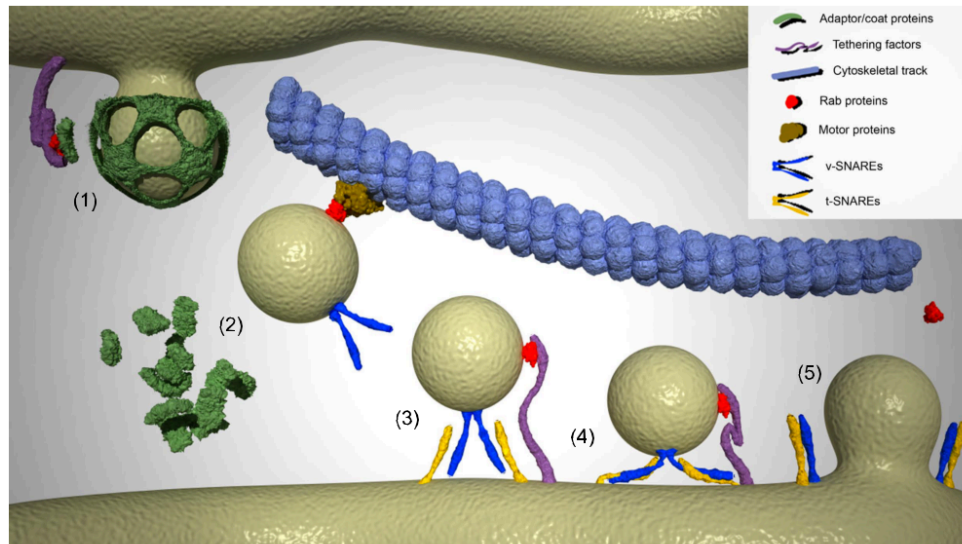


Figure 44: Vesicle budding and fusion.

- (1) Vesicle formation and coat assembly at the donor compartment.
 - (2) Vesicle uncoating and transport along cytoskeletal tracks.
 - (3) Tethering of vesicles to the acceptor compartment by Rab protein/tether factor complexes.
 - (4) Docking of vesicles to the acceptor compartment is mediated by v-SNAREs and t-SNAREs.
 - (5) Membrane fusion and release of cargo. Trans-SNARE complexes promote vesicle fusion.
- From reference: ²²⁴

Besides the classical mechanism of vesicle tethering however, Rab GTPases can mediate tethering in different ways. Rab GTPases located at the vesicle as well as the acceptor membrane can bind the same effector and thus mediate tethering over tens of nanometers²²⁵. Some Rab GTPases have also been shown to dimerize and could as such act as membrane tethers over smaller distances of less than 10 nm²²⁵. A third mechanism for Rab mediated tethering is the formation of a SNARE trans complex where the Rab GTPase recruits a SNARE binding regulator that binds to the SNAREs on the opposite membranes (Figure 45). Here, we describe a fourth mechanism by which the Rab GTPase is activated on the acceptor membrane and mediates tethering through direct binding of a transmembrane protein on the vesicle. Active Rab35 is bound to the future apical membrane (acceptor membrane) where it tethers apical vesicles through a direct interaction with the cytoplasmic tail of the transmembrane protein PODXL (Figure 45).

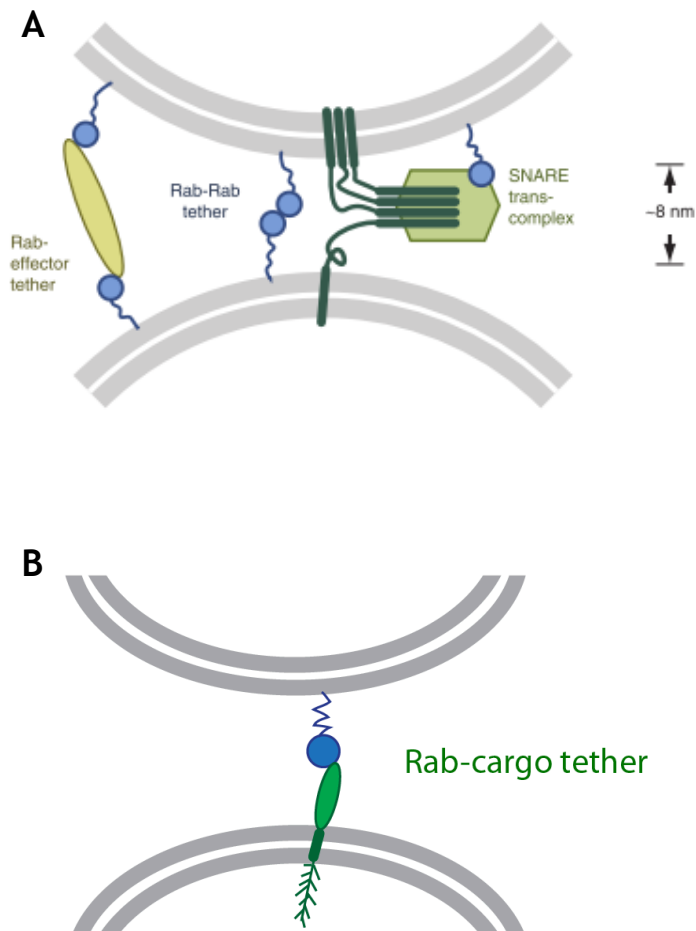


Figure 45: Rab-dependent tether mechanisms.

- (A) This scheme illustrates three well-characterized Rab-tether mechanisms: Rab effector tether, Rab-Rab tether and the SNARE trans-complex. From reference: ²²⁵
- (B) Proposed model for a Rab-cargo tether, showing a direct interaction between a Rab GTPase (blue) and a transmembrane cargo (green) (eg. Rab35 and PODXL).

A classical Rab tethering mechanism at the apical membrane in MDCK cysts has been well described for the case of Rab27 and Rab3. Vesicle-bound v-SNARE-like Slp4-a associates with the apical membrane-bound t-SNARE Stx3 and thus tethers Rab27A/Rab3/PODXL positive vesicle to the apical membrane in MDCK cysts⁶⁶. Depletion of either Stx3 or Slp4-a leads to an accumulation of intracellular vesicles, due to impaired vesicle fusion. In addition it was shown in Caco-2 3D cysts that Munc18-2 assists the Slp-4a/Stx3-mediated vesicle tethering by direct binding to both SNAREs²²⁶. Moreover, the v-SNARE Vamp7 interacts with Rab11 and Stx3, thus enabling Stx3 to form

a multi-Rab tethering complex comprising Rab3, Rab8, Rab27 and Rab11²²⁶. Rab8 and Rab11 are furthermore involved in the Exocyst-mediated tethering through interaction with the Exocyst subunit Sec15^{72,226,227}.

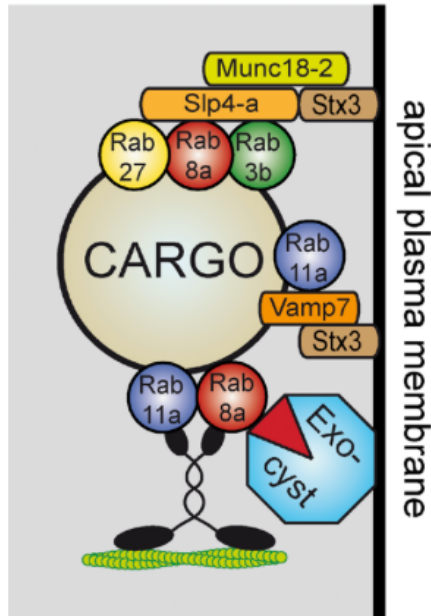


Figure 46: Delivery of apical cargo to the apical plasma membrane.

This scheme illustrates how apical vesicles are tethered at the apical plasma by multiple mechanisms. From reference: ²²⁶

The Exocyst is probably one of the best-studied plasma membrane tethering complexes. This octameric complex is comprised of Sec3, Sec5, Sec6, Sec8, Sec10, Sec15, Exo70 and Exo84. The exocyst associates with the plasma membrane via binding of Exo70 and Sec3 to $\text{PtdIns}(4,5)\text{P}_2$ ²²⁸⁻²³⁰ (Figure 47 and Figure 48). It tethers vesicles via binding of Sec15 to the Rab GTPases Rab11 and Rab8 whereas the subunits Sec5 and Exo84 can bind to RalA ²²⁰ and Exo70 and Sec3 bind additionally to Cdc42 ^{231,232}, Arf6 ¹²⁹ and RhoA ²³². The Exocyst has also been shown to act as a tethering complex at the apical membrane during MDCK cystogenesis⁷². Here, Rab11 and Rab8 cooperate to recruit Sec15 to the AMIS, which mediates vesicle tethering through interaction with other exocyst complex subunits (Sec10/Sec8) that are recruited to the AMIS via the Par3/aPKC complex^{72,227}.

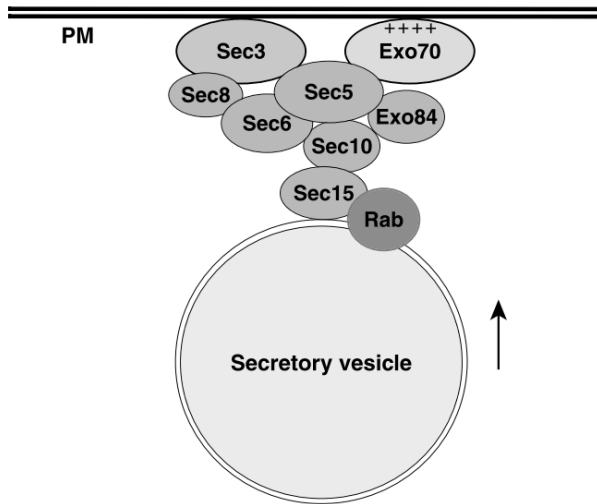


Figure 47: The composition of the Exocyst complex.

The Exocyst subunit Exo70 directly associates with $\text{PtdIns}(4,5)\text{P}_2$ at the plasma membrane (PM) via its positively charged residues. Exo70, together with Sec3, interact with other Exocyst subunits that are localized on the vesicle, thereby tethering the vesicle to the $\text{PtdIns}(4,5)\text{P}_2$ -rich plasma membrane. From reference: ²²⁸

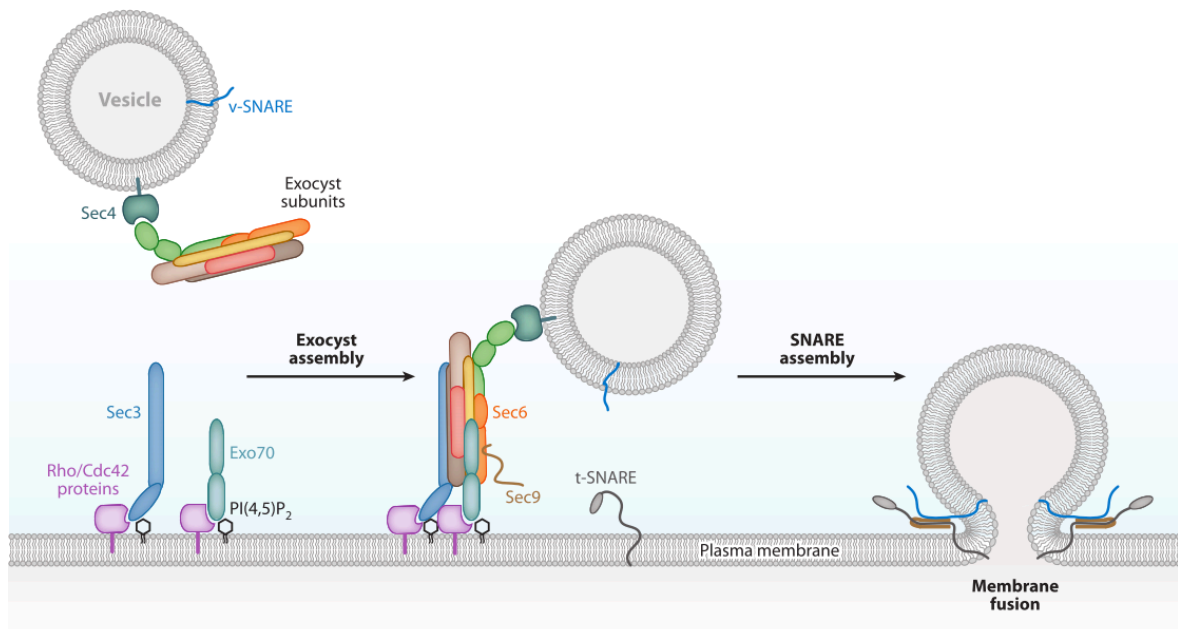


Figure 48: Exocyst-mediated vesicle tethering and fusion.

The Exocyst subunits Sec3 and Exo70 associate with the plasma membrane through interactions with Rho/Cdc42 and $\text{PtdIns}(4,5)\text{P}_2$, respectively. Formation of the exocyst complex mediates vesicle tethering and regulates SNARE complex assembly through interaction between Sec6 and the t-SNARE Sec9²³³, leading to membrane fusion. From reference: ²³⁴

The question that rises here is: why do so many different apical tethering mechanisms co-exist and why does only depletion of Rab35 lead to inversion of apico-basal polarity?

The tethering of apical vesicles needs to be a very robust process, since mis-localized apical proteins can have drastic consequences for an epithelial tissue. Moreover different tethering complexes can be differentially expressed in certain tissues to ensure tissue plasticity. One could also imagine that different tethering complexes act at different distances or are temporally differentially activated, thus having different tethering complexes activated for apical membrane initiation and maintenance. One should also consider that tethering of apical vesicle could be regarded as a stochastic event where single weak interactions cannot sufficiently tether vesicles, but a cascade of multiple tethering events could allow for robust vesicle tethering (Figure 49).

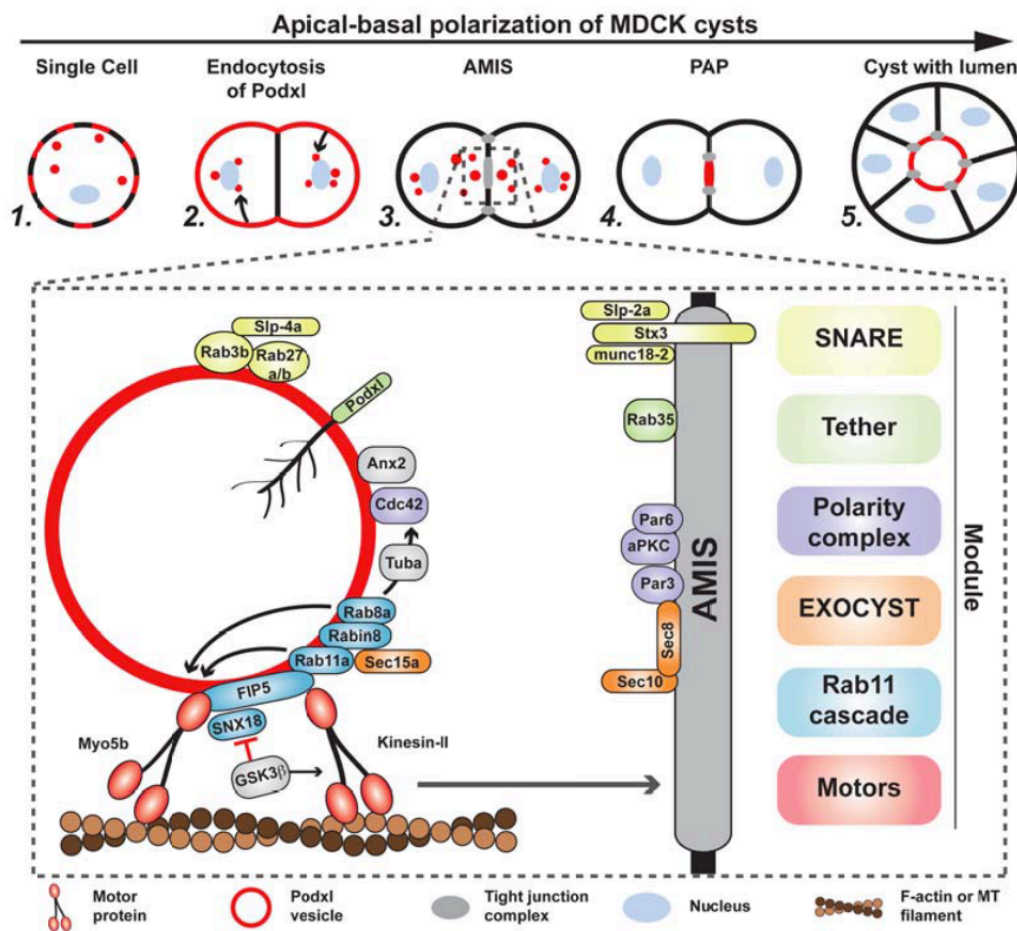


Figure 49 : Co-existence of multiple tethering complexes at the AMIS.

This scheme depicts how multiple tethering complexes, including Rab35, co-exist to ensure efficient tethering of apical vesicles at the AMIS. From reference: ²³⁵

3.4 Why does Rab35 depletion lead to inversion of AB polarity?

The Rab35 GTPase acts as a tether to capture PODXL-positive vesicles at the AMIS to facilitate their fusion. Depletion or inactivation of Rab35 disrupts this tethering mechanism and leads to an inversion of apico-basal polarity due to fusion of PODXL vesicles at the wrong plasma membrane domain. Likewise, disruption of the PODXL/Rab35 interaction through expression of the PODXL mutant V496A/Y500A that does not interact with Rab35 induces apico-basal polarity inversion.

In contrast, depletion of other tethering factors such as Syntaxin 3 or Exocyst subunits lead to an accumulation of apical cargo in the cytoplasm or the formation of multiple small lumen due to fusion to the wrong membrane, but do not induce polarity inversion.

Why does depletion of Rab35 lead to an inversion of apico-basal polarity? Is there a default pathway for PODXL-vesicles?

PODXL-vesicles trafficked in Rab11-positive recycling endosomes on the biosynthetic route through the TGN or on the transcytosis route from the basolateral to the apical domain. It was shown that PODXL trafficking to the apical membrane depends on a combination of the PDZ domain and NHERF1 interaction as well as glycosylation of the extracellular domain of PODXL¹⁵². Disruption of these apical targeting motifs leads to basolateral mistargeting of PODXL, suggesting that PODXL is indeed trafficked to basolateral membranes by default if apical sorting motifs are missing. This default pathway could also play a role in Rab35-depleted cysts. Although the actual apical targeting of PODXL is not impaired, the last step prior to fusion, the tethering of PODXL-vesicles, is inhibited and could thus activate the basolateral default pathway.

Could Rab35 be involved in the apical trafficking/sorting of PODXL-vesicles?

Since we did not observe a strong co-localization of Rab35 and PODXL or Rab35 and Rab11 on endosomes, it seems unlikely that Rab35 is involved in the actual trafficking of PODXL. Furthermore, ectopic expression of active Rab35 on the mitochondria leads to accumulation of PODXL-positive vesicles around the mitochondria even when endogenous Rab35 is depleted (unpublished results). This indicates that Rab35 is not required for the trafficking of PODXL to the mitochondrial membrane.

Could Rab35 binding to the PODXL cytoplasmic tail compete with other binding partners?

Interestingly, apico-basal polarity inversion upon Rab35 depletion can be rescued by expression of siRNA resistant Rab35 WT but not by the dominant active mutant Rab35 Q67L (data not shown). This indicates that the PODXL/Rab35 interaction needs to be regulated transiently and that Rab35 might compete with other proteins for the binding of the PODXL cytoplasmic tail. One could imagine that PODXL-vesicles are tethered at the AMIS via long distance tethers such as the Exocyst complex, from where they move closer to the Rab35/PODXL tether and the Slp-4/Stx3 tether that allows membrane fusion.

During the tethering steps, I propose that active Rab35 localized at the AMIS binds to the cytoplasmic tail of PODXL prior to Slp-4/Stx3 mediated membrane fusion. It is possible that the Rab35 binding could limit the access to the PODXL phosphorylation site at Ser-415, which was shown to be dephosphorylated by PP2A at the apical membrane⁷³. It was suggested that PP2A dephosphorylates PODXL and NHERF-1 at the apical membrane to allow formation of the PODXL/NHERF-1 complex to stabilize PODXL at the membrane. Interestingly, NHERF-1 can bind the Rab35 GAP EPI64B and could therefore recruit EPI64B to induce Rab35 inactivation and thus dissociation of PODXL to facilitate PODXL dephosphorylation and stabilization at the apical membrane.

However, this would explain why depletion of Rab35 or expression of the PODXL mutant could prevent stabilization of PODXL at the apical plasma membrane domain, but not why it then fuses to the basolateral plasma membrane.

Therefore, I can imagine two possible explanations how Rab35 depletion could induce polarity inversion:

1) Rab35 competes with another protein for the binding of the PODXL cytoplasmic tail.

Binding of Rab35 to the PODXL tail at the apical membrane could occupy the binding site for other proteins that are for example required for basolateral trafficking. In this case Rab35 would have a dual function at the apical membrane in assisting the tethering of PODXL-vesicles but also in preventing its basolateral trafficking.

This hypothesis requires an interaction between the PODXL cytoplasmic tail and another protein that mediates basolateral traffic (e.g. a Rab GTPase) or a minus-end directed motor. Mass spectrometry of co-immunoprecipitated proteins from PODXL WT in comparison to PODXL V496A/Y500A could reveal such a potential binding partner.

2) The Rab35/PODXL tether is dominant over the other tethering mechanisms.

However, during the initial steps of apico-basal polarity establishment, during the first cyst cytokinesis, the apical and basolateral domains are not yet defined. It was demonstrated by Bryant et al, that early MDCK cysts have to re-orientate the polarity axis, thus inducing the transcytosis of apical membrane proteins that are initially localized at the outer ECM-facing membrane⁷³. The endocytosis of PODXL is induced through β 1-integrin mediated signalling and PODXL phosphorylation by PKC β II. PODXL phosphorylation destabilizes the Ezrin/NHERF-1/PODXL complex and thus facilitates internalization and transcytosis.

Depleting Rab35 or blocking of the Rab35/PODXL interaction does not impair PODXL internalization as demonstrated by an antibody internalization assay in Rab35 depleted and control cells as well as PODXL mutant expressing MDCK cells (Supplementary Figure 6a-d in the published manuscript). Moreover it was recently shown in Hela cells that Rab35 is recruited onto clathrin coated vesicles after scission and therefore is not involved in the step of cargo internalization^{178,185}.

When Rab35 is depleted, it is true that PODXL appears very quickly at the basolateral membrane in early cystogenesis as observed by time-lapse microscopy. Nevertheless, PODXL is clearly observed in Rab11-positive recycling compartments and also in lower quantities at the cell-cell contacts in very early cysts upon Rab35 depletion. This demonstrates that PODXL internalization is indeed not impaired upon Rab35 depletion and that PODXL can be trafficked towards the cell-cell contacts, but finally fuses at the outer ECM-facing membrane.

2a) The Rab35/PODXL tether is dominant over the other tethering mechanisms and asymmetric PODXL distribution reinforces a positive feed-back loop

The definitive establishment and segregation of the apical and basolateral plasma membrane domain is likely a very fast process, driven by feed-back loops to create asymmetric protein distributions. Therefore it is likely that already little amounts of apical proteins (contained in PODXL-positive vesicles) can drive apical polarity establishment once they are enriched to a certain threshold. This means that once this threshold is reached, apical polarity complexes as well as kinases and phosphatases and the exocytic machinery would become enriched at this membrane. Hence, even apical tethering complexes such as the exocyst and Syntaxin 3 could become enriched at the ECM-facing membrane once the asymmetry of apical determinants is broken towards the “wrong”, ECM-facing membrane upon Rab35 depletion.

2b) The Rab35/PODXL tether is dominant over the other tethering mechanisms and the asymmetric distribution of PODXL is skewed to the basolateral membrane due to its larger surface.

If PODXL-vesicles were not directly targeted towards the apical membrane through Rab11-associated plus-end directed motors, then its delivery would occur randomized to the basolateral or the apical membrane. Nonetheless, its distribution would be skewed to the basolateral membrane due to its larger surface. This means that the cell has to overcome the advantage of basolateral vesicle targeting in order to enrich apical proteins at the much smaller apical membrane domain. The presence of tethering complexes at the apical membrane would represent one such mechanism that assists to accumulate PODXL-vesicles. The delivery of apical vesicle is furthermore likely a very dynamic process where many vesicles go back and forth and not every single vesicle that arrives at the apical membrane would automatically undergo apical fusion. Therefore, weakening of the tethering mechanism through depletion of Rab35 would allow vesicles to move back to the basolateral membrane and here, as mentioned before, a positive feed-back loop could help to establish an apical membrane at the CEM facing membrane and thus invert apico-basal polarity.

Taken together, I presented here different hypotheses that could explain why depletion of Rab35 or blocking of the PODXL/Rab35 interaction leads to a complete inversion of apico-basal polarity in MDCK cysts. Nonetheless, it needs to be emphasized that one of the major differences between the Rab35-mediated tethering compared to other tethering machineries is the fact that the Rab35/PODXL tethering complex does not interact directly with SNARE proteins (at least it has not been demonstrated yet). All of the here reviewed tethering complexes interact with SNARE proteins, thus disruption of these complexes not only disrupts tethering but possibly also fusion, which is required for polarity inversion.

3.5 Significance of other Rab-cargo interactions

Active, GTP-bound, Rab GTPases can interact with specific cytosolic effector proteins and recruits them to specific membranes. Through interaction with coat components, motor proteins and SNARES, Rab GTPase regulate the sorting, traffic, docking and fusion of vesicular cargo. However, Rab GTPases can also interact directly with the cytoplasmic domain of vesicular cargos.

The first direct Rab/cargo interaction was identified by Van Ijzendoorf et al. who demonstrated a direct binding between GTP-bound Rab3b and pIgR²³⁶. Binding of the ligand dIgA induces the dissociation of the Rab3b from pIgR to allow signalling through exocytosis and ligand release at the apical membrane. The interaction domain was mapped to the membrane -proximal 14 amino acids. Since then many other direct Rab-cargo interaction have been discovered including interactions with integrins^{237,238}, ion channels²³⁹⁻²⁴², GPCRs²⁴³⁻²⁴⁵ and intermediate filament proteins²⁴⁶⁻²⁴⁸. The human angiotension II type 1 receptor (AT₁R) belongs to the superfamily of GPCRs and can interact with Rab4, Rab5, Rab7 and Rab11 as shown by co-IP²⁴⁴. Furthermore these Rab GTPases compete for the binding to AT₁R, which was shown to occur within the last 10 aminoacids of the cytoplasmic tail. The binding of all RabGTPases was inhibited upon mutagenesis of the proline 354 and cysteine 355. However, it was only demonstrated that AT₁R could form a complex with the above-mentioned Rab GTPases, but it was not shown that these interactions are indeed direct. Rab11 in contrast has been shown to bind directly in a GTP dependent manner to the GPCR TP- β ²⁴⁵. Also in this case the interaction site is composed of a short amino acid sequence (335-344) within the cytoplasmic tail. Blocking of the direct interaction was shown to perturb the trafficking from Rab5-positive endosomes to Rab11-positive perinuclear recycling endosomes. Also Rab1 binds directly and GTP dependent to the cytoplasmic domain of the GPCR β 2-adrenergic receptor (β 2AR) to regulate its anterograde trafficking²⁴³. The binding of Rab1-GTP requires a dileucine motif, localized in the proximal part of cytoplasmic tail. Interestingly the same binding motif is also required for binding of Rab8 to β 2AR²⁴⁹. As

mentioned above, integrins can also bind directly to Rab GTPases as shown for Rab25 and $\alpha 5\beta 1$ ²³⁷ integrin and for Rab21 and $\alpha 2\beta 1$ integrin²³⁸. The interaction with Rab25 was demonstrated to be direct and GTP-dependent and drives cell migration and invasion of ovarian cancer cells in a 3D matrix by directing the localization of integrin-recycling vesicles²³⁷. Also the Rab21-integrin interaction was shown to be direct and to promote cell migration and adhesion in a breast cancer cell line²³⁸.

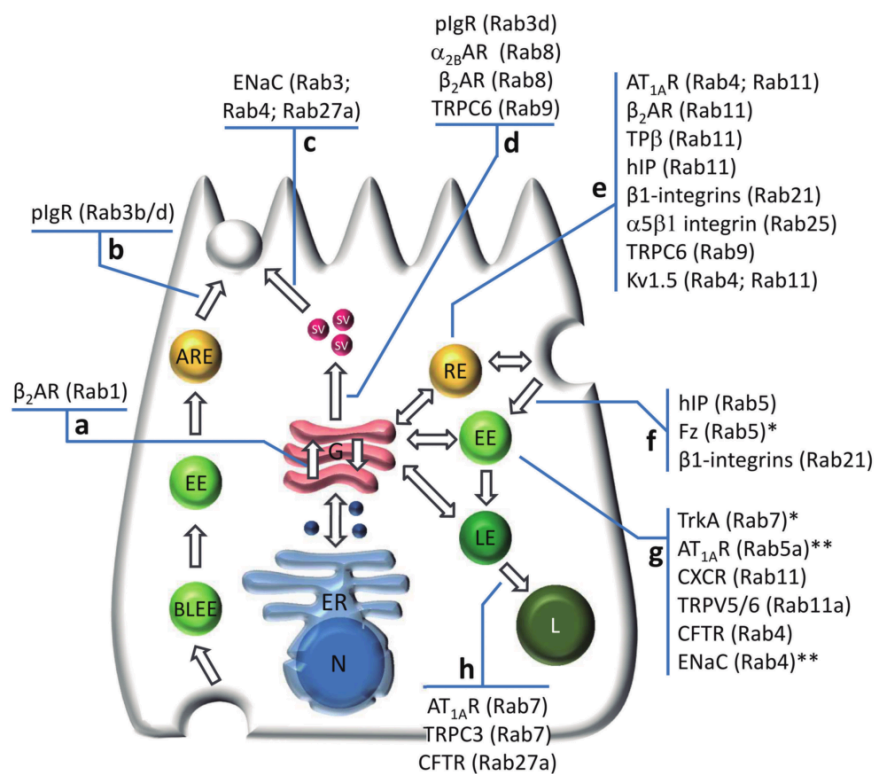


Figure 50: Rab GTPases-cargo direct interactions.

This scheme illustrates the known direct interaction between Rab GTPases and a transmembrane cargo.

- (a) Anterograde trafficking
- (b) Transcytosis
- (c) Exocytosis
- (d) Transport from TGN to PM
- (e) Recycling
- (f) Internalization
- (g) Endosomal sorting
- (h) Lysosomal delivery.

From reference: ²⁴⁷

It seems that Rab GTPase/cargo direct interactions are very specific and lack a common binding motif. The above-mentioned de Rab/cargo interactions regulate the traffic, recycling or the exocytosis of the cargo proteins and not the tethering of cargo vesicles, as it is the case for the PODXL/Rab35 interaction. The major difference between the above-mentioned interactions and the PODXL/Rab35 interaction is the particular plasma membrane localization of Rab35. None of the other here mentioned RabGTPases localize primarily to the plasma membrane and thus cannot function as a plasma membrane tether. If Rab/cargo interactions occur in *trans*, it is likely that these interaction facilitate the tethering between vesicles, for example to transfer cargo from Rab5-positive endosomes to Rab11-positive recycling endosomes as described for the Rab11/TP- β interaction²⁴⁵. However, Rab/cargo interactions can also occur in *cis*, thereby binding the transmembrane cargo while being localized on the same membrane and simultaneously binding to another partner such as a motor protein or another Rab GTPase. Furthermore, Rab/cargo direct interaction can regulate membrane traffic through competitive binding as shown for Rab3b, which competes for plgR binding with the ligand plgA to regulate apical exocytosis and ligand signalling²³⁶. However, the emerging role of Rab/cargo direct interaction requires further investigation and might open a completely new view on Rab GTPase regulated vesicular membrane traffic.

3.6 The role of Rab35 interacting proteins in apico-basal polarity establishment

The Rab35 effector OCRL

One effector protein of Rab35 is the phosphatidylinositol 5-phosphatase OCRL. Mutations of the *OCRL* gene can lead to the Occulo Renal Syndrome of Lowe and Dent2 disease, both characterized by congenital cataracts, mental and growth retardation and renal proximal tubule dysfunction (Fanconi syndrome)²⁵⁰. The preferred substrate of the

OCRL phosphatase are $\text{PtdIns}(4,5)\text{P}_2$ and $\text{PtdIns}(3,4,5)\text{P}_3$, which are converted to $\text{PtdIns}4\text{P}$ and $\text{PtdIns}(3,4)\text{P}$ respectively.

Rab35 was shown to interact directly with the phosphatase OCRL in HeLa cells and to regulate its localization at the intracellular bridge during cytokinesis. Correct localization of OCRL leads to conversion of $\text{PtdIns}(4,5)\text{P}_2$ to $\text{PtdIns}4\text{P}$ and prevents F-actin polymerization to allow successful abscission of the two daughter cells¹⁷⁹. Similarly OCRL is recruited onto new born endosomes by Rab35 in HeLa cells, which induces $\text{PtdIns}(4,5)\text{P}_2$ hydrolysis that allows uncoating and traffic these endosomes¹⁸⁵. A definite role for OCRL during MDCK cystogenesis has so far not been demonstrated. One study showed that depletion of OCRL impaired cyst formation when MDCK cells were cultured in a collagen/Matrigel mix²⁵¹, whereas another study showed only mild defects in MDCK cystogenesis (cultured in 100% Matrigel), but impaired cilia formation²⁵². However, none of these studies observed an inversion of apico-basal polarity upon OCRL depletion. When we cultured MDCK cells in 2% Matrigel, we did not observe any defects in cystogenesis upon OCRL depletion (Supplementary Fig. 6f,g of the published manuscript). Of note, OCRL shares 45% homology with the 5-phosphatase INPP5B, which could rescue OCRL depletion, as demonstrated in OCRL KO mice²⁵³. Interestingly, it has been shown that MDCK cells express significant levels of INPP5B, that could rescue the OCRL depletion²⁵⁴.

A role for Rab35 and OCRL (or INPP5B) during cytokinesis and endosomal traffic in MDCK cysts is likely, but has not been demonstrated yet. However the inversion of polarity upon Rab35 depletion is unlikely caused by cytokinesis defects, since depletion of OCRL alone does not affect cystogenesis. Moreover depletion of Cep55, a key player of cytokinesis, leads to a prolonged abscission time in MDCK cells grown on glass but does not impair cyst development (Supplementary Figure 4a,b in the published manuscript).

The Rab35 effector ACAP2

Arf6 was shown to negatively regulate Rab35 activation through the Rab35 GAP EPI64B, which was identified as an effector of Arf6. The Arf6 mediated regulation of Rab35 was

shown to regulate an endocytic pathway essential for cytokinetic abscission¹³². Interestingly, the Rab35 effector ACAP2 is also a GAP for Arf6, leading to mutual antagonistic regulation of Arf6 and Rab35 activation¹⁹². Arf6 activation in MDCK cysts was shown to induce lumen filling and multiple lumen as well as disruption of adherence junctions through enhanced growth factor receptor internalization and signalling¹³⁰. Arf6 depletion in contrast was shown to induce apico-basal polarity inversion through Rac1 inactivation and impaired laminin assembly¹¹⁷. Interestingly, it was shown in COS-7 cells that the Rab35/Arf6 mutual antagonism also plays a role in cell migration, EMT and tumorigenesis¹⁹⁸. Rab35 promotes cell-cell adhesion through maintaining cadherins at the cell surface. Furthermore Rab35 negatively regulates integrin recycling through ACAP2 mediated inhibition of Arf6. Depletion of Rab35 induces Arf6 activation, which leads to enhanced integrin and EGFR recycling and reduced recycling of cadherins, thus inhibiting cell-cell adhesions and promoting cell migration¹⁹⁸. The question that rises here is whether the Rab35 dependent apico-basal polarity inversion can be explained through Arf6 dysregulation and Rac1 inactivation. This is unlikely, since we could show that polarity inversion clearly depends on the direct interaction between PODXL and Rab35. Replacement of endogenous PODXL with the PODXL mutant V496A Y500A, unable to interact with Rab35, also leads to apico-basal polarity inversion. Although it was shown in one study that Arf6 depletion lead to Rac1 inactivation and therefore polarity inversion, it seems unlikely that Rac1 inactivation is mediated through Rab35, but further investigations would be necessary to clarify this point¹¹⁷.

The Rab35 GAP EPI64B

As mentioned above, Rab35 activity is negatively regulated by its GAP EPI64B. Interestingly, EPI64B binds to both PDZ domains of NHERF1 (EBP50), which binds to active Ezrin and PODXL²⁵⁵ at the plasma membrane. We demonstrated that active Rab35 binds to the cytoplasmic tail of PODXL to tether arriving PODXL endosomes at the future apical plasma membrane. The NHERF1/Ezrin/PODXL complex assembles upon membrane fusion to stabilize PODXL at the plasma membrane⁷³. It is possible that EPI64B is

required to inactivate Rab35 in order to disrupt the Rab35/PODXL interaction to enable assembly of the NHERF1/Ezrin complex. Another possibility would be that EPI64B inactivates Rab35 at the ECM-facing membrane and thus prevents Rab35 mediated PODXL tethering at the wrong plasma membrane. Both hypotheses will need further investigation to clarify the role EPI64B. However, EPI64B over-expression induces apico-basal polarity inversion in the presence of Rab35, thus demonstrating that EPI64B is the major Rab35 GAP in MDCK cysts.

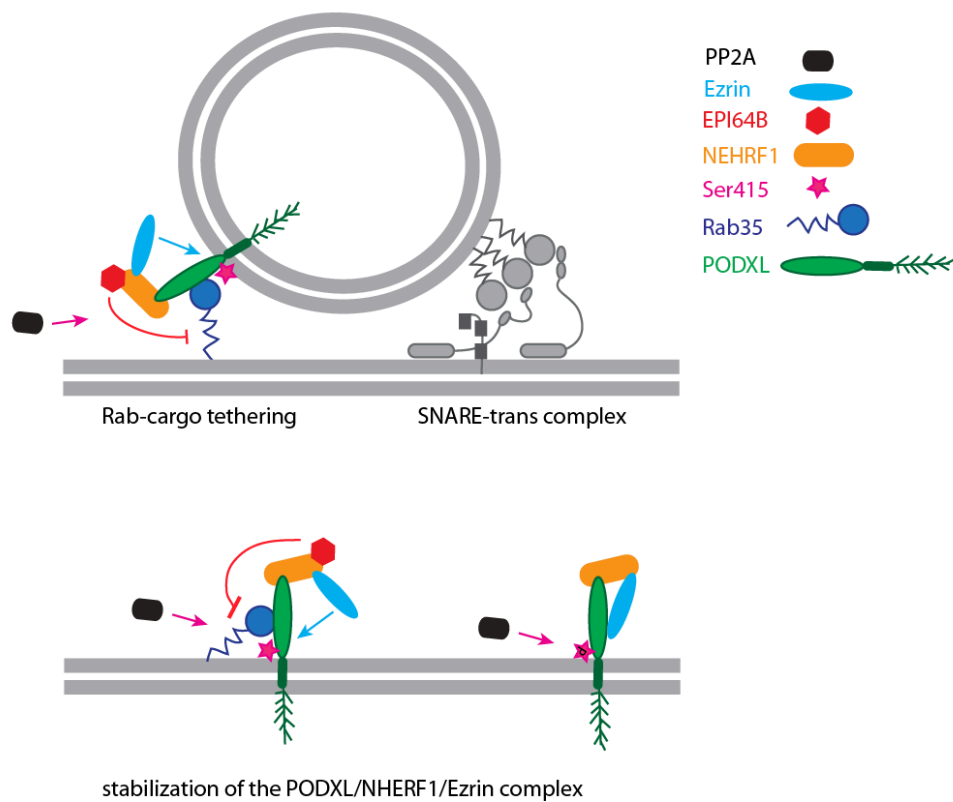


Figure 51: Model for EPI64B-mediated stabilization of the PODXL/NHERF1/Ezrin complex.

Rab35 GEFs: connecdenn1-3 and Folliculin

Other Rab35 interacting proteins are the Rab35 GEFs connecdenn1-3^{199,256} and the recently discovered GEF Folliculin²⁰⁴. Connecdenn1-3 have not been associated with any role in epithelial polarity so far, however it was shown that phosphorylated Connecdenn1 binds to 14-3-3²⁰³, a protein that also binds phosphorylated Par-3 at the apical domain during early polarity establishment²⁵⁷. Binding of 14-3-3 to Connecdenn1 releases its auto inhibition and increases its GEF activity as well as the binding to Rab35²⁰³. Hence, connecdenn1 could potentially activate Rab35 at the apical membrane through assistance of 14-3-3.

Although the GEF activity of Folliculin towards Rab35 was so far only demonstrated *in vitro* and not in cells²⁰⁴, Folliculin has been linked to epithelial polarity in two independent studies^{206,207}. It was shown that depletion of Folliculin impairs single lumen formation of T84 human colon carcinoma cells in Matrigel²⁰⁷ and in murine collecting duct mMCD3 cells cultured in Geltrex matrix²⁰⁶. Folliculin-depleted epithelial cysts display filled lumen, but not inversion of apico-basal polarity. However, the impaired lumen formation in these studies was linked to impaired Rho activation upon Folliculin depletion as well as defects in junction formation. Nevertheless it remains to be investigated whether depletion of Folliculin or connecdenn leads to polarity inversion in MDCK cells and could be thus identified as the major Rab35 GEF in MDCK cystogenesis.

3.7 Other potential functions for Rab35 in epithelial polarity

3.7.1 The role of Rab35 in subsequent cell divisions in MDCK cysts

During each cell division of cystogenesis, cells have to orientate their cell division axis, remodel junctions and deliver neosynthesized and recycled proteins to the newly defined membrane domains. The correct orientation of the mitotic spindle during mitosis is regulated through a polarized localization of the force generator complex ($G\alpha_i$, LGN, NuMA) that links the spindle microtubules to the cell cortex. $G\alpha_i$ binds to the plasma membrane via its G-protein coupled subunit and serves as an anchor for LGN. LGN in turn binds to NuMA, which associates to the dynein/dynactin complex and thus generates a pulling force on the astral microtubules^{87,258-261}. However the “correct” orientation of the mitotic spindle depends on the cell type, since cells can divide planar as in simple cuboidal epithelial monolayer, or perpendicular in a stratified epithelium such as the epidermis. In non-polarized Hela cells, it has been shown in the lab that the polarized cortex localization of the LGN/NuMA complex depends on $G\alpha_i$ and SLK mediated phosphorylation of ERM²⁵⁸. These results were also confirmed in apical progenitor cells of the mouse embryonic cortex²⁵⁸. However, it has not been investigated yet, whether this mechanism applies in polarized epithelial cells. During symmetric planar cell division as in MDCK cells, the apical localized aPKC/Par complex phosphorylates LGN and thus inhibits its binding to $G\alpha_i$ at the apical cortex²⁶². Indeed, impaired localization of the aPKC/Par complex through depletion of Cdc42, aPKC or Par3, results in randomized spindle orientation⁸⁵. Furthermore it was shown that Plexin-B2 localizes to the basolateral plasma membrane in MDCK cells and mouse kidney epithelial cells and controls the cell division axis through activation of Cdc42²⁶³. It was also shown that IQGAP is involved in planar spindle orientation in MDCK cells through modulating the cortical localization of NuMA²⁶⁴. However, it has been suggested that multiple mechanisms could compensate for each other to ensure robust spindle orientation²⁶⁵.

Defects in the orientation of the mitotic spindle have often been associated with multiple lumen phenotypes in MDCK cysts due to mistrafficked apical proteins or tumorogenesis at least in *Drosophila* in Lgl and Dlg mutants²⁶⁶.

However, the impact on misoriented spindles is under debate and seems to depend on the type of tissue. It has been shown in the imaginal wings disk of *Drosophila melanogaster* that misaligned spindles leads to extrusion of the perpendicular divided cells, which undergoes apoptosis. Inhibition of apoptosis in this context induces formation of a tumor-like cell mass²⁶⁷. On the other hand, it was shown in the developing ureteric bud of the mouse that epithelial cells can protrude out of the epithelial monolayer to round up for mitosis in the luminal space, while remaining connected to the epithelium via a basal process. During cytokinesis only one of the daughter cells inherit the basal process and re-inserts into the epithelium, while the other daughter cell, now localized in the luminal space does not undergo apoptosis, re-inserts a few cells further back into the epithelium²⁶⁸. In MDCK cysts in contrary, depletion of genes involved in spindle orientation is associated with either lumen filling or the multiple lumen phenotype^{68,83-85,87}.

A role for Rab35 in spindle orientation has not been investigated yet, although Rab35 was shown to localize to the meiotic spindle microtubules in mouse oocytes. Rab35 depletion in mouse oocytes leads abnormal spindle morphology, thus suggesting a role for Rab35 in spindle formation²⁶⁹. Of note, we did not observe any Rab35 at the mitotic spindle in GFP-Rab35 genome edited Hela cells (unpublished data).

Rab35 depletion in MDCK cysts leads to inverted polarity, but also to multiple lumens. Interestingly, the proportion of the inverted cyst phenotype, but not the multiple lumen phenotype, correlated with the efficiency of Rab35 depletion (Figure A in Annex). However, both phenotypes could be rescued by expression of RNAi or shRNA resistant Rab35 WT, indicating that both of these phenotypes are specific for Rab35. Nevertheless, further investigation is needed to determine the cause of the multiple lumen phenotype, since multiple lumen could form either through a misaligned spindle or through mistargeted apical proteins (Figure 52).

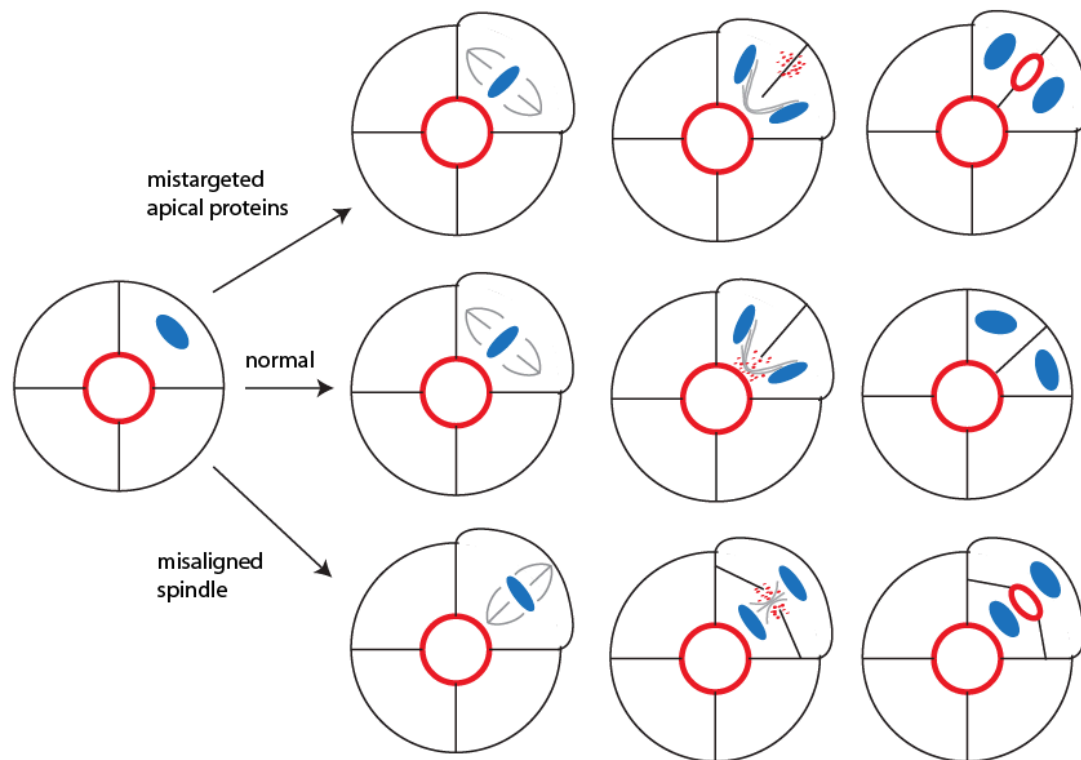


Figure 52: Development of multiple lumen in MDCK cysts

This scheme illustrates how MDCK cysts develop a single lumen in normal conditions or multiple lumens due to a misaligned spindle or due to mistargeted apical proteins.

To date, it is not known whether MDCK cells remain completely polarized during mitosis, although it was shown that adherence and tight junctions are maintained^{124,270}. Our unpublished data suggests that at least a part of PODXL is re-distributed and undergoes transcytosis during telophase in subsequent cell divisions. However, the contribution of neosynthesized PODXL to this transcytosed pool of PODXL is unknown. One could imagine several different potential models for subsequent cell divisions: In model (a) PODXL remains at its apical localization during mitosis at the 2-cell stage (Figure 53). After ingression of the furrow adherence and tight junctions are formed before cytokinetic abscission occurs and neo synthesized PODXL is trafficked towards the pre-existing apical membrane, where Rab35 is present. Here Rab35 could act as a tether for PODXL-vesicles as described for the first cell division.

In model (b) PODXL is endocytosed during mitosis, targeted towards the opposite poles and transcytosed, together with neosynthesized PODXL, to establish an apical membrane *de novo*. Also here Rab35 could act as a tether for PODXL-vesicles (Figure 53).

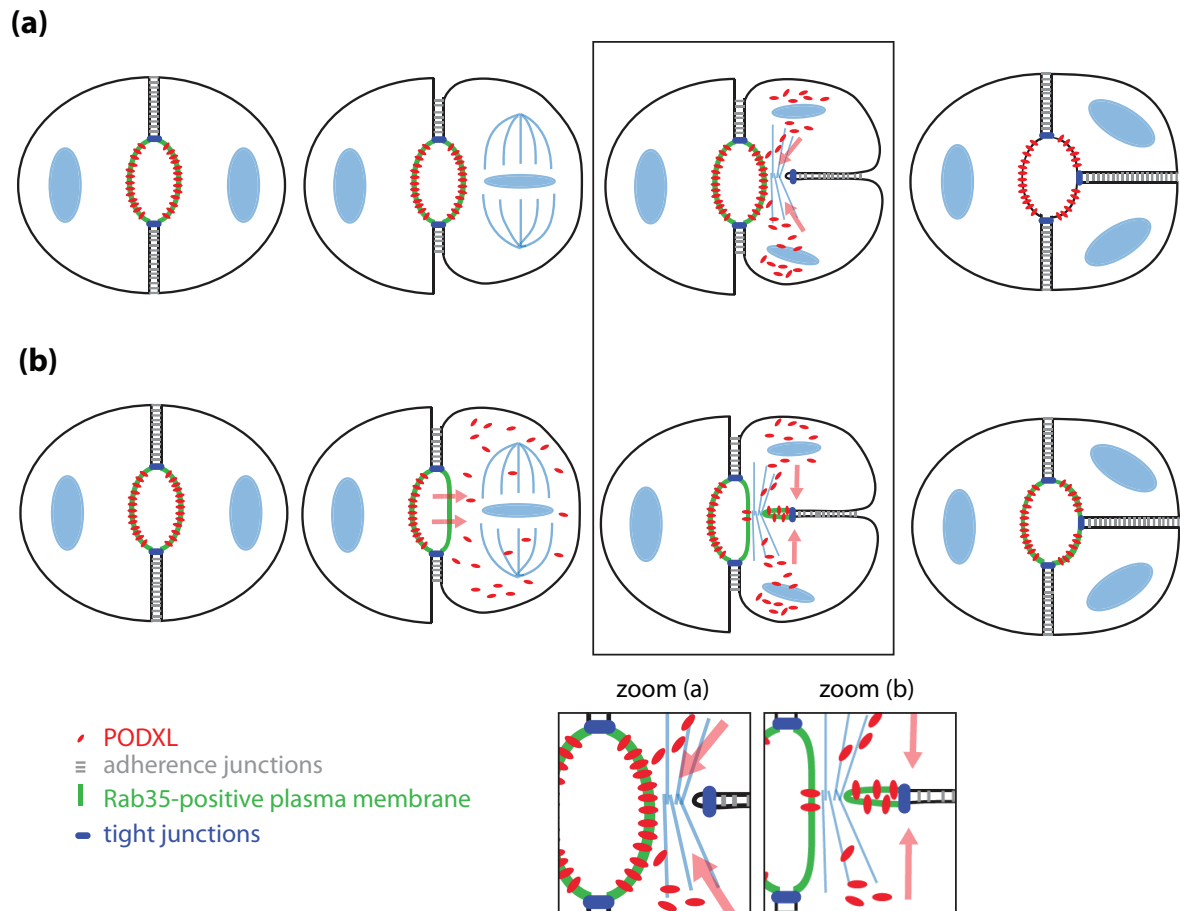


Figure 53: Rab35 and PODXL localization during the second cell division in MDCK cysts.

This scheme shows two models of PODXL and Rab35 localization during the second cell division in MDCK cysts.

During my thesis I have addressed the question whether Rab35 is involved in subsequent cell divisions in MDCK cysts after apico-basal polarity is already established (unpublished results). MDCK cells, stably expressing a Doxycycline repressible Rab35 shRNA were grown for 4 days in Matrigel to form cysts with a single open lumen. After 24 hours, doxycycline was washed out and expression of Rab35 shRNA was induced. MDCK cysts

were fixed after 24h (control) and after 3 days to assess the cyst phenotypes (Figure B in Annex). Interestingly, Rab35 depletion after apico-basal polarity establishment did not lead to inverted cysts, but lead to the formation of multiple lumen. This result indicates that Rab35 could be involved in the subsequent cell division after polarity establishment, although the mechanism by which Rab35 depletion induces multiple lumen remains speculative.

3.7.2 The Role of Rab35 in adherence junction integrity

Rab35 has been shown to regulate adherence junction formation. Depletion of Rab35 in COS-7 cells induces an accumulation of N- and E-cadherin in intracellular vesicles due to impaired recycling¹⁹⁸. Therefore Rab35 depletion decreases the cell surface localisation of cadherins and therefore decreases cell-cell adhesion. Furthermore Rab35 itself localizes to adherence junctions in C2C12 myoblasts and in Hela cells, where it regulates the recruitment of N- and M-cadherin to the junctions, their stabilization and their association with p120 catenin²⁰⁸. Interestingly, depletion or inactivation of Rab35 not only leads to an accumulation of cadherins in intracellular vesicles, but also reduces PtdIns(4,5)P₂ levels at the junctions. Moreover, PtdIns(4,5)P₂ was shown to be required for junction formation and for Rab35 recruitment, thus leading to a positive feed-back loop during adherence junction formation.

Surprisingly, to my knowledge, the requirement of adherence junctions for epithelial apico-basal polarity establishment has been barely investigated in vertebrate epithelia. One can assume that adherence junction formation plays an important role in polarity establishment since tight junctions develop from adherence junctions and proteins that are required for the establishment of polarity are often also required for junction formation as in the case of Par3 or Scribble. Moreover adherence junctions were shown

to regulate the position of the midbody¹²⁷ and thereby likely also the positioning of the apical lumen.

Interestingly, the importance of adherence junctions and lumen formation is well established in vascular lumen formation. Here the cells establish adherence junctions that are mainly composed of vascular-endothelial cadherin (VE-cadherin) and establish a lumen through delivery of anti-adhesive molecules (PODXL and Cd34) to the junctions to tear the membrane apart¹⁴⁸. Importantly, Par3 and Par6 associate with VE-cadherin and are required for lumen formation²⁷¹. The exocytosis of PODXL and Cd34 at the Par3/Par6 marked junctions follows the recruitment of F-actin and non-muscle myosin II that are required for cell shape remodelling¹⁴⁸ (Figure 54).

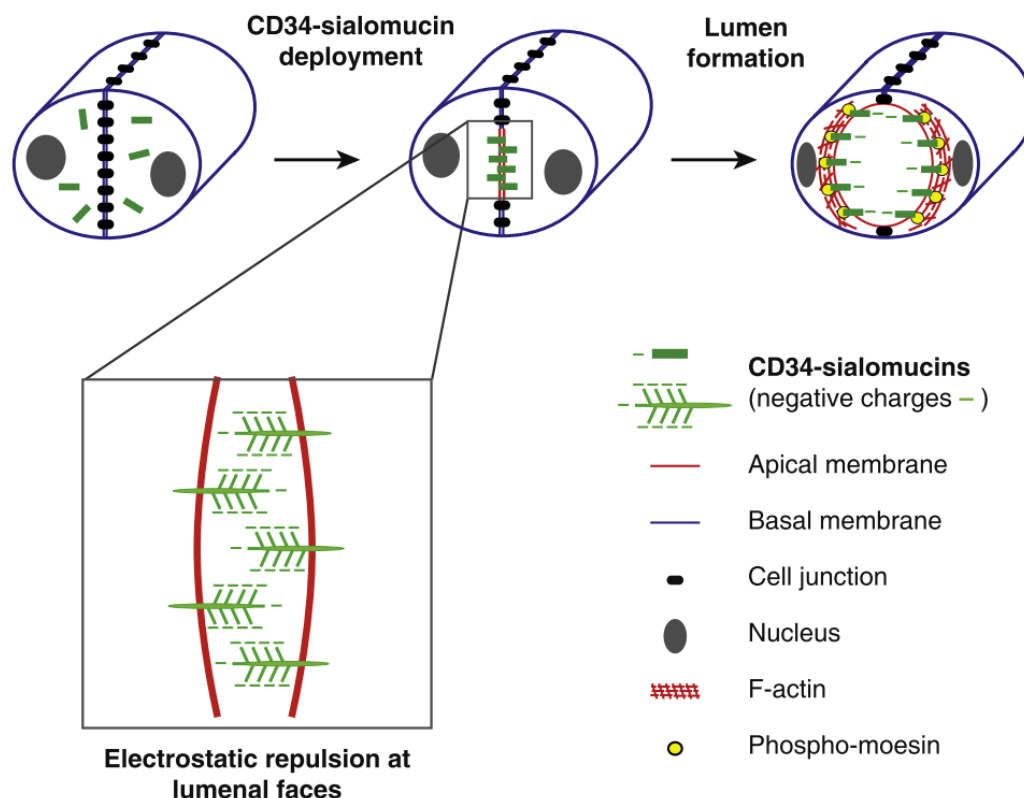


Figure 54: The function of electrostatic repulsion in vascular lumen formation.

This scheme illustrates how negatively charged sialomucins, like PODXL, CD34 or Endoglycan can induce electrostatic repulsion to separate to adjacent membranes in order to open a lumen. From reference: ²⁷²

However, to date nothing is known about Rab35 during vascular endothelial lumen formation. It is possible that Rab35 acts as a regulator for junction formation through recycling of VE-cadherin and as a tether for PODXL-vesicles. Interestingly, it has been shown *in vivo*, that also epithelial cells can establish lumen at pre-existing junctions through apical constriction without the need of preceding cell divisions^{51,273,274}. This raises the question of whether Rab35 could be also involved in apical membrane initiation and establishment without the requirement for cytokinesis. However, to answer this question further investigation would be required; for example by studying potential apical membrane and lumen formation of MDCK 2-cell aggregates that are not daughter cells.

3.8 Is the Rab35/ PODXL interaction a general mechanism?

It is possible that the Rab35/PODXL interaction in apico-basal polarity establishment presents a general mechanism that could be found *in vivo* in various tissues. Rab35, but not PODXL, is ubiquitously expressed in all human tissues. Although the expression of PODXL is restricted to certain tissues and cell types in adult tissues, PODXL is expressed in all three germ layers during mouse embryogenesis¹⁴⁰. Introduction of PODXL point mutations V496A /Y500A in mice could shed light on the impact of the Rab35/PODXL interaction *in vivo*. Moreover, these *in vivo* studies could for the first time link the inverted polarity phenotype observed in MDCK cells to a pathological phenotype *in vivo*, such as developmental defects or cancer initiation, progression or metastasis.

Interestingly, several somatic missense mutations of PODXL were found in samples from human carcinomas that are in close proximity to the Rab35 interaction domain.

transmembrane domain-----KDQQR**RL**TEELG**TV**EN**GY**HD**N**PTL-----DTHL* (human PODXL)

Rab35 binding domain

The PODXL mutant V496A /Y500A (canin) corresponds to V503A /Y507A for human PODXL.

Somatic mutation	Human tissue sample
R495W	pancreas carcinoma
E504K	skin malignant melanoma
G506S	skin malignant melanoma
D509N	skin malignant melanoma
D509G	large intestine carcinoma

(from: <http://cancer.sanger.ac.uk/cosmic>, a database for somatic mutations in cancer)

It would be of interest to investigate whether these somatic mutations found in human cancers abolish the interaction with Rab35 and whether these mutations also lead to apico-basal polarity inversion in MDCK cysts.

Moreover, it could be possible that Rab35 can interact with other members of the CD34 family such as CD34 or Endoglycan and thus could represent a general mechanism in tissues with differential expression of members of the CD34 family.

4 CONCLUSION AND FUTURE PERSPECTIVES

The major goal of my PhD project was to investigate PODXL as a potential novel effector of Rab35 during polarity establishment in 3D MDCK cysts. I found that PODXL is indeed a Rab35 effector, since the PODXL cytoplasmic binds directly and specifically to GTP-bound Rab35 *in vitro* and *in vivo*. PODXL is the first transmembrane protein discovered to interact directly with Rab35. Most Rab GTPase/transmembrane protein interactions involve transmembrane receptors, integrins or ion channels where the direct interaction is essential for the correct trafficking.

Initially, it seemed obvious that Rab35 could regulate the recycling of PODXL towards the apical membrane. However, time-lapse microscopy experiments revealed that PODXL, as previously reported, is transported in Rab11-positive recycling endosomes, showing only little overlap with Rab35-positive endosomes. This observation ruled out that Rab35 is recruited onto PODXL-positive endosomes to regulate its apical recycling. The only place where PODXL and co-localize was the apical, or future apical membrane, and PODXL was recruited onto this membrane after Rab35. Depletion of Rab35 in MDCK cysts leads to apico-basal polarity inversion, demonstrating for the first time that Rab35 is indeed involved in epithelial polarity establishment. However, the molecular cause of polarity inversion needs to be elucidated. Therefore, I set out to investigate whether the presence of GTP-Rab35 on the plasma membrane was sufficient to target PODXL to this membrane. Ectopic expression of active Rab35 on the outer mitochondrial membrane induced an accumulation of PODXL-positive in close apposition to the mitochondria. This demonstrated that active Rab35 acts as a potent tether for PODXL-positive vesicles through a direct and GTP-dependent interaction. This hypothesis was furthermore strengthened by the fact that inhibition of this direct interaction by expression of the PODXL mutant V496A Y500A completely abolished the Rab35 dependent tethering in MDCK cysts, leading to apico-basal polarity inversion.

This new concept of a direct Rab-cargo interaction at the acceptor membrane might shed light onto other Rab35-dependent pathways. Rab35 is a unique Rab GTPase

localized at the plasma membrane and could therefore represent a general tethering mechanism, which is not exclusive for PODXL. For example the role of Rab35 in exosome secretion might involve tethering of an unknown protein²⁷⁵. However, interactions with transmembrane proteins can easily be missed in Yeast-two hybrid screens due to their hydrophobic residues, which make them also difficult to detect by mass spectrometry.

To continue with the Rab35/PODXL interaction, further studies are needed to fully understand why Rab35 depletion or blocking of the PODXL/Rab35 interaction leads to apico-basal polarity inversion. Importantly, a very recent publication from the group of Fukuda confirms that loss of Rab35 by CRISPR/Cas9-mediated KO or depletion of Rab35 by siRNAs leads to apico-basal polarity inversion in MDCK cysts²⁷⁶. However, it was also shown that inverted Rab35-depleted cysts re-orient their polarity back to normal within 72h of culture in Matrigel. Contrarily to this result, I did not observe any re-orientation of polarity in Rab35-depleted cysts, even after 7 days of culture in Matrigel. The results obtained by the group of Fukuda might possibly reflect an adaptation of MDCK cells to the loss of Rab35 by up-regulation of an unknown rescue pathway. The levels of Rab35 depletion as well as the duration of depletion might explain why Rab35 depleted cysts can re-orient their polarity in some cases and why I did not observe any re-orientation even after 7 days in culture in my experiments.

In any case, it would be interesting to investigate further whether Rab35 depletion can indeed cause an up-regulation of other rescue pathways. In COS-7 cells for example it has been shown that Rab35 long-term depletion of Rab35 can up-regulate Rab5 by an unknown mechanisms, which has been suggested to compensate for the trafficking defect¹⁹⁹.

Furthermore, depletion of the Rab35 effector and ARF6 GAP ACAP2 or overexpression of Rab35 T76S T81A, a mutant that cannot interact with ACAP2, induces inversion of apico-basal polarity²⁷⁶. It would be interesting to investigate whether Rab35 T76S T81A can still interact with PODXL and whether inhibition of the Rab35/ACAP binding decreases Rab35 activity and thus indirectly influences the binding of PODXL to Rab35.

Moreover it would be interesting to investigate the role of Rab35 in subsequent cell division more in detail as well as the potential role for PODXL in cytokinetic abscission.

Interestingly, both, Rab35 and PODXL have been independently associated with tumorigenesis. Therefore, further studies are needed to investigate whether the Rab35/PODXL interaction could be involved in cancer development, progression or metastasis in various tissues, if disrupted. Finally, development of PODXL V496A/Y500A transgenic animal models such as mice or Zebrafish could be a useful tool to study the Rab35/PODXL interaction *in vivo*.

LIST OF REFERENCES

1. Kemphues, K. J., Priess, J. R., Morton, D. G. & Cheng, N. S. Identification of genes required for cytoplasmic localization in early *C. elegans* embryos. *Cell* **52**, 311-320 (1988).
2. Strome, S. & Wood, W. B. Immunofluorescence visualization of germ-line-specific cytoplasmic granules in embryos, larvae, and adults of *Caenorhabditis elegans*. *Proc. Natl. Acad. Sci. U. S. A.* **79**, 1558-62 (1982).
3. Watts, J. L. *et al.* par-6, a gene involved in the establishment of asymmetry in early *C. elegans* embryos, mediates the asymmetric localization of PAR-3. *Development* **122**, 3133-3140 (1996).
4. Tabuse, Y. *et al.* Atypical protein kinase C cooperates with PAR-3 to establish embryonic polarity in *Caenorhabditis elegans*. *Development* **125**, 3607-3614 (1998).
5. Hung, T. J. & Kemphues, K. J. PAR-6 is a conserved PDZ domain-containing protein that colocalizes with PAR-3 in *Caenorhabditis elegans* embryos. *Development* **126**, 127-135 (1999).
6. Takai, Y. & Nakanishi, H. Nectin and afadin: novel organizers of intercellular junctions. *J. Cell Sci.* **116**, 17-27 (2003).
7. Ooshio, T. *et al.* Cooperative roles of Par-3 and afadin in the formation of adherens and tight junctions. *J. Cell Sci.* **120**, 2352-2365 (2007).
8. Sato, T. *et al.* Regulation of the assembly and adhesion activity of E-cadherin by nectin and afadin for the formation of adherens junctions in Madin-Darby canine kidney cells. *J. Biol. Chem.* **281**, 5288-5299 (2006).
9. Ebnet, K. *et al.* The cell polarity protein ASIP / PAR-3 directly associates with junctional adhesion molecule (JAM). *EMBO J.* **20**, (2001).
10. Takekuni, K. *et al.* Direct binding of cell polarity protein PAR-3 to cell-cell adhesion molecule nectin at neuroepithelial cells of developing mouse. *J. Biol. Chem.* **278**, 5497-5500 (2003).
11. Chen, X. & Macara, I. G. Par-3 controls tight junction assembly through the Rac exchange factor Tiam1. *Nat. Cell Biol.* **7**, 262-269 (2005).
12. Nagai-Tamai Y, Mizuno K, Hirose T, Suzuki A, Ohno S. Regulated protein-protein interaction between aPCK and PAR-3 plays an essential role in the polarization of epithelial cells. *Genes to Cells* **7**, 1161-1171 (2002).
13. Benton, R. & St Johnston, D. *Drosophila* PAR-1 and 14-3-3 inhibit Bazooka/PAR-3 to establish complementary cortical domains in polarized cells. *Cell* **115**, 691-704 (2003).
14. Chartier, F. J.-M., Hardy, E. J.-L. & Laprise, P. Crumbs controls epithelial integrity by inhibiting Rac1 and PI3K. *J. Cell Sci.* **124**, 3393-3398 (2011).
15. Liu, K. D. *et al.* Rac1 is required for reorientation of polarity and lumen formation through a PI 3-kinase-dependent pathway. *Am. J. Physiol. Renal Physiol.* **293**, F1633-40 (2007).

16. Rodriguez-Boulan, E. & Macara, I. G. Organization and execution of the epithelial polarity programme. *Nat. Rev. Mol. Cell Biol.* **15**, 225-242 (2014).
17. Roignot, J., Peng, X. & Mostov, K. Polarity in mammalian epithelial morphogenesis. *Cold Spring Harb. Perspect. Biol.* **5**, (2013).
18. Apodaca, G. Opening ahead: early steps in lumen formation revealed. *Nat. Cell Biol.* **12**, 1026-8 (2010).
19. Iden, S. & Collard, J. G. Crosstalk between small GTPases and polarity proteins in cell polarization. *Nat. Rev. Mol. Cell Biol.* **9**, 846-59 (2008).
20. Gassama-Diagne, A. *et al.* Phosphatidylinositol-3,4,5-trisphosphate regulates the formation of the basolateral plasma membrane in epithelial cells. *Nat. Cell Biol.* **8**, 963-970 (2006).
21. Wu, H. *et al.* PDZ Domains of Par-3 as Potential Phosphoinositide Signaling Integrators. *Mol. Cell* **28**, 886-898 (2007).
22. Feng, W., Wu, H., Chan, L. N. & Zhang, M. Par-3-mediated junctional localization of the lipid phosphatase PTEN is required for cell polarity establishment. *J. Biol. Chem.* **283**, 23440-23449 (2008).
23. von Stein, W., Ramrath, A., Grimm, A., Müller-Borg, M. & Wodarz, A. Direct association of Bazooka/PAR-3 with the lipid phosphatase PTEN reveals a link between the PAR/aPKC complex and phosphoinositide signaling. *Development* **132**, 1675-1686 (2005).
24. Martin-Belmonte, F. *et al.* PTEN-mediated apical segregation of phosphoinositides controls epithelial morphogenesis through Cdc42. *Cell* **128**, 383-97 (2007).
25. Bucci, C. *et al.* The small GTPase rab5 function as a regulatory factor in the early endocytic pathway. *Cell* **70**, 715-728 (1992).
26. Bucci, C. *et al.* Rab5a is a common component of the apical and basolateral endocytic machinery in polarized epithelial cells. *Proc. Natl. Acad. Sci. U. S. A.* **91**, 5061-5 (1994).
27. van der Sluijs, P. *et al.* The small GTP-binding protein rab4 controls an early sorting event on the endocytic pathway. *Cell* **70**, 729-740 (1992).
28. Mukhopadhyay, A., Funato, K. & Stahl, P. D. Rab7 regulates transport from early to late endocytic compartments in *Xenopus* oocytes. *J. Biol. Chem.* **272**, 13055-13059 (1997).
29. Ng, E. L., Gan, B. Q., Ng, F. & Tang, B. L. Rab GTPases regulating receptor trafficking at the late endosome - lysosome membranes. *Cell Biochem. Funct.* 515-523 (2012).
30. Ullrich, O. & Molecular, E. Rab11 Regulates Recycling through the Pericentriolar Recycling Endosome. *J. Cell Biol.* **135**, 913-924 (1996).
31. Steinman, R. M., Mellman, I. S., Muller, W. A. & Cohn, Z. A. Endocytosis and the recycling of plasma membrane. *J. Cell Biol.* **96**, 1-27 (1983).
32. Eaton, S., Martin-belmonte, F., Cossart, P. & Helenius, A. Cargo sorting in the endocytic pathway: a key regulator of cell polarity and tissue dynamics. *Cold Spring Harb. Perspect. Biol.* **6**, a016899 (2014).

33. Cao, X., Surma, M. a & Simons, K. Polarized sorting and trafficking in epithelial cells. *Cell Res.* **22**, 793-805 (2012).
34. Stoops, E. H. & Caplan, M. J. Trafficking to the apical and basolateral membranes in polarized epithelial cells. *J. Am. Soc. Nephrol.* **25**, 1375-86 (2014).
35. Hase, K. *et al.* AP-1B-Mediated Protein Sorting Regulates Polarity and Proliferation of Intestinal Epithelial Cells in Mice. *Gastroenterology* **145**, 625-35 (2013).
36. Schuck, S. & Simons, K. Polarized sorting in epithelial cells: raft clustering and the biogenesis of the apical membrane. *J. Cell Sci.* **117**, 5955-5964 (2004).
37. Shafaq-Zadah, M., Brocard, L., Solari, F. & Michaux, G. AP-1 is required for the maintenance of apico-basal polarity in the *C. elegans* intestine. *Development* **139**, 2061-70 (2012).
38. Gillard, G. *et al.* Control of E-cadherin apical localisation and morphogenesis by a SOAP-1/AP-1/clathrin pathway in *C. elegans* epidermal cells. *Development* **1**, 1684-1694 (2015).
39. Lisanti, M. P., Caras, I. W., Davitz, M. A. & Rodriguez-Boulan, E. A glycopospholipid membrane anchor acts as an apical targeting signal in polarized epithelial cells. *J. Cell Biol.* **109**, 2145-2156 (1989).
40. Brown, D. A., Crise, B. & Rose, J. K. Mechanisms of Membrane Anchoring Affects Polarized Expression of Two Proteins in MDCK Cells. *Science.* **245**, 1499-501(1989)
41. Hannan, L. A., Lisanti, M. P., Rodriguez-Boulan, E. & Edidin, M. Correctly sorted molecules of a GPI-anchored protein are clustered and immobile when they arrive at the apical surface of MDCK cells. *J. Cell Biol.* **120**, 353-358 (1993).
42. Paladino, S. *et al.* Protein oligomerization modulates raft partitioning and apical sorting of GPI-anchored proteins. *J. Cell Biol.* **167**, 699-709 (2004).
43. Paladino, S., Sarnataro, D., Tivodar, S. & Zurzolo, C. Oligomerization is a specific requirement for apical sorting of glycosyl-phosphatidylinositol-anchored proteins but not for non-raft-associated apical proteins. *Traffic* **8**, 251-258 (2007).
44. Pang, S., Urquhart, P. & Hooper, N. M. N-glycans, not the GPI anchor, mediate the apical targeting of a naturally glycosylated, GPI-anchored protein in polarised epithelial cells. *J. Cell Sci.* **117**, 5079-86 (2004).
45. Yeaman, C. *et al.* The O-glycosylated stalk domain is required for apical sorting of neurotrophin receptors in polarized MDCK cells. *J. Cell Biol.* **139**, 929-940 (1997).
46. Luton, F., Hexham, MJ, Zhang, M, Mostov, KE. Identification of a cytoplasmic signal for apical transcytosis. *Traffic.* **10**, 1128-42 (2009).
47. DuBose, D. R., Wolff, S. C., Qi, A.-D., Naruszewicz, I. & Nicholas, R. a. Apical targeting of the P2Y(4) receptor is directed by hydrophobic and basic residues in the cytoplasmic tail. *Am. J. Physiol. Cell Physiol.* **304**, C228-39 (2013).
48. Marciano, D. K. A holey pursuit: lumen formation in the developing kidney. *Pediatr. Nephrol.* (2016). doi:10.1007/s00467-016-3326-4
49. Debnath, J. *et al.* The role of apoptosis in creating and maintaining luminal space

- within normal and oncogene-expressing mammary acini. *Cell* **111**, 29-40 (2002).
50. Debnath, J. & Brugge, J. S. Modelling glandular epithelial cancers in three-dimensional cultures. *Nat. Rev. Cancer* **5**, 675-88 (2005).
 51. Yang, Z. *et al.* De novo lumen formation and elongation in the developing nephron: a central role for afadin in apical polarity. *Development* **140**, 1774-84 (2013).
 52. Sigurbjörnsdóttir, S., Mathew, R. & Leptin, M. Molecular mechanisms of de novo lumen formation. *Nat. Rev. Mol. Cell Biol.* (2014). doi:10.1038/nrm3871
 53. Kamei, M. *et al.* Endothelial tubes assemble from intracellular vacuoles in vivo. *Nature* **442**, 453-456 (2006).
 54. Berry, K. L., Bülow, H. E., Hall, D. H. & Hobert, O. A C. elegans CLIC-like protein required for intracellular tube formation and maintenance. *Science* **302**, 2134-2137 (2003).
 55. Herwig, L. *et al.* Distinct cellular mechanisms of blood vessel fusion in the zebrafish embryo. *Curr. Biol.* **21**, 1942-1948 (2011).
 56. Schottenfeld-Roames, J, Rosa, JB, Ghabrial, AS. Seamless tube shape is constraint by endocytosis-dependent regulation of active Moesin. *Curr Biol.* **24**, 1756-1764 (2014).
 57. Schottenfeld-Roames, J. & Ghabrial, A. S. Whacked and Rab35 polarize dynein-motor-complex-dependent seamless tube growth. *Nat Cell Biol* **14**, 386-393 (2012).
 58. Lant, B. *et al.* CCM-3/STRIPAK promotes seamless tube extension through endocytic recycling. *Nat. Commun.* **6**, 6449 (2015).
 59. JayaNandanan, N., Mathew, R. & Leptin, M. Guidance of subcellular tubulogenesis by actin under the control of a synaptotagmin-like protein and Moesin. *Nat. Commun.* **5**, 3036 (2014).
 60. Ghabrial, A. S., Levi, B. P. & Krasnow, M. A. A systematic screen for tube morphogenesis and branching genes in the Drosophila tracheal system. *PLoS Genet.* **7**, (2011).
 61. Misfeldt, D. S., Hamamoto, S. T. & Pitelka, D. R. Transepithelial transport in cell culture. *Proc. Natl. Acad. Sci. U. S. A.* **73**, 1212-6 (1976).
 62. Richardson, JC, Simmons, NL. Demonstration of protein asymmetries in the plasma membrane of cultured renal (MDCK) epithelial cells by lactoperoxidase-mediated iodination. *FEBS Lett.* **105**, 201-4 (1979).
 63. Louvard, D. Apical membrane aminopeptidase appears at site of cell-cell contact in cultured kidney epithelial cells. *Proc. Natl. Acad. Sci. U. S. A.* **77**, 4132-4136 (1980).
 64. van Meer, G. & Simons, K. Viruses budding from either the apical or the basolateral plasma membrane domain of MDCK cells have unique phospholipid compositions. *EMBO J.* **1**, 847-52 (1982).
 65. Bacallao, R. *et al.* The subcellular organization of Madin-Darby canine kidney cells during the formation of a polarized epithelium. *J. Cell Biol.* **109**, 2817-2832

- (1989).
66. Gálvez-Santisteban, M. *et al.* Synaptotagmin-like proteins control the formation of a single apical membrane domain in epithelial cells. *Nat. Cell Biol.* **14**, 838-49 (2012).
 67. Wang, A. Z., Ojakian, G. K. & Nelson, W. J. Steps in the morphogenesis of a polarized epithelium. 137-152 (1990).
 68. Jaffe, A. B., Kaji, N., Durgan, J. & Hall, A. Cdc42 controls spindle orientation to position the apical surface during epithelial morphogenesis. *J. Cell Biol.* **183**, 625-33 (2008).
 69. Calero-Cuenca, F. J. *et al.* Nuclear fallout provides a new link between aPKC and polarized cell trafficking. *BMC Biol.* **14**, 32 (2016).
 70. Osmani, N., Peglion, F., Chavrier, P. & Etienne-Manneville, S. Cdc42 localization and cell polarity depend on membrane traffic. *J. Cell Biol.* **191**, 1261-1269 (2010).
 71. Ferrari, A., Veligodskiy, A., Berge, U., Lucas, M. S. & Kroschewski, R. ROCK-mediated contractility, tight junctions and channels contribute to the conversion of a preapical patch into apical surface during isochoric lumen initiation. *J. Cell Sci.* **121**, 3649-63 (2008).
 72. Bryant, D. M. *et al.* A molecular network for de novo generation of the apical surface and lumen. *Nat. Cell Biol.* **12**, 1035-45 (2010).
 73. Bryant, D. M. *et al.* A molecular switch for the orientation of epithelial cell polarization. *Dev. Cell* **31**, 171-87 (2014).
 74. Yasuda, T., Saegusa, C., Kamakura, S., Sumimoto, H. & Fukuda, M. Rab27 effector Slp2-a transports the apical signaling molecule podocalyxin to the apical surface of MDCK II cells and regulates claudin-2 expression. *Mol. Biol. Cell* **23**, 3229-39 (2012).
 75. Rozario, T. & DeSimone, D. W. The extracellular matrix in development and morphogenesis: A dynamic view. *Dev. Biol.* **341**, 126-140 (2010).
 76. Lu, P., Takai, K., Weaver, V. M. & Werb, Z. Extracellular matrix degradation and remodeling in development and disease. *Cold Spring Harb Perspect Biol* **3**, 1-24 (2011).
 77. Paszek, M. J. *et al.* Tensional homeostasis and the malignant phenotype. *Cancer Cell* **8**, 241-254 (2005).
 78. Leight, J. L., Wozniak, M. a., Chen, S., Lynch, M. L. & Chen, C. S. Matrix rigidity regulates a switch between TGF-1-induced apoptosis and epithelial-mesenchymal transition. *Mol. Biol. Cell* **23**, 781-791 (2012).
 79. Rodríguez-Fraticelli, A. E., Auzan, M., Alonso, M. a, Bornens, M. & Martín-Belmonte, F. Cell confinement controls centrosome positioning and lumen initiation during epithelial morphogenesis. *J. Cell Biol.* **198**, 1011-23 (2012).
 80. Lu, P., Weaver, V. M. & Werb, Z. The extracellular matrix: A dynamic niche in cancer progression. *J. Cell Biol.* **196**, 395-406 (2012).
 81. Wang, H., Lacoche, S., Huang, L., Xue, B. & Muthuswamy, S. K. Rotational motion

- during three-dimensional morphogenesis of mammary epithelial acini relates to laminin matrix assembly. *Proc. Natl. Acad. Sci. U. S. A.* **110**, 163-8 (2013).
82. Peng, J. *et al.* Phosphoinositide 3-kinase p110 δ promotes lumen formation through the enhancement of apico-basal polarity and basal membrane organization. *Nat. Commun.* **6**, 5937 (2015).
 83. Rodriguez-Fraticelli, A. E. *et al.* The Cdc42 GEF Intersectin 2 controls mitotic spindle orientation to form the lumen during epithelial morphogenesis. *J. Cell Biol.* **189**, 725-38 (2010).
 84. Qin, Y., Meisen, W. H., Hao, Y. & Macara, I. G. Tuba, a Cdc42 GEF, is required for polarized spindle orientation during epithelial cyst formation. *J. Cell Biol.* **189**, 661-9 (2010).
 85. Durgan, J., Kaji, N., Jin, D. & Hall, A. Par6B and atypical PKC regulate mitotic spindle orientation during epithelial morphogenesis. *J. Biol. Chem.* **286**, 12461-74 (2011).
 86. Hao, Y, Du, Q, Chen, X, Zheng, Z *et al.* Par3 Controls Spindle Pole Orientation in Epithelial Cells by aPKC-Mediated Phosphorylation of Pins at the Apical Cortex. *Curr Biol.* **20**, 1809-18 (2010).
 87. Zheng, Z. *et al.* LGN regulates mitotic spindle orientation during epithelial morphogenesis. *J. Cell Biol.* **189**, 275-288 (2010).
 88. Schlu, M. A. *et al.* Trafficking of Crumbs3 during Cytokinesis Is Crucial for Lumen Formation. **20**, 4652-4663 (2009).
 89. Li, D., Kuehn, E. W. & Prekeris, R. Kinesin-2 mediates apical endosome transport during epithelial lumen formation. *Cell. Logist.* **4**, 28928 (2014).
 90. Straight, SW, Shin, K, Fogg, VC *et al.* Loss of Pals1 expression leads to tight junction and polarity defects. *Mol. Biol. Cell* **15**, 1981-90 (2004).
 91. Shin, K., Straight, S. & Margolis, B. PATJ regulates tight junction formation and polarity in mammalian epithelial cells. *J. Cell Biol.* **168**, 705-711 (2005).
 92. Overeem, A. W., Bryant, D. M. & van IJzendoorn, S. C. D. Mechanisms of apical-basal axis orientation and epithelial lumen positioning. *Trends Cell Biol.* **25**, 476-485 (2015).
 93. Patil, P. U., D'Ambrosio, J., Inge, L. J., Mason, R. W. & Rajasekaran, A. K. Carcinoma cells induce lumen filling and EMT in epithelial cells through soluble E-cadherin-mediated activation of EGFR. *J. Cell Sci.* **128**, 4366-4379 (2015).
 94. Sakurai, A., Matsuda, M. & Kiyokawa, E. Activated Ras protein accelerates cell cycle progression to perturb Madin-Darby canine kidney cystogenesis. *J. Biol. Chem.* **287**, 31703-11 (2012).
 95. Bigorgne, A. E. *et al.* TTC7A mutations disrupt intestinal epithelial apicobasal polarity. *J. Clin. Invest.* **124**, 328-337 (2014).
 96. Michaux, G. *et al.* The localisation of the apical Par/Cdc42 polarity module is specifically affected in microvillus inclusion disease. *Biol. Cell* **108**, 19-28 (2016).
 97. Pettinato, G., Manivel, C. J., Panico, L., Sparano, L. & Petrella, G. Invasive Micropapillary Carcinoma of the Breast. *Am. J. Clin. Pathol.* **121**, 857-866 (2004).

98. Barbashina, V., Corben, A. D., Akram, M., Vallejo, C. & Tan, L. K. Mucinous micropapillary carcinoma of the breast: An aggressive counterpart to conventional pure mucinous tumors. *Hum. Pathol.* **44**, 1577-1585 (2013).
99. Haupt, B., Ro, J. Y., Schwartz, M. R. & Shen, S. S. Colorectal adenocarcinoma with micropapillary pattern and its association with lymph node metastasis. *Mod. Pathol.* **20**, 729-733 (2007).
100. Luna-Moré, S, Gonzalez, B, Acedo, C, Rodrigo, I, Luna, C. Invasive micropapillary carcinoma of the breast.;A new special type of invasive mammary carcinoma. *Pathol Res Pract.* **190**, 668-74 (1994).
101. Adams, S. A., Smith, M. E. F., Cowley, G. P. & Carr, L. A. Reversal of glandular polarity in the lymphovascular compartment of breast cancer. *J Clin Pathol* **57**, 1114-1117 (2004).
102. Adams, S. A., Sherwood, A. J. & Smith, M. E. F. Malignant mesothelioma: PAS-diastase positivity and inversion of polarity in intravascular tumour. *Histopathology* **41**, 260-262 (2002).
103. Kwon, G. Y. & Ro, J. Y. Micropapillary variant of urothelial carcinoma. *Adv. Urol.* **2011**, (2011).
104. Lubitz, C. C. *et al.* Hobnail variant of papillary thyroid carcinoma: an institutional case series and molecular profile. *Thyroid* **24**, 958-65 (2014).
105. Barresi, V., Branca, G., Vitarelli, E. & Tuccari, G. Micropapillary Pattern and Poorly Differentiated Clusters Represent the Same Biological Phenomenon in Colorectal Cancer: A Proposal for a Change in Terminology. *Am. J. Clin. Pathol.* **142**, 375-383 (2014).
106. Nassar, H. *et al.* Pathogenesis of invasive micropapillary carcinoma: role of MUC1 glycoprotein. *Mod. Pathol.* **17**, 1045-50 (2004).
107. Knowles, B. C. *et al.* Myosin Vb uncoupling from RAB8A and RAB11A elicits microvillus inclusion disease. *J. Clin. Invest.* **124**, 2947-2962 (2014).
108. Vogel, G. F. *et al.* Cargo-selective apical exocytosis in epithelial cells is conducted by Myo5B, Slp4a, Vamp7, and Syntaxin 3. *J. Cell Biol.* **211**, 587-604 (2015).
109. Ojakian, G. K. & Schwimmer, R. Regulation of epithelial cell surface polarity reversal by beta 1 integrins. *J. Cell Sci.* **107**, 561-576 (1994).
110. Nishiuchi, R. *et al.* Ligand-binding specificities of laminin-binding integrins: A comprehensive survey of laminin-integrin interactions using recombinant alpha3beta1, alpha6beta1, alpha7beta1 and alpha6beta4 integrins. *Matrix Biol.* **25**, 189-197 (2006).
111. Srichai, M. B., & Zent, R. Integrin Structure and Function. Cell-Extracellular Matrix Interactions in Cancer, *Springer New York*. pp. 19-41 (2010).
112. DeLeon, O. *et al.* Pak1 regulates the orientation of apical polarization and lumen formation by distinct pathways. *PLoS One* **7**, e41039 (2012).
113. Schoenenberger, C. a, Zuk, a, Zinkl, G. M., Kendall, D. & Matlin, K. S. Integrin expression and localization in normal MDCK cells and transformed MDCK cells lacking apical polarity. *J. Cell Sci.* **107**, 527-541 (1994).

114. Weir ML, Oppizzi ML, Henry MD, Onishi A, Campbell KP, Bissell MJ, Muschler JL. Dystroglycan loss disrupts polarity and β -casein induction in mammary epithelial cells by perturbing laminin anchoring. *J Cell Sci.* **119**, 4047-58 (2006).
115. Yu, W, Datta, A, et al. Beta1-Integrin Oriented Epithelial Polarity via Rac1 and Laminin. *Mol. Biol. Cell* **16**, 433-445 (2005).
116. Yu, W. *et al.* Involvement of RhoA, ROCK I and myosin II in inverted orientation of epithelial polarity. *EMBO Rep.* **9**, 923-929 (2008).
117. Monteleon, C. L. *et al.* Establishing epithelial glandular polarity: interlinked roles for ARF6, Rac1, and the matrix microenvironment. *Mol. Biol. Cell* **23**, 4495-505 (2012).
118. Yamaoka, M. *et al.* PI3K regulates endocytosis after insulin secretion by mediating signaling crosstalk between Arf6 and Rab27a. *J. Cell Sci.* **129**, 637-49 (2016).
119. Herszterg, S., Pinheiro, D. & Bella??che, Y. A multicellular view of cytokinesis in epithelial tissue. *Trends Cell Biol.* **24**, 285-293 (2014).
120. Hehnlly, H. & Doxsey, S. Polarity sets the stage for cytokinesis. *Mol. Biol. Cell* **23**, 7-11 (2012).
121. Le Bras, S. & Le Borgne, R. Epithelial cell division - multiplying without losing touch. *J. Cell Sci.* **127**, 5127-5137 (2014).
122. Founounou, N., Loyer, N. & Le Borgne, R. Septins Regulate the Contractility of the Actomyosin Ring to Enable Adherens Junction Remodeling during Cytokinesis of Epithelial Cells. *Dev. Cell* **24**, 242-255 (2013).
123. Reinsch, S. & Karsenti, E. Orientation of spindle axis and distribution of plasma membrane proteins during cell division in polarized MDCKII cells. *J. Cell Biol.* **126**, 1509-26 (1994).
124. Baker, J. & Garrod, D. Epithelial cells retain junctions during mitosis. *J. Cell Sci.* **104**, 415-425 (1993).
125. Hsu, Y.-H. *et al.* Podocalyxin EBP50 ezrin molecular complex enhances the metastatic potential of renal cell carcinoma through recruiting Rac1 guanine nucleotide exchange factor ARHGEF7. *Am. J. Pathol.* **176**, 3050-61 (2010).
126. Guillot, C.; Lecuit, T. Mechanics of Epithelial Tissue. *Science* **340**, 1185-1189 (2013).
127. Morais-de-Sá, E. & Sunkel, C. Adherens junctions determine the apical position of the midbody during follicular epithelial cell division. *EMBO Rep.* **14**, 696-703 (2013).
128. Li, D., Mangan, A., Cicchini, L., Margolis, B. & Prekeris, R. FIP5 phosphorylation during mitosis regulates apical trafficking and lumenogenesis. *EMBO Rep.* **15**, 428- (2014).
129. Fielding, A. B. *et al.* Rab11-FIP3 and FIP4 interact with Arf6 and the exocyst to control membrane traffic in cytokinesis. *EMBO J.* **24**, 3389-99 (2005).
130. Tushir, J. S. *et al.* Unregulated ARF6 Activation in Epithelial Cysts Generates Hyperactive Signaling Endosomes and Disrupts Morphogenesis. **21**, 2355-2366

(2010).

131. Schweitzer, J. K., Sedgwick, A. E. & D'Souza-Schorey, C. ARF6-mediated endocytic recycling impacts cell movement, cell division and lipid homeostasis. *Semin. Cell Dev. Biol.* **22**, 39-47 (2011).
132. Chesneau, L. *et al.* An ARF6/Rab35 GTPase cascade for endocytic recycling and successful cytokinesis. *Curr. Biol.* **22**, 147-153 (2012).
133. Comer, F. I. & Parent, C. a. Phosphoinositides specify polarity during epithelial organ development. *Cell* **128**, 239-40 (2007).
134. Janetopoulos, C., Borleis, J., Vazquez, F., Iijima, M. & Devreotes, P. Temporal and spatial regulation of phosphoinositide signaling mediates cytokinesis. *Dev. Cell* **8**, 467-477 (2005).
135. Nielsen, J. S. & McNagny, K. M. Novel functions of the CD34 family. *J. Cell Sci.* **121**, 4145-4145 (2008).
136. Dekan, G., Gabel, C. & Farquhar, M. G. Sulfate contributes to the negative charge of podocalyxin, the major sialoglycoprotein of the glomerular filtration slits. *Proc. Natl. Acad. Sci. U. S. A.* **88**, 5398-402 (1991).
137. Kerjaschki, D., Sharkey, D. J. & Farquhar, M. G. Identification and characterization of podocalyxin-the major sialoprotein of the renal glomerular epithelial cell. *J. Cell Biol.* **98**, 1591-6 (1984).
138. Sawada, H., Stukenbrok, H., Kerjaschki, D. & Farquhar, M. G. Epithelial polyanion (podocalyxin) is found on the sides but not the soles of the foot processes of the glomerular epithelium. *Am. J. Pathol.* **125**, 309-18 (1986).
139. Horvat, R., Hovorka, A., Dekan, G., Poczewski, H. & Kerjaschki, D. Endothelial cell membranes contain podocalyxin--the major sialoprotein of visceral glomerular epithelial cells. *The Journal of Cell Biology* **102**, 484-491 (1986).
140. Doyonnas, R. *et al.* Plenary paper Podocalyxin is a CD34-related marker of murine hematopoietic stem cells and embryonic erythroid cells. *Blood* **105**, 4170-4178 (2005).
141. Vitureira, N., McNagny, K., Soriano, E. & Burgaya, F. Pattern of expression of the podocalyxin gene in the mouse brain during development. *Gene Expr. Patterns* **5**, 349-54 (2005).
142. Palmer, R. E. *et al.* WT1 regulates the expression of the major glomerular podocyte membrane protein Podocalyxin. *Curr. Biol.* **11**, 1805-9 (2001).
143. Butta, N. *et al.* Role of transcription factor Sp1 and CpG methylation on the regulation of the human podocalyxin gene promoter. *BMC Mol. Biol.* **7**, 17 (2006).
144. Doyonnas, R. *et al.* Anuria, omphalocele, and perinatal lethality in mice lacking the CD34-related protein podocalyxin. *J. Exp. Med.* **194**, 13-27 (2001).
145. Schnabel, E., Anderson, J. M. & Farquhar, M. G. The tight junction protein ZO-1 is concentrated along slit diaphragms of the glomerular epithelium. *J. Cell Biol.* **111**, 1255-1263 (1990).
146. Charest, P. M. & Roth, J. Localization of sialic acid in kidney glomeruli: regionalization in the podocyte plasma membrane and loss in experimental

- nephrosis. *Proc. Natl. Acad. Sci. U. S. A.* **82**, 8508-8512 (1985).
147. Doyonnas, R. *et al.* Anuria, omphalocele, and perinatal lethality in mice lacking the CD34-related protein podocalyxin. *J. Exp. Med.* **194**, 13-27 (2001).
 148. Strilić, B. *et al.* The molecular basis of vascular lumen formation in the developing mouse aorta. *Dev. Cell* **17**, 505-15 (2009).
 149. Takeda, T., Go, W. Y., Orlando, R. a & Farquhar, M. G. Expression of podocalyxin inhibits cell-cell adhesion and modifies junctional properties in Madin-Darby canine kidney cells. *Mol. Biol. Cell* **11**, 3219-32 (2000).
 150. Larrucea, S. *et al.* Expression of podocalyxin enhances the adherence, migration, and intercellular communication of cells. *Exp. Cell Res.* **314**, 2004-15 (2008).
 151. Larrucea, S. *et al.* Podocalyxin enhances the adherence of cells to platelets. *Cell. Mol. Life Sci.* **64**, 2965-2974 (2007).
 152. Meder, D., Shevchenko, A., Simons, K. & Füllekrug, J. Gp135/podocalyxin and NHERF-2 participate in the formation of a preapical domain during polarization of MDCK cells. *J. Cell Biol.* **168**, 303-13 (2005).
 153. Nielsen, J. S. *et al.* The CD34-related molecule podocalyxin is a potent inducer of microvillus formation. *PLoS One* **2**, e237 (2007).
 154. A Bipartite Signal Regulates the Faithful Delivery of Apical Domain Marker Podocalyxin/Gp135. *Mol. Biol. Cell* **18**, 986-994 (2007).
 155. Orlando, R. a *et al.* The glomerular epithelial cell anti-adhesin podocalyxin associates with the actin cytoskeleton through interactions with ezrin. *J. Am. Soc. Nephrol.* **12**, 1589-98 (2001).
 156. Takeda, T., McQuistan, T., Orlando, R. A. & Farquhar, M. G. Loss of glomerular foot processes is associated with uncoupling of podocalyxin from the actin cytoskeleton. *J. Clin. Invest.* **108**, 289-301 (2001).
 157. Breton, S. *et al.* The B1 subunit of the H+ATPase is a PDZ domain-binding protein: Colocalization with NHE-RF in renal B-intercalated cells. *J. Biol. Chem.* **275**, 18219-18224 (2000).
 158. Schmieder, S., Nagai, M., Orlando, R. a, Takeda, T. & Farquhar, M. G. Podocalyxin activates RhoA and induces actin reorganization through NHERF1 and Ezrin in MDCK cells. *J. Am. Soc. Nephrol.* **15**, 2289-98 (2004).
 159. Kobayashi, T., Notoya, M., Shinosaki, T. & Kurihara, H. Cortactin interacts with podocalyxin and mediates morphological change of podocytes through its phosphorylation. *Nephron. Exp. Nephrol.* **113**, e89-96 (2009).
 160. Al-Momany, a., Li, L., Alexander, R. T. & Ballermann, B. J. Clustered PI(4,5)P2 accumulation and ezrin phosphorylation in response to CLIC5A. *J. Cell Sci.* **127**, 5164-5178 (2014).
 161. Ojakian, G. K. & Schwimmer, R. The polarized distribution of an apical cell surface glycoprotein is maintained by interactions with the cytoskeleton of Madin-Darby canine kidney cells. *J. Cell Biol.* **107**, 2377-2387 (1988).
 162. Ojakian, G. K., Schwimmer, R. & Herz, R. E. Polarized insertion of an intracellular glycoprotein pool into the apical membrane of MDCK cells. *Am. J.*

Physiol. **258**, C390-C398 (1990).

163. Cheng, H.-Y. *et al.* Molecular identification of canine podocalyxin-like protein 1 as a renal tubulogenic regulator. *J. Am. Soc. Nephrol.* **16**, 1612-22 (2005).
164. Freedman, B. S. *et al.* Modelling kidney disease with CRISPR-mutant kidney organoids derived from human pluripotent epiblast spheroids. *Nat. Commun.* **6**, 8715 (2015).
165. McNagny, K. M. *et al.* Podocalyxin in the Diagnosis and Treatment of Cancer, Advances in cancer Management, Prof. Ravinder Mohan (Ed.), InTech (2012).
166. Laitinen, A. *et al.* Podocalyxin as a Prognostic Marker in Gastric Cancer. *PLoS One* **10**, e0145079 (2015).
167. Saukkonen, K. *et al.* Podocalyxin is a marker of poor prognosis in pancreatic ductal adenocarcinoma. *PLoS One* **10**, 1-7 (2015).
168. Liu, Y. & Jiang, Y.-G. Podocalyxin Promotes Glioblastoma Multiforme Cell Invasion and Proliferation via β -Catenin Signaling. *PLoS One* **9**, e111343 (2014).
169. Sizemore, S., Cicek, M., Sizemore, N., Ng, K. P. & Casey, G. Podocalyxin increases the aggressive phenotype of breast and prostate cancer cells in vitro through its interaction with ezrin. *Cancer Res.* **67**, 6183-91 (2007).
170. Graves, M. L. *et al.* The cell surface mucin podocalyxin regulates collective breast tumor budding. *Breast Cancer Res.* **18**, 11 (2016).
171. Amo, L. *et al.* Podocalyxin-like protein 1 functions as an immunomodulatory molecule in breast cancer cells. *Cancer Lett.* **368**, 26-35 (2015).
172. Snyder, K. A. *et al.* Podocalyxin enhances breast tumor growth and metastasis and is a target for monoclonal antibody therapy. *Breast Cancer Res.* **17**, 46 (2015).
173. Vitureira, N. *et al.* Podocalyxin is a novel polysialylated neural adhesion protein with multiple roles in neural development and synapse formation. *PLoS One* **5**, e12003 (2010).
174. Sudhaman, S. *et al.* Discovery of a frameshift mutation in podocalyxin-like (PODXL) gene, coding for a neural adhesion molecule, as causal for autosomal-recessive juvenile Parkinsonism. *J. Med. Genet.* **53**, 540-6 (2016).
175. Stenmark, H. Rab GTPases as coordinators of vesicle traffic. *Nat. Rev. Mol. Cell Biol.* **10**, 513-25 (2009).
176. Li, F. *et al.* The role of the hypervariable C-terminal domain in Rab GTPases membrane targeting. *Proc. Natl. Acad. Sci.* **111**, 2572-2577 (2014).
177. Heo, W. Do *et al.* Clusters to the Plasma Membrane. *Science* (80-.). **1458**, 1458-1461 (2007).
178. Kouranti, I., Sachse, M., Arouche, N., Goud, B. & Echard, A. Rab35 Regulates an Endocytic Recycling Pathway Essential for the Terminal Steps of Cytokinesis. *Curr. Biol.* **16**, 1719-1725 (2006).
179. Dambournet, D. *et al.* Rab35 GTPase and OCRL phosphatase remodel lipids and F-actin for successful cytokinesis. *Nat. Cell Biol.* **13**, 981-988 (2011).

180. Sato, M. *et al.* Regulation of endocytic recycling by *C. elegans* Rab35 and its regulator RME-4, a coated-pit protein. *EMBO J* **27**, 1183-1196 (2008).
181. Shah, M., Baterina, O. Y., Taupin, V. & Farquhar, M. G. ARH directs megalin to the endocytic recycling compartment to regulate its proteolysis and gene expression. *J. Cell Biol.* **202**, 113-127 (2013).
182. Gao, Y. *et al.* Recycling of the Ca²⁺-activated K⁺ channel, KCa2.3, is dependent upon RME-1, Rab35/EPI64C, and an N-terminal domain. *J. Biol. Chem.* **285**, 17938-17953 (2010).
183. Davey, J. R. *et al.* TBC1D13 is a RAB35 Specific GAP that Plays an Important Role in GLUT4 Trafficking in Adipocytes. *Traffic* **13**, 1429-1441 (2012).
184. Nandez, R. *et al.* A role of OCRL in clathrin-coated pit dynamics and uncoating revealed by studies of Lowe syndrome cells. *Elife* **3**, e02975 (2014).
185. Cauvin, C. *et al.* Rab35 GTPase Triggers Switch-like Recruitment of the Lowe Syndrome Lipid Phosphatase OCRL on Newborn Endosomes. *Curr. Biol.* 120-128 (2015).
186. Klinkert, K. , Echard, A. Rab35 GTPase: a central regulator of phosphoinositides and F-actin in endocytic recycling and beyond. (2016).
187. Echard, A. Connecting membrane traffic to ESCRT and the final cut. *Nat Cell Biol* **14**, 983-985 (2012).
188. Kobayashi, H. & Fukuda, M. Rab35 establishes the EHD1-association site by coordinating two distinct effectors during neurite outgrowth. *J Cell Sci* **126**, 2424-2435 (2013).
189. Giridharan, S. S. P., Cai, B., Naslavsky, N. & Caplan, S. Trafficking cascades mediated by Rab35 and its membrane hub effector, MICAL-L1. *Commun. Integr. Biol.* **5**, 384-387 (2012).
190. Kobayashi, H., Etoh, K., Ohbayashi, N. & Fukuda, M. Rab35 promotes the recruitment of Rab8, Rab13 and Rab36 to recycling endosomes through MICAL-L1 during neurite outgrowth. *Biol. Open* **3**, 803-14 (2014).
191. Walseng, E., Bakke, O. & Roche, P. A. Major histocompatibility complex class II-peptide complexes internalize using a clathrin- and dynamin-independent endocytosis pathway. *J. Biol. Chem.* **283**, 14717-14727 (2008).
192. Kobayashi, H. & Fukuda, M. Rab35 regulates Arf6 activity through centaurin-beta2 (ACAP2) during neurite outgrowth. *J Cell Sci* **125**, 2235-2243 (2012).
193. Chevallier, J. *et al.* Rab35 regulates neurite outgrowth and cell shape. *FEBS Lett.* **583**, 1096-1101 (2009).
194. Kobayashi, H., Etoh, K. & Fukuda, M. Rab35 is translocated from Arf6-positive perinuclear recycling endosomes to neurite tips during neurite outgrowth. *Small GTPases* **5**, e29290 (2014).
195. Abe, Y. *et al.* A Small Ras-like protein Ray/Rab1c modulates the p53-regulating activity of PRPK. *Biochem. Biophys. Res. Commun.* **344**, 377-85 (2006).
196. Crockett, D. K., Lin, Z., Elenitoba-Johnson, K. S. & Lim, M. S. Identification of NPM-ALK interacting proteins by tandem mass spectrometry. *Oncogene* **23**, 2617-

- 2629 (2004).
197. Sheach, L. a *et al.* Androgen-related expression of G-proteins in ovarian cancer. *Br. J. Cancer* **101**, 498-503 (2009).
 198. Allaire, P. D. *et al.* Interplay between Rab35 and Arf6 controls cargo recycling to coordinate cell adhesion and migration. *J. Cell Sci.* **126**, 722-31 (2013).
 199. Allaire, P. D. *et al.* The Connecdenn DENN Domain: A GEF for Rab35 Mediating Cargo-Specific Exit from Early Endosomes. *Mol. Cell* **37**, 370-382 (2010).
 200. Tang, Y. *et al.* MicroRNA-720 promotes in vitro cell migration by targeting Rab35 expression in cervical cancer cells. *Cell Biosci.* **5**, 56 (2015).
 201. Zhu, Y. *et al.* Rab35 is required for Wnt5a/Dvl2-induced Rac1 activation and cell migration in MCF-7 breast cancer cells. *Cell. Signal.* **25**, 1075-1085 (2013).
 202. Wheeler, DB, Zoncu, R, Root, DE *et al.* Identification of an oncogenic RAB protein. *Science.* **350**, 211-7 (2015).
 203. Kulasekaran, G. *et al.* Phosphorylation-dependent Regulation of Connecdenn/DENND1 Guanine Nucleotide Exchange Factors. *J. Biol. Chem.* **290**, 17999-18008 (2015).
 204. Nookala, R. K. *et al.* Crystal structure of folliculin reveals a hidDENN function in genetically inherited renal cancer. *Open Biol.* **2**, 120071 (2012).
 205. Schmidt, L. S. & Linehan, W. M. Molecular genetics and clinical features of Birt-Hogg-Dubé syndrome. *Nat. Rev. Urol.* **12**, 558-569 (2015).
 206. Nahorski, M. S. *et al.* Folliculin interacts with p0071 (plakophilin-4) and deficiency is associated with disordered RhoA signalling, epithelial polarization and cytokinesis. *Hum. Mol. Genet.* **21**, 5268-79 (2012).
 207. Medvetz, D. a *et al.* Folliculin, the product of the Birt-Hogg-Dube tumor suppressor gene, interacts with the adherens junction protein p0071 to regulate cell-cell adhesion. *PLoS One* **7**, e47842 (2012).
 208. Charrasse, S., Comunale, F., De Rossi, S., Echard, A. & Gauthier-Rouviere, C. Rab35 regulates cadherin-mediated adherens junction formation and myoblast fusion. *Mol Biol Cell* **24**, 234-245 (2013).
 209. Zhang, J., Fonovic, M., Suyama, K., Bogoy, M. & Scott, M. P. Rab35 controls actin bundling by recruiting fascin as an effector protein. *Science (80-.).* **325**, 1250-1254 (2009).
 210. Marat, A. L., Ioannou, M. S. & McPherson, P. S. Connecdenn 3/DENND1C binds actin linking Rab35 activation to the actin cytoskeleton. *Mol. Biol. Cell* **23**, 163-75 (2012).
 211. Shim, J. *et al.* Rab35 mediates transport of Cdc42 and Rac1 to the plasma membrane during phagocytosis. *Mol Cell Biol* **30**, 1421-1433 (2010).
 212. Klinkert, K., Rocancourt, M., Houdusse, A. & Echard, A. Rab35 GTPase couples cell division with initiation of epithelial apico-basal polarity and lumen opening. *Nat. Commun.* **7**, 11166 (2016).
 213. Blasky, A. J., Mangan, A. & Prekeris, R. Polarized Protein Transport and Lumen

- Formation During Epithelial Tissue Morphogenesis. *Annu Rev Cell Dev Biol.* **31**, 575-91 (2015).
214. Pinal, N. *et al.* Regulated and polarized PtdIns(3,4,5)P₃ accumulation is essential for apical membrane morphogenesis in photoreceptor epithelial cells. *Curr. Biol.* **16**, 140-149 (2006).
 215. Sivars, U, Aivazian, D, Pfeffer, SR. Yip3 catalyses the dissociation of endosomal Rab-GDI complexes. *Nature* **425**, 846-851 (2003).
 216. Dirac-Svejstrup, A. B., Sumizawa, T. & Pfeffer, S. R. Identification of a GDI displacement factor that releases endosomal Rab GTPases from Rab-GDI. *EMBO J.* **16**, 465-472 (1997).
 217. Chavrier, P. *et al.* Hypervariable C-terminal domain of rab proteins acts as a targeting signal. *Nature* **353**, 769-772 (1991).
 218. Wu, Y. *et al.* Membrane targeting mechanism of Rab GTPases elucidated by semisynthetic protein probes. *Nat. Chem. Biol.* **6**, 534-540 (2010).
 219. Chen, Y. A. & Scheller, R. H. SNARE-mediated membrane fusion. *Nat. Rev. Mol. Cell Biol.* **2**, 98-106 (2001).
 220. Bröcker, C., Engelbrecht-Vandré, S. & Ungermann, C. Multisubunit tethering complexes and their role in membrane fusion. *Curr. Biol.* **20**, 943-952 (2010).
 221. Sogaard, M. *et al.* A rab protein is required for the assembly of SNARE complexes in the docking of transport vesicles. *Cell* **78**, 937-948 (1994).
 222. Ravichandran, V., Chawla, A. & Roche, P. A. Identification of a Novel Syntaxin- and Synaptobrevin/VAMP-binding Protein, SNAP-23, Expressed in Non-neuronal Tissues. *J. Biol. Chem.* **271**, 13300-13303 (1996).
 223. Cheatham, B. *et al.* Insulin-stimulated translocation of GLUT4 glucose transporters requires SNARE-complex proteins. *Proc. Natl. Acad. Sci. U. S. A.* **93**, 15169-15173 (1996).
 224. Vázquez-Martínez, R. & Malagón, R. Rab proteins and the secretory pathway: The case of Rab18 in neuroendocrine cells. *Front. Endocrinol.* **2**, 1-9 (2010).
 225. Lo, S.-Y. *et al.* Intrinsic tethering activity of endosomal Rab proteins. *Nat. Struct. Mol. Biol.* **19**, 40-7 (2012).
 226. Vogel, G. F. *et al.* Cargo-selective apical exocytosis in epithelial cells is conducted by Myo5B, Slp4a, Vamp7, and Syntaxin 3. *The Journal of Cell Biology* **211**, 587-604 (2015).
 227. Zuo, X., Fogelgren, B. & Lipschutz, J. H. The small GTPase Cdc42 is necessary for primary ciliogenesis in renal tubular epithelial cells. *J. Biol. Chem.* **286**, 22469-22477 (2011).
 228. He, B., Xi, F., Zhang, X., Zhang, J. & Guo, W. Exo70 interacts with phospholipids and mediates the targeting of the exocyst to the plasma membrane. *EMBO J.* **26**, 4053-4065 (2007).
 229. Liu. Phosphatidylinositol 4,5-Bisphosphate Mediates the Targeting of the Exocyst to the Plasma Membrane for Exocytosis in Mammalian Cells. (2007).

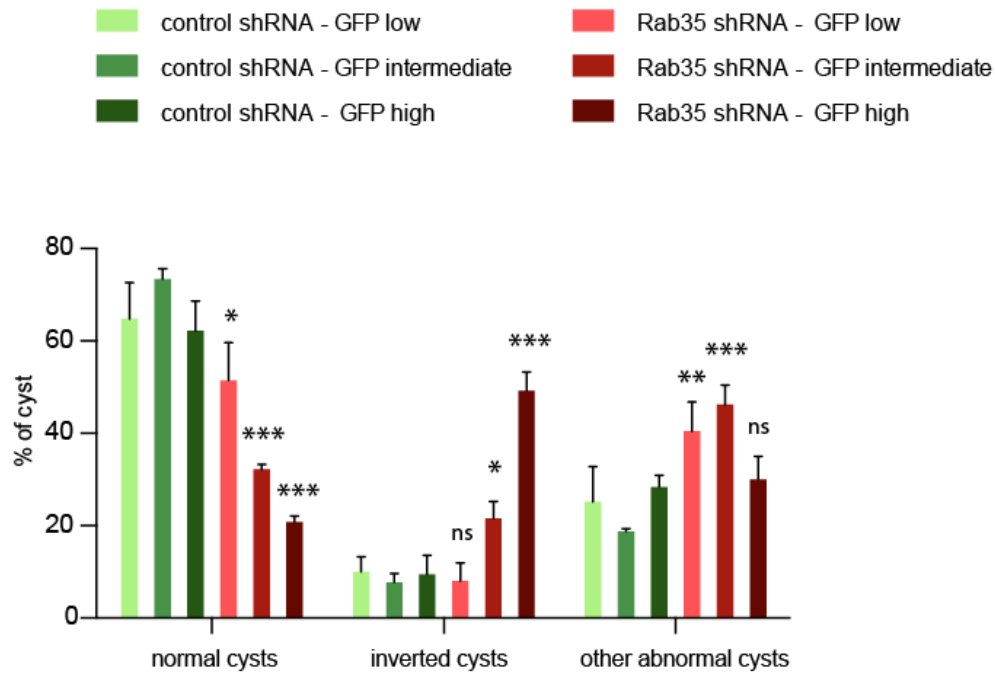
230. Chia, P. Z. C. & Gleeson, P. a. Membrane tethering. *F1000Prime Rep.* **6**, 74 (2014).
231. Dudek, S. M. *et al.* The Exo70 Subunit of the Exocyst Is an Effector for Both Cdc42 and Rho3 Function in Polarized Exocytosis. *Mol. Biol. Cell* **21**, 4042-4056 (2010).
232. Zhang, X. *et al.* Membrane association and functional regulation of Sec3 by phospholipids and Cdc42. *J. Cell Biol.* **180**, 145-158 (2008).
233. Sivaram, M. V. S., Saporita, J. A., Furgason, M. L. M., Boettcher, A. J. & Munson, M. Dimerization of the exocyst protein Sec6p and its interaction with the t-SNARE Sec9p. *Biochemistry* **44**, 6302-6311 (2005).
234. Yu, I.-M. & Hughson, F. M. Tethering factors as organizers of intracellular vesicular traffic. *Annu. Rev. Cell Dev. Biol.* **26**, 137-56 (2010).
235. Roman-fernandez, A., Bryant, D. M., Road, S. & Estate, G. Complex polarity: building multicellular tissues through apical membrane traffic. *Traffic.* (2016)
236. van IJzendoorn, S. C. D., Tuvim, M. J., Weimbs, T., Dickey, B. F. & Mostov, K. E. Direct interaction between Rab3b and the polymeric immunoglobulin receptor controls ligand-stimulated transcytosis in epithelial cells. *Dev. Cell* **2**, 219-228 (2002).
237. Caswell, P. T. *et al.* Rab25 Associates with alpha5beta1 Integrin to Promote Invasive Migration in 3D Microenvironments. *Dev. Cell* **13**, 496-510 (2007).
238. Pellinen, T. *et al.* Small GTPase Rab21 regulates cell adhesion and controls endosomal traffic of beta1-integrins. *J. Cell Biol.* **173**, 767-780 (2006).
239. Saxena, S. K., Kaur, S. & George, C. Rab4GTPase modulates CFTR function by impairing channel expression at plasma membrane. *Biochem. Biophys. Res. Commun.* **341**, 184-191 (2006).
240. Saxena, S. K., Horiuchi, H. & Fukuda, M. Rab27a regulates epithelial sodium channel (ENaC) activity through synaptotagmin-like protein (SLP-5) and Munc13-4 effector mechanism. *Biochem. Biophys. Res. Commun.* **344**, 651-657 (2006).
241. Saxena, S. K. & Kaur, S. Rab27a negatively regulates CFTR chloride channel function in colonic epithelia: Involvement of the effector proteins in the regulatory mechanism. *Biochem. Biophys. Res. Commun.* **346**, 259-267 (2006).
242. McEwen, D. P. *et al.* Rab-GTPase-dependent endocytic recycling of Kv1.5 in atrial myocytes. *J. Biol. Chem.* **282**, 29612-29620 (2007).
243. Hammad, M. M., Kuang, Y. Q., Morse, A. & Dupré, D. J. Rab1 interacts directly with the β_2 -adrenergic receptor to regulate receptor anterograde trafficking. *Biol. Chem.* **393**, 541-546 (2012).
244. Esseltine, J. L., Dale, L. B. & Ferguson, S. S. G. Rab GTPases bind at a common site within the angiotensin II type I receptor carboxyl-terminal tail: evidence that Rab4 regulates receptor phosphorylation, desensitization, and resensitization. *Mol. Pharmacol.* **79**, 175-84 (2011).
245. Hamelin, E., Thériault, C., Laroche, G. & Parent, J. L. The intracellular trafficking of the G protein-coupled receptor TPb depends on a direct interaction with Rab11. *J. Biol. Chem.* **280**, 36195-36205 (2005).

246. Cogli, L., Progida, C., Bramato, R. & Bucci, C. Vimentin phosphorylation and assembly are regulated by the small GTPase Rab7a. *Biochim. Biophys. Acta - Mol. Cell Res.* **1833**, 1283-1293 (2013).
247. Aloisi, A. L. & Bucci, C. Rab GTPases-cargo direct interactions: fine modulators of intracellular trafficking. *Histol. Histopathol.* **28**, 839-49 (2013).
248. Smythe, E. Direct interactions between rab GTPases and cargo. *Molecular Cell* **9**, 205-206 (2002).
249. Dong, C. *et al.* Rab8 interacts with distinct motifs in 2B- and 2-Adrenergic receptors and differentially modulates their transport. *J. Biol. Chem.* **285**, 20369-20380 (2010).
250. Leahey, A., Charnas, L. R. & Nussbaum, R. L. Nonsense mutations in the OCRL-1 gene in patients with the oculocerebrorenal syndrome of Lowe. **2**, 461-463 (1993).
251. Grieve, A. G. *et al.* Lowe Syndrome protein OCRL1 supports maturation of polarized epithelial cells. *PLoS One* **6**, e24044 (2011).
252. Rbaibi, Y1, Cui, S, Mo, D, Carattino, M, Rohatgi, R *et al.* OCRL1 Modulates Cilia Length in Renal Epithelial Cells Youssef. **10**, 54-56 (2013).
253. Jänne, P. A. *et al.* Functional overlap between murine Inpp5b and Ocr11 may explain why deficiency of the murine ortholog for OCRL1 does not cause Lowe syndrome in mice. *J. Clin. Invest.* **101**, 2042-2053 (1998).
254. Cui, S. *et al.* OCRL1 function in renal epithelial membrane traffic. *Am. J. Physiol. Renal Physiol.* **298**, F335-45 (2010).
255. Reczek, D. & Bretscher, a. Identification of EPI64, a TBC/rabGAP domain-containing microvillar protein that binds to the first PDZ domain of EBP50 and E3KARP. *J. Cell Biol.* **153**, 191-206 (2001).
256. Allaire, P. D., Mcpherson, P. S. & Ritter, B. Rab GTPases. **1298**, 217-231 (2015).
257. Hurd, T. W. *et al.* Phosphorylation-Dependent Binding of 14-3-3 to the Polarity Protein Par3 Regulates Cell Polarity in Mammalian Epithelia. *Curr. Biol.* **13**, 2082-2090 (2003).
258. Machicoane, M. *et al.* SLK-dependent activation of ERMs controls LGN-NuMA localization and spindle orientation. *J. Cell Biol.* **205**, 791-799 (2014).
259. Kotak, S., Busso, C. & Gönczy, P. NuMA interacts with phosphoinositides and links the mitotic spindle with the plasma membrane. *EMBO J.* **33**, 1-16 (2014).
260. Du, Q., Stukenberg, P. T. & Macara, I. G. A mammalian Partner of inscuteable binds NuMA and regulates mitotic spindle organization. *Nat. Cell Biol.* **3**, 1069-75 (2001).
261. Morin, X. & Bellaiche, Y. Mitotic Spindle Orientation in Asymmetric and Symmetric Cell Divisions during Animal Development. *Dev. Cell* **21**, 102-119 (2011).
262. Fuchs, E. Par3-mInsc and Gai3 cooperate to promote oriented epidermal cell. **16**, 758-769 (2014).

263. Xia, J. *et al.* Semaphorin-Plexin Signaling Controls Mitotic Spindle Orientation during Epithelial Morphogenesis and Repair. *Dev. Cell* **33**, 299-313 (2015).
264. Bañón-Rodríguez, I. *et al.* EGFR controls IQGAP basolateral membrane localization and mitotic spindle orientation during epithelial morphogenesis. *EMBO J.* **33**, 129-145 (2014).
265. Dan T., B. & Daniel, S. J. Spindle orientation: What if it goes wrong? *Semin. Cell Dev. Biol.* **34**, 140-145 (2014).
266. Knoblich, J. A. Europe PMC Funders Group Asymmetric cell division : recent developments and their implications for tumour biology. **11**, 849-860 (2014).
267. Nakajima, Y., Meyer, E. J., Kroesen, A., McKinney, S. A. & Gibson, M. C. Epithelial junctions maintain tissue architecture by directing planar spindle orientation. *Nature* **500**, 359-362 (2013).
268. Packard, A. *et al.* Luminal Mitosis Drives Epithelial Cell Dispersal within the Branching Ureteric Bud. *Dev. Cell* **27**, 319-330 (2013).
269. Wang, H. H. *et al.* Rab3A, Rab27A, and Rab35 regulate different events during mouse oocyte meiotic maturation and activation. *Histochem. Cell Biol.* (2016).
270. Herszterg, S., Leibfried, A., Bosveld, F., Martin, C. & Bellaiche, Y. Interplay between the dividing cell and its neighbors regulates adherens junction formation during cytokinesis in epithelial tissue. *Dev. Cell* **24**, 256-70 (2013).
271. Iden, S. *et al.* A distinct PAR complex associates physically with VE-cadherin in vertebrate endothelial cells. *EMBO Rep.* **7**, 1239-1246 (2006).
272. Robbins, R. M. & Beitel, G. J. Vascular lumen formation: negativity will tear us apart. *Curr. Biol.* **20**, 973-5 (2010).
273. Rasmussen, J. P., Reddy, S. S. & Priess, J. R. Laminin is required to orient epithelial polarity in the *C. elegans* pharynx. *Development* **139**, 2050-2060 (2012).
274. Bedzhov, I. & Zernicka-Goetz, M. Self-organizing properties of mouse pluripotent cells initiate morphogenesis upon implantation. *Cell* **156**, 1032-44 (2014).
275. Hsu, C. *et al.* Regulation of exosome secretion by Rab35 and its GTPase-activating proteins TBC1D10A-C. *J. Cell Biol.* **189**, 223-232 (2010).
276. Mrozowska, P. S. & Fukuda, M. Regulation of podocalyxin trafficking by Rab small GTPases in 2D and 3D epithelial cell cultures. *J Cell Biol.* **213**, 355-69 (2016)

ANNEX

a



b

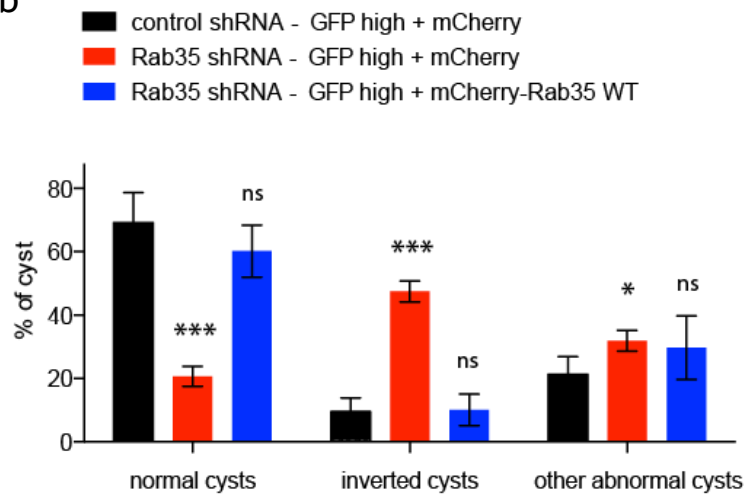


Figure A: Rab35 depletion levels correlate with cyst phenotypes

- (a) MDCK cells stably expressing either Rab35 shRNA IHRES GFP or control shRNA IHRES GFP were sorted for low, intermediate and high GFP expressing cells and seeded into Matrigel. Cysts were fixed after 48 hours and cyst phenotypes were quantified. $p < 0.05$ (*), $p < 0.01$ (**), $p < 0.001$ (***), ns: not significant. (compared to corresponding control)
- (b) MDCK cells stably expressing either Rab35 shRNA IHRES GFP (high) control shRNA IHRES GFP (high) were transfected with either mCherry alone or with mCherry-Rab35 WT for 24h and seeded into Matrigel. Cysts were fixed after 48h and cyst phenotypes were quantified. $p < 0.05$ (*), $p < 0.001$ (***), ns: not significant.

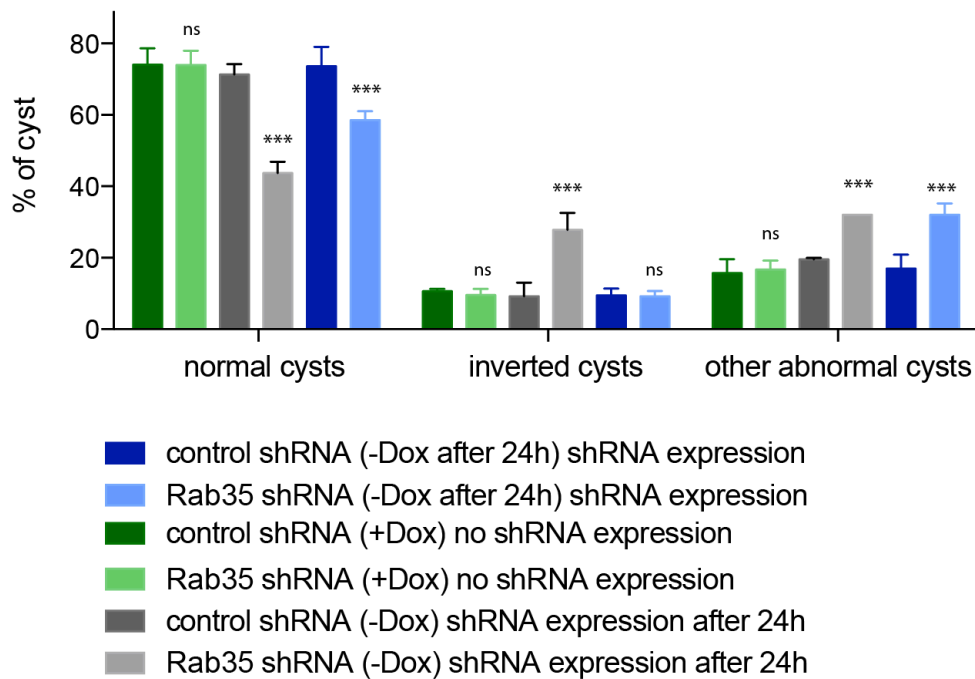


Figure B: Inversion of apico-basal polarity inversion requires Rab35 depletion during the first cell division of cyst development.

MDCK Tet-Off cells stably expressing either Rab35 shRNA or control shRNA under a tetracycline-regulated promoter were either cultured in the presence of Doxycycline (shRNA not expressed) or without Doxycycline (shRNA expressed).

Cyst phenotypes were quantified after 4 days in Matrigel.

Blue bars show cyst phenotypes in MDCK cells expressing control (dark blue) and Rab35 shRNA (light blue) without any Doxycycline: shRNAs are expressed throughout the cyst development.

Green bars show cyst phenotypes in MDCK cells expressing control (dark green) and Rab35 shRNA (light green) in the presence of Doxycycline: shRNAs are not expressed.

Grey bars show cyst phenotypes in MDCK cells expressing control (dark grey) and Rab35 shRNA (light grey), which were cultured initially in the presence of Doxycycline (shRNAs not expressed) and were then shifted into Doxycycline-free culture medium (24h after seeding into Matrigel), leading to shRNA expression only after the first cell division in Matrigel. Note that depletion of Rab35 after the first cell division does not lead to apico-basal polarity inversion, but to other abnormal phenotypes. $p < 0.05$ (*), $p < 0.01$ (**), $p < 0.001$ (***), ns: not significant. (compared to corresponding control)

Review

Rab35 GTPase: A Central Regulator of Phosphoinositides and F-actin in Endocytic Recycling and Beyond

Kerstin Klinkert^{1,2,3} and Arnaud Echard^{1,2*}

¹Membrane Traffic and Cell Division Lab, Cell Biology and Infection Department, Institut Pasteur, 25-28 rue du Dr Roux, 75724 Paris, France

²Centre National de la Recherche Scientifique, UMR3691, 75015 Paris, France

³Sorbonne Universités, Université Pierre et Marie Curie, Université Paris 06, Institut de formation doctorale, 75252 Paris, France

*Corresponding author: Arnaud Echard, arnaud.echard@pasteur.fr

Abstract

Rab35 is one of the first discovered members of the large Rab GTPase family, yet it received little attention for 10 years being considered merely as a Rab1-like GTPase. In 2006, Rab35 was recognized as a unique Rab GTPase localized both at the plasma membrane and on endosomes, playing essential roles in endocytic recycling and cytokinesis. Since then, Rab35 has become one of the most studied Rabs involved in a growing number of cellular functions, including endosomal trafficking, exosome release, phagocytosis, cell migration, immunological synapse formation and neurite outgrowth. Recently, Rab35 has been acknowledged as an oncogenic GTPase with activating mutations being found in cancer patients. In this review, we provide a comprehensive summary of known Rab35-dependent cellular functions and detail the few Rab35

effectors characterized so far. We also review how the Rab35 GTP/GDP cycle is regulated, and emphasize a newly discovered mechanism that controls its tight activation on newborn endosomes. We propose that the involvement of Rab35 in such diverse and apparently unrelated cellular functions can be explained by the central role of this GTPase in regulating phosphoinositides and F-actin, both on endosomes and at the plasma membrane.

Keywords actin, cancer, cell migration, cytokinesis, endosomes, membrane traffic, phagocytosis, phosphoinositides, PtdIns(4,5) P_2 , Rab GTPase

Received 2 May 2016, revised and accepted for publication 12 June 2016, uncorrected manuscript published online 21 June 2016

Rab35: an evolutionarily conserved Rab GTPase localized both on endosomes and at the plasma membrane

Rab GTPases are key regulators of membrane trafficking in eukaryotic cells, and regulate multiple steps of intracellular transport by controlling vesicle budding, lipid remodeling, interaction with molecular motors and the cytoskeleton, vesicle tethering and fusion (1). This is achieved by the localization of GTP-bound (active) Rab GTPase at the cytoplasmic surface of specific intracellular compartments

and by the recruitment of particular effectors by each Rab (1). Rab35 was first cloned from human skeletal muscle in 1994 and found to be ubiquitously expressed (2). Systematic sequencing later revealed that Rab35 is conserved in all animal metazoans and seems to even predate the rise of metazoans, as it has been identified in an organism that branched off from the premetazoan lineage after fungi, but before choanoflagellates (3). Rab35 was initially called H-Ray and later Rab1C due to its high sequence similarity to Rab1A and Rab1B, and indeed Rab35 clusters with Rab1A and Rab1B in the now complete phylogenetic tree

of Rab GTPases (3). However, despite strong homology of Rab35 with Rab1A and B in the catalytic GTPase domain and switch regions, they clearly differ in the last C-terminal 30 amino acids. Accordingly, Rab35 and the two Rab1 isoforms have distinct membrane localizations as well as different cellular functions. Rab1A and Rab1B localize to the endoplasmic reticulum (ER) and Golgi and regulate ER-to-Golgi vesicular traffic (1), whereas Rab35 localizes to both endosomes and the plasma membrane, as detailed below. A distinct feature of Rab35 is its evolutionarily conserved polybasic C-terminal extremity. Interestingly, the plasma membrane localization of Rab35 is GTP-dependent and involves this region through its direct binding to the negatively charged phosphoinositides PtdIns(4,5) P_2 and PtdIns(3,4,5) P_3 (4–6).

Initial studies suggested that overexpressed GFP-Rab35 could shuttle between the plasma membrane, cytosol and nucleus (7), although the later is thought to be an artifact of overexpression (8). However, endogenous Rab35 and episomally expressed epitope tagged-Rab35 are localized both at the plasma membrane and on a fraction of endosomes in mammalian cells (8–13), which has been recently confirmed using genome-edited cell line (14). This dual localization is conserved, as it is also found in *Caenorhabditis elegans* (15). To our knowledge, Rab35 is a unique Rab in animal cells by being clearly localized both at the plasma membrane and on endosomes. The significance of specific roles for Rab35 at the plasma membrane will be discussed later.

Rab35 promotes endocytic recycling

Rab35 was first identified in a comprehensive RNAi screen for cytokinesis defects in *Drosophila* S2 cells (8), in the search for regulators linking membrane traffic with the physical separation of the daughter cells at the end of mitosis (16,17). An increase of binucleated cells was observed upon depletion of Rab5, Rab11 and Rab35, with loss of Rab35 giving the strongest phenotype. Cytokinesis failure was associated with the presence of large intracellular vacuoles suggesting a trafficking block. Further investigation in HeLa cells revealed that Rab35 controls a fast endocytic recycling pathway from endosomes to the plasma membrane. Consequently, depletion or inactivation of Rab35 using the dominant-negative mutant Rab35 S22N led to an

accumulation of endocytic carriers such as transferrin (Tf) and Tf receptor (TfR) at the limiting membrane of intracellular vacuoles (8,13). Defects in TfR recycling were later confirmed in Rab35-depleted cells (18).

The key role of Rab35 in endocytic recycling was further strengthened when Rab35 was identified in a *C. elegans* genetic screen for yolk endocytosis in oocytes (15). Loss-of-function mutations in Rab35 (also known as RME-5, or receptor-mediated endocytosis-5) result in strong defects in yolk protein internalization associated with an accumulation of yolk receptors in dispersed small vesicles. Careful phenotypic analysis revealed that Rab35 functions at the level of cortical endosomes in the early steps of endocytic recycling, a finding recently confirmed in HeLa cells (14). Epistasis experiments in *C. elegans* also suggested that Rab35 functions in a recycling pathway in parallel to that controlled by Rab11, consistent with a role for Rab35 in fast endocytic recycling in mammals (8).

Rab35-dependent endocytic recycling back to the plasma membrane has actually been reported for diverse cargoes. Specifically, Rab35 controls the trafficking of major histocompatibility complex class-II (MHC-II)-peptides in HeLa-CIITA cells (9), MHC-I in COS-7 cells and HeLa cells (12,19,20), T-cell receptor (TCR) in Jurkat T cells (13), Ca²⁺-activated K⁺ channel KCa2.3 in human embryonic kidney cells and human microvascular endothelial cells (HMEC-1) (21), Megalin in L2 rat yolk sac cells when autosomal recessive hypercholesterolemia (ARH) is depleted (22), GLUT4 in adipocytes (23), M- and N-Cadherin in C2C12 and COS-7 cells (10,20) and β 1-integrin in COS-7 and HeLa cells (11,20). In addition, Rab35 depletion or inactivation also perturbs trafficking from the endosomes to the trans Golgi network (TGN) of internalized Shiga toxin (24), or CI-mannose-6-phosphate receptors (14).

Altogether, there is clear evidence that Rab35 controls the trafficking of unrelated cargoes at the level of endosomes, indicating that Rab35 plays a fundamental and conserved role after cargo internalization.

OCRL, MICAL-L1 and ACAP2: three key effectors of Rab35 in endocytic trafficking

Effector proteins bind specifically to active, GTP-bound Rabs, and mediate their cellular effects. Three Rab35

effectors, OCRL, MICAL-L1 and ACAP2 have been characterized and explain the role of Rab35 in regulating phosphoinositides on endosomes, endosomal fission and cargo recycling.

OCRL

Initial work in *Drosophila* and human cells indicated that Rab35 plays a critical role in regulating the levels of the PtdIns(4,5) P_2 lipid on endosomes (8). Inactivation of Rab35 using Rab35 S22N dominant-negative mutant induces the formation of intracellular vacuoles that are abnormally rich in PtdIns(4,5) P_2 , suggesting that Rab35 limits this phosphoinositide in normal cells. Interestingly, these vacuoles are rapidly covered by the PtdIns(4,5) P_2 -binding protein SEPTIN2 and slowly accumulate F-actin. The delocalization of SEPTIN2 from the plasma membrane onto these vacuoles likely explains the cleavage furrow instability and cytokinesis failure observed upon Rab35 inactivation in human cells, or Rab35 depletion in *Drosophila* cells (8).

This raised the question of why PtdIns(4,5) P_2 accumulates on endosomes when Rab35 is inactivated. GTP-bound Rab35 is known to bind directly to the PtdIns(4,5) P_2 phosphatase OCRL (25,26), an enzyme that selectively hydrolyses PtdIns(4,5) P_2 into PtdIns4P (27–31). Mutations in OCRL are responsible for the Oculo-Cerebro-Renal syndrome of Lowe, a rare genetic disease characterized by reabsorption defects in renal cells, congenital cataract and mental impairment (27–29,31). At the cellular level, OCRL depletion perturbs endocytic recycling and trafficking from endosomes to the TGN (32,33), which is reminiscent of the defects observed after Rab35 depletion.

A recent study revealed that GTP-bound Rab35 directly recruits OCRL onto clathrin-coated endosomes, just after their scission from the plasma membrane (14). In addition, depletion of either Rab35 or OCRL leads to accumulation of PtdIns(4,5) P_2 - and F-actin-binding proteins on enlarged peripheral endosomes, and delays trafficking of internalized mannose-6-phosphate receptor to the TGN. Similarly, Rab35 depletion leads to the accumulation of N- and M-cadherin in transferrin-, clathrin- and AP2-positive endosomes in C2C12 myoblasts (10). Altogether, Rab35 functions with OCRL to promote PtdIns(4,5) P_2 hydrolysis

on newborn endosomes, hence clathrin uncoating and subsequent trafficking and sorting steps from early endosomes (14). This indicates a crucial role of Rab35 in defining the lipid identity of peripheral endosomes before they fuse to give rise to early endosomes.

MICAL-L1 and ACAP2

In addition, Rab35 plays a later role on recycling endosomes positive for ARF6 (34,35), through the coordinated recruitment of the Rab35 effectors MICAL-L1 and the ARF6 GAP centaurin β 2/ACAP2 (25,36). This mechanism has been particularly well studied during neurite outgrowth in PC12 cells in response to NGF stimulation (37–41). Expression of a partially constitutive active mutant (Rab35 Q67L) (42) promotes neurite outgrowth in PC12 cells and in N1E-115 cells, whereas expression of a constitutively active mutant of ARF6 inhibits neurite outgrowth and endocytic recycling (34,38,43,44). Upon nerve growth factor (NGF) stimulation, Rab35 accumulates on ARF6-positive perinuclear recycling endosomes and recruits both MICAL-L1 and ACAP2 (36,38). Then, MICAL-L1 together with ACAP2 controls the recruitment of EHD1, a protein inducing membrane fission due to its similarities to dynamin (39,40,45). Mechanistically, MICAL-L1 associates directly with EHD1, whereas ACAP2 promotes EHD1 recruitment indirectly through the inactivation of ARF6 and thereby maintenance of PtdIns4P, a scaffold factor for EHD1 (39). This is consistent with previous findings indicating that Rab35 is required for EHD1 recruitment on recycling endosomes (12). In parallel to promoting fission of tubular endosomes through EHD1, MICAL-L1 also recruits downstream Rabs (namely Rab8, Rab13 and Rab36), which promote recycling (36,40). Thus, Rab35 plays a pivotal role on ARF6-positive recycling endosomes both by inactivating ARF6 and by recruiting MICAL-L1, which in turn recruits additional Rabs and EHD1 (Figure 1).

In addition to the Rab35/ARF6 antagonism described above, the correct sorting of cargoes that enter by clathrin-independent endocytosis (such as CD44, CD98 and CD147) depends on Rab35 activation and ARF6 inactivation on sorting/recycling endosomes (44). When clathrin-mediated endocytic pathway is inhibited, ARF6-GTP levels are upregulated and functional experiments indicate that Rab35 is on the contrary

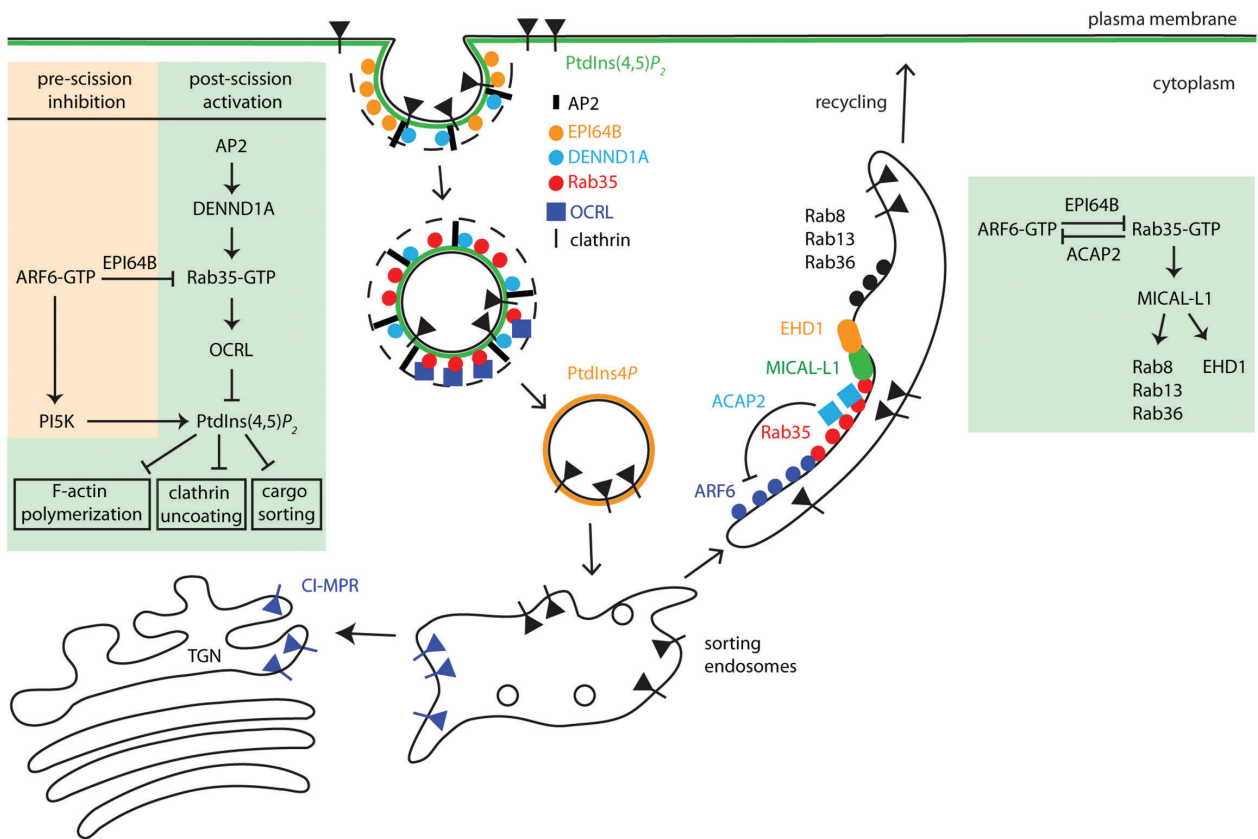


Figure 1: Functions of Rab35 in membrane traffic. PtdIns(4,5)P₂ homeostasis during endocytosis and recycling is regulated by Rab35 and its effectors. In clathrin-coated pits, PtdIns(4,5)P₂ levels (green) are high: ARF6 directly recruits the PtdIns 5-kinase and inhibits Rab35 activation by recruiting its RabGAP EPI64 (orange circles). After scission of the endosome from the plasma membrane, the AP2-binding Rab35 GEF DENND1A (light blue circle) activates Rab35 (red circles) on newborn endosomes, where it recruits the PtdIns(4,5)P₂ phosphatase OCRL (blue squares). This promotes PtdIns(4,5)P₂ hydrolysis, clathrin uncoating and cargo sorting. On the recycling endosomes Rab35 activation, which antagonizes with ARF6 activation through the Rab35 effector ACAP2 (light blue square), recruits MICAL-L1 (green ovals) and thereby EHD1 (orange ovals) and other Rab GTPases (black circles) to allow scission of the tubular endosomes and to promote recycling to the plasma membrane.

inactivated. As a consequence, the sorting of cargoes of the ARF6-dependent pathway is perturbed (44). At the molecular level, one can imagine that depletion of clathrin inhibits Rab35 activation, as it depends on AP2/clathrin-binding guanine exchange nucleotide factors (GEFs) (12,14,15). As a consequence, the Rab35 effector ACAP2 may not be properly recruited on recycling endosomes, which would translate into abnormally elevated levels of ARF6-GTP. Consistent with this mechanism, the levels of ARF6-GTP clearly increase when Rab35 is depleted (20). Altogether, there is clear evidence that Rab35 negatively regulates ARF6 activation on recycling endosomes, which is important for correct recycling of cargoes. Such a

Rab35/ARF6 antagonism has been further confirmed during the regulation of oligodendrocyte differentiation (46).

GEFs and GAPs control tight activation of Rab35 on newborn endosomes

The Rab35 GTP/GDP cycle is governed by interaction with GEFs and GTPase-activating proteins (GAPs) (1). Several Rab35 GEFs and GAPs have been identified (47), the best characterized being DENND1A and EPI64A-C, which altogether regulate a burst of Rab35 activation on newborn endosomes.

Rab35 GEFs

DENND1 family

DENND1A is a major GEF for Rab35 in the endocytic pathway (48). In mammals, the DENND1 family is composed of DENND1A (also known as *conneccenn1*), DENND1B (*conneccenn2*) and DENND1C (*conneccenn3*). The DENN domain (*differentially expressed in neoplastic versus normal cells*) is an evolutionarily conserved module present in all eukaryotes (49,50), first identified as a Rab-binding module in the Rab6/Rab11 interacting protein Rab6ip1 (51,52), and later found to display Rab GEF activity (48). The first hint that DENND1A functions as a Rab35 GEF came through the identification of its *C. elegans* homologue (RME4) in the same screen for mutants defective in receptor-mediated endocytosis of yolk proteins that identified Rab35/RME5 (15). Epistasis experiments indicated that RME4 acts upstream of Rab35 in endocytic recycling, and mutations in RME4 and RME5 lead to similar trafficking defects (15). Finally, RME4 interacts specifically with GDP-bound Rab35, suggesting that it acts as a Rab35 GEF (15). It was subsequently demonstrated that indeed DENND1A is a *bona fide* GEF for Rab35 *in vitro* (12). Importantly, disrupting DENND1A function impairs trafficking through endosomes, as observed upon Rab35 depletion in several cell types (12,14,15), indicating that it is a functional Rab35 GEF. Of note, DENND1A might have other yet-to-be-identified target(s), as the RME4 mutant has a stronger endocytic phenotype than the RME5 mutant in *C. elegans*, at least in certain cell types (15).

Before knowing that it is a Rab35 GEF, DENND1A/*conneccenn1* had been previously characterized as a novel clathrin-coated vesicle (CCV) component, which interacts directly with clathrin, with the α -ear of the endocytic clathrin adaptor AP-2, and with the accessory proteins intersectin, endophilin A1 and adaptin-ear-binding coat-associated protein (NECAP) (53,54). Accordingly, DENND1A partially colocalizes with AP-2 (12,15). An exceptional feature of DENND1A is its strong interaction with the surface of CCVs *in vitro*, even under conditions where clathrin is removed, suggesting a role after CCV formation (53). This strong association likely results from combined interactions between DENND1A and Rab35 itself, and with the AP-2, accessory proteins, 14-3-3 proteins and phosphoinositides (12,55). Detailed

TIRF-microscopy-based analysis recently revealed that DENND1A is loaded onto CCVs just after the scission of CCPs from the plasma membrane and a few seconds before Rab35 itself (14). AP-2 binding is necessary, but not sufficient to explain the DENND1A recruitment profile, as AP-2 is present in CCPs well before CCVs scission from the plasma membrane. Altogether, multiple reports indicate that DENND1A is a major Rab35 GEF that activates Rab35 on CCVs to promote endocytic recycling of various cargoes after internalization.

Among the 26 DENN-containing proteins in Man, three (DENND1A, DENND1B and DENND1C, plus alternative spliced variants) constitute the DENND1 subfamily (48,50). The Rab35/DENND1B complex was the first crystal structure of a Rab/DENN-containing protein solved, and it provided hints on how DENN GEFs act at the molecular level (56). All members of the DENND1 family have robust, although differential GEF activity toward Rab35 and interact with the clathrin machinery (57). Indeed, DENND1A-C associates with AP-2 (through different mechanisms), clathrin and phosphoinositides (12,48,57,58). DENND1B is expressed more broadly than DENND1A, and might functionally replace DENND1A, although clear differences in AP-2-colocalization and CCV binding exist (57). DENND1C is distinct as it displays an additional *in vitro* GEF activity for Rab13 (but weaker than for Rab35) (59,60), and as it binds directly to actin and partially colocalizes with the actin cytoskeleton (60). In contrast to DENND1A-B that activates Rab35 on endosomes, DENND1C is important for activating Rab35-mediated functions in actin remodeling (60), as described later.

Folliculin

Folliculin (FLCN) is a potential Rab35 GEF and displays a selective GEF activity toward Rab35, at least *in vitro* (61). The primary sequence of FLCN does not reveal a discernable DENN domain, but unexpectedly, the atomic structure of the C-terminal part of FLCN revealed the presence of a DENN module (61). Loss-of-function mutations in FLCN leads to a rare genetic disease, the Birt-Hogg-Dubé syndrome (BHD) characterized by benign skin tumors and elevated incidence of renal carcinomas (62). FLCN impacts on numerous cell functions and regulates for instance mTORC signaling (63), as recently found for Rab35 (see

below). However, further studies are needed to demonstrate whether FLCN is a functional Rab35 GEF in cells.

Rab35 GAPs

TBC1D10A-C/EPI64A-C

While Rab35-GTP inhibits ARF6 by recruiting ACAP2 as described above, ARF6-GTP also inhibits Rab35 activation. Indeed, ARF6-GTP directly interacts with EPI64A-C (*TBC1D10A-C*) (64), which constitutes a family of functional GAPs for Rab35 (13,19,24,65). Consequently, overexpression of either a constitutively active mutant of ARF6 (ARF6 Q67L), EPI64, or a dominant-negative of Rab35 (Rab35 S22N) all lead to the formation of PtdIns(4,5) P_2 -rich vacuoles that block endocytic cargo recycling and inhibit cytokinesis (13,19,21). In addition, ARF6-GTP and EPI64 both reduce the levels of Rab35-GTP in cells (19), as measured by a high affinity trap with a domain of RUSC2 (66). Tissue expression of EPI64A-C differs, and each of these GAPs likely regulates Rab35 in a cell type-specific manner (13,19). Interestingly, ARF6 is present in clathrin-coated pits (19,67), where it recruits EPI64B, thus preventing activation of Rab35 in CCPs (19). Total internal reflection fluorescence (TIRF)-microscopy confirmed that EPI64B is present on CCPs, but not on CCVs (14), likely because it is retained at the cell cortex through its interaction with the Ezrin-interacting protein EBP50 (64).

The presence of the Rab35 GAP EPI64B before CCP scission combined to the recruitment just after the scission of the Rab35 GEF DENND1A explains the precise spatial and temporal activation of Rab35 on newborn clathrin-coated endosomes (14). This mechanism of regulation ensures that Rab35 recruits OCRL only after CCP scission in order to hydrolyze PtdIns(4,5) P_2 . Before CCP scission, PtdIns(4,5) P_2 production is essential for recruiting key CCP proteins. It is favored both by ARF6 (which interacts with a PtdIns4P 5-kinase) and by preventing Rab35 activation thus OCRL recruitment. On the contrary, after scission, Rab35 is activated and recruits OCRL on newborn endosomes. This induces PtdIns(4,5) P_2 hydrolysis and promotes clathrin uncoating (14) (Figure 1). In conclusion, ARF6 and Rab35 are part of a putative bi-stable switch: ARF6-GTP inhibits Rab35 activation through binding to Rab35 GAP EPI64, whereas Rab35-GTP inhibits ARF6 activation through binding to ARF6 GAP

ACAP2 (Figure 1). In other words, it is predicted that at a membrane it is either Rab35-GTP/ARF6-GDP, or Rab35-GDP/ARF6-GTP. As described in the last section this could be important to control local phosphoinositide levels and F-actin dynamics.

Skywalker/TBC1D24

Mutations in the neuronal Rab35 GAP Skywalker (*TBC1D24*) revealed that Rab35 is implicated in endosomal sorting of synaptic vesicle proteins in *Drosophila* neuromuscular junctions (68). Increasing the levels of active Rab35 facilitates endosomal trafficking, which boosts neurotransmission. Whether *TBC1D24* inactivates Rab35 only in neurons and whether this regulation is evolutionarily conserved remains to be investigated.

TBC1D13

Upon insulin stimulation glucose transport in adipocytes is stimulated by the translocation of the glucose transporter GLUT4 from internal membranes to the plasma membrane. Overexpression of the Rab GAP *TBC1D13* prevents GLUT4 translocation following insulin stimulation and reduces Rab35 activation in cells (69). Furthermore, *TBC1D13* is a Rab35 specific GAP *in vitro* and the defects observed after *TBC1D13* overexpression could be rescued by coexpression of a constitutively active Rab35 Q67L mutant. In addition, *TBC1D13* is also a Rab10 effector suggesting a potential Rab cascade whereby Rab10 recruits *TBC1D13* to inactivate Rab35 on a compartment that remains to be characterized (69). Further work will be needed using Rab35- or *TBC1D13*-depleted cells to confirm a role for activation of endogenous Rab35 in the trafficking of GLUT4 upon insulin stimulation, and to potentially extend the role(s) in other cell types of this ubiquitously expressed GAP.

Rab35 functions in immunity and phagocytosis

As mentioned above, Rab35 regulates the trafficking of key immune receptors: MHC-I, MHC-II-peptide complex and the TCR (9,12,13,19,20).

Depletion of Rab35 in COS-7 cells indeed inhibits the recycling of MHC-I back to the plasma membrane after its

internalization through clathrin-independent endocytosis. This leads to an accumulation of MHC-I in early endosomes due to failure of EHD1 recruitment onto early endosomes (12,20). Inactivation of Rab35 in HeLa cells also leads to the intracellular accumulation of MHC-I, here in vacuoles that are positive for TfR, but negative for early endosome markers such as Rab5 and EEA1 (19).

In addition, mature MHC-II-peptide complexes are endocytosed in a clathrin-independent manner and their recycling requires Rab35 (9). Expression of ARF6 T27N, or Rab35 S22N dominant-negative mutants in HeLa-CIITA cells both induces the accumulation of MHC class-II on vesicular structures positive for ARF6, Rab35 and EHD1, and impairs recycling.

Finally, the formation of the immune synapse requires enrichment of TCR and other signaling molecules at the contact site between T cells and antigen presenting cells. Inactivation of Rab35 by overexpression of Rab35 GAP EPI64C (preferentially expressed in hematopoietic cells), or of the dominant-negative mutant Rab35 S22N inhibits TCR recycling (13). Altogether, this prevents TCR enrichment at the contact site and impairs conjugate formation. The role of Rab35 in TCR recycling has been recently confirmed in mouse T_H2 cells (70). Depletion of Rab35 or mutations in DENND1B delays TCR down-regulation from the cell surface following receptor activation, thus enhances TCR signaling, increases T_H2 cytokine production and leads to hyperallergic responses (70). It remains to be established how Rab35 regulates TCR internalization that could be indirect, as Rab35 is loaded on endosomes only after internalization (14). Interestingly, impaired Rab35 activation is linked to asthma, as human T_H2 cells from patients harboring asthma-associated DENND1B variants phenocopy Dennd1b^{-/-} T_H2 cells.

Besides being involved in normal trafficking of immune receptors, Rab35 also contributes to immunity by regulating phagocytosis. During FcR-mediated phagocytosis in macrophages Rab35 is found at the base of the phagocytic cup (71). Depletion or inactivation of Rab35 leads to decreased phagocytosis due to impaired membrane extensions and phagocytic cup formation. Conversely, GTP-bound Rab35 recruits ACAP2 to inactivate ARF6, which promotes actin-rich protrusions and is necessary

for the final phagosome closure. Interestingly, Rab35 is deactivated immediately after phagosome formation, while ARF6 gets transiently activated (72). This tight regulation is necessary for successful phagocytosis and highlights again the mutual Rab35/ARF6 antagonism already described above in the trafficking section. A role for Rab35 in phagocytosis and innate immunity has also been described in *Drosophila* (73,74). Rab35 mutant flies show strong susceptibility to infection and inactivation of Rab35 strongly inhibits the formation of actin-rich protrusions required for phagocytosis (74).

Hijacking of the Rab35 pathway by pathogens

Intracellular pathogens often use and modulate their host cells' trafficking machineries to direct proteins and membranes to their vacuole, which is required for pathogen survival and replication. The bacteria *Legionella pneumophila* induces posttranslational modifications of host Rab GTPases Rab1 and Rab35 to modulate endocytic and exocytic pathways, respectively (75). *Legionella* secretes two enzymes that covalently modify host Rab1 and Rab35: DrrA (which mediates the covalent attachment of an AMP moiety to a specific tyrosine or AMPylation) and AnkX (which mediates the covalent attachment of phosphocholine moiety to a specific serine or phosphocholination) (75,76). Consequently, AnkX expression reduces Rab35 binding to its GEF DENND1A and mimics Rab35 depletion. In addition, phosphocholination reduces the extraction of Rab35 from membranes by GDI (GDP dissociation inhibitor), at least *in vitro* (5,76). Besides AnkX, *Legionella* secrete another effector protein (LepB) that *in vitro* displays GAP activities toward Rab1, Rab3, Rab8, Rab13 and Rab35 (77). Thus, different bacterial effectors target Rab35 and its inactivation is central for *Legionella* infection.

In urinary tract infections caused by intracellular uropathogenic *Escherichia coli* (UPEC), Rab35 facilitates UPEC survival within vacuoles in bladder epithelial cells (18). Indeed, UPEC enhances the expression of both Rab35 and TfR and recruits these proteins to UPEC-containing vacuoles, thereby enhancing iron delivery into the vacuole. In addition, Rab35 helps UPEC to escape lysosomal degradation, which further promotes intracellular survival of UPEC. The compartment occupied by UPEC reassembles that of *Anaplasma phagocytophilum* and also recruits

Rab35 (78), perhaps to similarly promote iron delivery to the bacteria.

Rab35 is also known to play a role in the extracellular release of the *Bacillus anthracis* virulence factor anthrax lethal toxin. In RPE cells, both Rab11 and Rab35 are required for the delivery of exosomes loaded with the toxin into the extracellular medium (79). Apart from infection, the role for Rab35 in exosome secretion had been demonstrated in oligodendrocytes and in MDCK cells (65,80). Interestingly, expression of active Rab35 Q67L reduces the motility of LysoTracker-labeled vesicles, suggesting that active Rab35 might promote vesicle tethering to facilitate membrane fusion and exosome secretion (65). A similar Rab35-dependent tethering mechanism has been recently demonstrated during apico-basal polarity establishment in renal epithelial cells, as described in the next section.

Rab35 functions in cytokinesis and cell polarity

Cell division and cell polarity are two processes that are tightly linked to each other, and Rab35 has not only been implicated in both processes, but also couples them.

The importance of Rab35 in cytokinesis was first discovered in a RNAi screen in *Drosophila* S2 cell for cytokinesis defects, as mentioned above (8). Depending on the level of Rab35 depletion/activation, *Drosophila* or human cells display either bridge instability leading to binucleated cells, or delayed abscission (26). As found on newborn endosomes in interphase cells, Rab35 controls OCRL localization at the plasma membrane of the cytokinetic bridge connecting the daughter cells. This allows PtdIns(4,5) P_2 hydrolysis that is necessary for preventing F-actin accumulation during late cytokinesis, and thus for successful abscission. Indeed, abscission in HeLa cells is greatly delayed in OCRL- or Rab35-depleted cells, and this is associated with increased levels of PtdIns(4,5) P_2 and F-actin at the bridge. Interestingly, low nontoxic doses of Latrunculin-A rescue the delay in abscission indicating that Rab35/OCRL controls actin clearance necessary for completion of abscission (26). Unexpectedly, Rab35 has also been involved in an earlier step of cell division, in the formation and maintenance of microtubule-based meiotic spindles in mice oocytes

(81). Depletion of Rab35 in oocytes induces abnormal and multipolar spindles and decreases polar body extrusion. How Rab35 could influence spindle morphology remains to be investigated and could possibly involve PtdIns(4,5) P_2 and thus septins.

Recently, Rab35 has been found to couple cytokinesis with the establishment of apico-basal polarity in MDCK cyst development (82). MDCK cells cultured in matrigel form single cell layer spheres (cysts) with a central apical lumen. Each cyst results from the successive division of a single, initially unpolarized cell. Strikingly, inactivation of Rab35 leads to cysts with complete inversion of apico-basal polarity and lacking open lumens. In normal cysts, Rab35 targets intracellular vesicles transporting aPKC, Cdc42, Crumbs3 and the lumen promoting factor podocalyxin to the membrane surrounding the first cytokinetic bridge, which defines the apical initiation site. Rab35 is enriched at the cleavage furrow and tethers apical-vesicles through a direct interaction with the cytoplasmic tail of podocalyxin. Therefore, PODXL is a novel effector of Rab35 and Rab35 physically couples cytokinesis with initiation of apico-basal polarity. The importance of Rab35 in apical polarity in 3D MDCK cysts has been confirmed recently (83). Interestingly, ACAP2 is an effector of Rab35 in 3D but not in 2D cultures, highlighting the fundamental differences in trafficking between the two conditions (83). Importantly, the implication of Rab35 in polarity establishment has also been reported *in vivo* in seamless tube formation in *Drosophila* tracheal terminal cells (84). Growth of seamless tubes is polarized along the proximodistal axis and is regulated by Rab35 and its GAP Whacked (a homologue of EPI64A-C). GTP-bound Rab35 directs the transport of apical membrane vesicles to the distal tip of terminal cell branches to induce seamless tube growth. Interestingly,

Rab35 functions in cell migration and cancer

The first potential link between Rab35 and tumorigenesis came from the existence in lymphoma cells of a complex between Rab35 and the oncogenic chimeric kinase NPM-ALK, but the functional significance of this interaction needs to be investigated (85). Along the same line, Rab35 was found associated with the p53 kinase PRPK and overexpression experiments suggest it may regulate

p53 transcriptional activity (7). Furthermore, Rab35 might represent a biomarker of ovarian cancer, as Rab35 expression is upregulated in this cancer (86).

Rab35 depletion in COS-7 cells leads to phenotypes resembling epithelial–mesenchymal transition (EMT), including decreased cell adhesion and increased cell migration, which is often observed for cancer cells (20). In COS-7 cells, Rab35 activity and the mutual antagonism with ARF6 are required to maintain N- and E-cadherin at the cell surface to promote cell–cell adhesion (20). This is consistent with previous studies showing that Rab35 depletion inhibits C2C12 myoblast fusion through impaired cadherin recycling to the plasma membrane (10). Rab35 is proposed to inhibit cell migration through ACAP2-dependent inactivation of ARF6, which results in an inhibition of the β 1-integrin and epidermal growth factor (EGF) receptor recycling (20). However, a separate study in HeLa and MDA-MB-231 cells did not detect a role for Rab35 in β 1-integrin recycling, but instead an inhibitory role of Rab35 in β 1-integrin internalization (11). The reason for this apparent discrepancy is not known, but it could depend on differences in cell types and experimental setups (see discussions in 11 and 20).

In cancer cells Rab35 activation is regulated through several mechanisms. First, Rab35 expression is suppressed in a subset of cancers characterized by elevated ARF6 activity (20), reinforcing the notion of the ARF6/Rab35 antagonism. Furthermore, Rab35 is negatively regulated by microRNA-720 (miR-720), which is upregulated in cervical tumors (87). In HeLa cells overexpression of miR-720 diminishes Rab35 expression and thereby promotes cell migration (87), as also observed in COS-7 cells (20).

In contrast with the studies mentioned above, Rab35 depletion does not promote, but instead inhibits cell migration when breast cancer MCF-7 cells are stimulated by Wnt5a (88). Here, Rab35 acts downstream of Wnt5a and Dvl2 and upstream of Rac1 to promote cell migration, although the mechanisms by which Wnt5a and Dvl2 activate Rab35 and Rac1, respectively, remain to be established. Altogether, the role of Rab35 in cell migration is thus complex, depending on the cell type and might be influenced by external cues that modulate signal transduction pathways.

Quite recently, Rab35 has been directly linked to cancer through its regulatory role in the phosphatidylinositol-3-kinase (PI3K)/ AKT signaling pathway (89), as previously noted (20). Depletion of Rab35 suppresses phosphorylation-induced AKT activation in different cell types, whereas expression of a GTP-bound Rab35 Q67L mutant induces constitutive AKT signaling. Rab35 functions downstream of growth factor receptors and upstream of PDK1 and mTORC2, possibly by regulating PI3K as Rab35-GTP co-immunoprecipitated with the lipid kinase. Expression of active Rab35 is sufficient to drive PDGFR- α into Lamp2-positive endosomes even in absence of ligands, leading to constitutive AKT phosphorylation. Interestingly, AKT-dependent phosphorylation releases the auto-inhibition of the Rab35 GEF DENND1A, thus increasing GEF activity and binding to Rab35 and in such a way promotes Rab35 activation (55). Hence, Rab35 activation and AKT phosphorylation potentially act together in a positive feedback loop. Importantly, in human cancers two somatic Rab35 mutations were found to constitutively activate PI3K/AKT signaling. When overexpressed in HeLa cells the same mutations phenocopied the expression of GTP-locked Rab35, suppressing apoptosis and promoting cellular transformation. Altogether, this suggests that Rab35-dependent recycling of specific growth factor receptors plays a driving role in cancer development.

Rab35: a key regulator of F-actin at the plasma membrane

At first sight the cellular functions of Rab35 seem to be very diverse: endocytic recycling, cytokinesis, phagocytosis, migration, neurite outgrowth, membrane protrusion, cancer and infection (Figure 2). However, many of these regulatory functions in actin dynamics can be explained by a common, fundamental role played by Rab35 at the plasma membrane. Indeed, Rab35 regulates many actin-based phenomena. Rab35 depletion inhibits neurite outgrowth (38–40,60) and membrane extension (74,90), as mentioned previously. Interestingly, Rab35 colocalizes with Cdc42, Rac1 and RhoA in PC12 and N1E-115 and BHK neuronal cells, activates Cdc42 and stimulates neurite outgrowth in a Cdc42-dependent manner through actin remodeling (37). In addition, Rab35 translocates from

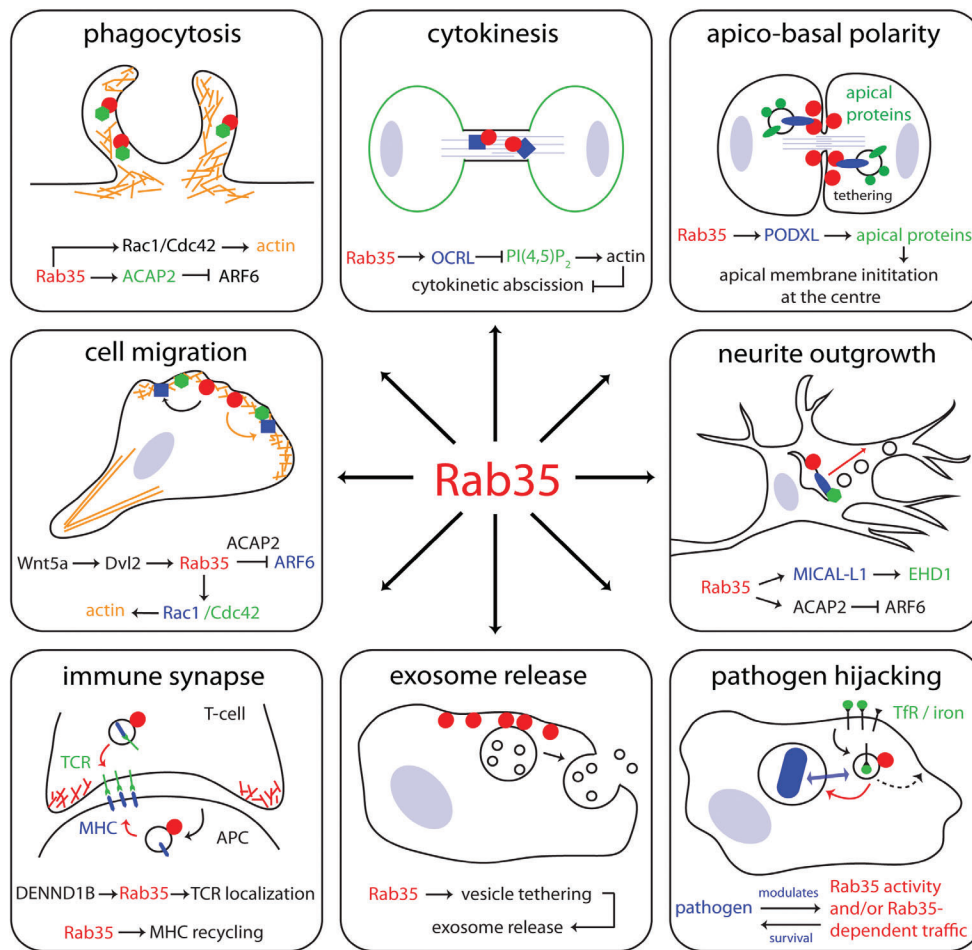


Figure 2: Functions of Rab35 at the plasma membrane. Rab35 (red circles) regulates many cellular functions in association with specific effector proteins. Note that most cellular functions involve the regulation of F-actin polymerization either through Rac1/Cdc42 activation, ARF6 inactivation or through OCRL-mediated PtdIns(4,5)P₂ hydrolysis.

recycling endosomes to neurite tips upon NGF stimulation (91). Finally, Rab35 also regulates Rac activity in Wnt5-induced migration (88), as well as Rac and Cdc42 localization during phagocytosis in *Drosophila* (74). Altogether, there is a body of evidence arguing for an important role for Rab35 in local targeting and activation of both Rac and Cdc42 at the plasma membrane. How Rab35 promotes Rac and/or Cdc42 activation is a key open question for future studies.

Consistent with a strong link between Rab35 and the actin cytoskeleton, inactivation of Rab35 during *Drosophila* development induces malformation of bristles that are actin-based structures (90). Malformed bristles are caused by loose and disconnected actin, suggesting a direct role

for Rab35 in actin organization. Accordingly, the actin bundling protein fascin is an effector of Rab35 and overexpression of fascin can rescue the bristle phenotype induced by Rab35 depletion, placing fascin downstream of Rab35. Using *Drosophila* S2 cells it was further demonstrated that active Rab35 ectopically expressed at the mitochondrial membrane was sufficient to induce actin bundling around the mitochondria (90). Consistent with Rab35 promoting actin-based protrusions, overexpression of the constitutively active mutant Rab35 Q767L leads to long cell extensions in BHK cells, *Drosophila* S2 and SL2 cells, NIH3T3, Jurkat T cells and HeLa cells (4,13,37,60,74,90,92). Co-overexpression of DENND1C and wild-type Rab35 has an even greater impact on the formation of cell protrusions, indicating that in cell shape

morphology changes the actin-binding GEF DENND1C is likely responsible for Rab35 activation (60). However, it would be important to test this idea directly in DENND1C-depleted cells. Interestingly, the colocalization between Rab35 and fascin is enhanced when DENND1C is overexpressed in mammalian cells. Thus, it is proposed that DENND1C is recruited by actin, then locally activates Rab35, which in turn recruits fascin to induce actin filament bundling and membrane protrusions (60).

In other cellular functions involving Rab35 such as cytokinesis, phagocytosis or migration, several other Rab35 effectors regulating PtdIns(4,5) P_2 levels (e.g. OCRL and ACAP2) could contribute to regulate local F-actin remodeling in parallel to ARF6, Rac and Cdc42 (26,71,93,94).

Conclusions and open questions

Rab35 plays a fundamental and evolutionarily conserved role in endocytic recycling of diverse cargos from the endosomes to the plasma membrane. This trafficking function relies on Rab35 effectors that promote PtdIns(4,5) P_2 hydrolysis and clathrin uncoating after endosome scission from the plasma membrane (OCRL), fission of tubular recycling endosomes through the recruitment of additional Rabs and EHD1 (MICAL-L1) and inactivation of the ARF6 GTPase on recycling endosomes (ACAP2). Rab35 appears a few seconds after endosome scission and as its colocalization with the early endosomal marker Rab5 is limited, it is postulated that Rab35 is recruited transiently on newborn endosomes and is lost from early endosomes (14). While the Rab35 GEF on newborn endosome is the AP2-binding protein DENND1A, the identity of the GEF(s) acting at the level of recycling endosomes remains elusive. The functions of Rab35 and ARF6 are interdependent, as the Rab35 GAP EPI64 is an effector of ARF6 and the ARF6 GAP ACAP2 is an effector of Rab35. The potential mutual antagonism between Rab35 activation and ARF6 activation has been reported in many instances, but visualizing the conversion of Rab35-GTP by ARF6-GTP (and vice versa) on internal membranes will require the development of GTP-specific biosensors for live-cell imaging.

Besides being localized on endosomes, Rab35 is a unique Rab GTPase due to its presence at the plasma membrane.

However, it is difficult to determine what is the importance of Rab35 in directly recruiting effectors at the plasma membrane, versus the importance of endosomal Rab35 in delivering effectors to the plasma membrane. Actually, Rab35-dependent trafficking appears to target Rac and Cdc42 to the plasma membrane during phagocytosis and during neurite outgrowth, and to be a major positive regulator of their activation through mechanisms that remain to be discovered. In addition, Rab35 favors protrusions by recruiting the actin-bundling factor fascin. A major question for the future is to identify the GEFs that locally activate Rab35 at the plasma membrane during cell migration, cytokinesis, membrane protrusions and phagocytosis. As on endosomes, Rab35 recruits the PtdIns(4,5) P_2 phosphatase OCRL at the plasma membrane to regulate local actin clearance during cytokinesis. It is likely that the same functional module regulates actin clearance at the base of the phagocytic cup during phagosomal closure, as described for both OCRL and Rab35 (93,94). We thus speculate that Rab35-recruitment of OCRL and F-actin remodeling might be an ancestral function of Rab35 both on endosomes and at the plasma membrane.

Posttranslational modifications such as phosphocholination and AMPylation of Rab35 seem to play a major role in successful bacterial infection. Surprisingly, little is known about Rab35 posttranslational modifications that might modulate Rab35 function in normal cells. Clearly, geranylgeranylation of the C-terminus of Rab35 is not sufficient to explain its unique plasma membrane localization (as Rabs in general are prenylated at their C-terminus), which critically depends on its polybasic tail. Rab35 is phosphorylated at least nine positions (<http://www.phosphonet.ca>), notably in the C-terminal extremity (SKRKKRCC). One can imagine that phosphorylation of the tail will change the affinity of Rab35 for the plasma membrane and thus regulates Rab35 distribution between endosomes and the plasma membrane. Phosphorylation of another small GTPase RhoA at S188 is known to regulate its association with the plasma membrane (95) giving credence to the notion that S194 phosphorylation might do the same for Rab35.

There is also an urgent need for animal models to understand Rab35 functions *in vivo*. Surprisingly, loss-of-function mutants in *C. elegans* and *Drosophila*

melanogaster are viable, although they affect yolk internalization and increase susceptibility to infections, respectively (15,74). Other Rab GTPases are strongly upregulated after Rab35 depletion (e.g. Rab5) (12), suggesting potential functional compensations. However, *rab35* KO is embryonic lethal in mice (see discussion in 21) and future work will certainly reveal interesting functions of Rab35 during development. Finally, identifying additional Rab35 effectors will be essential in the future, and together with specific GEFs, might directly connect Rab35 to a number of diseases such as asthma, the Lowe syndrome, the BHD syndrome and cancer.

Acknowledgments

We thank all the past and current Lab members for discussions, and G. Langsley for critical reading of the manuscript and discussions about Rab phosphorylation.

Work in the Echard Lab is supported by Institut Pasteur, CNRS, FRM (Equipe FRM DEQ20120323707, FDT20150532389), INCa (2014-1-PL BIO-04-IP1), ANR (AbCyStem), Schlumberger Foundation for Research and Education, IXCore foundation and Association Syndrome de Lowe.

The Editorial Process File is available in the online version of this article.

References

- Stenmark H. Rab GTPases as coordinators of vesicle traffic. *Nat Rev Mol Cell Biol* 2009;10:513–525.
- Zhu AX, Zhao Y, Flier JS. Molecular cloning of two small GTP-binding proteins from human skeletal muscle. *Biochem Biophys Res Commun* 1994;205:1875–1882.
- Klopper TH, Kienle N, Fasshauer D, Munro S. Untangling the evolution of Rab G proteins: implications of a comprehensive genomic analysis. *BMC Biol* 2012;10:71.
- Heo WD, Inoue T, Park WS, Kim ML, Park BO, Wandless TJ, Meyer T. PI(3,4,5)P3 and PI(4,5)P2 lipids target proteins with polybasic clusters to the plasma membrane. *Science* 2006;314:1458–1461.
- Gavriljuk K, Itzen A, Goody RS, Gerwert K, Kottling C. Membrane extraction of Rab proteins by GDP dissociation inhibitor characterized using attenuated total reflection infrared spectroscopy. *Proc Natl Acad Sci U S A* 2013;110:13380–13385.
- Li F, Yi L, Zhao L, Itzen A, Goody RS, Wu YW. The role of the hypervariable C-terminal domain in Rab GTPases membrane targeting. *Proc Natl Acad Sci U S A* 2014;111:2572–2577.
- Abe Y, Takeuchi T, Imai Y, Murase R, Kamei Y, Fujibuchi T, Matsumoto S, Ueda N, Ogasawara M, Shigemoto K, Kito K. A Small Ras-like protein Ray/Rab1c modulates the p53-regulating activity of PRPK. *Biochem Biophys Res Commun* 2006;344:377–385.
- Kouranti I, Sachse M, Arouche N, Goud B, Echard A. Rab35 regulates an endocytic recycling pathway essential for the terminal steps of cytokinesis. *Curr Biol* 2006;16:1719–1725.
- Walseng E, Bakke O, Roche PA. Major histocompatibility complex class II-peptide complexes internalize using a clathrin- and dynamin-independent endocytosis pathway. *J Biol Chem* 2008;283:14717–14727.
- Charrasse S, Comunale F, De Rossi S, Echard A, Gauthier-Rouviere C. Rab35 regulates cadherin-mediated adherens junction formation and myoblast fusion. *Mol Biol Cell* 2013;24:234–245.
- Argenzio E, Margadant C, Leyton-Puig D, Janssen H, Jalink K, Sonnenberg A, Moolenaar WH. CLIC4 regulates cell adhesion and beta1 integrin trafficking. *J Cell Sci* 2014;127:5189–5203.
- Allaire PD, Marat AL, Dall'Armi C, Di Paolo G, McPherson PS, Ritter B. The Connecden DENN domain: a GEF for Rab35 mediating cargo-specific exit from early endosomes. *Mol Cell* 2010;37:370–382.
- Patino-Lopez G, Dong X, Ben-Aissa K, Bernot KM, Itoh T, Fukuda M, Kruhlak MJ, Samelson LE, Shaw S. Rab35 and its GAP EPI64C in T cells regulate receptor recycling and immunological synapse formation. *J Biol Chem* 2008;283:18323–18330.
- Cauvin C, Rosendale M, Gupta-Rossi N, Rocancourt M, Larraufie P, Salomon R, Perrais D, Echard A. Rab35 GTPase triggers switch-like recruitment of the Lowe syndrome lipid phosphatase OCRL on newborn endosomes. *Curr Biol* 2016;26:120–128.
- Sato M, Sato K, Liou W, Pant S, Harada A, Grant BD. Regulation of endocytic recycling by *C. elegans* Rab35 and its regulator RME-4, a coated-pit protein. *EMBO J* 2008;27:1183–1196.
- Echard A, Hickson GR, Foley E, O'Farrell PH. Terminal cytokinesis events uncovered after an RNAi screen. *Curr Biol* 2004;14:1685–1693.
- Mierzwa B, Gerlich DW. Cytokinetic abscission: molecular mechanisms and temporal control. *Dev Cell* 2014;31:525–538.
- Dikshit N, Bist P, Fenlon SN, Pulloor NK, Chua CE, Scidmore MA, Carlyon JA, Tang BL, Chen SL, Sukumaran B. Intracellular uropathogenic *E. coli* exploits host Rab35 for iron acquisition and survival within urinary bladder cells. *PLoS Pathog* 2015;11:e1005083.
- Chesneau L, Dambournet D, Machicoane M, Kouranti I, Fukuda M, Goud B, Echard A. An ARF6/Rab35 GTPase cascade for endocytic recycling and successful cytokinesis. *Curr Biol* 2012;22:147–153.
- Allaire PD, Seyed Sadr M, Chaineau M, Seyed Sadr E, Konefal S, Fotouhi M, Maret D, Ritter B, Del Maestro RF, McPherson PS. Interplay between Rab35 and Arf6 controls cargo recycling to coordinate cell adhesion and migration. *J Cell Sci* 2013;126:722–731.
- Gao Y, Balut CM, Bailey MA, Patino-Lopez G, Shaw S, Devor DC. Recycling of the Ca²⁺-activated K⁺ channel, KCa2.3, is dependent upon RME-1, Rab35/EPI64C, and an N-terminal domain. *J Biol Chem* 2010;285:17938–17953.
- Shah M, Bateria OY Jr, Taupin V, Farquhar MG. ARH directs megalin to the endocytic recycling compartment to regulate its proteolysis and gene expression. *J Cell Biol* 2013;202:113–127.
- Davey JR, Humphrey SJ, Junutula JR, Mishra AK, Lambright DG, James DE, Stockli J. TBC1D13 is a Rab35 specific gap that plays an important role in GLUT4 trafficking in adipocytes. *Traffic* 2012;13:1429–1441.

24. Fuchs E, Haas AK, Spooner RA, Yoshimura S, Lord JM, Barr FA. Specific Rab GTPase-activating proteins define the Shiga toxin and epidermal growth factor uptake pathways. *J Cell Biol* 2007;177:1133–1143.
25. Kanno E, Ishibashi K, Kobayashi H, Matsui T, Ohbayashi N, Fukuda M. Comprehensive screening for novel rab-binding proteins by GST pull-down assay using 60 different mammalian Rabs. *Traffic* 2010;11:491–507.
26. Dambournet D, Machicoane M, Chesneau L, Sachse M, Rocancourt M, El Marjou A, Formstecher E, Salomon R, Goud B, Echard A. Rab35 GTPase and OCRL phosphatase remodel lipids and F-actin for successful cytokinesis. *Nat Cell Biol* 2011;13:981–988.
27. Lowe M. Structure and function of the Lowe syndrome protein OCRL1. *Traffic* 2005;6:711–719.
28. Pirruccello M, De Camilli P. Inositol 5-phosphatases: insights from the Lowe syndrome protein OCRL. *Trends Biochem Sci* 2012;37:134–143.
29. Mehta ZB, Pietka G, Lowe M. The cellular and physiological functions of the Lowe syndrome protein OCRL1. *Traffic* 2014;15:471–487.
30. Echard A. Phosphoinositides and cytokinesis: the "PIP" of the iceberg. *Cytoskeleton* 2012;69:893–912.
31. Cauvin C, Echard A. Phosphoinositides: lipids with informative heads and mastermind functions in cell division. *Biochim Biophys Acta* 2014;1851:832–843.
32. Choudhury R, Diao A, Zhang F, Eisenberg E, Saint-Pol A, Williams C, Konstantakopoulos A, Lucocq J, Johannes L, Rabouille C, Greene LE, Lowe M. Lowe syndrome protein OCRL1 interacts with clathrin and regulates protein trafficking between endosomes and the trans-Golgi network. *Mol Biol Cell* 2005;16:3467–3479.
33. Vicinanza M, Di Campli A, Polishchuk E, Santoro M, Di Tullio G, Godi A, Levchenko E, De Leo MG, Polishchuk R, Sandoval L, Marzolo M, De Matteis MA. OCRL controls trafficking through early endosomes via PtdIns4,5P(2)-dependent regulation of endosomal actin. *EMBO J* 2011;30:4970–4985.
34. Grant BD, Donaldson JG. Pathways and mechanisms of endocytic recycling. *Nat Rev Mol Cell Biol* 2009;10:597–608.
35. D'Souza-Schorey C, Chavrier P. ARF proteins: roles in membrane traffic and beyond. *Nat Rev Mol Cell Biol* 2006;7:347–358.
36. Rahajeng J, Giridharan SS, Cai B, Naslavsky N, Caplan S. MICAL-L1 is a tubular endosomal membrane hub that connects Rab35 and Arf6 with Rab8a. *Traffic* 2012;13:82–93.
37. Chevallier J, Koop C, Srivastava A, Petrie RJ, Lamarche-Vane N, Presley JF. Rab35 regulates neurite outgrowth and cell shape. *FEBS Lett* 2009;583:1096–1101.
38. Kobayashi H, Fukuda M. Rab35 regulates Arf6 activity through centaurin-beta2 (ACAP2) during neurite outgrowth. *J Cell Sci* 2012;125:2235–2243.
39. Kobayashi H, Fukuda M. Rab35 establishes the EHD1-association site by coordinating two distinct effectors during neurite outgrowth. *J Cell Sci* 2013;126:2424–2435.
40. Kobayashi H, Etoh K, Ohbayashi N, Fukuda M. Rab35 promotes the recruitment of Rab8, Rab13 and Rab36 to recycling endosomes through MICAL-L1 during neurite outgrowth. *Biol Open* 2014;3:803–814.
41. Etoh K, Fukuda M. Structure-function analyses of the small GTPase Rab35 and its effector protein Centaurin-beta2/ACAP2 during neurite outgrowth of PC12 cells. *J Biol Chem* 2015;290:9064–9074.
42. Langemeyer L, Nunes Bastos R, Cai Y, Itzen A, Reinisch KM, Barr FA. Diversity and plasticity in Rab GTPase nucleotide release mechanism has consequences for Rab activation and inactivation. *Elife* 2014;3:e01623.
43. Radhakrishna H, Donaldson JG. ADP-ribosylation factor 6 regulates a novel plasma membrane recycling pathway. *J Cell Biol* 1997;139:49–61.
44. Dutta D, Donaldson JG. Sorting of independent cargo proteins depends on Rab35 delivered by clathrin-mediated endocytosis. *Traffic* 2015;16:994–1009.
45. Giridharan SS, Caplan S. MICAL-family proteins: complex regulators of the actin cytoskeleton. *Antioxid Redox Signal* 2013;20:2059–2073.
46. Miyamoto Y, Yamamori N, Torii T, Tanoue A, Yamauchi J. Rab35, acting through ACAP2 switching off Arf6, negatively regulates oligodendrocyte differentiation and myelination. *Mol Biol Cell* 2014;25:1532–1542.
47. Chaineau M, Ioannou MS, McPherson PS. Rab35: GEFs, GAPs and effectors. *Traffic* 2013;14:1109–1117.
48. Marat AL, Dokainish H, McPherson PS. DENN domain proteins: regulators of Rab GTPases. *J Biol Chem* 2011;286:13791–13800.
49. Levivier E, Goud B, Souchet M, Calmels TP, Morron JP, Callebaut I. uDENN, DENN, and dDENN: indissociable domains in Rab and MAP kinases signaling pathways. *Biochem Biophys Res Commun* 2001;287:688–695.
50. Zhang D, Iyer LM, He F, Aravind L. Discovery of novel DENN proteins: implications for the evolution of eukaryotic intracellular membrane structures and human disease. *Front Genet* 2012;3:283.
51. Janoueix-Lerosey I, Jollivet F, Camonis J, Marche PN, Goud B. Two-hybrid system screen with the small GTP-binding protein Rab6. Identification of a novel mouse GDP dissociation inhibitor isoform and two other potential partners of Rab6. *J Biol Chem* 1995;270:14801–14808.
52. Miserey-Lenkei S, Waharte F, Boulet A, Cuif MH, Tenza D, El Marjou A, Raposo G, Salamero J, Heliot L, Goud B, Monier S. Rab6-interacting protein 1 links Rab6 and Rab11 function. *Traffic* 2007;8:1385–1403.
53. Allaire PD, Ritter B, Thomas S, Burman JL, Denisov AY, Legendre-Guillemin V, Harper SQ, Davidson BL, Gehring K, McPherson PS. Connecdenn, a novel DENN domain-containing protein of neuronal clathrin-coated vesicles functioning in synaptic vesicle endocytosis. *J Neurosci* 2006;26:13202–13212.
54. Ritter B, Denisov AY, Philie J, Allaire PD, Legendre-Guillemin V, Zylbergold P, Gehring K, McPherson PS. The NECAP PHear domain increases clathrin accessory protein binding potential. *EMBO J* 2007;26:4066–4077.
55. Kulasekaran G, Nossova N, Marat AL, Lund I, Cremer C, Ioannou MS, McPherson PS. Phosphorylation-dependent regulation of connecdenn/DENND1 guanine nucleotide exchange factors. *J Biol Chem* 2015;290:17999–18008.

56. Wu X, Bradley MJ, Cai Y, Kummel D, De La Cruz EM, Barr FA, Reinisch KM. Insights regarding guanine nucleotide exchange from the structure of a DENN-domain protein complexed with its Rab GTPase substrate. *Proc Natl Acad Sci U S A* 2011;108:18672–18677.
57. Marat AL, McPherson PS. The connectenn family, Rab35 guanine nucleotide exchange factors interfacing with the clathrin machinery. *J Biol Chem* 2010;285:10627–10637.
58. Girard M, Allaire PD, McPherson PS, Blondeau F. Non-stoichiometric relationship between clathrin heavy and light chains revealed by quantitative comparative proteomics of clathrin-coated vesicles from brain and liver. *Mol Cell Proteomics* 2005;4:1145–1154.
59. Yoshimura S, Gerondopoulos A, Linford A, Rigden DJ, Barr FA. Family-wide characterization of the DENN domain Rab GDP-GTP exchange factors. *J Cell Biol* 2010;191:367–381.
60. Marat AL, Ioannou MS, McPherson PS. Connectenn 3/DENND1C binds actin linking Rab35 activation to the actin cytoskeleton. *Mol Biol Cell* 2012;23:163–175.
61. Nookala RK, Langemeyer L, Pacitto A, Ochoa-Montano B, Donaldson JC, Blaszczyk BK, Chirgadze DY, Barr FA, Bazan JF, Blundell TL. Crystal structure of folliculin reveals a hidDENN function in genetically inherited renal cancer. *Open Biol* 2012;2:120071.
62. Nickerson ML, Warren MB, Toro JR, Matrosova V, Glenn G, Turner ML, Duray P, Merino M, Choyke P, Pavlovich CP, Sharma N, Walther M, Munroe D, Hill R, Maher E, et al. Mutations in a novel gene lead to kidney tumors, lung wall defects, and benign tumors of the hair follicle in patients with the Birt-Hogg-Dube syndrome. *Cancer Cell* 2002;2:157–164.
63. Tsun ZY, Bar-Peled L, Chantranupong L, Zoncu R, Wang T, Kim C, Spooner E, Sabatini DM. The folliculin tumor suppressor is a GAP for the RagC/D GTPases that signal amino acid levels to mTORC1. *Mol Cell* 2013;52:495–505.
64. Hanono A, Garbett D, Reczek D, Chambers DN, Bretscher A. EPI64 regulates microvillar subdomains and structure. *J Cell Biol* 2006;175:803–813.
65. Hsu C, Morohashi Y, Yoshimura S, Manrique-Hoyos N, Jung S, Lauterbach MA, Bakhti M, Gronborg M, Mobius W, Rhee J, Barr FA, Simons M. Regulation of exosome secretion by Rab35 and its GTPase-activating proteins TBC1D10A-C. *J Cell Biol* 2010;189:223–232.
66. Fukuda M, Kobayashi H, Ishibashi K, Ohbayashi N. Genome-wide investigation of the Rab binding activity of RUN domains: development of a novel tool that specifically traps GTP-Rab35. *Cell Struct Funct* 2011;36:155–170.
67. Montagnac G, de Forges H, Smythe E, Gueudry C, Romao M, Salamero J, Chavrier P. Decoupling of activation and effector binding underlies ARF6 priming of fast endocytic recycling. *Curr Biol* 2011;21:574–579.
68. Uytterhoeven V, Kuenen S, Kasprovicz J, Miskiewicz K, Verstreken P. Loss of skywalker reveals synaptic endosomes as sorting stations for synaptic vesicle proteins. *Cell* 2011;145:117–132.
69. Davey JR, Humphrey SJ, Junutula JR, Mishra AK, Lambright DG, James DE, Stockli J. TBC1D13 is a RAB35 specific GAP that plays an important role in GLUT4 trafficking in adipocytes. *Traffic* 2012;13:1429–1441.
70. Yang CW, Hojer CD, Zhou M, Wu X, Wuster A, Lee WP, Yaspan BL, Chan AC. Regulation of T cell receptor signaling by DENND1B in TH2 cells and allergic disease. *Cell* 2016;164:141–155.
71. Egami Y, Fukuda M, Araki N. Rab35 regulates phagosome formation through recruitment of ACAP2 in macrophages during FcγR-mediated phagocytosis. *J Cell Sci* 2011;124:3557–3567.
72. Egami Y, Fujii M, Kawai K, Ishikawa Y, Fukuda M, Araki N. Activation-inactivation cycling of Rab35 and ARF6 is required for phagocytosis of zymosan in RAW264 macrophages. *J Immunol Res* 2015;2015:429439.
73. Stroschein-Stevenson SL, Foley E, O'Farrell PH, Johnson AD. Identification of Drosophila gene products required for phagocytosis of *Candida albicans*. *PLoS Biol* 2006;4:e4.
74. Shim J, Lee SM, Lee MS, Yoon J, Kweon HS, Kim YJ. Rab35 mediates transport of Cdc42 and Rac1 to the plasma membrane during phagocytosis. *Mol Cell Biol* 2010;30:1421–1433.
75. Mukherjee S, Liu X, Arasaki K, McDonough J, Galan JE, Roy CR. Modulation of Rab GTPase function by a protein phosphocholine transferase. *Nature* 2011;477:103–106.
76. Goody PR, Heller K, Oesterlin LK, Muller MP, Itzen A, Goody RS. Reversible phosphocholination of Rab proteins by *Legionella pneumophila* effector proteins. *EMBO J* 2012;31:1774–1784.
77. Mihai Gazdag E, Streller A, Haneburger I, Hilbi H, Vetter IR, Goody RS, Itzen A. Mechanism of Rab1b deactivation by the *Legionella pneumophila* GAP LepB. *EMBO Rep* 2013;14:199–205.
78. Huang B, Hubber A, McDonough JA, Roy CR, Scidmore MA, Carlyon JA. The *Anaplasma phagocytophilum*-occupied vacuole selectively recruits Rab-GTPases that are predominantly associated with recycling endosomes. *Cell Microbiol* 2010;12:1292–1307.
79. Abrami L, Brandi L, Moayeri M, Brown MJ, Krantz BA, Leppla SH, van der Goot FG. Hijacking multivesicular bodies enables long-term and exosome-mediated long-distance action of anthrax toxin. *Cell Rep* 2013;5:986–996.
80. Kwon SH, Liu KD, Mostov KE. Intercellular transfer of GPRC5B via exosomes drives HGF-mediated outward growth. *Curr Biol* 2014;24:199–204.
81. Wang HH, Cui Q, Zhang T, Wang ZB, Ouyang YC, Shen W, Ma JY, Schatten H, Sun QY. Rab3A, Rab27A, and Rab35 regulate different events during mouse oocyte meiotic maturation and activation. *Histochem Cell Biol* 2016;145:647–657.
82. Klinkert K, Rocancourt M, Houdusse A, Echard A. Rab35 GTPase couples cell division with initiation of epithelial apico-basal polarity and lumen opening. *Nat Commun* 2016;7:11166.
83. Mrozowska PS, Fukuda M. Regulation of podocalyxin trafficking by Rab small GTPases in 2D and 3D epithelial cell cultures. *J Cell Biol* 2016;213:355–369.
84. Schottenfeld-Roames J, Ghabrial AS. Whacked and Rab35 polarize dynein-motor-complex-dependent seamless tube growth. *Nat Cell Biol* 2012;14:386–393.

85. Crockett DK, Lin Z, Elenitoba-Johnson KS, Lim MS. Identification of NPM-ALK interacting proteins by tandem mass spectrometry. *Oncogene* 2004;23:2617–2629.
86. Sheach LA, Adeney EM, Kucukmetin A, Wilkinson SJ, Fisher AD, Elattar A, Robson CN, Edmondson RJ. Androgen-related expression of G-proteins in ovarian cancer. *Br J Cancer* 2009;101:498–503.
87. Tang Y, Lin Y, Li C, Hu X, Liu Y, He M, Luo J, Sun G, Wang T, Li W, Guo M. MicroRNA-720 promotes in vitro cell migration by targeting Rab35 expression in cervical cancer cells. *Cell Biosci* 2015;5:56.
88. Zhu Y, Shen T, Liu J, Zheng J, Zhang Y, Xu R, Sun C, Du J, Chen Y, Gu L. Rab35 is required for Wnt5a/Dvl2-induced Rac1 activation and cell migration in MCF-7 breast cancer cells. *Cell Signal* 2013;25:1075–1085.
89. Wheeler DB, Zoncu R, Root DE, Sabatini DM, Sawyers CL. Identification of an oncogenic RAB protein. *Science* 2015;350:211–217.
90. Zhang J, Fonovic M, Suyama K, Bogoy M, Scott MP. Rab35 controls actin bundling by recruiting fascin as an effector protein. *Science* 2009;325:1250–1254.
91. Kobayashi H, Etoh K, Fukuda M. Rab35 is translocated from Arf6-positive perinuclear recycling endosomes to neurite tips during neurite outgrowth. *Small GTPases* 2014;5:e29290.
92. Chua CE, Lim YS, Tang BL. Rab35 – a vesicular traffic-regulating small GTPase with actin modulating roles. *FEBS Lett* 2009;584:1–6.
93. Marion S, Mazzolini J, Herit F, Bourdoncle P, Kambou-Pene N, Hailfinger S, Sachse M, Ruland J, Benmerah A, Echard A, Thome M, Niedergang F. The NF-kappaB signaling protein Bcl10 regulates actin dynamics by controlling AP1 and OCRL-bearing vesicles. *Dev Cell* 2012;23:954–967.
94. Kuhbacher A, Dambournet D, Echard A, Cossart P, Pizarro-Cerda J. Phosphatidylinositol 5-phosphatase oculocerebrorenal syndrome of Lowe protein (OCRL) controls actin dynamics during early steps of *Listeria monocytogenes* infection. *J Biol Chem* 2012;287:13128–13136.
95. Lang P, Gesbert F, Delespine-Carmagnat M, Stancou R, Pouchelet M, Bertoglio J. Protein kinase A phosphorylation of RhoA mediates the morphological and functional effects of cyclic AMP in cytotoxic lymphocytes. *EMBO J* 1996;15:510–519.

RESUME

L'établissement de la polarité apico-basale dans les tissus épithéliaux est étroitement lié à la division cellulaire, mais les mécanismes moléculaires sous-jacents n'ont pas encore été établis. A l'aide d'un modèle de culture en 3 dimensions de cellules rénales (MDCK), j'ai montré que lors du développement d'un cyst, la GTPase Rab35 joue un rôle majeur dans l'établissement de la polarité et le positionnement du lumen pendant la première division cellulaire. Au niveau moléculaire, Rab35 permet de coupler l'initiation de la polarité apico-basale avec la cytokinèse via l'attachement au sillon de clivage de vésicules intracellulaires contenant des déterminants clé de l'établissement de la polarité. Ces vésicules transportent notamment les protéines aPKC, Cdc42, Crumbs3 ainsi que le facteur d'ouverture de la lumière Podocalyxin. De plus, l'attachement de ces vésicules au sillon de clivage dépend de l'interaction directe entre Rab35 et la queue cytoplasmique de Podocalyxin. Par conséquent, l'inactivation de Rab35 entraîne une inversion complète de la polarité apico-basale des kystes 3D. J'ai mis en évidence un nouveau mécanisme de ciblage des vésicules intracellulaire au site de clivage dépendant de la protéine Rab35 impliqué à la fois dans l'initiation de la polarité apico-basale et dans l'ouverture de la lumière au centre du cyst.

Mot clés: polarité épithélial, cytokinèse, Podocalyxin, Rab35 GTPase, 3D MDCK cysts

ABSTRACT

Establishment and maintenance of apico-basal polarity in epithelial organs must be tightly coupled with cell division, but the underlying molecular mechanisms are largely unknown. Using 3D cultures of renal MDCK cells (cysts), I found that the Rab35 GTPase plays a crucial role in polarity initiation and apical lumen positioning during the first cell division of cyst development. At the molecular level, Rab35 physically couples cytokinesis with the initiation of apico-basal polarity by tethering intracellular vesicles containing key apical determinants at the cleavage site. These vesicles transport aPKC, Cdc42, Crumbs3 and the lumen promoting factor Podocalyxin, and are tethered through a direct interaction between Rab35 and the cytoplasmic tail of Podocalyxin. Consequently, Rab35 inactivation leads to complete inversion of apico-basal polarity in 3D cysts. This novel and unconventional mode of Rab-dependent vesicle targeting provides a simple mechanism for triggering both initiation of apico-basal polarity and lumen opening at the centre of cysts.

Keywords: Epithelial polarity, cytokinesis, Podocalyxin, Rab35 GTPase, 3D MDCK cysts